Abstract

SACHET, EDWARD. Transition Metal Oxides for Infrared Optoelectronics. (Under the direction of Jon-Paul Maria.)

Plasmonics, a field of study in optoelectronics, describes the interaction of free charge carriers in conductors with electromagnetic radiation. Under certain illumination conditions, free charge carriers can become resonant with the electric field component of the light used. This resonance results in a bound electromagnetic wave with unique optical properties that can be utilized for a variety of sensing, spectroscopy and optoelectronic applications.

Historically, plasmonic phenomena were restricted to metallic material systems such as gold and silver, and the light used to excite plasmonic phenomena was part of the UV-VIS energy range of the electromagnetic spectrum. In recent years however, a growing interest in lower energy plasmonics, particularly at infrared energies, emerged from the plasmonics community. Migrating plasmonic phenomena to the infrared regime will enable new technologies such as novel infrared emitters and detectors, advanced IR-spectroscopy techniques, heat assisted data storage or heat scavenging.

Facilitating this transition however will require advances in materials development. The plasmonic host materials employed for UV-VIS applications, in particular the noble metals, are inept to support low loss plasmonics at infrared energies. Novel plasmonic host materials, preferably with tunable properties to cover a wide range of resonance energies, are needed.

This dissertation explores the use of transition metal oxides as plasmonic materials for the mid-infrared (2-10 μm wavelength) energy range. In particular, two material systems, ZnO and CdO, are studied and their applicability towards mid-IR plasmonics is assessed. Additionally, a simulation method to predict plasmonic properties of arbitrary materials has been developed in combination with an infrared spectroscopy technique that allows to experimentally interrogate the plasmonic properties of thin film samples. These techniques are complimentary and yield directly comparable results allowing for an efficient testing of theory against experiment.

The study of heavily doped zinc oxide led to an important proof of concept, demonstrating that wide band gap conducting oxides are indeed applicable for plasmonics in the mid-infrared. However, the ZnO material system revealed the limiting factors present

in most transition metal oxides. At the high doping levels needed to support mid-infrared plasmons (>1x10^{20} cm^{-3}) the transport properties degrade. Charge carrier mobilities are low which translates into high optical losses for plasmonic applications. A material that combines high charge carrier concentrations with high carrier mobilities is needed for optimal performance in the infrared. Scattered literature reports suggested that doped CdO might exhibit this rare combination of transport properties.

This lead to the development of a MBE based deposition technique for CdO doped with dysprosium (CdO:Dy). Ideal transport properties for mid-IR plasmonics were found and the material was thoroughly characterized in its structural, transport, optical, and thermal properties. CdO:Dy can sustain extremely large room temperature electron mobilities of >300 $cm^2V^{-1}s^{-1}$ for a free carrier concentration range of 8x10^{19}-5x10^{20} cm^{-3} . A crystal defect based model was proposed to describe the structure/property relations leading to the unusual transport properties of CdO:Dy, and the model was tested experimentally. Complimentary *ab initio* calculations using density functional theory (DFT) were performed for additional verification of the proposed mechanism.

The final part of this thesis describes the application of thin films of CdO:Dy to investigate the absorption mode mixing of plasmons with gas absorptions in the infrared. A significantly increased infrared absorption is found when these two resonant phenomena are combined. Based on the modeling technique developed for this work, the enhancement mechanism was identified and theoretically described. The plasmonic mode-mixing enhancement compares favorably to conventional enhanced infrared absorption measurement schemes based on thin noble metal films. The mode-mixing enhancement infrared absorption effect represents the first step towards technological application using the materials and methods developed in this work.

Transition Metal Oxides for Infrared Optoelectronics

by
Edward Sachet

A dissertation submitted to the Graduate Faculty of
North Carolina State University
in partial fulfillment of the
requirements for the Degree of
Doctor of Philosophy

Materials Science and Engineering

Raleigh, North Carolina

2015

APPROVED BY:

Stefan Franzen Professor of Chemistry	Douglas Irving Associate Professor of Materials Science
Zlatko Sitar Professor of Materials Science	Jon-Paul Maria Professor of Materials Science Chair of Advisory Committee

Dedication

To my parents Monika and Robert who might wonder what I do all day long

Biography

The author was born January 9^{th}, 1986 to parents Monika Sachet and Robert Schick of Vienna, Austria. He attended the Vienna University of Technology where he studied Chemistry. In 2010, he graduated with a Master of Science degree focusing on the Metallurgy of the less common metals under the supervision of Prof. Wolf-Dieter Schubert. His master thesis was an industry cooperation with the goal to develop alternative alloy binder systems for tungsten carbide hardmetals. After graduation he remained with the Vienna University of Technology as a Research Assistant, focusing on in-situ studies of the high temperature sintering process of cemented carbides.

In 2011, he was awarded a Fulbright scholarship and joined Prof. Jon-Paul Maria's group at North Carolina State University to pursue his doctorate. His project focused on the development and characterization of novel materials that support surface plasmon resonance in the mid-infrared energy range of the electromagnetic spectrum.

Acknowledgements

I would first like to thank my advisor Prof. Jon-Paul Maria for his persistence in convincing me to work with him on this project. In a large part it is due to Dr. Maria's infectious enthusiasm towards science that led this project far beyond what was originally conceived. Without his endless optimism and personal guidance I would have given up numerous times, on occasions when no experiment worked and every single piece of equipment seemed to fail simultaneously. I would also like to thank him for creating a working environment that strikes the delicate balance of productivity, seriousness and good times. Finally, for being a friend and introducing me to aspects of the american life that would have remained hidden otherwise...

All current and former members of the Electronic Oxides group that I had the pleasure of working with: Michelle Casper, Nicole Estrich, David Harris, David Hook, Xiaoyu Kang, Kyle Kelley, John Leonard, William Luke, Ed Mily, Beth Paisley, Bennet Rogers, Tina Rost, Chris T. Shelton, Alex Smith and J.B. Weld. You guys are awesome! I thank you for all the help in the lab, fruitful discussions, pranks and your friendship which made my tenure at NC-State an enjoyable time.

Prof. Stefan Franzen, for co-advising this thesis, and asking the right questions to motivate me and strengthen my interest in fundamental science. His former group member Joshua Guske, for introducing me to the field of plasmonics and sharing his knowledge. I would like to thank Joshua Harris, Benjamin Gaddy, Prof. Douglas Irving, Brian Donovan, Prof. Patrick Hopkins, Jon Ihlefeld and Prof. Stefano Curtarolo for playing an important role in my biggest academic achievement so far. Furthermore, Prof. Wolf-Dieter Schubert who remained as mentor and friend.

I would also like to thank the Austrian Fulbright commission for supporting me. Without their vision and guidance, I would have never dared to study in the USA.

Finally, my sister Catherine and my parents Monika and Robert who supported me and my academic pursuits throughout my life.

Table of Contents

List of Tables

List of Figures

Chapter 1

Surface Plasmon Polaritons

1.1 Motivation for this work

Surface Plasmon Polaritons (SPP) are bound electromagnetic surface waves that can propagate along a metal/dielectric interface. These waves are caused by a collective oscillation of free electrons within the metal and result in electromagnetic fields that decay exponentially, perpendicular to the interface, into the metal as well as the dielectric. A simple visualization of the electric fields caused by a SPP at a 2D interface is depicted in figure 1.1.
SPP surface waves can be coupled to by incoming electromagnetic radiation, thus they offer an direct link between an optical signal (incoming light) and an electrical signal (collective electron oscillation). Furthermore, the bound surface wave has a shorter wavelength than the incoming light, and can therefore confine light into sub-wavelength length scales. This implies, that SPPs can be used for sub-wavelength optics and to bypass the diffraction limit.

Historically, SPPs have been investigated in noble metals, which support SPPs in the ultraviolet (UV) and visible (UV-VIS) parts of the electromagnetic spectrum. Following a full understanding of these phenomena, various technologies utilizing the properties of metal-bound SPPs have been developed and successfully commercialized. Metal-SPP based technologies have become a vital part of biochemical sensing or sub-wavelength imaging applications.
Recently, the research field encompassing all plasmonic phenomena, *Plasmonics*, is growing increasingly fast with an ever higher number of research publications published each year. This new found interest in the field is mostly fueled by the realization that SPPs are not exclusive to metal/dielectric interfaces. SPPs can be supported by a number of material

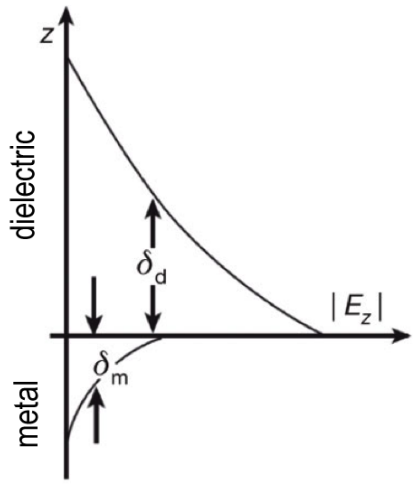

Figure 1.1 2D schematic of a SPP at a metal/dielectric interface; the exponentially decaying electric fields are perpendicular to the interface. δ indicates the confinement width of the electromagnetic field for the metal (δ_m) and dielectric (δ_d).

classes, such as semiconductors, half-metals, liquids or conductive metal oxides (CMOs). The contrast to metal based SPPs, these material classes support SPPs at lower energies, at longer wavelengths than the UV-VIS regime that is accessible using noble metals. Shifting - and understanding - plasmonic phenomena to lower energies, can open up exciting new possibilities for SPP based technologies.

One spectral region of interest is the infrared (IR). The infrared band carries heat, vibrational information about chemical bonding and is widely used for telecommunication purposes. Combining these characteristics with SPPs and SPP based technologies, can enable high value-added technologies for applications such as advanced chemical sensing, heat harvesting, data storage, infrared detectors and emitters or light and heat harvesting applications. In the context of these promises and the lively research community, the motivation for this work was to find and optimize materials that can support infrared plasmonics, with a focus on the mid-IR region of the electromagnetic spectrum. New materials were created, characterized, and tested towards their applicability for the technologies mentioned above.

1.2 Historical Overview

Surface plasmon polaritons were first observed 1902 by Wood, who studied the interaction of light with gratings. He noticed dark bands in the reflected spectrum off of metal backed diffraction gratings and published his observations in the same year[1]. Figure 1.2 depicts the original figure published in his work. The dark reflection bands that were found, are

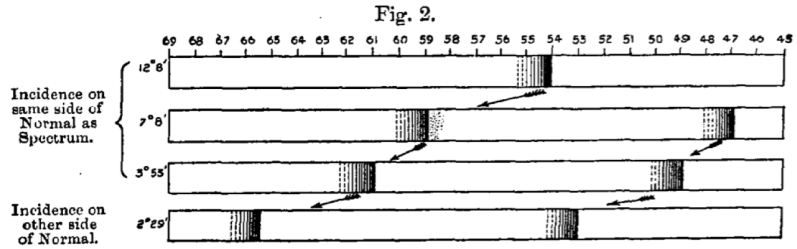

Figure 1.2 First experimental observation of SPPs as published by Wood in 1902[1].

still known as *Wood's anomalies* today. Similar observations were made by Lord Rayleigh, who published a course theory describing the anomalies in 1907[2]. Wood published his own theory to explain the observed optical phenomena[3], however both theories could not accurately explain the observed spectra. In the years to come, both scientists made significant contributions to understand the nature of surface plasmons and Wood refined his views on the topic in 1935[4].
Several decades later, Palmer refined the theories, by solving the polarization dependencies of Wood's anomalies[5,6]. Unrelated research into the energy loss to electron beams in gaseous systems and metal films[7,8] contributed the missing pieces. The realization by Pines and Bohm, that the observed energy losses are caused by a collective oscillation of free electrons, an oscillating electron plasma, was the most important contribution[9–11]. Soon thereafter it was realized, that these plasma oscillations are present at a metal *surface*, with field components that extended away from the metal into the surrounding medium. This implied, that these oscillations can be modified by changes in the environment of the surface[12], which is the key to most SPP based sensing technologies.

1.3 Surface Plasmon Resonance

Starting in the 1960s, Kretschmann[13–15] and Raether[16], and independently Otto[17], published the first complete theories on SPPs. More importantly, both Kretschmann-Raether and Otto described a simple, reliable coupling mechanism to drive SPPs on metal surfaces and study their properties. These coupling schemes are still known as the *Kretschmann-Raether*- and the *Otto*-configurations.
In order to elaborate on these coupling schemes we first have to introduce a model system, comprising of a thin metal layer and a dielectric. To further describe the dielectric properties of both components, we assume the dielectric to exhibit constant dielectric properties with energy (a non-dispersive medium) and with no loss ($\epsilon_1 = const.$; $\epsilon_2 = 0$). To describe the dielectric function of the metal, we assume a lossless cloud of electrons freely propagating

within the metallic crystal. The negatively charged electrons do not interact with the positively charged nuclei within the crystal lattice. This model is known as the lossless Drude model[18,19]. Within this model, we can describe the energy (frequency) dependent dielectric function of our model metal as:

$$\epsilon_{Drude} = \epsilon_\infty(1 - \frac{\omega_p^2}{\omega}) \tag{1.1}$$

Where ϵ_{Drude} is the dielectric function, ϵ_∞ is the high frequency limit of the dielectric function and ω_p is the characteristic plasma frequency of the material. The dispersion relation, that summarizes possible combinations of wave-vector and energy that allow a SPP to propagate is given by:

$$k_{SPP} = \frac{\omega}{c}\sqrt{\frac{\epsilon_A\epsilon_B}{\epsilon_A + \epsilon_B}} \tag{1.2}$$

where ϵ_A and ϵ_B represent the properties of the dielectric and the metal, respectively. Further we define the frequency as ω and the speed of light as c. A derivation for this dispersion relation is presented at the end of this chapter (1.7). If we now assume ϵ_∞=1 and the dielectric constant of medium A to be unity ($\epsilon_A = 1$), we can normalize all energies to the plasma frequency (ω_p) using:

$$\Omega \equiv \frac{\omega}{\omega_p} \tag{1.3}$$

we then set:

$$K \equiv \frac{k}{k_p} \tag{1.4}$$

with:

$$k_p = \frac{\omega_p}{c} \tag{1.5}$$

and insert into equation 1.2, yielding a simplified SPP dispersion that allows to explore the coupling mechanisms:

$$K = \sqrt{\frac{\Omega^2 - 1}{2\Omega^2 - 1}} \cdot \Omega \tag{1.6}$$

A plot of this dispersion relation in energy-wavevector space is depicted in figure 1.3. We can see that the dispersion yields two discrete branches, with an energy gap. The upper limit of this energy gap is found to be equal to the plasma frequency ω_p. The higher energy branch corresponds to the radiative bulk plasmon polariton (BPP), which describes the plasma oscillation in the bulk of the metallic material. The focus of this work is the branch at energies below ω_p, the surface plasmon polariton (SPP) branch. The SPP dispersion summarizes all possible combinations of wavevector (in plane, thus k_x) and energy of this surface wave. Using this description, we can explore how to interact or couple to this surface wave, using electromagnetic radiation, or beams of light.

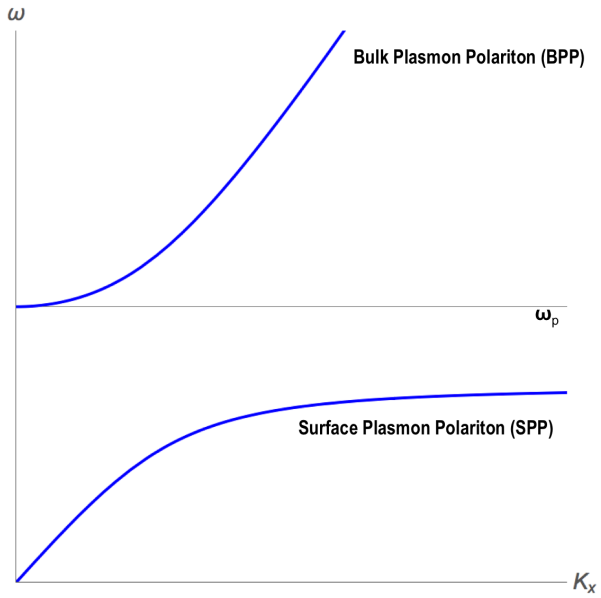

Figure 1.3 SPP dispersion for a lossless Drude metal. The two branches in the dispersion correspond to the surface plasmon polariton (SPP) and the (radiative) bulk plasmon polariton (BPP). The horizontal grey line denotes the plasma frequency ω_p.

The dispersion relation of light propagating through a medium with $\epsilon = 1$ in energy-wavevector space can be summarized as:

$$k_{light} = \frac{\omega_{light}}{c} \tag{1.7}$$

This is commonly known as a *light line*. If we plot this equation together with the SPP dispersion curve (now limiting the energy scale to values $< \omega_p$) we yield figure 1.4. The light line (green) does not intersect the SPP dispersion at any energy. This implies, that light propagating in a medium with $\epsilon = 1$ can not couple to a SPP. The in plane wavevector at any given energy is always smaller then the wavevector of the SPP. In order to enable a coupling, the wavevector (=momentum) of the incoming light needs to be raised. This is where Otto and Kretschmann-Raether achieved their brake troughs. They realized, that by passing the light through a prism of an optically denser medium ($\epsilon > 1$), the momentum of the propagating light could be increased. In the model picture depicted in figure 1.4, this corresponds to a tilt of the light line towards higher momenta. If we increase the dielectric constant of the propagation medium, we have to modify equation 1.7 to (assuming a lossless dielectric medium ϵ_D):

$$k_{light} = \frac{\omega_{light} \cdot \sqrt{\epsilon_D}}{c} \tag{1.8}$$

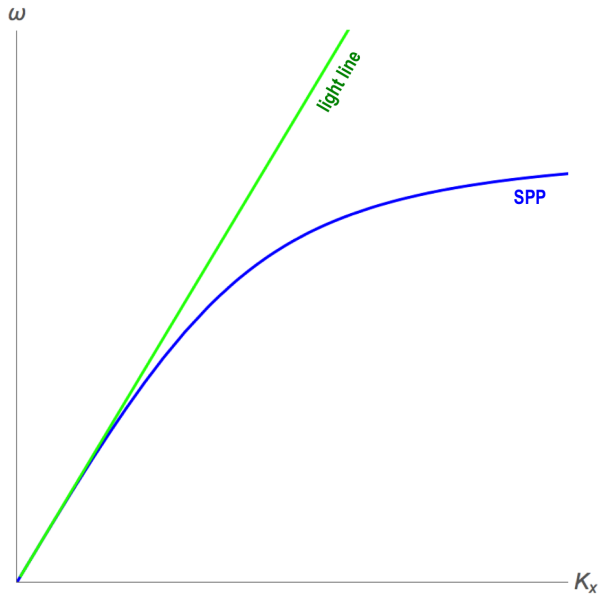

Figure 1.4 SPP dispersion (blue) with a light line (green) corresponding to light propagating in a dielectric medium with $\epsilon = 1$. No intersection of theses two features can be found.

The resulting dispersion picture is depicted in figure 1.5 . In this scenario, the light line is shifted towards higher momenta, thus intersecting the SPP dispersion curve at one point. This indicates that coupling is possible if we can match the wavevector of the incoming light experimentally.
Otto and Kretschmann-Raether realized, that if they used a total internal reflection geometry, this becomes possible. Figures 1.6 and 1.7 depict the Kretschmann-Raether and Otto configuration respectively. Upon total internal reflection, an evanescent field is created[20,21]. This wave carries the same wavevector as the original, internally reflected wave. In both configurations, this evanescent field is brought in contact with the metal surface, either by propagating through the metal film (Kretschmann-Raether) or by propagating through an air gap (Otto). If the in-plane component (k_x) and energy of this field matches the SPP dispersion, coupling occurs and the incoming light becomes resonant with the SPP. This phenomenon is called *surface plasmon resonance* (SPR). In order to achieve SPR, the in-plane component at a given energy can be varied in both configurations by varying the incident angle of the light (Θ_i). If we only consider the in-plane component of the light line, we can summarize this as:

$$k_{x(light)} = \frac{\omega_{light} \cdot \sqrt{\epsilon_D} \sin \Theta_i}{c} \tag{1.9}$$

An example on how this affects the light line is given in figure 1.8. We can immediately see,

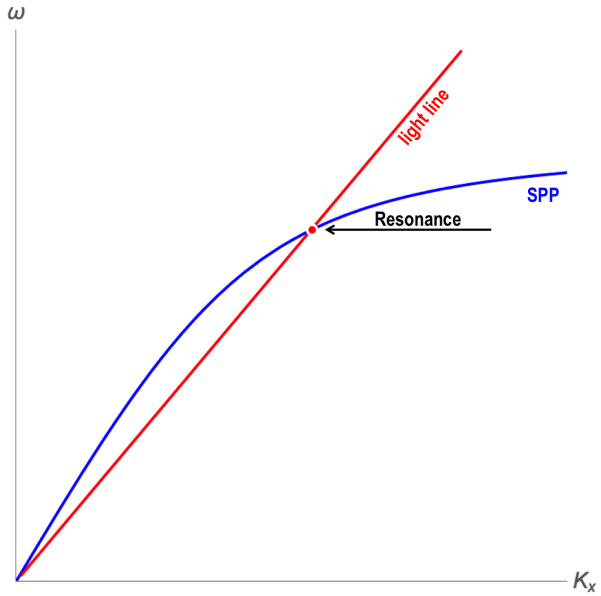

Figure 1.5 SPP dispersion and lightline for light propagating in an optically dense ($\epsilon > 1$) medium. The overlap of the lightline with the SPP dispersion indicates a possible resonance condition (coupling).

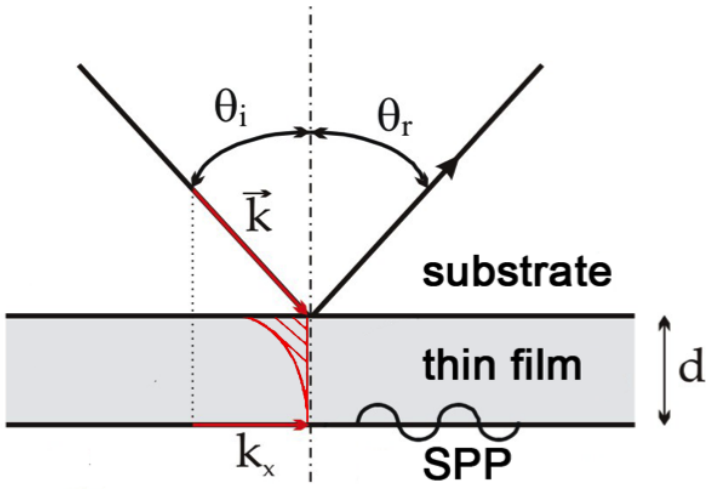

Figure 1.6 Schematic of the Kretschmann configuration. Total internal reflection creates an evanescent field (red) that penetrates the metal film. The in-plane component (k_x) of this field is the projection down onto the interface and can be varied by varying the incident angle (Θ_i) of the light beam. This configuration thus allows to match the wavevector of the incoming light to the SPP by varying the incidence angle.

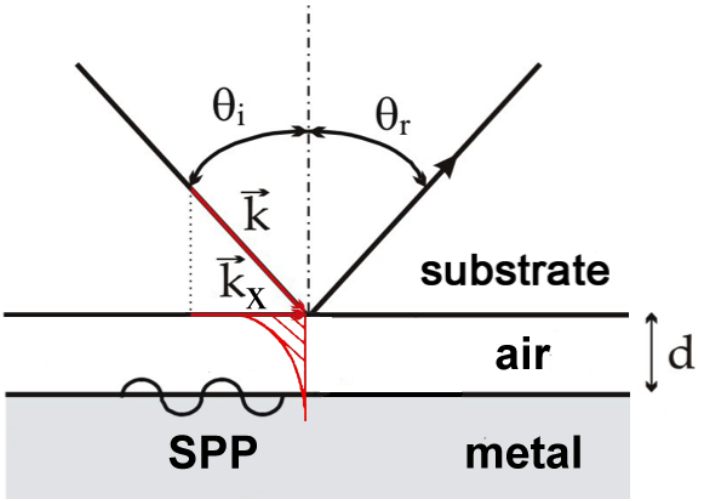

Figure 1.7 Schematic of the Otto configuration. Total internal reflection creates an evanescent field (red) that propagates through an air gap into the metal film. The in-plane component (k_x) of this field is the projection down onto the interface and can be varied by varying the incident angle (Θ_i) of the light beam. This configuration thus allows to match the wavevector of the incoming light to the SPP by varying the incidence angle.

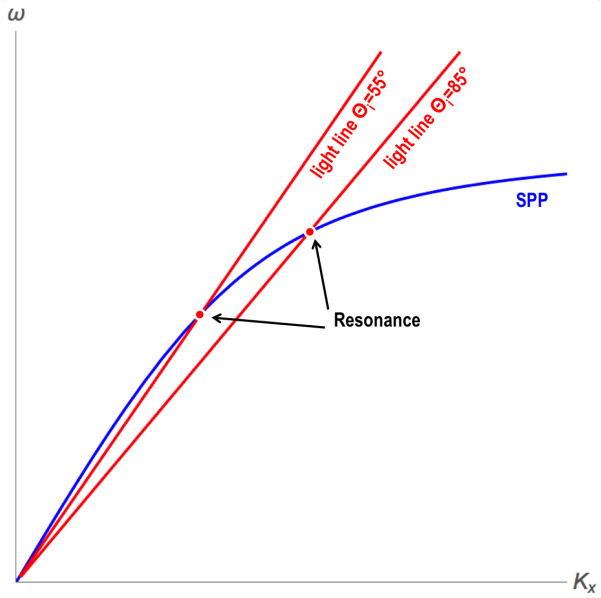

Figure 1.8 Varying the incidence angle and in-plane component of a light line. By changing the angle, resonance can be achieved at different energies (and k_x).

that a variation of the incidence angle allows us to achieve SPR at varying energies.

Upon SPR, the incoming light energy is absorbed by the SPP, which results in a drop of the internally reflected light intensity in the experimental configurations described above. This provides a convenient way to find a resonance condition: By varying either the incidence angle (with constant light energy) or by scanning the incoming energy at a constant incidence angle, we can monitor the reflected light intensity. A resonance condition is experimentally found if the reflected light intensity reaches a minimum. If we consider both of these cases in more detail it becomes important to add that there is a strong polarization dependence for these experiments. Only incoming light polarized in such a way, that it's electric field has an in-plane component that can match the SPPs wavevector, can couple to the SPP. *In the Kretschmann- or Otto-configurations, this condition is only met by p-polarized light.*

To highlight the importance of this polarization dependence, we can simulate an experiment in either of the coupling schemes using the ideal Drude metal described above. First, the energy of the light will be held constant, and the incidence angle is varied. Thus, the light line is tilted towards higher momenta. The reflected light intensity is monitored as R and plotted as a function of angle for two polarization states, s- and p-polarized. The results are depicted in figure 1.9.

For the p-polarized case (blue, panel b), the resonance with the SPP can easily be seen as an observed minimum in the reflected light intensity R. The s-polarized case does not exhibit such a minimum, since s-polarized light does not have a matching in-plane component of the electromagnetic wavevector and can thus not couple to the SPP. Alternatively, we can simulate an experiment where the angle of incidence is held constant. At a constant angle, the energy is scanned. This experiment is summarized in figure 1.10.

Again, for the p-polarized case (blue, panel b) we find a minimum in the reflected light intensity, indicating a resonance condition. S-polarized light can not couple to the SPP, thus the recorded reflected light intensity does not exhibit any features, indicating no interaction with the SPP.

These experiments can theoretically be performed in either the Kretschmann-Raether (to shorten: Kretschmann) or the Otto configuration. Since I exclusively used the Kretschmann configuration for this work, we will from now on assume the use of the Kretschmann configuration throughout the rest of this thesis.

The theoretical experiments depicted in figures 1.9 and 1.10 illustrate how the Kretschmann configuration can be used to optically characterize the SPP dispersion of a given material. By recording resonance conditions over a wide incident angle range, we can extract a sufficient amount of data points to measure the SPP dispersion over a wide range of energy. Experimentally, we are using a combination of both approaches outlined here, since a variable angle, spectroscopic experiment is used that accommodates the Kretschmann configuration.

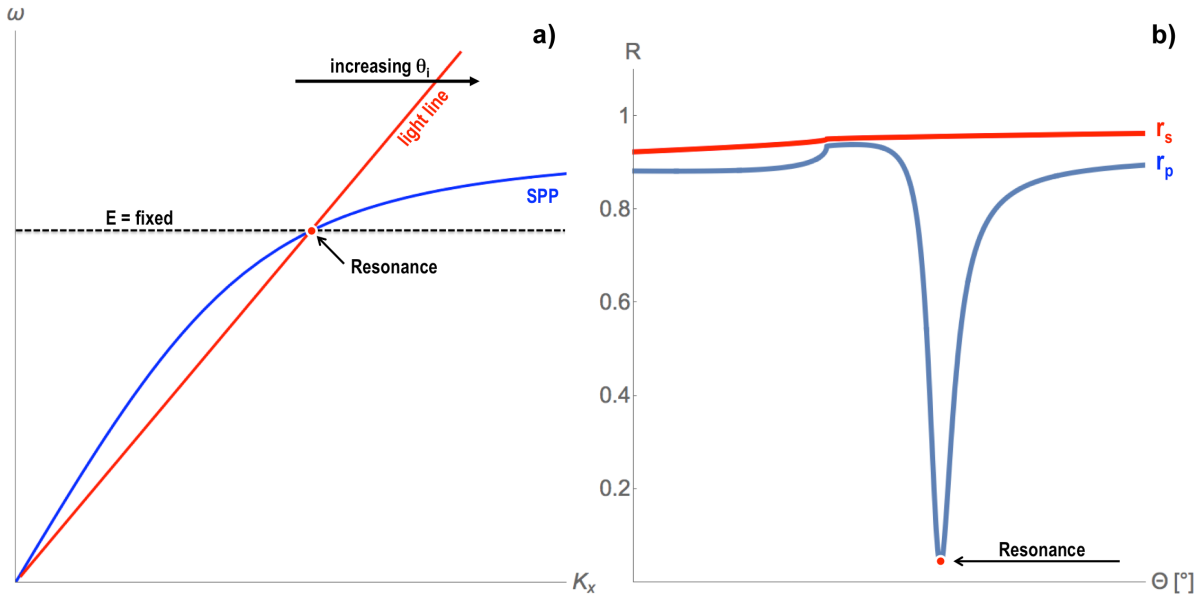

Figure 1.9 Simulated reflection experiment demonstrating the strong polarization dependence for SPR. a) The performed experiment can be summarized in the dispersion picture as tilting the light line while keeping the energy of the light constant. b) Monitoring the reflected light intensities: The blue trace corresponds to the observed reflectance (R) for p-polarized light. A minimum, corresponding to a resonance condition is found. The red trace, for s-polarized light, does not exhibit such a minimum, since s-polarized light cannot couple to a SPP in this experiment.

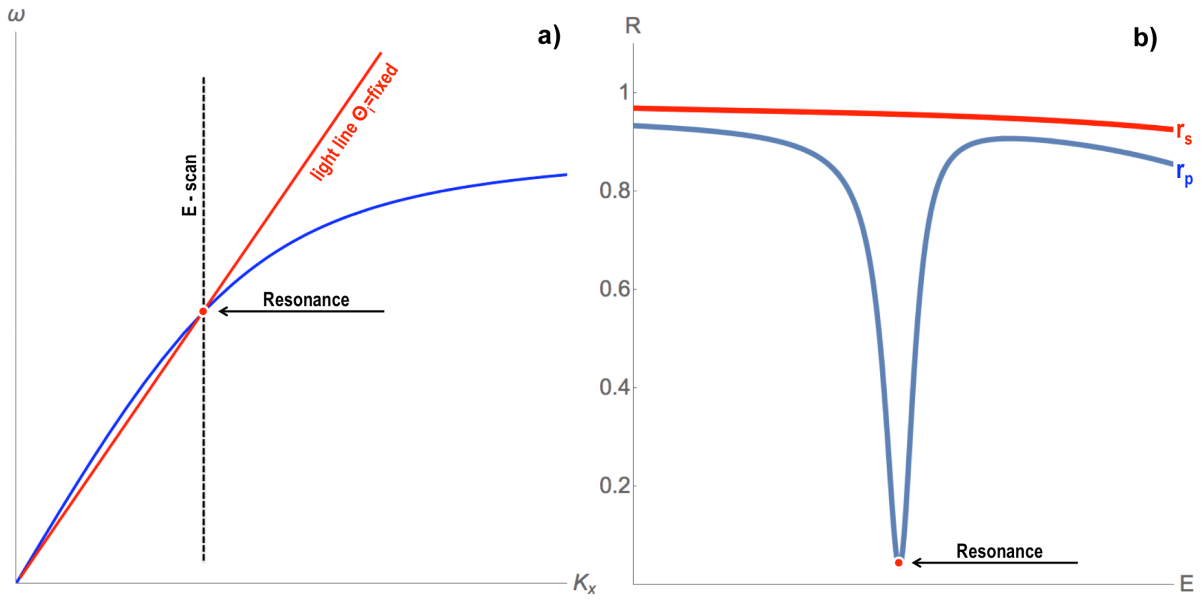

Figure 1.10 Simulated reflection experiment demonstrating the strong polarization dependence for SPR with varying energy. a) The performed experiment can be summarized in the dispersion picture as scanning vertically in energy at a constant in-plane component (fixed lightline). b) Monitoring the reflected light intensities: The blue trace corresponds to the observed reflectance R for p-polarized light. A minimum, corresponding to a resonance condition is found. The red trace, for s-polarized light, does not exhibit such a minimum, since s-polarized light cannot couple to a SPP in this experiment.

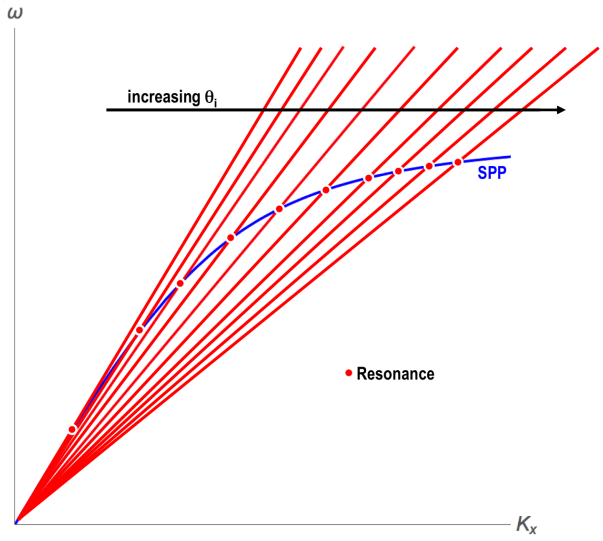

Figure 1.11 Various incidence angles in the Kretschmann configuration for SPP mapping. A series of scans at varying angles can be used to couple to the SPP at different energies.

In these experiments, we acquire data as reflected light intensity (reflectance) in energy-angle space. To realize how this connects to the SPP dispersion, we can consider a series of experiments following the procedure outlined in figure 1.9. By repeating the recording of polarization dependent reflectance as a function of incident angles at various energies, or vice versa, we can gradually map the SPP dispersion in angle and energy space. In the dispersion picture, this can be summarized as a series of light lines intersecting the SPP dispersion at different energies. Figure 1.11 illustrates this using multiple light lines corresponding to a wide range of incident angles in the Kretschmann configuration. By recording the angle/energy combination for each individual lightline that corresponds to the resonance (thus experimentally the angle/energy combination at which a minimum in p-polarized reflectance was observed), we are mapping the SPP dispersion. Upon plotting these points as a function of angle and energy, we create a map of the SPP dispersion in angle/energy space. Figure 1.12 illustrates this conversion. This plasmonic map represents the SPP dispersion converted into angle/energy space. If a sufficient number of data points is compiled, an accurate experimental description of the SPP dispersion can be achieved. Since the angle/energy parameter space can be directly accessed experimentally using the Kretschmann configuration, it is the main way of analyzing the plasmonic properties of materials in this work. Considering that the in-plane wavevector and the incident angle in the Kretschmann configuration are connected through the optical properties of the prism used in the Kretschmann configuration experiment, we can accurately extract the plasmonic properties and dispersion of any thin film material using this technique of reflectivity mapping.

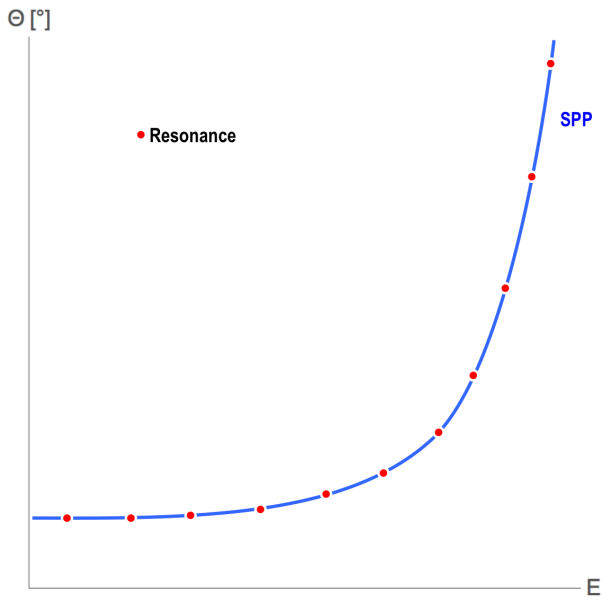

Figure 1.12 Mapping of the SPP dispersion in angle/energy space. By compiling all observed resonance conditions we can map the SPP dispersion in angle/energy space. This is of utmost importance for this work, since we can directly access this parameter space experimentally.

A real example from this work, recorded using the IR-VASE ellipsometer and the Kretschmann configuration, is depicted in figure 1.13. Details on how this data was recorded can be found in the experimental section, chapter 2.3.6. From this reflectivity map, the connection with the idealized description of this mapping procedure (fig. 1.12) can be seen. The SPP dispersion is depicted as an arc of low reflectivity R (darker shades). This arc follows a similar pattern of angle/energy combinations to the idealized data. From this reflectivity map, the plasmonic properties of the material probed in this experiment could be extracted. Because this is experimental data using real (thus non-ideal) materials, as apposed to the ideal examples used above, there are a number of features in this map that have to be further characterized and accounted for. The details on how to describe non-idealities, such as lossy metallic layers, dispersive optical components and atmospheric effects can be found in the modeling section, chapter 3.

1.4 SPR-Technologies

This section will give a brief overview of current uses of plasmonic phenomena in science and technology. It is by no means complete, however it should give the reader an idea of the versatile ways plasmonic phenomena have been utilized. All of these techniques contributed

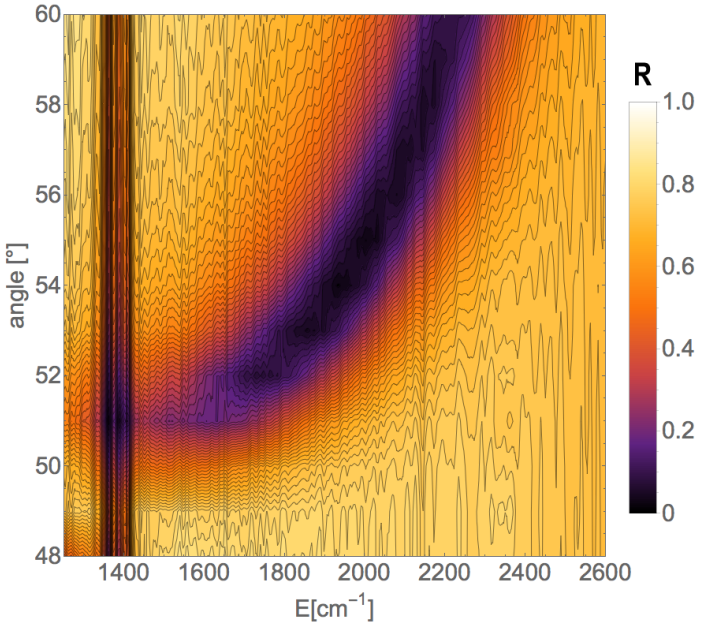

Figure 1.13 Example experimental reflectivity map. The plasmon dispersion can be seen as an arc of low reflectivity R (darker shades) in angle/energy space.

to the growing interest into the field if plasmonics. Selected recent works are cited to give an over-view and a starting point for literature research into any of the fields presented.

1.4.1 SPR-Surface sensing

The highest impact technologies based on surface plasmons and their properties are SPR-Biosensing techniques. These technologies can be used to monitor minute changes in refractive index on chemically functionalized surfaces. This technology has been successfully used in screening for novel drugs[22], to study the kinetics of protein-binding reactions[23,24] or the high throughput quality control of pharmaceutical proteins[25]. All of these techniques are based on the same property of surface plasmon polaritons: Their remarkable sensitivity towards changes in their dielectric environment.

If we consider the SPP dispersion equation:

$$k = k_{SPP} = \frac{\omega}{c}\sqrt{\frac{\epsilon_m \epsilon_d}{\epsilon_m + \epsilon_d}} \tag{1.10}$$

we find that the dispersion is dependent on the dielectric properties of the metal used (ϵ_m) and the dielectric environment (ϵ_d). The metals properties can be considered constant throughout

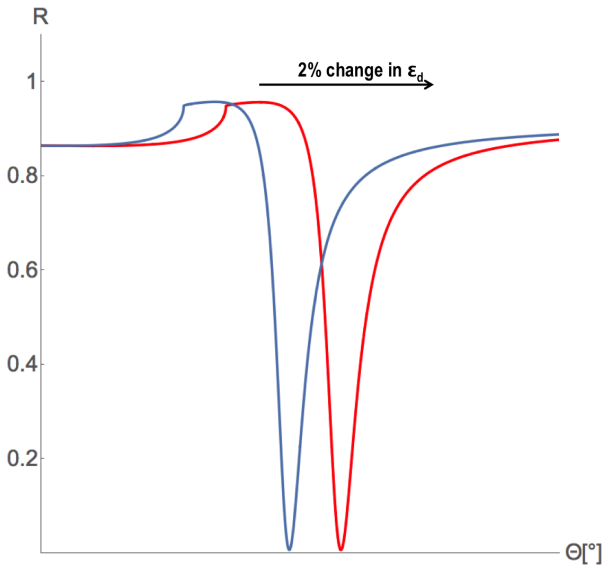

Figure 1.14 Angular sensitivity of SPR measurements. A pronounced angular shift in the position of the reflectance minimum can be found upon a change of the dielectric constant in the environment of 2%.

an experiment, however the dielectric environment (ϵ_d) can change with time. If that is the case, the resulting SPP dispersion will change dynamically, which can be recorded as a change in the outcome of an experiment. One can consider a Kretschmann configuration experiment where we monitor a reflectivity minimum as a function of incidence angle, as described in fig.1.9. The position of the observed reflectivity minimum is governed by the materials used (ϵ_m, ϵ_d) and the energy of the light that is incident. The remarkable property of SPPs is, that this resonance condition can vary *greatly* even with minute changes of the dielectric environment ϵ_d. To illustrate this, we can simulate and compare the outcome of the Kretschmann type experiment upon changing the dielectric constant of the environment (ϵ_d) by only 2%. Figure 1.14 depicts the results. It can clearly be seen, that even small changes induce a large shift in the position of the observed resonance minimum.

In SPR based technologies, the change in the dielectric constant can be caused by the binding of molecules to surfaces. Within the evanescent field caused by total internal reflection, even sub-monolayer coverage of analyte molecules can change the refractive index in proximity of the metal film to the extent that it can be measured by SPR. Chemical functionalization can govern what kind of molecules are able to bind to the sensor surface, making this technique extremely versatile. The theoretical maximum sensitivity of a gold based sensing scheme was estimated to be as high as 600°/unit of index of refraction[26].

1.4.2 Plasmonics technologies beyond the diffraction limit

Conventional microscopy is limited in resolution due to the diffraction limit, defined by Abbe as[27]:

$$d = \frac{\lambda}{2n \sin \Theta} \tag{1.11}$$

Here, d is the resulting spot size for a light converging through a medium with refractive index n at an angle Θ. This implies, that for diffraction based optics, the resolution for visible light wavelengths is limited to, e.g., 250 nm for green light with λ=500 nm. Clearly, this resolution is not sufficient to image objects at the nano-scale, where feature sizes can be easily < 1nm. Therefore, this technologically important length domain is not accessible for conventional light based microscopy.

The field confinement enabled by the bound surface wave, the SPP, can allow light to be squeezed in significantly smaller spaces, thus in principle enabling optical techniques to access the nano-lengthscales and nano imaging[28]. SPP bound to silver and gold surfaces or hole arrays have been demonstrated to enhance the resolution for 500 nm light to about 70 nm, a 7x improvement for imaging[29]. Using an tapered metallic tip design to concentrate the electric field in the near field of a conventional microscope objective, allowed the resolution to be enhanced even further[30]. The state of the art in plasmon assisted near field imaging is a tapered wave guide design. Light is bound to a SPP propagating along a gold/SiO_2 interface formed by an optical fiber[31]. This fiber tapers in diameter down to a sub 100 nm gap. Essentially, SPPs are being used to squeeze visible light into a small spot that can be rastered over the area of interest for hyper-spectral spectroscopy. Figure 1.15 depicts the design. Other pointed-probe techniques have been demonstrated to break the resolution limit of microscopy[32], however, plasmonic wave guide based designs are as of now the highest performing designs[33,34].

1.4.3 Plasmonic field enhancement

The very strong localization, and thus enhancement, of the electric field due to plasmons, is routinely used to amplify electric field based spectroscopy techniques. Certain metal geometries can act as antennas for incoming light and concentrate electric field to a very small (relative to the wavelength of the radiation used) point in space. Within these small volumina, enormous electric fields, relative to the incoming radiation, can be achieved[35]. The most iconic antenna design is the plasmonic bow-tie antenna, depicted in figure 1.16. This simple design can become resonant with incoming, visible light (normal to the image plane) and create electric field enhancements in the space between them. For the example given in figure 1.16, the gap is about 20 nm. The enhancement from such architectures has been measured to be in the order of 10^3(ref.[36]). The high electric fields created, can be utilized to

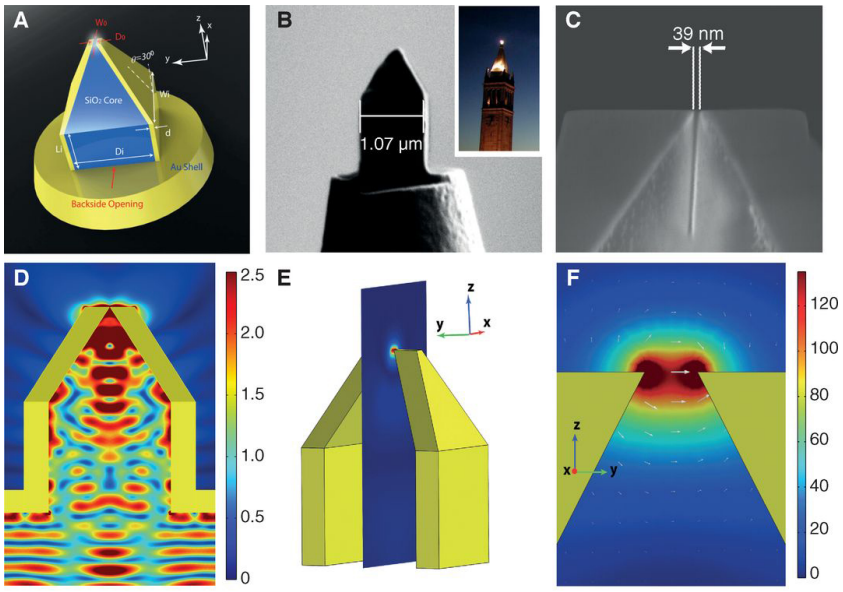

Figure 1.15 Tapered wave guide design for near-field imaging. a-c) Design of the tapered plasmon wave guide d-f) Electric field distributions within the wave guide[31].

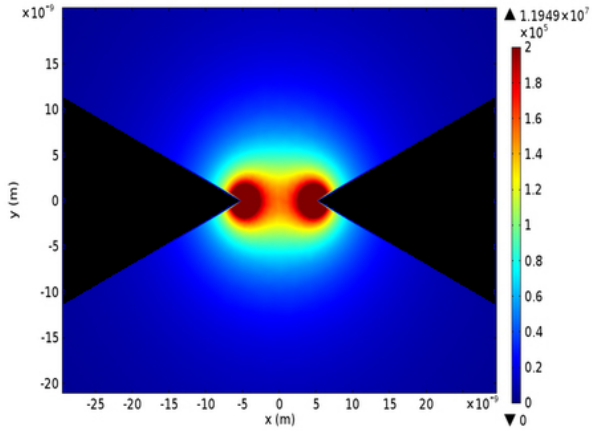

Figure 1.16 Electric field distribution around a metallic bow-tie antenna. Between the two triangular lobes, very strong electric fields can be created, once the antenna becomes resonant with the incoming radiation (top view).

sample the small focusing volumes of these antenna designs, with spectroscopy techniques based on VIS wavelengths.

Utilizing bow-tie antenna designs, scanning near-field microscopy probes were fabricated, that enable photoluminescence (PL) spectroscopy of single quantum dot structures[37]. Scanning near-field fluorescent spectroscopy was demonstrated using metallic antennas[38] and improved to a lateral resolution of 10 nm[39]. Utilizing plasmonic antennas suspended in solutions, this approach could be extended to the liquid domain[40]. Further improvements of the technique allowed for the fluorescent probing of individual nano-dots[41] and even individual molecules[42,43].

Another important use of plasmon-concentrated electric fields is the efficiency enhancement of photovoltaic (PV) devices. The efficiency of solar cells can be improved by utilizing plasmonic structures to concentrate the incoming light in the semiconductor. The same semiconductor volume can therefore harvest more of the incoming radiation[44]. Experimentally demonstrated, working designs are based on corrugated metal/semiconductor interfaces[45], or the embedding of plasmonic particles into the PV-structure[46,47]. It is important to note, that these principles can be extended to non-traditional PV devices, such as organic solar cells[48]. In theory, a large variety of geometries can be used to enhance the absorption of solar cells[49].

1.5 Towards Infrared Surface Plasmon Polaritons

Interestingly, despite all of the technologies and advances mentioned above, plasmonics has yet to be established in the mid-IR energy ranges. As mentioned in the beginning of this work, mid-IR plasmonics would enable exciting new technologies. The lack of progress however, is due to the fact that suitable materials, that can support low-loss plasmon oscillations at mid-IR energies, are rare. To understand why, it is helpful to recall the simplified plasmon dispersion as was depicted in figure1.3.

The horizontal gray line indicated the plasma frequency of the model material. It becomes evident, that plasmonic phenomena are connected to the plasma frequency in a given material. As a matter of fact, the upper limit in energy of a SPP is directly proportional to the plasma frequency ($\omega_{SPP} \propto \omega_p$). At this point, we will leave this statement as is. For a much more thorough explanation of the connection between the plasma frequency and the SPP dispersion see chapter 3. In a metal, the plasma frequency is directly proportional to the amount of free charge carriers ($\omega_p \propto n$), thus the SPP dispersion is directly proportional to the free carrier concentration in a material ($\omega_{SPP} \propto n$). We can use these connections, to estimate the free carrier concentrations needed, to support plasmonic phenomena in a certain range of the electromagnetic spectrum. The result can be seen in figure 1.17, and gives an overview of the *plasmonic material spectrum*.

From this figure, we can estimate, that a material with roughly 1x10^{19} to 1x10^{20} carri-

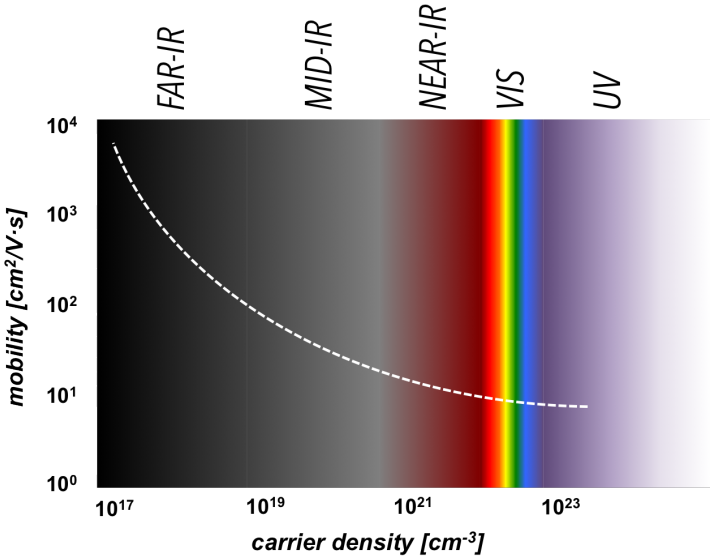

Figure 1.17 The plasmon material spectrum. A approximation of the carrier densities needed to support plasmonics at a certain range within the electromagnetic spectrum. The dotted trace indicates typical mobility values for materials exhibiting the respective free carrier concentrations.

ers cm^{-3} is needed to support mid-IR plasmonics. Finding such a material is, however, a formidable challenge. We can populate the plasmon material spectrum with several material classes and indicate the respective carrier concentration ranges that these materials exhibit. The result is depicted in figure 1.18 .

It can be seen, that neither traditional semiconductors, nor traditional metals can access this free carrier concentration range. For very few semiconductors, such as GaN for example, the carrier concentration can be raised into the $1x10^{20}$ cm^{-3} range[50]. If possible though, another important material property inevitably degrades, the free carrier mobility (μ). At this point in the manuscript, we simply state that for a given carrier concentration, a material should always exhibit the highest possible carrier mobility, in order to be a high quality plasmonic host material (For a thorough explanations of the connection of SPP dispersion and free carrier mobility, see chapter 3). It turns out, that in highly doped semiconductors the mobilities are disappointingly low. In other words, even if a semiconductor is dope-able to an extend that it supports mid-IR plasmonics, the low free carrier mobility will limit the performance of this material. This connection between carrier concentration and mobility can be easily seen in reference data for silicon, the prototypical semiconductor, as depicted in figure 1.19. With increasing donor density, the free carrier mobility drops steeply. Similar trends can be found in almost any semiconducting material, which is why this material class is not suitable for high-quality mid-IR plasmonics.

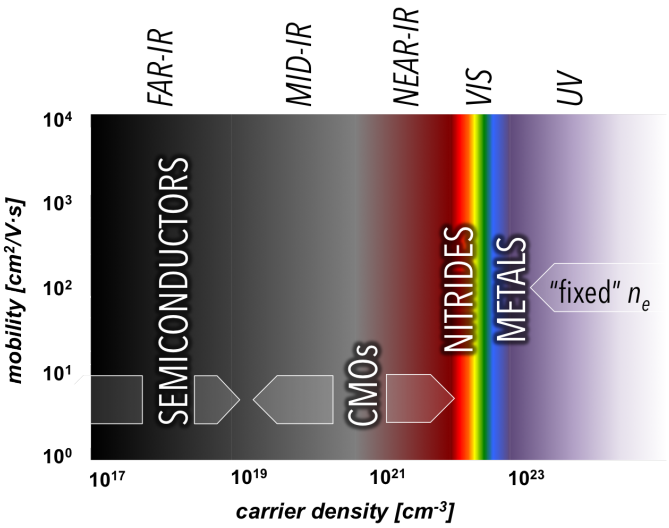

Figure 1.18 The plasmon material spectrum populated with material classes. The ranges in terms of free carrier concentration that can be accessed by several classes of materials is indicated.

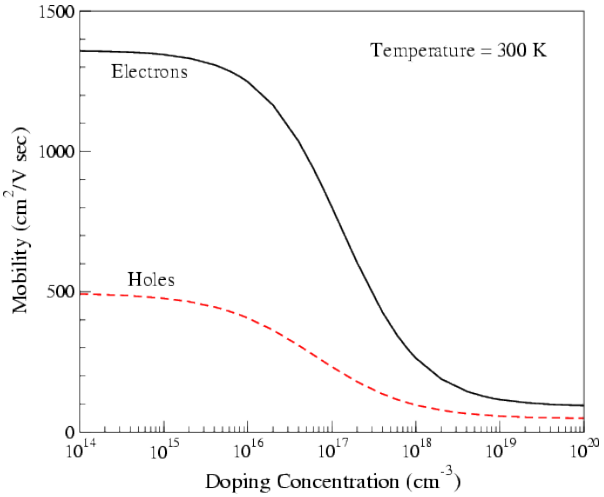

Figure 1.19 Room-temperature mobilities of electrons and holes in Si as a function of dopant concentration.

If we consider the higher energy range of the plasmon material spectrum as depicted in fig. 1.18, we find the metals. Metals have the highest free carrier concentration of any material, about 1 electron per atom ($\sim 10^{23}$ cm^{-3}). This allows them to be excellent hosts for UV[51,52] and VIS plasmonics. Some metals can also be used for near-infrared plasmonic applications. However,the carrier concentration cannot be sufficiently lowered to support mid-IR plasmonics. Similar properties can be found with metallic nitrides, such as TiN. The carrier concentration supports near-IR to VIS plasmonics[53,54], but cannot be lowered to sufficiently low concentrations.

Patterned metal surfaces can exhibit mid-IR plasmonics, so-called *spoof-plasmons*[55–58]. Unfortunately, the SPPs supported by these structures are extremely lossy and the structures are difficult to fabricate, and thus not applicable towards mid-IR technologies.

Emerging 2D materials, such as graphene or MoS_2 are promising candidate materials for plasmonic applications over a wide range of the electromagnetic spectrum, with potential applications reaching from the ThZ-region to VIS light energies[59–62]. As of now, research into this new class of materials is still nascent and the potential for mid-IR plasmonics can not be evaluated at this point in time. Recent observations indicate, that optical damping pathways in 2D materials might limit the performance for the mid-IR[63,64].

This leaves us with the material class depicted in figure 1.18, conductive metal oxides (CMOs), that support the necessary carrier concentration range to access mid-IR energies.

1.6 Surface Plasmon Polaritons in Conductive Metal Oxides

Conductive metal oxides are a doped metal oxides, whose conductivity arises either through intrinsic defect formation, such as the formation of oxygen vacancies, or through intentional doping with impurities. These materials can be highly doped (up to $\sim 10^{22}$ cm^{-3}) and are thus ideal candidates for mid-IR plasmonic. Furthermore, since the free carriers within the CMOs are arise due to doping, their plasma frequency can be tuned, by controlling the concentration of dopants. This is adding additional functionality over metallic systems who's carrier concentrations are mostly fixed as a material property.

A large number of publications can be found on a variety of materials, indicating the broad interest and potential applicability of these materials towards mid-IR plasmonics. Indium Tin Oxide (ITO) is probably the best investigated CMO material that can support surface plasmon resonance in the IR[65–67]. Doped variants of ZnO, using either aluminum (AZO) or gallium (GZO) as n-type dopants, are also well investigated plasmonic host materials[68–71]. Multilayer structures comprised of metal oxides also exhibit infrared plasmon resonance[72]. Unfortunately, all investigated oxide materials to-date, share a similar property trend as highly doped semiconducting materials: The free carrier mobilities are very modest, severely limiting the potential for low loss plasma oscillations in the mid-IR[73,74]. This is where the focus of this thesis ties in. It is supposed to present a fundamental investigation into whether we can

use material science, structure-property relations, to maintain the advantageous properties of CMOs, such as the tunability of the free carrier concentration, and increase the carrier mobility to levels that will enable low-loss mid-IR surface plasmon resonance.

1.7 Derivation

For completeness of this introduction, a brief derivation for the dispersion relation of a SPP propagating along a metal/dielectric boundary is presented. The derivation is guided by[75] and[76]. A complete derivation can be found in[16] and[77].

Without current or charge, Maxwell's equations are:

$$\nabla \cdot \mathbf{E} = 0 \tag{1.12}$$

$$\nabla \cdot \mathbf{B} = 0 \tag{1.13}$$

$$\nabla \times \mathbf{E} = -\frac{\partial \mathbf{B}}{\partial t} \tag{1.14}$$

$$\nabla \times \mathbf{B} = \mu_0 \mu \epsilon_0 \epsilon \frac{\partial \mathbf{E}}{\partial t} \tag{1.15}$$

Additionally:

$$\mathbf{D} = \epsilon_0 \epsilon \mathbf{E} = \epsilon_0 \mathbf{E} + \mathbf{P} \tag{1.16}$$

$$\mathbf{B} = \mu_0 \mu \mathbf{H} = \mu_0 \mathbf{H} + \mu_0 \mathbf{M} \tag{1.17}$$

Setting $\mu = 1$, taking the curl of 1.14 and combining with 1.15 the field equations can be found:

$$\nabla \times \nabla \times \mathbf{E} = \mu_0 \epsilon_0 \epsilon \frac{\partial^2 \mathbf{E}}{\partial t^2} \tag{1.18}$$

$$\nabla \times \nabla \times \mathbf{B} = \mu_0 \epsilon_0 \epsilon \frac{\partial^2 \mathbf{B}}{\partial t^2} \tag{1.19}$$

Introducing a vector identity:

$$\nabla \times \nabla \times \mathbf{A} = \nabla \nabla \cdot \mathbf{A} \nabla^2 \mathbf{A} \tag{1.20}$$

Which is used in 1.18 and 1.19 to get:

$$\nabla \nabla \cdot \mathbf{E} \nabla^2 \mathbf{E} = -\mu_0 \epsilon_0 \epsilon \frac{\partial^2 \mathbf{E}}{\partial t^2} \tag{1.21}$$

$$\nabla\nabla\cdot\mathbf{B}\nabla^2\mathbf{B} = -\mu_0\epsilon_0\epsilon\frac{\partial^2\mathbf{B}}{\partial t^2} \tag{1.22}$$

The speed of light is $c = \epsilon_0\mu_0^{-\frac{1}{2}}$,

$$\nabla\nabla\cdot\mathbf{E}\nabla^2\mathbf{E} = -\frac{\epsilon}{c}\frac{\partial^2\mathbf{E}}{\partial t^2} \tag{1.23}$$

$$\nabla\nabla\cdot\mathbf{B}\nabla^2\mathbf{B} = -\frac{\epsilon}{c}\frac{\partial^2\mathbf{B}}{\partial t^2} \tag{1.24}$$

Using Fourier transform to convert from time and space domains into radial frequency and wavevector domain:

$$\nabla \rightarrow \imath\mathbf{k} \tag{1.25}$$

$$\frac{\partial}{\partial_t} \rightarrow \imath\omega \tag{1.26}$$

The resulting wave equations are now:

$$-\mathbf{k}\,\mathbf{k}\cdot\mathbf{E} + k^2\mathbf{E} = \epsilon\frac{\omega^2}{c^2}\mathbf{E} \tag{1.27}$$

$$-\mathbf{k}\,\mathbf{k}\cdot\mathbf{B} + k^2\mathbf{B} = \epsilon\frac{\omega^2}{c^2}\mathbf{B} \tag{1.28}$$

We are looking for a transverse wave, where $\mathbf{k}\cdot\mathbf{E} = 0$ and $\mathbf{k}\cdot\mathbf{B} = 0$. The resulting wave equations are:

$$k^2\cdot\mathbf{E} = \epsilon\frac{\omega^2}{c^2}\mathbf{E} \tag{1.29}$$

$$k^2\cdot\mathbf{B} = \epsilon\frac{\omega^2}{c^2}\mathbf{B} \tag{1.30}$$

which can be generalized as:

$$k^2 = \epsilon\frac{\omega^2}{c^2} \tag{1.31}$$

This represents the generalized dispersion relation for transverse waves in dielectric media. To find if such a wave can exist at the interface of a meta and a dielectric, we define a geometry in figure 1.20:

Additionally, the following boundary conditions are applied:

$$\mathbf{D}_{\perp A} - \mathbf{D}_{\perp B} = 0 \tag{1.32}$$

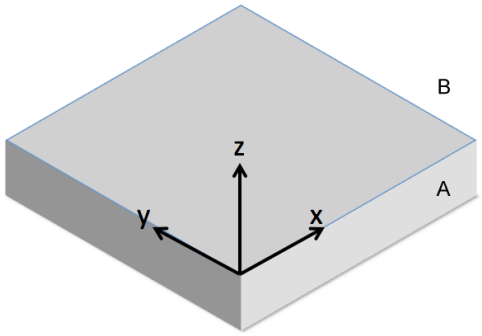

Figure 1.20 Schematic of the coordinate system used along a metal/dielectric boundary

$$\mathbf{E}_{\parallel A} - \mathbf{E}_{\parallel B} = 0 \tag{1.33}$$

$$\mathbf{B}_{\perp A} - \mathbf{B}_{\perp B} = 0 \tag{1.34}$$

$$\mathbf{H}_{\parallel A} - \mathbf{H}_{\parallel B} = 0 \tag{1.35}$$

For a transverse wave propagating along the interface A/B we can then formulate:

$$E_{zA} = -H_{ya}\frac{k_x}{\omega\epsilon_0\epsilon_A} \tag{1.36}$$

$$E_{zB} = -H_{yB}\frac{k_x}{\omega\epsilon_0\epsilon_B} \tag{1.37}$$

$$E_{xA} = H_{yA}\frac{k_{zA}}{\imath\omega\epsilon_0\epsilon_A} \tag{1.38}$$

$$E_{xB} = -H_{yB}\frac{k_{zB}}{\imath\omega\epsilon_0\epsilon_B} \tag{1.39}$$

Applying the boundary conditions 1.32-1.35:

$$E_{xA} = E_{xB} \tag{1.40}$$

$$H_{yA} = H_{yB} \tag{1.41}$$

and

$$\frac{\epsilon_A}{k_{zA}} = -\frac{\epsilon_B}{k_{zB}} \tag{1.42}$$

This implies that either ϵ_A or ϵ_B need to be negative, thus one of the materials at the interface needs to be metallic ($\epsilon < 0$) at the frequency range of interest. If we now apply the wave equation 1.29 to the electric field expression for the interface materials

$$\mathbf{E}_A = (E_{xA}\hat{x} + E_{zA}\hat{z})e^{-\imath\omega t + \imath k_x x - k_{zA} z} \tag{1.43}$$

$$\mathbf{E}_B = (E_{xB}\hat{x} + E_{zB}\hat{z})e^{-\imath\omega t + \imath k_x x - k_{zB} z} \tag{1.44}$$

we find:

$$k_{zA}^2 \mathbf{E}_A - k_x^2 \mathbf{E}_A = \epsilon_A \frac{\omega^2}{c^2} \mathbf{E}_A \tag{1.45}$$

$$k_{zB}^2 \mathbf{E}_B - k_x^2 \mathbf{E}_B = \epsilon_B \frac{\omega^2}{c^2} \mathbf{E}_B \tag{1.46}$$

With equation 1.42 we find:

$$k = k_{SPP} = \frac{\omega}{c} \sqrt{\frac{\epsilon_A \epsilon_B}{\epsilon_A + \epsilon_B}} \tag{1.47}$$

This is the dispersion relation for a Surface Plasmon Polariton (SPP), a standing wave existing at the interface of materials with the optical properties ϵ_A and ϵ_B.

Chapter 2

Experimental Details

This chapter will summarize experimental techniques and parameters that have been used throughout this work. A description of all simulation techniques used can be found in chapter 3.

2.1 Pulsed Laser Deposition (PLD)

2.1.1 Target Preparation

Ceramic PLD target were prepared using a powder route. Metal oxide powders for ZnO- (Alfa Aesar, 99.99+ % trace metal basis) and CdO-Targets (Sigma Aldrich, 99.99+ % trace metal basis) were pressed into a 1.25 inch metal die at 16000 psi using a pneumatic laboratory press. The pressed ZnO pellets were then sintered in Air using a Sentro Tech box furnace at 1250°C for 12h (initial ramp rate 15°C/min). The resulting 1 inch targets exhibited 97% theoretical density ($\rho_{ZnO} = 5.61$ g/cm^{-3}).
The pressed CdO pellets were sintered using a Lindberg controlled atmosphere tube furnace. Throughout the sintering process, the target was held under an atmosphere of 100 % O_2 with a flow of 10 mm^3/sec. The sintering temperature was 700°C held for 8 hours with an initial ramp rate of 10°C/min. *The exhaust gases were directed into the adjacent laboratory hood using teflon tubing.* The resulting 1 inch targets exhibited 98 % theoretical density ($\rho_{CdO} = 8.15$ g/cm^{-3}). Figures 2.1 and 2.2 depict typical XRD scans of the resulting targets.

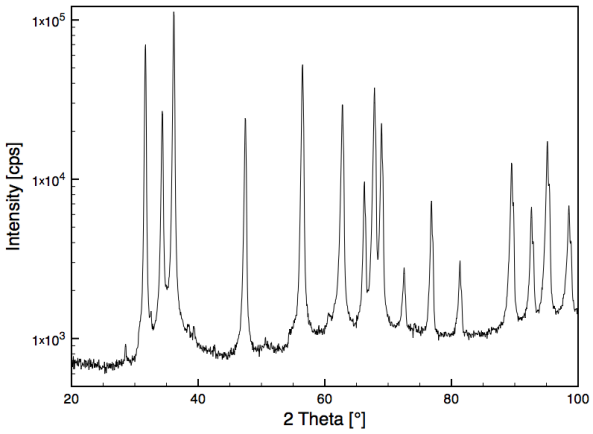

Figure 2.1 XRD of a typical ZnO target

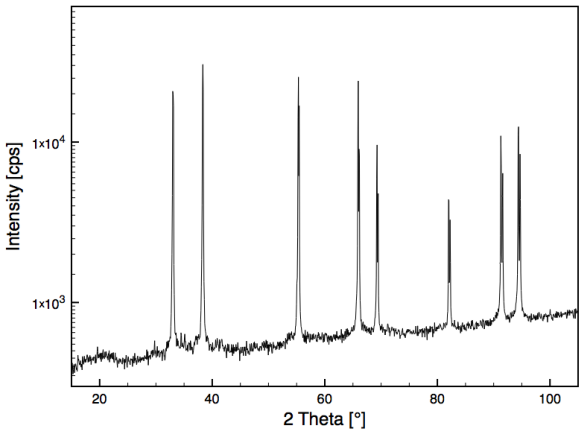

Figure 2.2 XRD of a typical CdO target

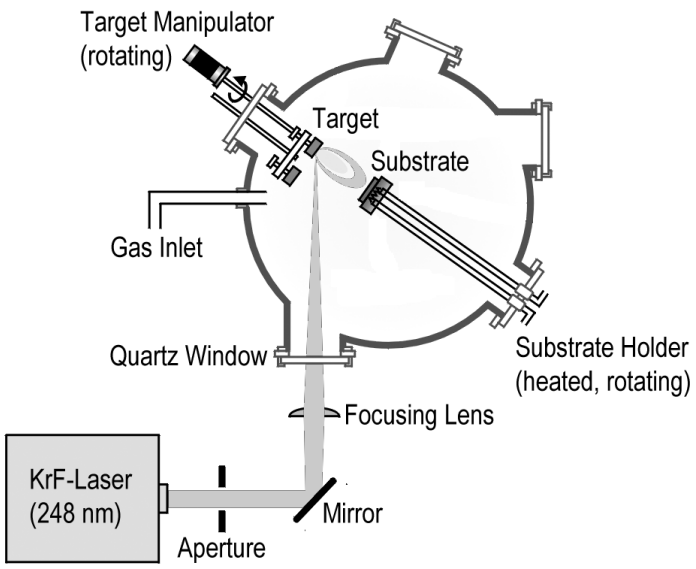

Figure 2.3 Schematic of the PLD system used for this work

2.1.2 PLD-System

PLD depositions were carried out using a custom build PLD deposition chamber. A Coherent Compex Pro 102F KrF laser with a wavelength of 248 nm was used for ablation. Figure 2.3 depicts a schematic of the deposition system. The target carousel can hold up to five targets that can be selected *in-situ*. The target is continuously rotated during ablations. The heated substrate holder rotates continuously ±360°.
Prior to deposition, the respective substrates were mounted on the target manipulator using silver paint which was dried in air at 80°C. The mounted targets on the manipulator were then introduced into the system and the deposition chamber was evacuated to a base pressure of $<1\text{x}10^{-5}$ Torr.

2.1.3 PLD-Deposition

2.1.3.1 ZnO

For ZnO deposition, typical parameters used where:

Substrate temperature 600-750°C

Target substrate distance 55-100 mm

Background O_2 pressure 1-100 mTorr

Laser energy density 0.6-1.2 J/cm^2

Pulse repetition rate 3-10 Hz

2.1.3.2 CdO

For CdO deposition, typical parameters used where:

Substrate temperature 300-500°C

Target substrate distance 55-100 mm

Background O_2 pressure 10-30 mTorr

Laser energy density 1.5 J/cm^2

Pulse repetition rate 10 Hz

At substrate temperatures above 500°C, evaporation would occur, and no film growth could be observed.

2.2 Molecular Beam Epitaxy (MBE)

All MBE growth for this work was carried out using a Perkin-Elmer 435 MBE. Figure 2.4 depicts a schematic of the deposition system. Three metal effusion sources were available for Mg, Cd and Dy (doping effusion cell) with individual PID temperature control. Oxygen could be supplied either as molecular oxygen or from a custom built inductively coupled, radio frequency plasma source (RF-ICP source) for increased oxygen activity. A schematic of the ICP source can be seen in figure 2.5. Samples were mounted on a Mo puck for deposition and substrate temperature was controlled using a infrared pyrometer aimed at the puck center.

2.2.1 Sample Preparation

Prior to deposition, single crystal substrates were cleaned with the following procedure: Rinse in solvents with decreasing polarity, DI Water/Acetone/Ethanol/Methanol. For hygroscopic substrates, the water was omitted. Following the rinse, the samples where cleaned for 10 minutes using a UV-Ozone sample cleaner. The substrate where then mounted on a Mo puck using a very thin, continuous layer of silver paint. Following the sample mounting, the puck was heated to 140°C for 20 minutes on a hot plate to dry the silver paste.
The hot puck was then transferred into the load lock of the MBE system and immediately pumped down. After reaching a load lock pressure of $<1x10^{-7}$ Torr the sample was transferred into the growth chamber.

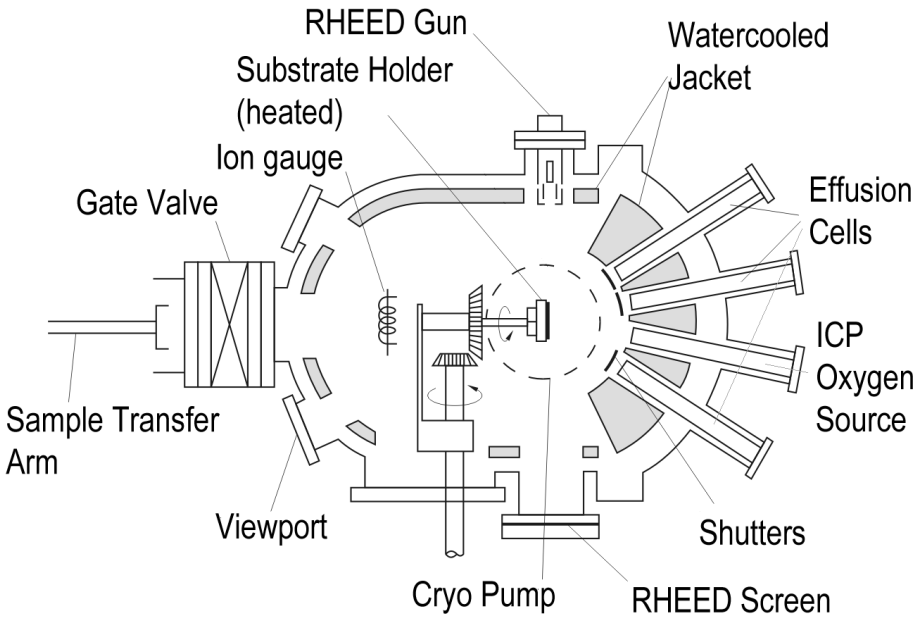

Figure 2.4 Schematic of the MBE deposition system

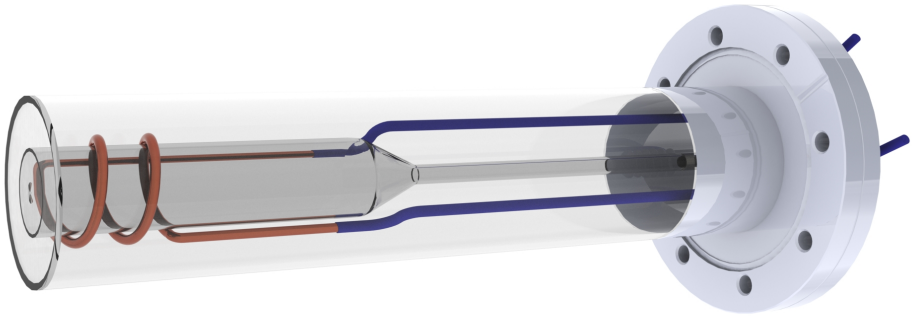

Figure 2.5 Schematic of the custom built RF-ICP Oxygen source used for this work

2.2.2 MBE-Deposition

For plasma assisted growth, the ICP-source was started as first step. To strike the plasma, the O_2 pressure was raised to 1x10^{-5} Torr. At this pressure, turning the RF generator on will result in a faint, capacitavely coupled, oxygen plasma. After adjusting the load/tune on the RF matching unit for highest possible forward power, lowering the oxygen pressure will strike an inductively coupled plasma. The plasma can be run with 230W forwards power with the reflecting power <10 W. Accessible deposition pressures when using the ICP source range from 6x10^{-7}-1x10^{-5} Torr.
After a stable plasma emission is reached, the effusion cells and the sample heater where brought to deposition temperature, with the effusion cell shutters remaining closed. Upon reaching stable cell- and substrate-temperatures (within ±1°C), the shutters were opened to initiate growth.
For non plasma assisted growth, the start-up procedure for the ICP source was omitted and the effusion cells and the substrate could be brought up to temperature right after sample puck transfer.
Typical deposition parameters for CdO:Dy growth used for this work:

Substrate temperature 200-500°C

Cd-Cell temperature 200-240°C resulting in a calculated Cd flux of 2-5x10^{13} (at cm^2 s^2)

Dy-Cell temperature 900-1100°C resulting in a calc. Dy flux of 1x10^8 to 3.5x10^{12} (at cm^2 s^2)

Mg-Cell temperature 280-360°C resulting in a calculated Mg flux of 0.5-6x10^{13} (at cm^2 s^2)

Background O_2 pressure 1-5x10^{-6} Torr

ICP-source RF power 200-250 W resulting in a atomic O-flux of 0.8-1.2x10^{14} (at cm^2 s^2)

For non-oxide substrates such as GaN, GaAs or Si, the substrate temperature was held <300°C to avoid evaporation off of the heated substrates during growth. Typical CdO growth rates observed where 0.9 nm/min. Growth rates where monitored using a quartz crystal monitor (QCM), however this method proved to be unreliable for plasma assisted growth. Consequently, growth rates where backed out from film thicknesses measured using either (depending on thickness) profilometry or x-ray reflectivity.

2.3 Sample Characterization

2.3.1 X-ray Diffraction (XRD)

X-ray diffraction experiments were carrier out using a Panalytical Empyrean Platform with multiple available optics. Bragg-Brentano diffraction data for phase identification was recorded

using a programmable divergence slit incidence beam optic with a 1-D strip detector as receiving optic. Single crystal diffraction and diffraction of epitaxial thin films was recorded using a parallel beam configuration with either a Goebel-mirror or a double bounce hybrid monochrometer on the incidence beam side. A parallel plate collimator (PPC, 0.18°) with a Xe-proportional counter was used on the receiving side for parallel beam measurements. For rocking curves, the proportional counter was mounted on a rocking curve attachment.
X-ray reflectivity data was recorded using either of the parallel beam options and data analysis was carried out using Panalytical Reflectivity software.

2.3.2 Atomic Force Microscopy (AFM)

AFM data was recorded using an Asylum MFP-3D AFM. Si AFM tips (Aspire, conical 300 kHz, 40 N/m) were used to record height and phase surface data in tapping mode.

2.3.3 Scanning Electron Microscopy (SEM)

High resolution SEM images were recorded using a FEI VERIOS field emission scanning electron microscope. Typical operating settings were a working distance of 4 mm, a beam acceleration voltage of 1kV and current of 1 pA. The stage bias was typically varied between 0.5-2 kV.

2.3.4 Transport Measurements

Room-temperature transport data were measured with the Van-der-Pauw technique using an Ecopia HMS-3000 Hall Measurement System. Temperature-dependent transport measurements were carried out using a custom-built transport probe in a Quantum Design PPMS. For temperature dependent Hall data, the Ecopia HMS-3000 system was interfaced with the PPMS, by connecting the pin-outs of the PPMS sample holder to the Ecopia interface. In this configuration, the PPMS was used to control the temperature and magnetic field, whereas the software of the Ecopia HMS-3000 was used to record the Hall data and calculate the transport properties.

2.3.5 Ellipsometry

To record variable angle, spectroscopic ellipsometry data (VASE), a Woollam VASE and IR-VASE have been used to record UV-VIS and IR VASE data respectively. For modeling and data analysis, Woollams WVase-software has been used.

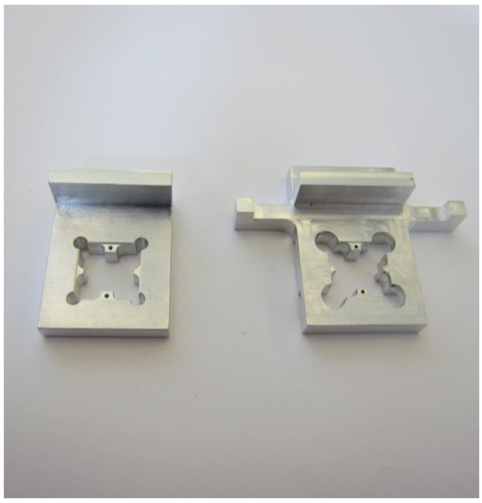

Figure 2.6 Custom sample holders for SPR Spectroscopy to be used on the sample stage of a IR-VASE.

2.3.6 Surface Plasmon Resonance Spectroscopy

To record IR-reflectivity data in the Kretschmann configuration, the IR-VASE has been modified with a custom sample stage. The design went trough multiple iterations that enhanced the SPR capabilities and added functionality. The simplest setup comprises of an aluminum sample holder with a cutout to accommodate 1x1 cm thin film samples.
Figure 2.6 depicts two of the sample holder geometries developed for this work. The central cutout allows for the placement of a 1x1 cm sample, with the metallic film facing down. The sample can then be covered with a prism (CaF_2). To ensure good optical contact, an index matching fluid (Cargille Series M 1.720) needs to be applied between the sample and the prism. The assembly can then be mounted on the IR-VASE sample stage using a Thorlabs prism holder (PM4/M) attached to the stage. Figure 2.7 depicts the mounted assembly. Once secured on the sample stage, the IR-VASE can be aligned to the sample, through the prism, and reflectivity data can be recorded as a function of angle and energy. Figure 2.8 depicts the mounted assembly and indicates the experimental beam path (dotted red) in the Kretschmann configuration.

Further functionality was added by designing a flow cell sample holder. This design allows to expose the SPR sample to controlled atmospheres. Figure 2.9 depicts the SPR flow cell holder mounted on the IR-Vase sample stage. Technical drawings off all custom designed parts can be found in Appendix A. Experimentally collected data was exported using WVASE software and compiled into tabulated data of polarization dependent reflectance vs. wavelength. Data processing and plotting of reflectivity maps was performed using Wolfram

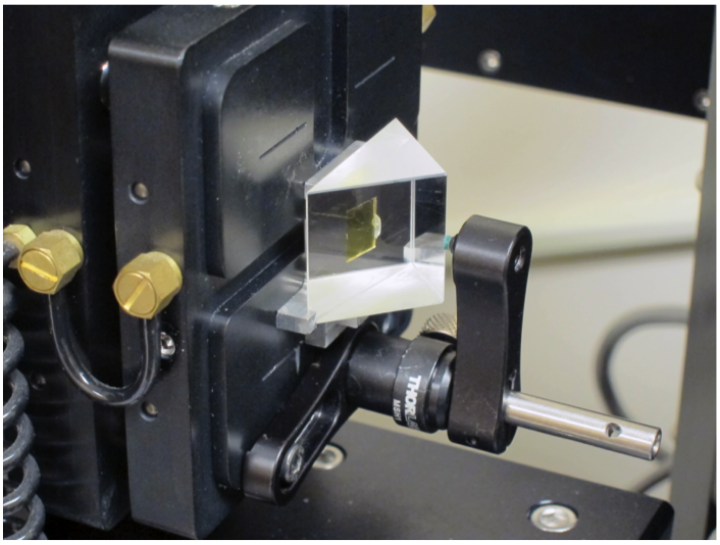

Figure 2.7 Custom SPR stage mounted on IR-VASE sample stage to record SPR data. The sample can be seen in orange through the prism, together with a drop of index matching fluid.

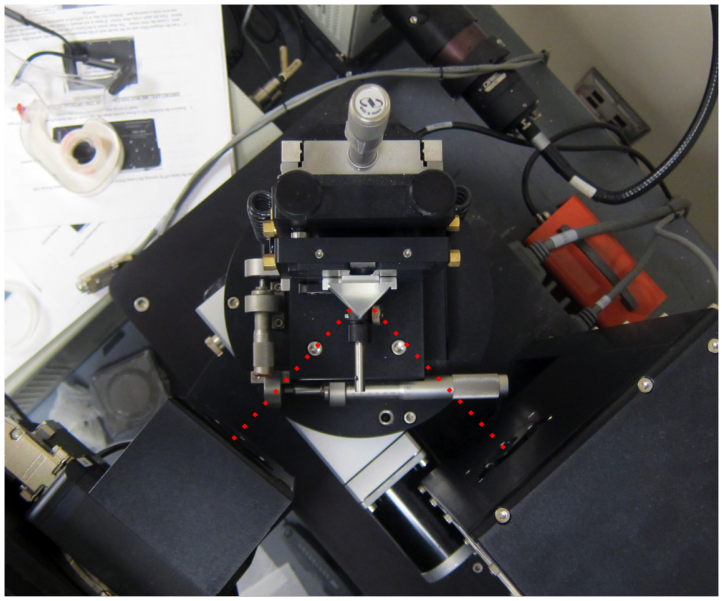

Figure 2.8 Beam path for an SPR experiment using the IR-VASE; the beam path is indicated as a red-dotted line. The source and detector are mounted on a goniometer, allowing to vary the incident angle of the probe light and the detector position.

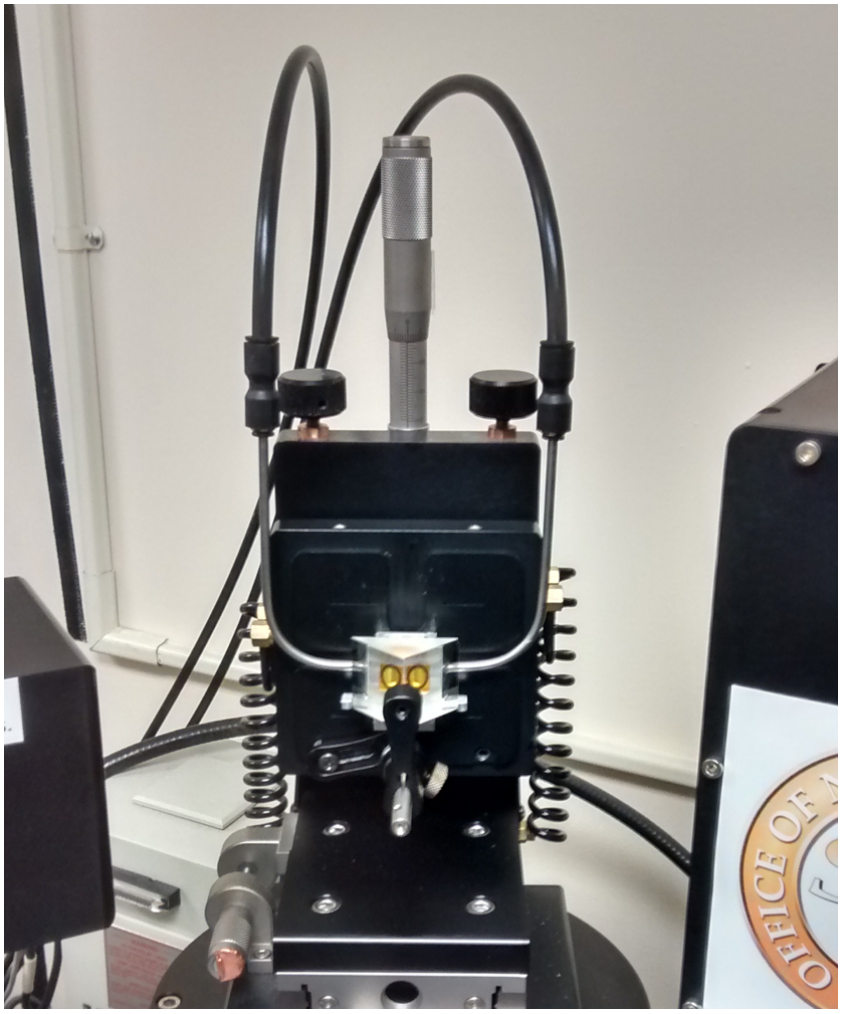

Figure 2.9 Custom built SPR Flow Cell mounted on the IR-VASE sample stage. The gas lines running from the top allow to expose the SPR sample to controlled atmospheres.

Mathematica.

Chapter 3

Modeling

For this work it proved to be of importance to develop a reliable modeling scheme that can predict the optical/plasmonic properties of thin films and their optical response in the conducted experiments. In order to plan experiments efficiently, it proved to be valuable to be able to predict the optical/plasmonic properties of the studied material system. Doing so allowed for efficient planning of experiments and fast realization of targeted sample characteristics. Furthermore, modeling experimental data was exceedingly helpful in interpreting and understanding the optical behavior of novel plasmonic materials. All modeling was performed using Wolfram Mathematica. The code written for this work is available in the Appendix (B).

3.1 The Drude Model

Throughout this work, we used the Drude formalism to describe the dielectric properties of plasmonic materials for the mid-IR. It has been shown, that this approach is accurate for degeneratively doped semiconductors[65,73,78–80]. Using this formalism, the dielectric properties of any material can be described according to equation 3.1 and 3.2.

$$\epsilon_1 = \epsilon_\infty - \frac{\omega_p^2}{\omega + \gamma^2} \tag{3.1}$$

$$\epsilon_2 = \frac{\gamma \omega_p^2}{\omega(\omega + \gamma^2)} \tag{3.2}$$

with

$$\omega_p^2 = \frac{nq^2}{m_{eff}\epsilon_0} \tag{3.3}$$

and

$$\gamma = \frac{q}{\mu m_{eff}} \tag{3.4}$$

ϵ_∞ High frequency dielectric constant

ω_p Plasma frequency

γ Damping term

n Free carrier concentration

q Electron charge

m_{eff} Effective electron mass

ϵ_0 Permittivity of free space

μ Free carrier mobility

This model allows to describe the dielectric properties of any material with only four input parameters: The free carrier concentration n, the electron mobility μ, the high frequency dielectric constant ϵ_∞ and the effective mass of the free carriers m_{eff}. These parameters are readily available for most semiconducting materials, or can be measured through a combination of Hall-effect measurements and ellipsometry. Therefore, this model allows to describe the dielectric properties of prospective plasmonic materials and simulate their plasmonic response. In this way, an initial screening of materials can be done without the need to invest time into developing and optimizing growth methods.
It is important to note, that the Drude model does not capture the dielectric functions of materials accurately over the entire electromagnetic spectrum. Especially at higher energies, at UV-VIS frequencies, the model is unable to describe electronic transition phenomena and other physical processes that change the dielectric response at frequencies above the IR-bands. However, for the scope of this work, which focuses on the infrared portion of the electromagnetic spectrum, it is an accurate description of the optical properties of semiconductors and has been successfully used to describe the optical properties of semiconductors with free carrier concentrations ranging from $1.0\text{x}10^{19}$-$1.0\text{x}10^{21}$ cm^{-3} .
If we consider a generic material with a given n, μ, m_{eff} and ϵ_∞ we can plot the dielectric function with it's real and imaginary components as depicted in fig. 3.1. From this figure, we can infer the important characteristics of the Drude dielectric function. The real part (solid) steadily decreases with decreasing energy, with a characteristic point where the sign

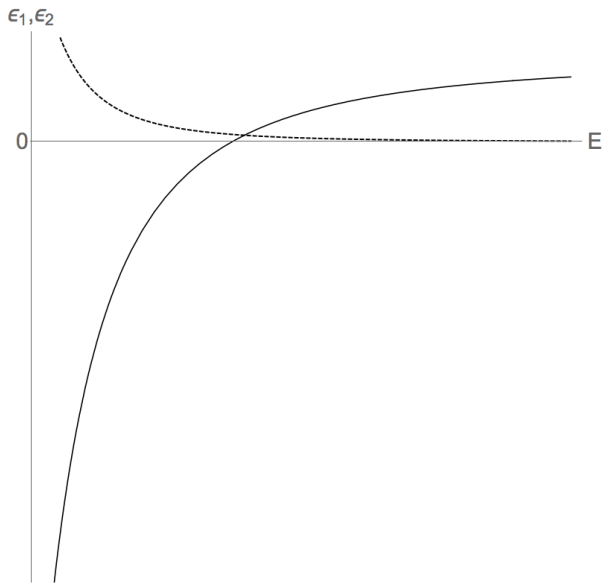

Figure 3.1 Example of a Drude dielectric function; The real part (solid) and imaginary part (dashed) are shown as a function of energy.

of ϵ_1 changes from positive to negative, the *cross-over frequency*. At energies lower than this characteristic energy, the real part of the dielectric function falls steeply. This is the energy range of interest for plasmonics. At energies above the cross-over frequency, the material does not support any plasmonic oscillations.
The imaginary part (dashed), also called the loss tangent, follows a different trend. The loss is generally low at energies above the cross-over frequency, and exponentially increases for energies below the cross-over of ϵ_1. This describes the major challenge for plasmonic materials: A material that supports plasmons ($\epsilon_1 < 0$) is inherently lossy, if the dielectric function follows the Drude formalism.
To understand how the Drude dielectric functions depend on the material properties, we can vary the input parameters individually and compare the resulting dielectric functions. The resulting dielectric functions are depicted in figure 3.2. In panel 3.2a we can see the resulting dielectric functions upon variation of the free carrier concentration. An increase in n shifts the cross-over frequency of ϵ_1 towards higher energies. This reveals one of the major advantages of semiconductors as plasmonic materials. Since we can vary the free carrier concentration in semiconductors via doping, the cross-over frequency becomes tunable. Thus, the energies at which plasmonic behavior can occur ($<$ cross-over frequency) can be varied, the material's plasmonic behavior can be tuned in energy space by varying the free carrier concentration.
If we consider variation of the free carrier mobility (fig. 3.2b), we can see that variation of the

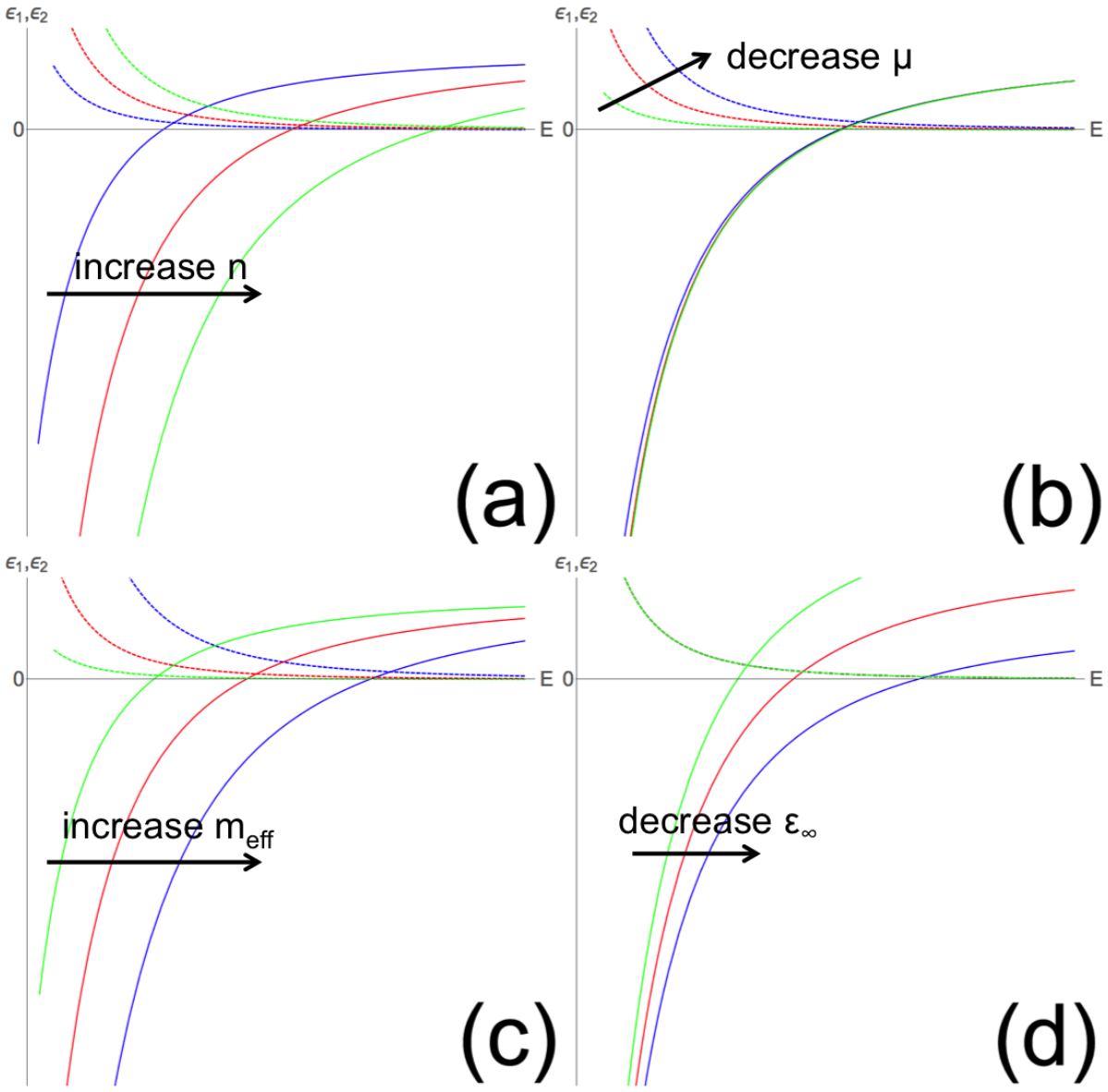

Figure 3.2 The effect of material properties on the resulting Drude dielectric functions. a) variation of the free carrier concentration n b) variation of the free carrier mobility μ c) variation of the carrier effective mass m_{eff} d) variation of the high frequency dielectric constant ϵ_∞

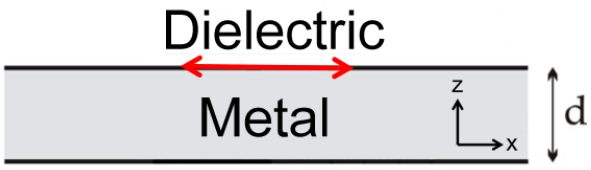

Figure 3.3 2D representation of the model system.

mobility does not affect ϵ_1. It does however strongly influence the resulting loss tangent ϵ_2. With increasing mobility, the loss function decreases with respect to the cross-over energy. This implies, that for a given carrier concentration, high carrier mobility will always result in a lower loss tangent and is therefor generally desirable for a plasmonic host material.

In panel 3.2c a variation of the effective electron mass can be seen. An increasing effective electron mass has similar effects on ϵ_1 as the free carrier concentration. Higher effective masses result in a cross-over frequency that is shifted towards higher energies. There is a small effect on the loss tangent, as can be deduced from equations 3.4 and 3.2, however the effect is almost negligible when compared to the impact of the carrier's mobility.

Finally, panel 3.2d depicts a variation of the high frequency dielectric constant. From equations 3.1 and 3.2 we can see that only ϵ_1 is modified. The loss tangent remains unchanged. The real part of the dielectric function however is changed significantly. An increasing effective mass will shift the cross-over frequency towards higher energies, and will increase the rate of change of ϵ_1 when moving to lower energies. The dielectric function falls steeper through the cross-over point into negative ϵ_1 values.

In summary, we can see how the four input parameters for the Drude model shape the resulting dielectric function. In real materials, those properties are usually linked and can not always be varied independently. However, it is important to understand the influence of each individual parameter to find new plasmonic host materials and to optimize the properties for a plasmonic application.

3.2 Surface Plasmon Polariton Dispersion

In section 1.7 the derivation for a bound surface wave, the surface plasmon polariton, in a metal/dielectric interface was presented. For a thin film geometry, the problem can be reduced to 2 dimension, as the two in plane directions are equivalent, given the fact that there is no anisotropy in the thin film's dielectric properties. We can thus consider a 2-dimensional model system as depicted in figure 3.3.

From the derivation in 1.7 we understand that in order to fulfill the boundary conditions for a SPP, equation 3.5 must be fulfilled.

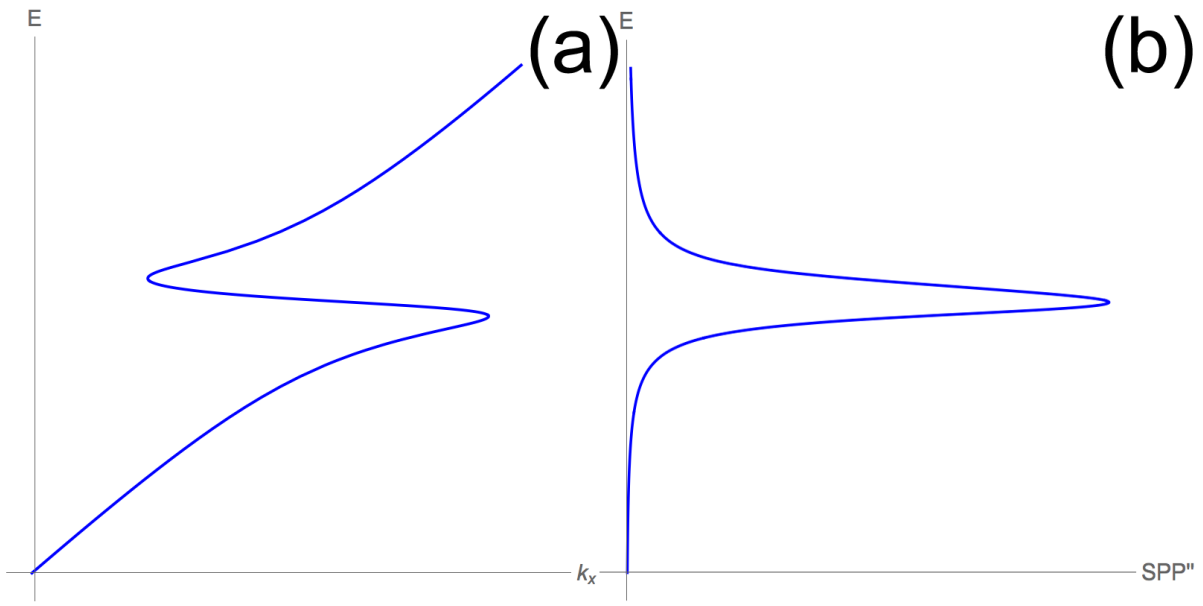

Figure 3.4 Real and imaginary part of the SPP dispersion. a) the real part of the SPP dispersion in energy wavevector space b) the imaginary part of the SPP dispersion (dimensionless).

$$\begin{pmatrix} k^2 - \frac{\omega^2}{c^2}\epsilon_{xx} & 0 & 0 \\ 0 & k^2 - \frac{\omega^2}{c^2}\epsilon_{yy} & 0 \\ 0 & 0 & \frac{\omega^2}{c^2}\epsilon_{zz} \end{pmatrix} \cdot \begin{pmatrix} E_x \\ E_y \\ E_z \end{pmatrix} = 0 \tag{3.5}$$

Since the x and y directions are identical, we can solve for k_{xx} and yield equation 3.6. This is the SPP dispersion relation.

$$k_{xx} = k_{yy} = \frac{\omega}{c}\sqrt{\frac{\epsilon_m \epsilon_d}{\epsilon_m + \epsilon_d}} \tag{3.6}$$

It can be seen, that this dispersion relation is dependent on the dielectric properties of the metal and the dielectric. The dielectric is typically non dispersive, such as air ($\epsilon = 1.00054$). The metal dielectric function however can be described using the Drude formalism described in 3.1. Since the dielectric function is a complex function, the resulting dispersion relation will also be a complex function. We can split the dispersion function into a real and imaginary part and plot the results in energy vs. in-plane wavevector (k_{xx}) space. The result is depicted in figure 3.4. In comparison to the ideal material discussed in chapter 1.3, we do not find two distinct branches in the dispersion and there is no energy gap separating the SPP and BPP dispersion. The dispersion is continuous and the two branches are connected by a lossy

region (see fig. 3.4b). This is a direct result of the non-ideality of the plasmonic material, the metal in the 2-dimensional model. It can be seen that the account for a real material, that is not lossless, adds a layer of complexity to the model, as the loss has to be treated with a complex function.

In the 2-dimensional model we considered the x- and y-directions to be identical. For the z-direction however, we have to consider a different scenario, which is depicted in figure 3.5.

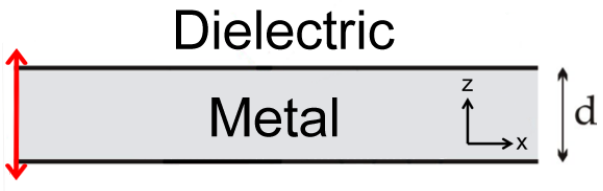

Figure 3.5 2D representation of the model system.

The approach according to equation 3.5 can be solved for k_{zz}resulting in equation 3.7.

$$\epsilon_{zz} = 0 \tag{3.7}$$

This implies, that there is another mode propagating along the z-direction, that is non dispersive. If we combine this solution with the Drude dielectric function, we find that the mode is supported right at the cross over frequency, when $\epsilon_1 = 0$. Therefor, thin films of Drude metals support an additional plasmon mode perpendicular to the thin film surface, called the screened-bulk plasmon polariton (SBPP)[66]. Figure 3.6 summarizes all possible modes for the 2-dimensional model system in energy/wave-vector space.

3.3 SPR in the Kretschmann Rather configuration

To model the coupling of radiation to one of the plasmon modes described in 3.2 using the Kretschmann configuration, the 2 dimensional model has to be extended. As mentioned in chapter 1.3, the momentum of light has to be increased in order to achieve a resonance condition with a SPP. In the Kretschmann configuration, this is done by propagating the light through a prism with a refractive index > 1. Figure 3.7 depicts a 2D schematic of the Kretschmann configuration. Light propagates through an optical denser medium (substrate) at an angle Θ_i and a wavevector k. If this angle reaches the critical angle of the substrate/thin film interface (defined by the respective refractive indices), total internal reflection is achieved and the light gets reflected at an angle Θ_r. Upon internal reflection an evanescent field is

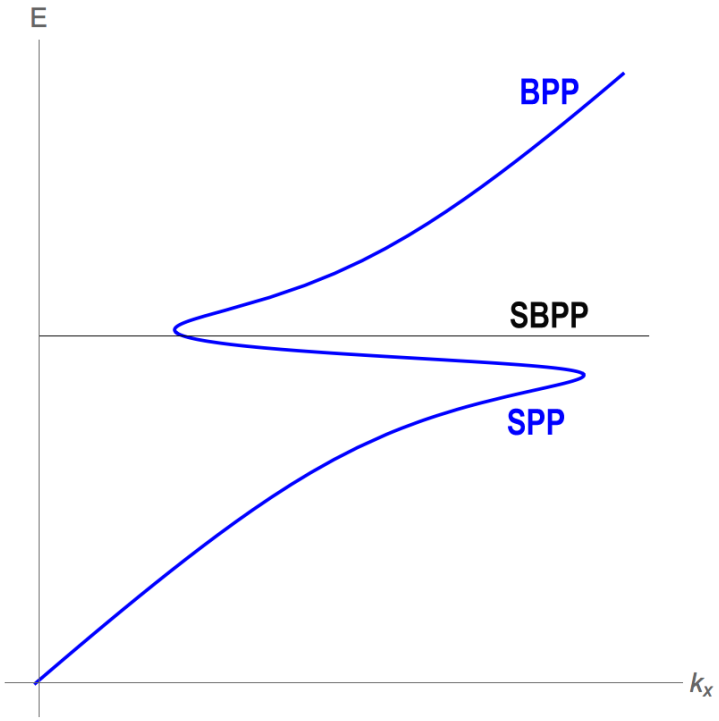

Figure 3.6 Summary of supported modes; SPP (blue) and SBPP (black) modes with their respective dispersion relations in energy/wavevector space.

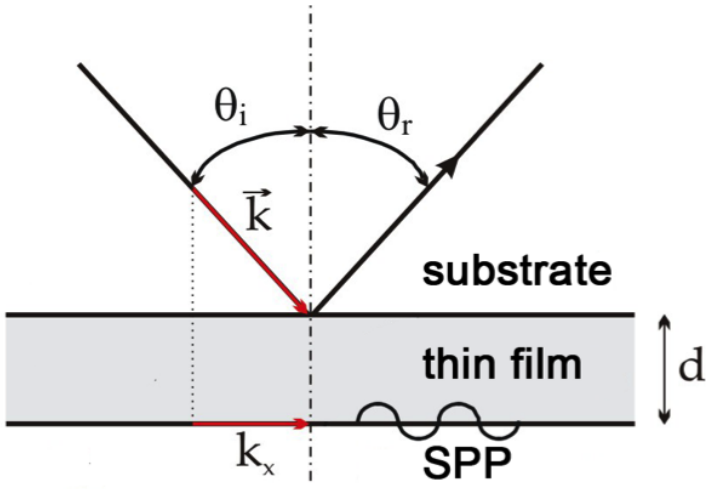

Figure 3.7 2D schematic of the Kretschmann configuration to couple light with a surface plasmon polariton supported by a thin film/dielectric interface.

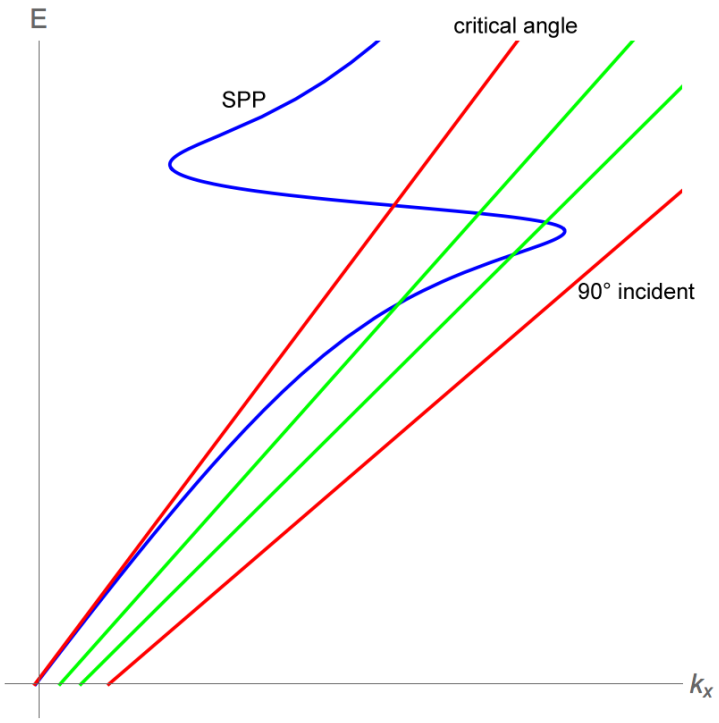

Figure 3.8 SPP dispersion plotted with examples of light lines. The red lines indicate the limit for a Kretschmann experiment, the critical angle and 90 degrees incidence. The green lightlines indicate incidence angles at which coupling to the SPP can be achieved.

created that propagates the light through the plasmonic thin film. The evanescent field has an in-plane component (k_x) that can be seen as the projection of the incoming light wave down onto the thin film surface. Varying Θ_i will vary k_x. To simulate whether we can achieve coupling of the incoming light to the SPP dispersion, we can calculate the light lines according to equation 3.8 with n being the refractive index of the substrate material.

$$\omega = \frac{ck}{n} \sin \Theta_i \tag{3.8}$$

The resulting light lines can then be plotted in the same energy/wave-vector space as the SPP dispersion. Figure 3.8 illustrates an example using the generic SPP dispersion used in fig. 3.6 by assuming a substrate refractive index of 2. The red light lines indicate the limits of Θ_i for the Kretschmann type experiment. The upper limit is the critical angle Θ_c defined by the refractive index combination of the substrate/thin film. The lower limit corresponds to 90 degrees incident angle, at which point the the light propagates parallel to the thin film. At angles $\Theta_c < \Theta_i < 90$ the light lines will intersect with the SPP dispersion, indicating that a

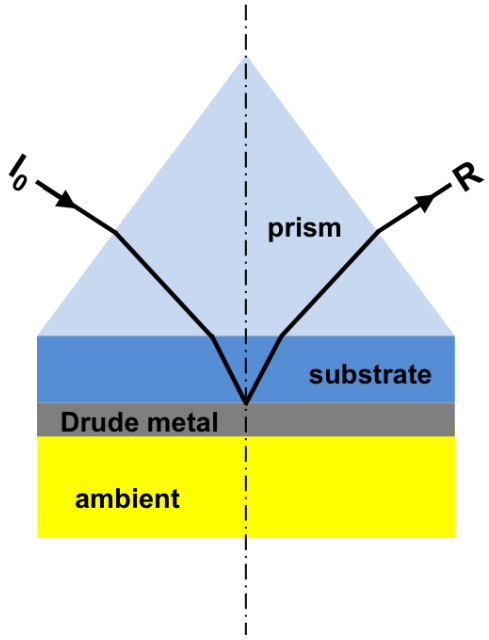

Figure 3.9 Schematic of the model system in the Kretschmann Rather configuration and its individual components.

coupling to the SPP is possible under these conditions. By varying the incident angle and energy and simultaneously monitoring the reflected light intensity, the plasmonic properties of thin films can be experimentally determined using the Kretschmann configuration.

This coupling mechanism was used in combination with an IR-VASE to extract the plasmonic properties of thin films grown for this work. The measurement procedure is described in chapter 2.3.6. Experimentally, reflectivity data is collected in angle-energy space. Therefore, the modeling was designed to compute reflectivity data in angle-energy space. Because of this, the methodology of using energy/wavevector space as simulation domain would yield results that are not directly comparable to experimental data. Even though angle and in-plane wave-vector are related, a conversion is not straight forward as the experimental beam path includes further optical elements and refraction events than the ones captured by the simple three layer model depicted in figure 3.7. By including all optical elements of the IR-VASE experiment, simulated data could be produced that is directly comparable to experimentally acquired data.

Fig. 3.9 depicts a schematic of the entire system to model. In order to yield data that is directly comparable to experimental data, the entire beam path through the experiment has to be captured in the model. The IR-beam propagates through air, enters the prism and finally

the substrate where it is totally internally reflected. The optical properties of those elements have thus to be included in the simulation and are accounted for as real and imaginary components of the respective dielectric functions over the mid-IR energy range. The materials typically used are CaF_2 or Al_2O_3 for the prism, and MgO, Al_2O_3 or GaN for the substrate material. The optical properties of the Drude metal film is described by the Drude model as a function of free carrier concentration, free carrier mobility, effective electron mass and high frequency dielectric constant. The ambient can be defined either via a constant (non-dispersive medium, typically air) or by a dielectric function (to account for absorption of gases etc.).

Once all materials are defined, the simulation calculates a ray trace from the IR-source through the prism into the substrate using Snell's law.

$$\frac{sin\Theta_1}{sin\Theta_2} = \frac{n_2}{n_1} \tag{3.9}$$

The resulting angle within the substrate is then used to calculate the reflectance of the three layer system comprising of substrate/Drude metal/environment. This can be analytically solved for p- and s- polarized light using the Airy equation[81]. The polarization dependent reflectance of a single interface is described by the Fresnel equations:

$$\text{p-polarized light: } r_p = \frac{n_i cos\Theta_i - n_t cos\Theta_t}{n_i cos\Theta_i + n_t cos\Theta_t} \tag{3.10}$$

$$\text{s-polarized light: } r_s = \frac{n_t cos\Theta_i - n_i cos\Theta_t}{n_t cos\Theta_i + n_i cos\Theta_t} \tag{3.11}$$

The total polarization dependent reflectance from the three (film/substrate/ambient) interface is then calculated for a film thickness d_f:

$$r = \frac{r_1 + r_2 exp(2ib)}{1 + r_1 r_2 exp(2ib)} \tag{3.12}$$

with

$$b = \frac{2\pi d_f}{\lambda}\sqrt{n_{film}^2 - n_{substrate}^2 sin^2\Theta_i} \tag{3.13}$$

The simulation iterates through the desired incident angle and energy range and ultimately compiles a map of reflectance vs. incidence angle. Figures 3.10-3.12 depict examples of the output for a generic material. The data can be calculated using the total reflectance defined as $R=R_p/R_s$, or as the reflectivity of the individual polarizations R_p and R_s. Using $R=R_p/R_s$ has the distinct advantage, that atmospheric and other absorptions that are present in both polarizations, cancel out and the result is a less noisy experiment.

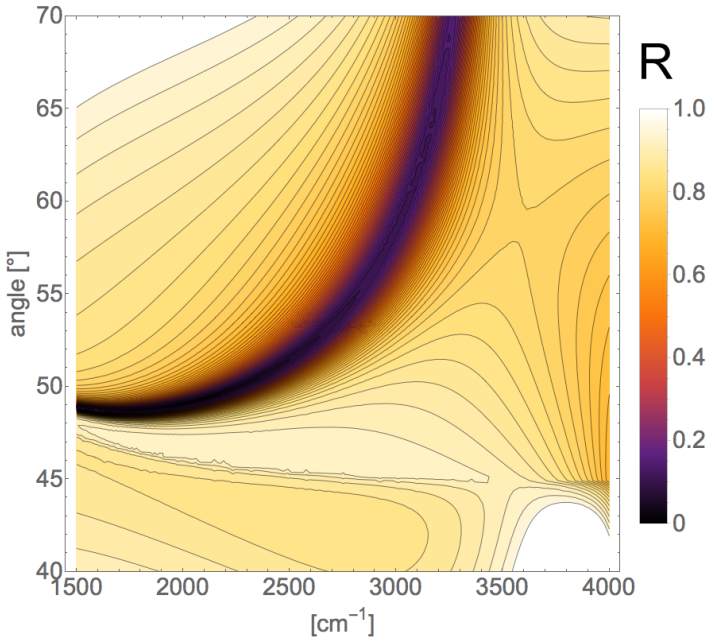

Figure 3.10 Simulated reflectivity data for an generic thin film depicting R in angle and energy space.

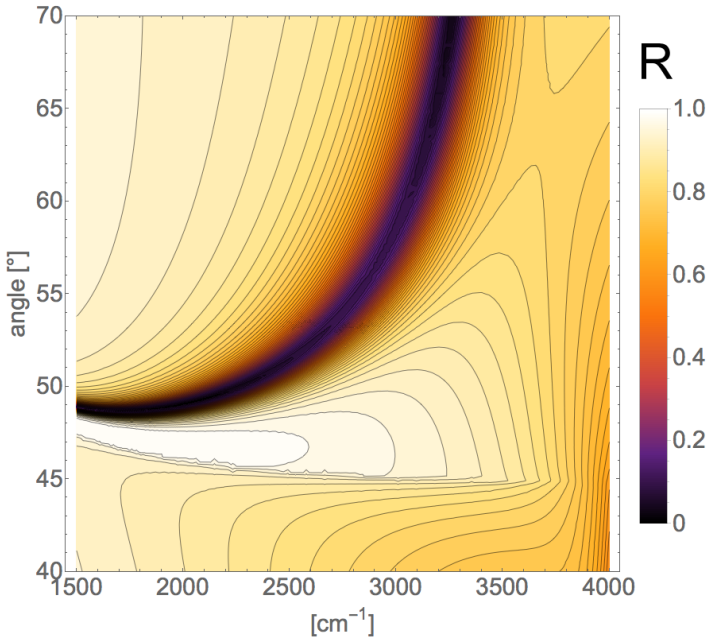

Figure 3.11 Simulated reflectivity data for an generic thin film depicting r_p in angle and energy space.

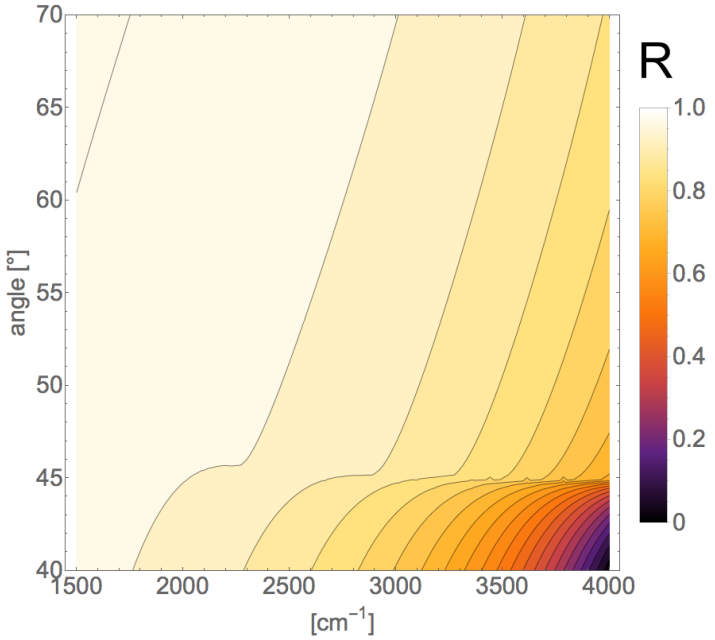

Figure 3.12 Simulated reflectivity data for an generic thin film depicting r_s in angle and energy space.

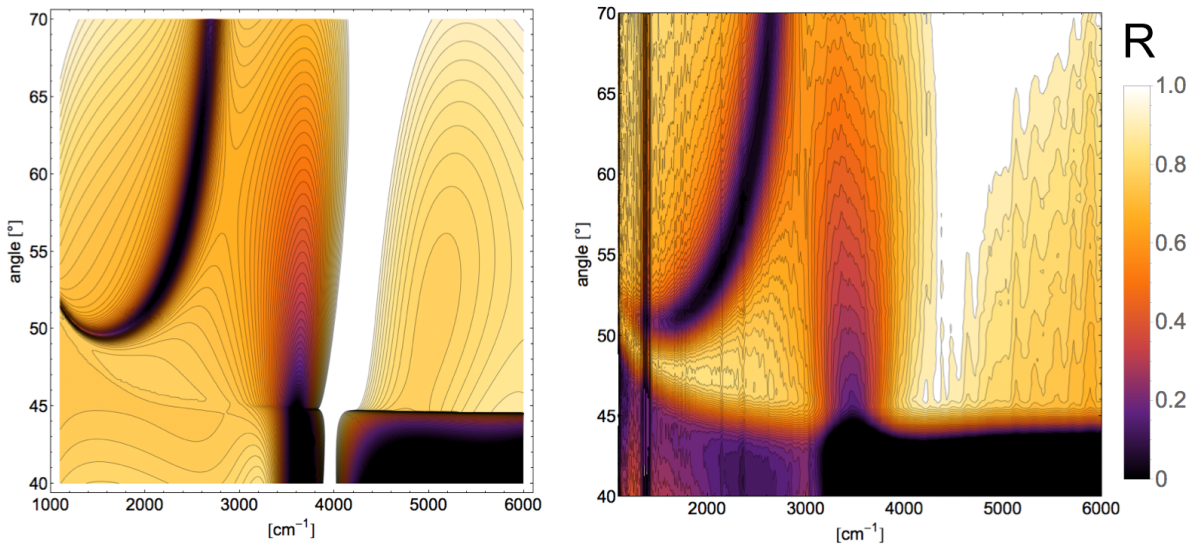

Figure 3.13 Comparison of simulated and experimental reflectivity data for a CdO thin film on MgO (100) substrate. CdO properties: d=500 nm, n=1.45x10^{20} cm^{-3} , μ=450 cm^{2}V^{-1}s^{-1} .

Since the simulations include the entire experimental setup, one can yield simulated data that is in excellent agreement with experimental data, provided the plasmonic material can be accurately described using the Drude formalism. An example is given in figure 3.13 for one of the cadmium oxide thin films deposited for this work. The simulation accurately describes the band of low reflectivity corresponding to the SPP dispersion. The arc of low reflectivity is a projection of the SPP dispersion into angle/energy space. Thus, by recording the reflectivity one can extract information about the SPP dispersion. The dispersiveness of the critical angle towards lower energies is captured as well. This can be seen as a warping of the horizontal line around 45°towards lower energies. This is due to the different dispersion of the substrate and prism materials used in the simulation. Without including the dispersion of all materials used in the the measurement setup, the simulations would not accurately capture the reflectivities at lower energies. The vertical lines around 1200 cm^{-1} are caused by a dim band in the IR-VASE output spectrum, thus the experiment produces very noisy (low intensity) data around those frequencies.

Ultimately, a combination of 3D and 2D simulations has been used throughput this work to interpret experimental data and to design and optimize sample parameters such as film thickness, carrier concentration or different substrate materials with varying properties.

3.4 Modeling to understand material property/optical response relations

The simulations introduced above can be used to understand material property/optical response relations without having to perform time consuming experimental series. In real material systems it is very unlikely that a single property can be isolated and changed independently of all other properties that influence the plasmonic behavior. Nevertheless, it became extremely useful throughout this work being able to do so using simulations. This allowed to get a better understanding of the individual impacts of material properties on the plasmonic properties. It also allowed to screen prospective new materials faster, testing the applicability for plasmonics without having to optimize a growth method first.

In the following section, various examples will be given to demonstrate how the plasmonic properties of a generic material change, if a specific materials property is changed. In more detail, all four Drude model specific parameters (n, μ,m_{eff} and ϵ_∞) and the sample thickness will be varied and the computed reflectivity maps will be presented and discussed.

3.4.1 Film thickness

For a Kretschmann type SPR experiment, the evanescent field propagating through the metallic thin film undergoes a phase shift. This is due to the loss inherent to the metallic film. This implies, that not only the in-plane wave-vector and energy of the incoming radiation has to be matched to the SPP to achieve coupling. The phase shift has to be accounted for as well. The phases can be matched by varying the thickness of the thin film. This thickness dependence is accurately captured by the model described above.

Experimentally this means, that a third parameter, the phase, has to be matched together with energy and in-plane wave-vector by varying the thin film thickness. To demonstrate the effect of the metallic films thickness on the observed reflectivity, figure 3.14 depicts the SPR response of a generic film with 4 different thicknesses. Panel a) in figure 3.14 depicts R for a generic film with a thickness of 50 nm. A strong, angle independent absorption can be seen. This corresponds to coupling to the SBPP, as described in 3.3. Coupling to this mode is only possible for thin films, more precisely for films with thicknesses below the skin depth of the material at the coupling energy[66]. With increasing the thickness to 150 nm, as can be seen in panel b), the SBPP mode almost fully suppressed, and the overall reflectivity is high with only small indications of coupling at low energies. For this thickness, no resonance condition is matched, resulting in a rather featureless reflectivity map. Upon further increasing the thickness to 250 nm, panel c), one can see increasingly strong coupling to the SPP, as indicated by the characteristic arc shape of the angle and energy dependent absorption. In panel d) the thickness is increased to 350 nm and a strong coupling to the SPP over the entire angle/energy range depicted can be seen.

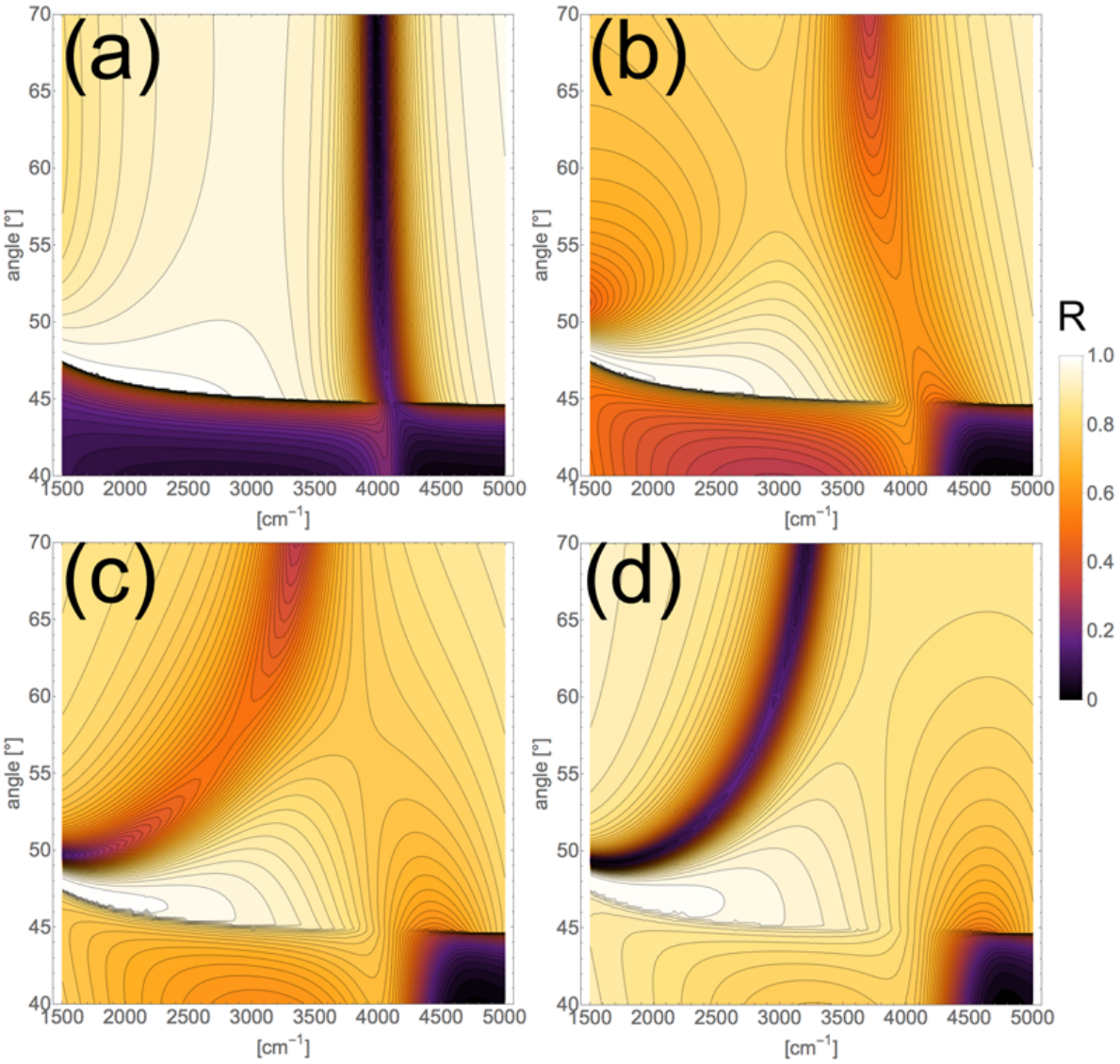

Figure 3.14 The effect of varying the film thickness within a material system on the resulting SPR reflectivity maps; all Drude parameters are held constant. a) 50 nm b) 150 nm c) 250 nm d) 350 nm.

To optimize film thickness for specific coupling at certain energies/angles, two dimensional simulation can be employed. By keeping either incidence angle or the energy constant, one can simulate the effect of a change in thickness on the resulting reflectance (coupling). This method is very useful for simulating the thickness needed to achieve maximum coupling at a certain incidence angle or energy. Figure 3.15 depicts an example of the effect of varying film thickness for the generic material at a constant incidence angle of 60 degrees. It can be seen that R varies significantly with changing thickness.

Analogous, varying the thickness while keeping the energy constant can be used to optimize the coupling at a given energy and extracting the resulting resonance angle. An example for the generic material is depicted in figure 3.16.

3.4.2 Carrier concentration

Increasing the carrier concentration changes the plasma frequency ω_p of the Drude metal. This will shift the resulting SPP dispersion towards higher energies. The step wise increase in n depicted in figure 3.17 a)-d) translates this into angle/energy space. One can see the plasmonic arc shift to higher energies with increasing carrier concentration. The absorption strength varies since the film thickness is held constant throughout the 4 panels.

3.4.3 Carrier mobility

Changing mobility has a very pronounced effect on the resulting reflectivities. The simulated reflectivity map for a generic material with an electron mobility of 50 $cm^2V^{-1}s^{-1}$ as depicted in figure 3.18 a) exhibits a very broad, slightly dispersive absorption band. The SPP dispersion is effectively smeared out. Upon further increasing the mobility (panels b)-d)) the resulting reflectivity arc sharpens up, giving a clear picture of the SPP dispersion. This is due to the decreased loss in the imaginary part of he SPP dispersion that is mostly influenced by the damping term $gamma$ as described in equation 3.2. From this set of simulated maps it becomes obvious why a high carrier mobility is usually favorable for plasmonic materials.

3.4.4 Effective mass

A variation of the effective mass has similar effects as changing the carrier concentration. From equation 3.1 we can see that a decreasing m_{eff} will shift the SPP dispersion towards higher energies resulting in a increasingly higher energy absorption of the SPP. This can be seen in panels a)-d) of figure 3.19, where the plasmonic absorption arc shifts further to the right (higher energies) with decreasing m_{eff}.

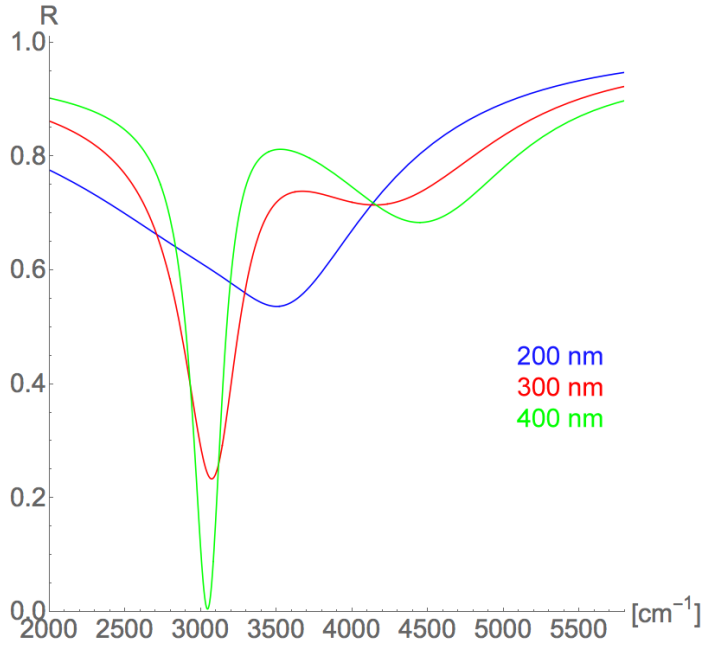

Figure 3.15 Reflectance as a function of film thickness for a generic film in energy space. The strong dependence of R on the film thickness can be seen.

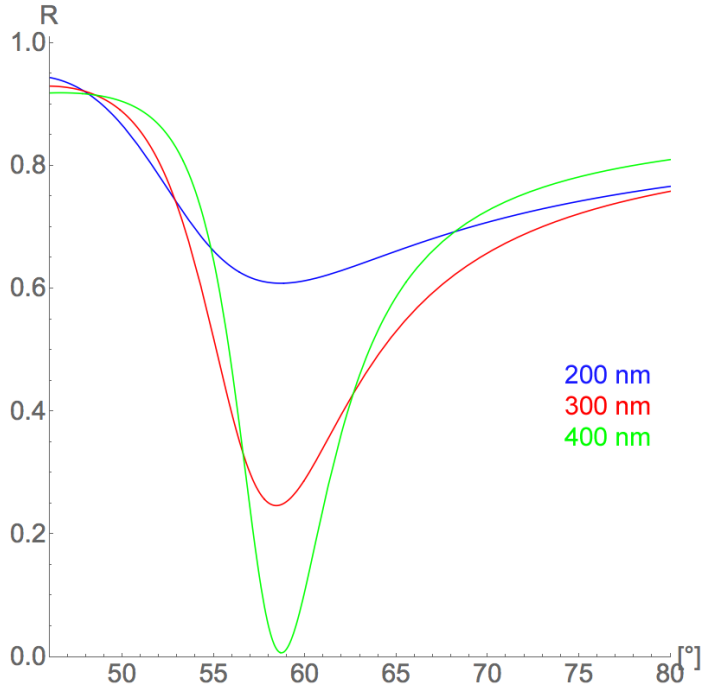

Figure 3.16 Reflectance as a function of film thickness for a generic film in angle space. The strong dependence of R on the film thickness can be seen.

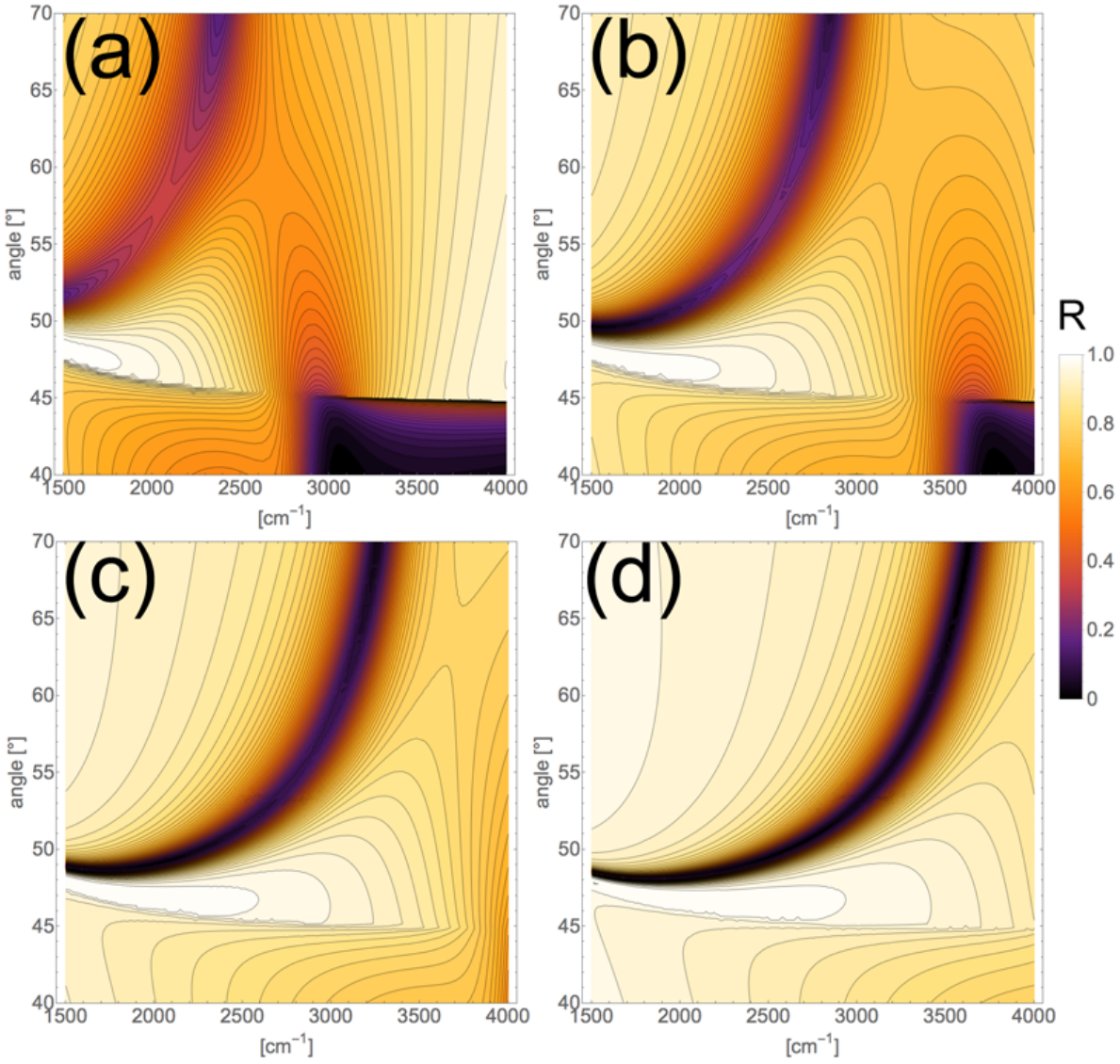

Figure 3.17 The effect of varying the carrier concentration within a material system on the resulting SPR reflectivity maps; all other Drude parameters and the film thickness are held constant. a) 1.0×10^{20} cm^{-3} b) 1.5×10^{20} cm^{-3} c) 2.0×10^{20} cm^{-3} d) 2.5×10^{20} cm^{-3} .

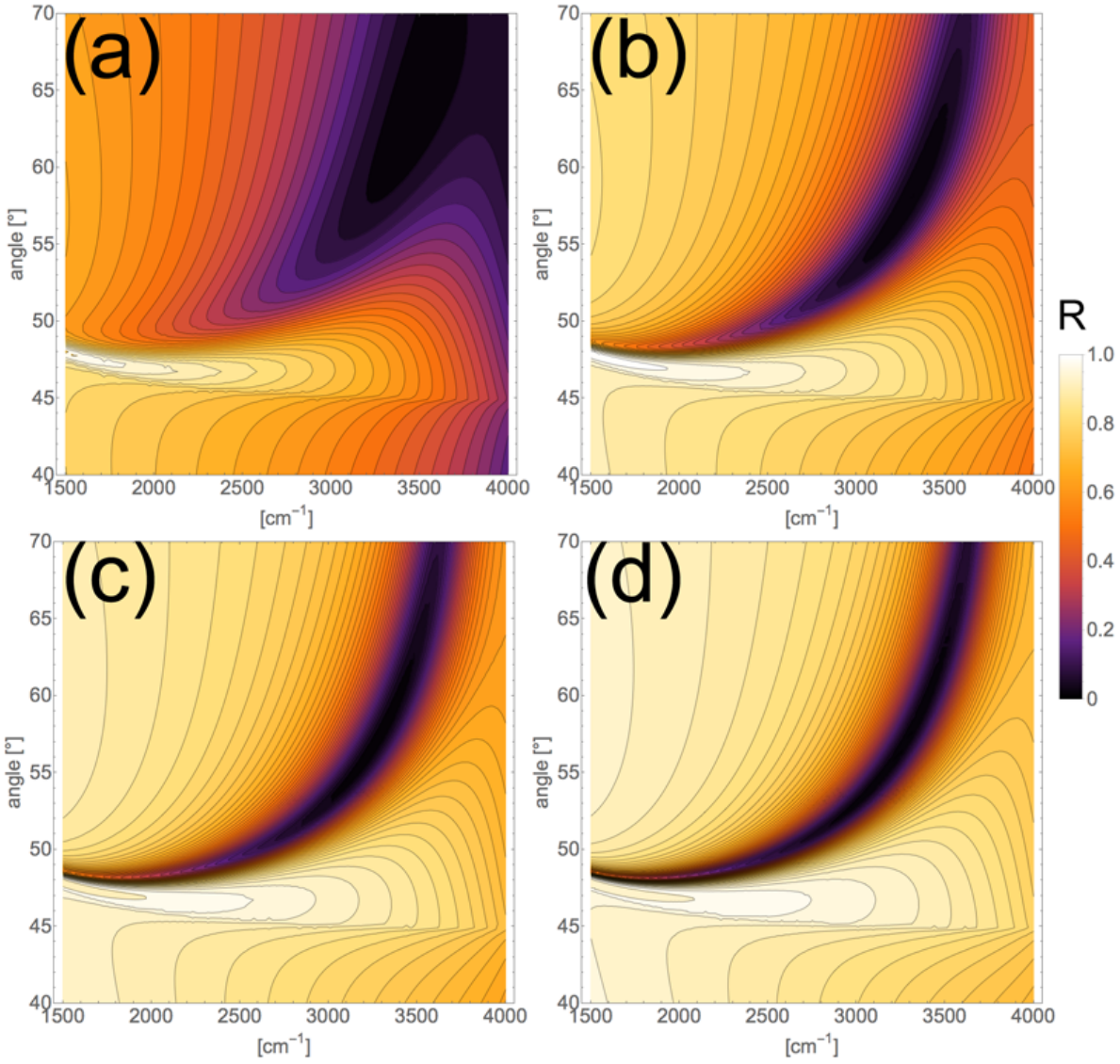

Figure 3.18 The effect of varying the carrier mobility within a material system on the resulting SPR reflectivity maps; all other Drude parameters and film thickness are held constant. a) 50 $cm^2V^{-1}s^{-1}$ b) 100 $cm^2V^{-1}s^{-1}$ c) 150 $cm^2V^{-1}s^{-1}$ d) 200 $cm^2V^{-1}s^{-1}$.

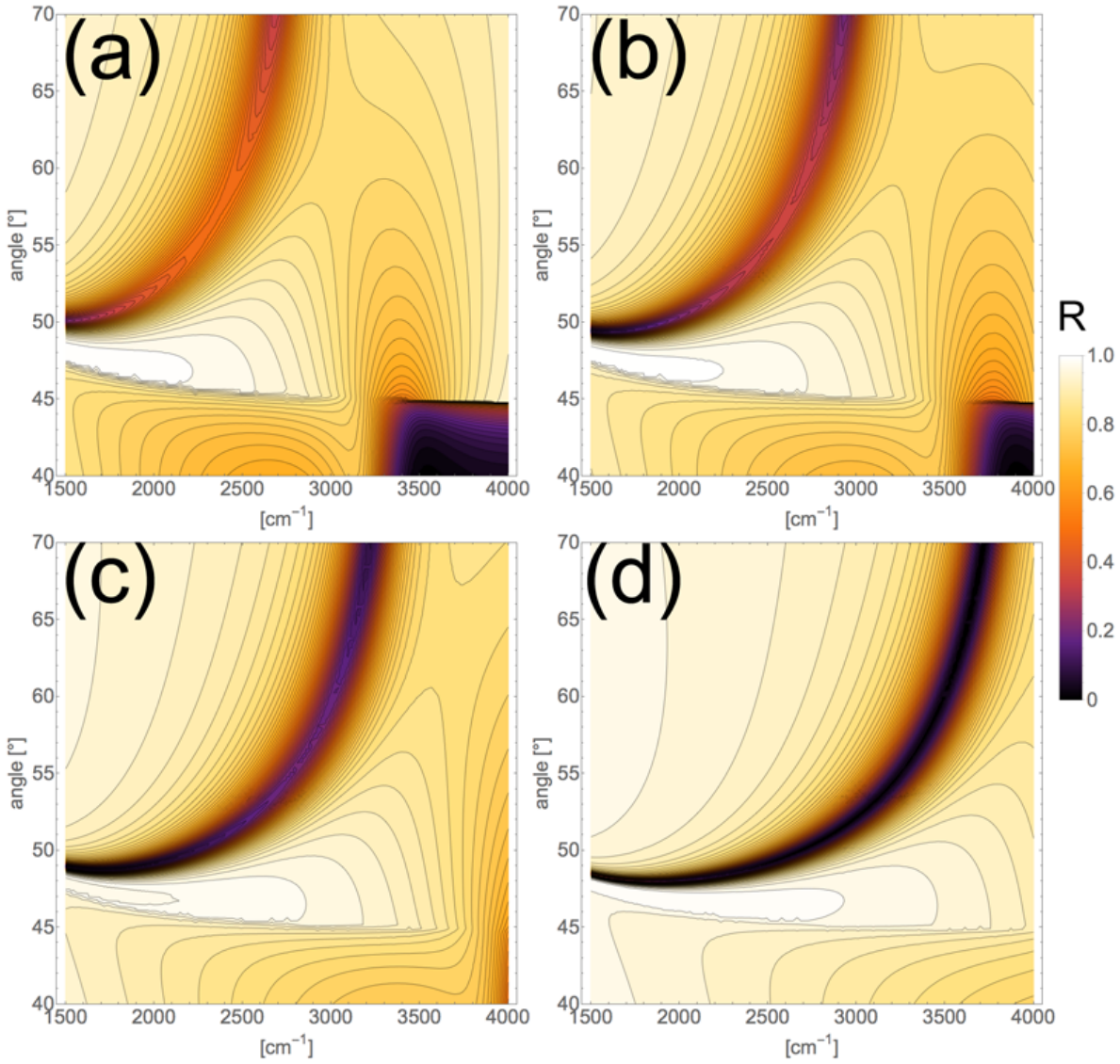

Figure 3.19 The effect of varying the carrier effective mass within a material system on the resulting SPR reflectivity maps; all other Drude parameters are held constant. a) m_{eff}=0.4 b) m_{eff}=0.33 c) m_{eff}=0.27 d) m_{eff}=0.2 .

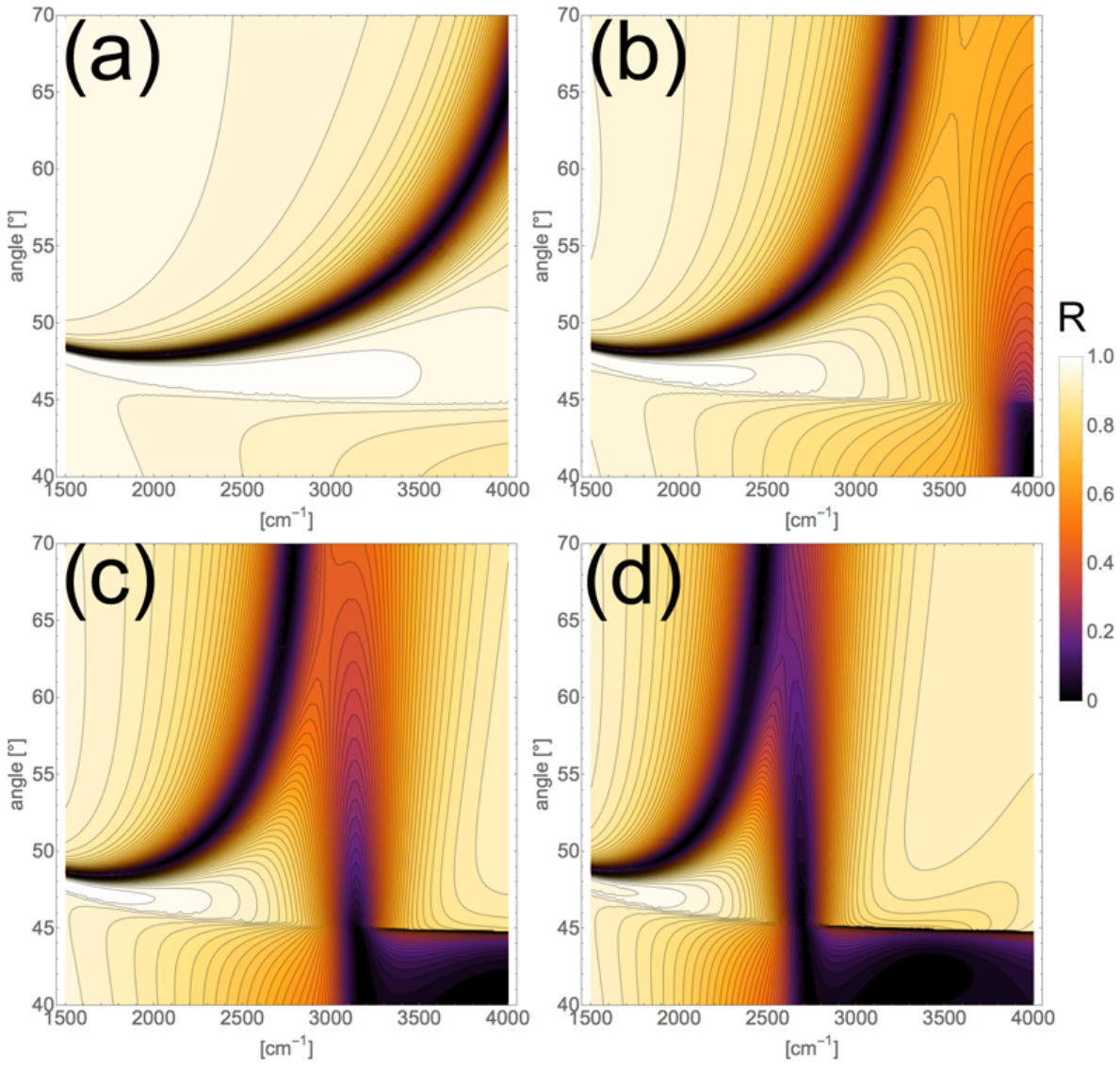

Figure 3.20 The effect of varying the high frequency dielectric constant within a material system on the resulting SPR reflectivity maps; all other Drude parameters are held constant. a) ϵ_∞=4 b) ϵ_∞=8 c) ϵ_∞=12 d) ϵ_∞=16.

3.4.5 High frequency dielectric constant

To understand the effects of a changing high frequency dielectric constant on SPR reflectivity measurements, it is helpful to examine the effects this variation has on the dielectric function of the Drude metal. This has been discussed in figure 3.2. The change in cross-over frequency in combination with the changing second derivative of ϵ_1 results in the compression effect that is depicted in figure 3.20. Panels a)-d) depict the reflectivities corresponding to an increasing high frequency dielectric constant. The result is a shift of the SPP dispersion towards lower energies. Furthermore, the SPP and BSPP modes move closer together in energy.

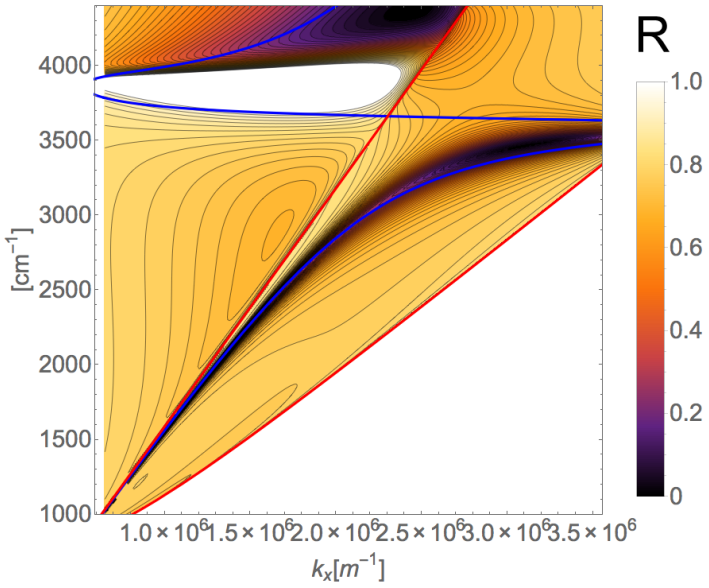

Figure 3.21 Reflectivity map in wave-vector/energy space. The SPP dispersion is plotted in blue and the critical angle as well as the 90 °incidence light lines are plotted in red

3.5 SPR in the Kretschmann Rather configuration; wavevector/energy space

It is possible to calculate reflectivities and reflectivity maps in wavevector/energy space. This is useful if the full dispersion needs to be plotted on the same map as the reflectivities. Figure 3.21 shows an example for a generic material. It is noticeable, that in this representation, the light lines (red) are not exactly straight lines. This is due to the fact that the simulation code includes the optical dispersion data of the substrate material, which warps the light line slightly (the refractive index changes at lower energies). Even though this simulation method can be helpful, in the context of the Kretschmann configuration it does not convey a lot of useful information, since most of the maps parameter space is not experimentally accessible. Only the area within in cone formed by the two light lines can be experimentally probed. The white area below the 90° light line corresponds to incident angles greater than 90° and is therefor not feasible in the Kretschmann configuration.

This data representation can however be used to identify modes. By overlaying calculated dispersion curves and the reflectivity data, thickness dependencies and the transition between modes becomes easier to interpret. Despite some advantages of this method over the angle/energy representations, the latter was mostly used for this work.

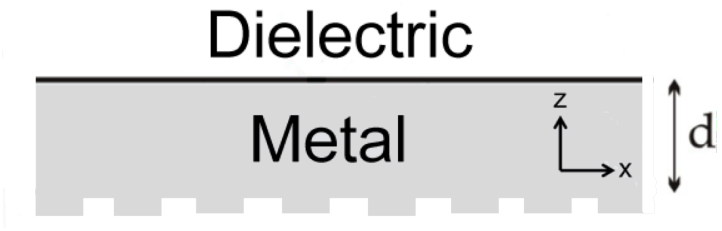

Figure 3.22 Schematic of a grating used to couple to SPPs

3.6 SPR grating coupling

In order to achieve momentum matching of light to SPPs we so far considered propagation trough an optically dens medium. Coupling light propagating through free space is not possible in a planar geometry. To enable the coupling of light from free space to SPPs, optical gratings can be used. A grating can supply the necessary momentum increase to incoming light, allowing light propagating in free space to couple to SPPs by interacting with the grating. The possible momentum transfer can be described with a grating vector $k_{\vec{G}}$, with:

$$k_{\vec{G}} = \frac{2\pi}{a} \tag{3.14}$$

where a is the length of the repeat unit of the grating (the grating pitch). This vector can be added or subtracted from the lights momentum. In energy/wave vector space, this shifts the light line by the magnitude of $k_{\vec{G}}$ in the positive or negative direction. This quickly becomes very confusing, since gratings can also add/subtract multiples of the grating vector ($\pm k_{\vec{G}}, \pm 2k_{\vec{G}}, ...$) and the light can propagate in the positive and negative k_x direction relative to the thin film plane. Figure 3.22 depicts a schematic of a grating on top of a metal film. In this case, the grating is made out of the same material as the metal, however this is not necessary for a grating to work.

Since the light does not have to propagate through the substrate, it can couple to two SPP dispersions. The air/metal interface supports a SPP, and additionally, the substrate/metal interface can also support an SPP, since both are dielectric/metal interfaces. The substrate/metal SPP is not accessible with the Kretschmann configuration and limited to lower energies (relative to ω_p of the metal). This circumstance complicates the matter further, since there are two dispersion curves that the (grating modified) light lines can couple to. In an effort to simplify this problem, a code was written that visualizes all the possible light lines and SPP dispersions for a given substrate/thin film combination and grating vector. The program features interactive options that allow to visualize selective light lines at different incidence angles, the SPP dispersions and the added/subtracted grating vectors. An example is given

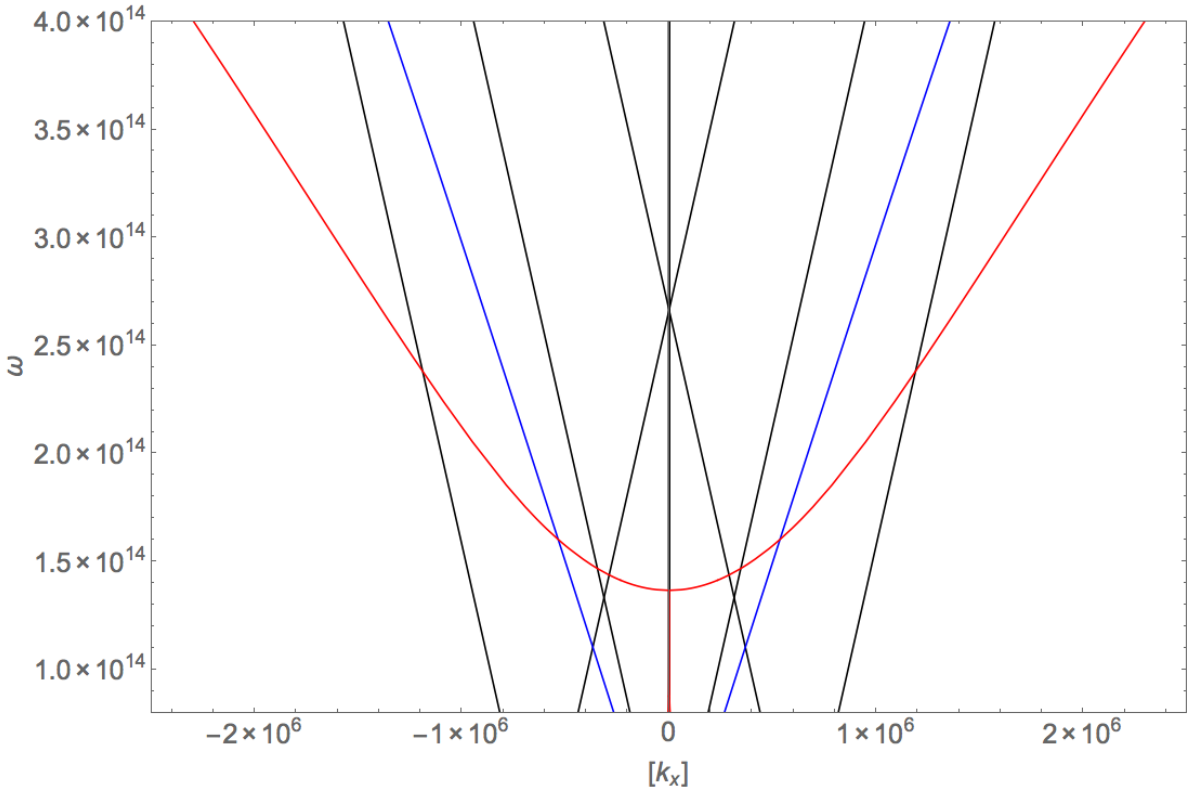

Figure 3.23 Grating coupling to SPPs. An example of the code output depicting energy/wave-vector space. The air/metal SPP is plotted in blue, the substrate/metal SPP in red and the light lines for 45°incidence are plotted in black for freely propagating and $\pm k_{\vec{G}}$ light

in figure 3.23.

The air/metal SPP is plotted in blue, the substrate/metal SPP in red and the light lines for 45° incidence are plotted in black for freely propagating and $\pm k_{\vec{G}}$ light. Every intersection of a light line with a SPP dispersion allows for coupling to the SPP. Therefore, there are many more coupling opportunities to a single SPP dispersion when compared to the Kretschmann configuration.

To fully appreciate the complexity of grating vector multiples and changing incidence angles (which will tilt all light lines in this picture), one should compile the code found in Appendix B. It allows for direct control of all input variables and dynamically updates the resulting figure. This allows to fully explore the coupling opportunities with gratings to SPP dispersions.

3.7 Importance of modeling in the context of this work

For this work, the search for novel materials that support SPR at mid-IR energies, these simulations added substantial efficiency and understanding. A significant amount of time was spent creating and optimizing the code. However, the possibility to explore the plasmonic properties of any material *in silico* streamlined our efforts and allowed to design very efficient experimental strategies. Significantly more time could be spent optimizing a material rather than testing it for it's applicability for mid-IR plasmonics. By researching literature values for Drude parameters for candidate materials, many potential materials could be excluded form experimental work since it became obvious, using these simulations, that their properties will not allow to support SPR in the mid-IR. On the other hand, for promising materials all the experimental parameters could be optimized using the simulations, allowing for faster progression in the research.

Chapter 4

Mid-infrared surface plasmon resonance in Zinc Oxide semiconductor thin films

Published in Applied Physics Letters, Volume 102, Issue 5 (2013) – DOI: 10.1063/1.4791700

Edward Sachet[1], Mark Losego[2], Joshua Guske[3], Stefan Franzen[3] and Jon-Paul Maria[1]

[1]Department of Materials Science, North Carolina State University, Raleigh, NC
[2]Department of Chemical & Biomolecular Engineering, North Carolina State University, Raleigh, NC
[3]Department of Chemistry, North Carolina State University, Raleigh, NC

4.1 Abstract

Surface plasmon resonance (SPR) in semiconducting materials at mid-infrared (mid-IR) energies offers the potential for new plasmonic functionalities and integration schemes. Mainstream semiconductors are transparent to mid-IR energies, thus a tightly integrated monolithic package for SPR sensing becomes feasible. We report mid-IR surface plasmon resonance in Zinc Oxide (ZnO) as a model material for semiconductors with $4x10^{19}$ to $8x10^{19}$ cm^{-3} carriers. The surface plasmon modes were characterized using spectroscopic IR-ellipsometry and compared to a reflectivity simulation. The data confirms the feasibility of mid-IR SPR, shows a generic ability for plasmon tuning, and demonstrates the predictive

power of the reflectivity model.

4.2 Main text

Surface plasmon resonance (SPR) is a well-established sensing technique for detecting minute changes in the refractive index at the surface of a conducting medium. The technique commonly employs a visible light source to excite a surface plasmon at a thin metal film/dielectric interface. The resonant conditions of the plasmon are highly sensitive to the refractive index of the dielectric, which leads to an extreme sensitivity to adsorbates when the dielectric is air or a liquid. This method is used routinely in the life-science community to detect reversible binding reactions of proteins to functionalized surfaces[82–84] and in a more recent report, surface plasmons were demonstrated gas sensors[85,86]. Gold and silver are the commonly used plasmonic materials since they are relatively inert and metallic thus offering high carrier concentrations and limited chemical interactions. For metals, absorption due to plasmon resonance is mostly confined to ultraviolet and visible (UV/VIS) light energies. This is due to the direct correlation of charge carrier density, plasma frequency (ω_p) and the resonant frequency of the surface plasmon (ω_{sp}), which can be roughly estimated as $\omega_{sp} \approx \omega_p/\sqrt{2}$ in air[65]. Since the carrier density in a metal can only be varied slightly, there are limited opportunities for tuning the resonance frequency. Consequently, most SPR sensor devices are based on UV/VIS-transparent substrates such as glass to couple light into the plasmonic film. Semiconductors offer several advantages over metals: The carrier density can span several orders of magnitude using well-understood doping techniques and there are obvious opportunities for monolithic integration of SPR-active surfaces and light sources. With a typical carrier concentration of about $5\text{x}10^{19}$ cm^{-3} we predict SPR to occur around 2000 cm^{-1}, the mid-IR range. Mainstream semiconductors such as Si, Ge or GaAs are all transparent to those energies, allowing their use as transparent substrates. Consequently, it is feasible to integrate a solid-state light source into a semiconductor heterostructure that also includes the active plasmonic thin film. Furthermore, the carrier concentration of the active film can be tuned to match its SPR frequency to the exact frequency of the light source. In principle, this could eliminate the need for external optics and lead to miniaturization of SPR based technologies. Some wide bandgap semiconductors, especially oxides, are more chemically inert than metals and could be used as sensors in extreme conditions, such as corrosive liquids or higher temperature environments. Furthermore, the comparatively lower carrier densities use light with longer wavelengths thus a significantly longer probing range from the sensing device. This occurs because the wavelength of the surface plasmon polariton (SPP) excited by the pumping light is directly proportional to the wavelength of the incident radiation[87]. The evanescent wave associated with the SPP decays exponentially into the sensing medium orthogonal to the films surface and probes the surrounding dielectric. Since the evanescent wave decays within roughly 1/3 of its wavelength, IR energies can increase significantly the probe of SPR based

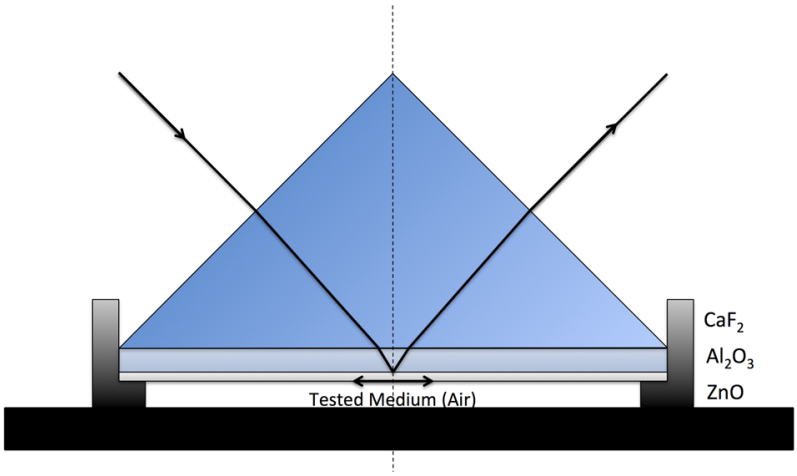

Figure 4.1 Experimental setup demonstrating the Kretschmann-Raether configuration for SPR measurements

sensors. This would allow, for example, biosensors to probe a larger volume, which would in principle increase the sensitivity and signal-to-noise ratio. Demonstrating SPR in the mid-IR could ultimately lead to monolithically integrated SPR sensors, combining semiconductor technology and reliability with the sensing characteristics of surface plasmons. In this study, we demonstrate SPR supported by a heteroepitaxial thin film of ZnO (bandgap 3.37 eV) in the mid-IR (*i.e.*, between 1700-4000 cm^{-1}) and we provide a quantitative spectroscopic model to predict and understand the measured reflectivity dependence.

Heteroepitaxial thin films of zinc oxide (ZnO) were prepared by pulsed laser deposition (PLD) from a ceramic ZnO target. The ceramic was sintered from ZnO powder (99.99+% metal basis) at 1250°C for 8h and was ablated by a krypton fluride (KrF) excimer laser (248nm) at a typical energy density of 0.67 J/cm^2 and 10 Hz pulse repetition rate with an oxygen background pressure of 10 mTorr. Double side epitaxial-polished c-plane sapphire was used as substrate for deposition at a target-substrate distance of 100 mm. The thin films were characterized by x-ray diffraction (XRD) using a Panalytical Empyrean XRD and the electrical properties were measured using an Ecopia HMS-3000 Hall Measurement System. SPR measurements were performed using a Wollam IR-VASE spectroscopic ellipsometer in the Kretschmann-Raether configuration. A right angle CaF_2 prism was used to couple light into the sapphire substrate mounted onto a custom-built sample holder. To optimize the optical connection, index-matching fluid (Cargille Series M 1.720) was applied between the prism and the sapphire surface. The assembly was then mounted onto the motorized theta-2theta ellipsometer stage. This configuration supports angle, wavelength, frequency as well as phase interrogating measurements and therefor allows the investigation of all

SPR responses reported so far[88]. The reflectivity data was recorded for r- and s-polarized light and ultimately compiled into angle and frequency dependent maps that visualize the ZnO plasmonic response. Simulated maps of the plasmonic response are calculated using a companion Mathematica code (which is available for download from the online version of this article). The model system used is depicted in FIG. 4.1. Snell's law was used to account for the change in incident angle in respect to the sample stage as the light passes the air/prism interface and the prism/substrate interface. Reflectivity data was then calculated from the sapphire/ZnO/air interfaces. To model the dielectric constant of the ZnO films, a free electron Drude model was used. In this model, the real (ϵ_r) and imaginary (ϵ_i) dielectric functions are given by Eq. (4.1) and (4.2)

$$\epsilon_r = \epsilon_\infty - \frac{\omega_p^2}{\omega + \gamma^2} \tag{4.1}$$

$$\epsilon_i = \frac{\gamma\omega_p^2}{\omega(\omega + \gamma^2)} \tag{4.2}$$

where ω_p is the plasma frequency (Eq. 4.3), ϵ_∞ is the high frequency dielectric constant and γ is a damping term (Eq. 4.4).

$$\omega_p^2 = \frac{nq^2}{m_e\epsilon_0} \tag{4.3}$$

$$\gamma = \frac{q}{\mu m_e} \tag{4.4}$$

The plasma frequency is directly dependent on the carrier density (n) where q is the electron charge (1.602x10^{-19}C), ϵ_0 is the permittivity of free space, m_e is the effective electron mass and μ is the electron mobility.
The reflectance at an interface was described by the Fresnel equations:

$$r_p = \frac{n_i cos\Theta_i - n_t cos\Theta_t}{n_i cos\Theta_i + n_t cos\Theta_t} \tag{4.5}$$

$$r_s = \frac{n_t cos\Theta_i - n_i cos\Theta_t}{n_t cos\Theta_i + n_i cos\Theta_t} \tag{4.6}$$

where the complex refractive indices of the incident material (n_i) and the transmitted material (n_t) together with the incident angle Θ are used to calculate the reflectance for both p- and s-polarized light. To calculate the refractive index of the modeled film, the relation $n = |\epsilon|^2$ was used.
The total reflectance from the sapphire/ZnO/air interface can be calculated using the Airy formula[81]

$$r = \frac{r_1 + r_2 exp(2ib)}{1 + r_1 r_2 exp(2ib)} \tag{4.7}$$

Table 4.1 Summary of the electrical and structural properties of the ZnO thin films

Sample	Thickness [nm]	Carrier conc. [cm^{-3}]	Mobility [$cm^2V^{-1}s^{-1}$]	FWHM (00.2) [°]
A	400	$8x10^{19}$	20	0.5
B	600	$4.5x10^{19}$	18	0.6
C	600	$6x10^{19}$	18	0.6

with

$$b = \frac{2\pi d_f}{\lambda}\sqrt{n_{film}^2 - n_{substrate}^2 sin^2\Theta_i} \tag{4.8}$$

where λ is the incident light wavelength, d_f is the film's thickness and r_1 and r_2 are the calculated reflectances from interface 1 and 2. Additionally, the back reflection from the CaF_2/sapphire interface was calculated using Eq. 4.5-4.6 and added to the calculated reflectivity data. The data is ultimately compiled into maps of the total reflectance in angle and wavenumber space (Eq. 4.9).

$$R = \frac{R_p}{R_s} = \frac{|r_p|^2}{|r_s|^2} \tag{4.9}$$

In previous publications[73], we considered the refractive index of the substrate and prism to be constant. However, since the refractive indices of the materials used for this study vary significantly in the mid-IR, the dispersion of CaF_2 and the sapphire substrates was measured over the energy range used and included in the model.

Three different ZnO films of different thickness were selected for this study. Table 4.1 summarizes the electrical and structural properties as determined by XRD and Hall effect measurements. The defect chemistry in ZnO is known to favor oxygen vacancies created by the Schottky reaction $0 = V_Z n^{\times} + V_O^{\times}$ with further ionization of the oxygen vacancies according to $V_O^{\times} = V_O^{\bullet\bullet} + 2\,e^-$ [89]. All three films were prepared to be highly oxygen deficient to reach the desired electron concentration of about $5x10^{19}$ cm^{-3} . The crystallographic orientation of all films can be summarized by the epitaxial relationship (00.1)ZnO||(00.1)Al_2O_3 and [2-1.0] ZnO||[1-1.0] Al_2O_3. FIG. 4.2 is a phi-scan of off-axis ZnO and Al_2O_3 reflections that confirms the expected epitaxial registry. The expected six fold symmetry of the off-axis ZnO reflection as well as the 30° rotation of the ZnO lattice relative to the sapphire oxygen sub-lattice is apparent.

To calculate the thin film reflectivity data, the electrical properties summarized in Table 4.1 were used as input parameters. The relative electron effective mass me was estimated to be 0.32 (Ref.[90]) at the carrier concentrations used. The high frequency dielectric constant ϵ_∞ was set to be 3.4[91]. The calculated maps were then compared to the measured data as

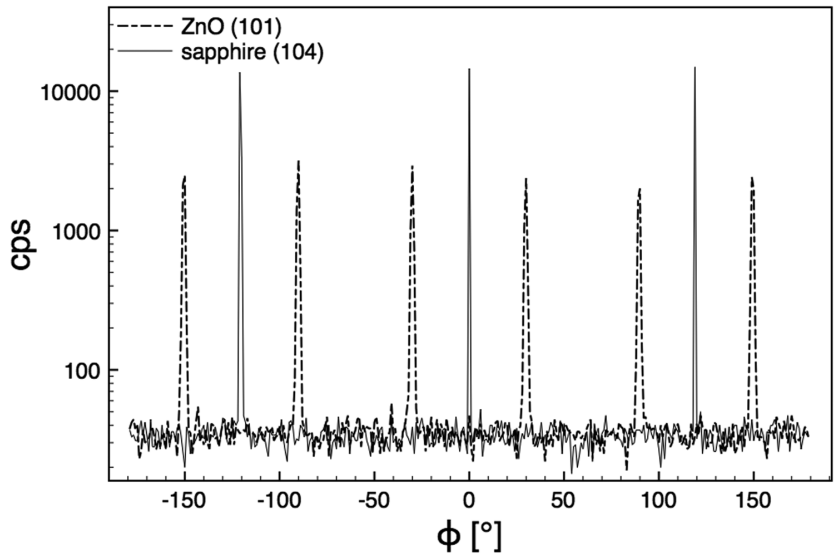

Figure 4.2 XRD phi-scans of the ZnO (101)/substrate (104) reflection demonstrating the epitaxial relationship of the ZnO films to the c-plane sapphire

depicted in FIG 4.3 and FIG 4.4. All of the measured maps feature a prominent absorption line around 3000 cm^{-1}, that can be attributed to absorption of Diiodomethane that is a component of the index matching fluid[92]. The white areas in FIG. 4.3-4.4 correspond to data points where the rp/rs-ratio is >1. The data for these fields can be plotted, but a color scale that emphasizes the SPR absorption was used, and only R-values ranging from 0-1 are visible. The first comparison of simulation and measurement (FIG. 4.3 a, b and c) depicts a narrow angular section around the critical angle of the sapphire/air interface of the 800 nm ZnO film (sample C). Since the refractive index of sapphire is dispersive in the mid-IR, there is a significant curvature of the critical angle towards higher angels at lower energies. The shift in the critical angle can be explained by wavelength dependent dielectric functions of CaF_2 and sapphire at wavenumbers <6000 cm^{-1}. Assuming a constant refractive index for sapphire and CaF_2, the simulated critical angle would be at a constant angle and the simulation would loose significant accuracy as is depicted in FIG 3a. By accounting for the dispersion, the simulated reflectivity shows good agreement with the measurement and predicts all features in the empirical reflectivity data (FIG 4.3 b,c). This comparison underlines the importance of including dispersion data for reflectivity simulations in the mid-IR.

Simulated and measured SPR responses for the ZnO thickness series is depicted in FIG.4.4 a,b (sample A), FIG.4.4 c,d (sample B) and FIG.4.4 e,f (sample C). The model captures the reflectivity dips in both the angle and frequency dependent axes and also reproduces the change of the SPR response with increasing film thickness. The SPR dip shifts towards

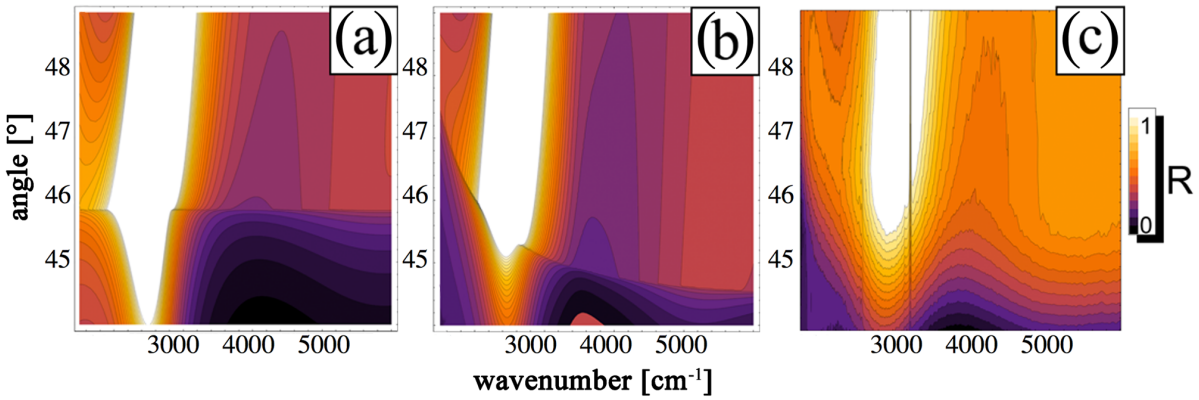

Figure 4.3 Comparison of simulation and experiment for reflectivity data around the critical angle of an 800 nm ZnO thin film (sample C). Comparing simulation with constant dispersion (a) to simula- tion including dispersion for CaF2 and sapphire (b) to experimental data (c). The increase in accuracy upon including dispersion is demonstrated. All data are depicted in the same parameter space.

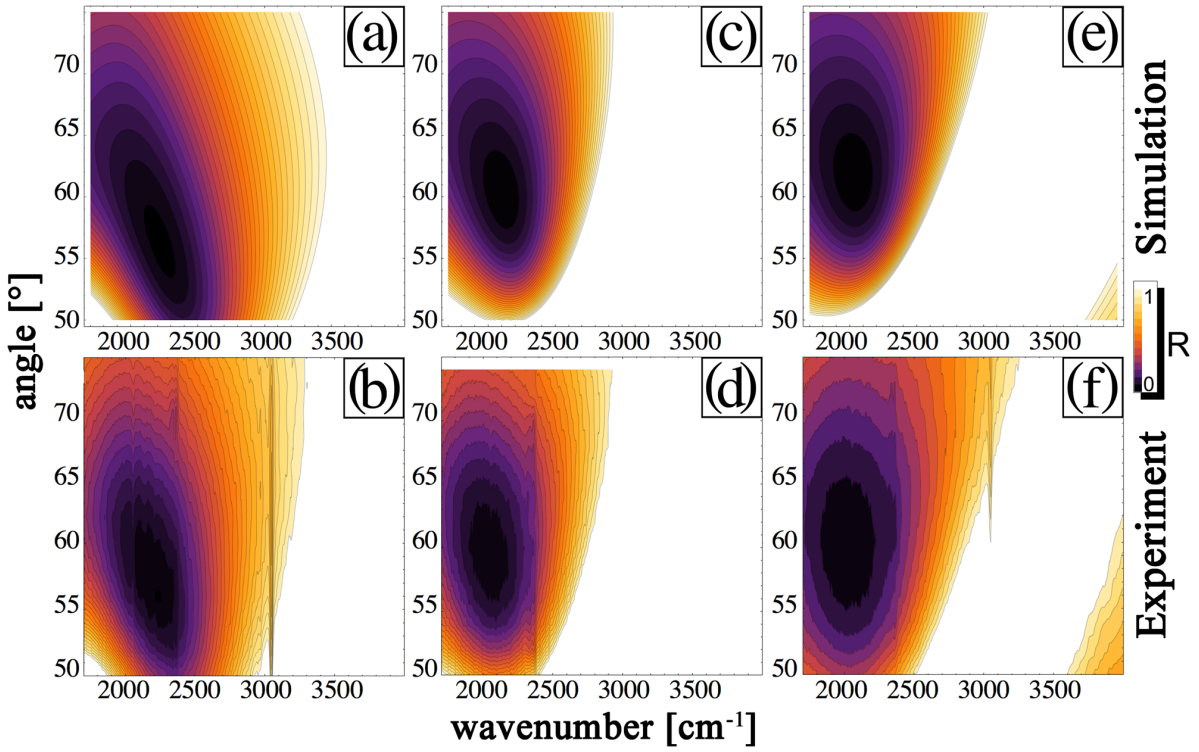

Figure 4.4 Reflectivity data for ZnO thin films and comparison to simulations. The data-pairs compare experiment to simulation for ZnO films with 400 nm (a) and (b), 600nm (c) and (d), and 800nm (e) and (f) film thicknesses. All data are depicted in the same parameter space.

higher angles for increased film thickness (FIG.4.4 e,f), and thicker films (sample B and C) lack the pronounced tilt in the reflectivity minima evident in the 400nm film (sample A). Practically speaking, for a single wavelength illumination, thicker films will show a smaller angular shift. This SPR broadening with increasing film thickness is captured in the simulated data. At higher angles, the model underestimates slightly the back reflection from the sapphire/prism interface, particularly towards lower energies. However, this only seems to offset the observed SPR dips to slightly lower reflectivity values. The general shape, hence the angle and frequency dependence of the SPR is not affected. This effect can be explained by the loss of transparency for sapphire at wavenumbers lower than 1700 cm^{-1}. At these energies and incident angles, the absorption is different for r- and s-polarized light resulting in an inaccurate r_p/r_s calculation. FIG. 4.5 illustrates this effect via a reflectivity map of a sapphire substrate without a ZnO film. The reflectivity data for this sample can be considered as a background for all measurements using the CaF_2/sapphire configuration and accounts for the deviations between the simulated and measured SPR response. If needed, these artifacts can be avoided by choosing prism/substrate combinations that are fully transparent over the investigated range.

In conclusion, we demonstrate surface plasmon resonance in semiconductor thin films and validate experimentally a mathematical model for mid-IR energies. Based on a free electron Drude model, the plasmonic response of semiconductors with carrier densities between 4-8x10^{19} cm^{-3} was simulated and compared to experimental data. Including wavelength-dependent data for the optics and substrates is essential to account for the strong dispersion of IR transparent materials for the energies used. With these adaptations, simulated data accurately predicted SPR in the ZnO films used as model system for this study. Since the free electron modeling approach proved to be accurate for modeling SPR in transparent conducting oxides, the method can be extended to predict SPR in other semiconducting materials, as long as their electrical properties are know. The code included in this publication therefor offers a powerful research tool for predicting plasmonic phenomena in a broad range of technologically interesting materials. Finally, observing SPR in semiconductor thin films opens up exciting possibilities for plasmonic research. The entire material class of semiconductors with their diverse and readily modifiable electronic properties can now be explored. Mid-IR energies are particularly interesting as they facilitate monolithical integration of SPR active thin films into semiconductor heterostructures transparent to those energies. As such, semiconductor based SPR will likely become an important technique that enables miniaturized and fully integrated sensor technologies.

Acknowledgments

We would like to thank Dr. Genzer and Dr. Kiril Efimenko from the department of chemical engineering at NCSU for granting generous access to the IR-ellipsometer.

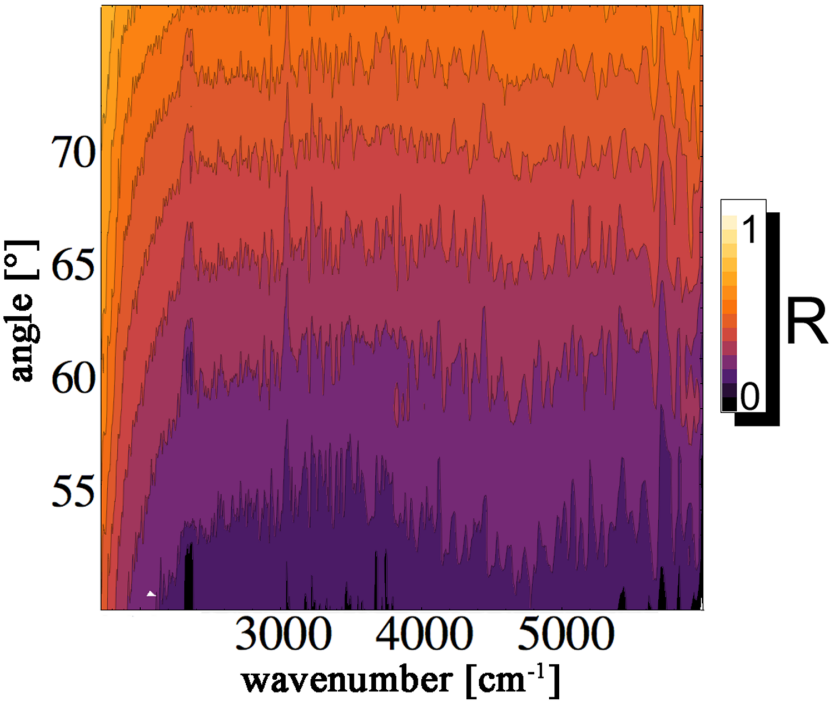

Figure 4.5 Reflectivity data for a bare sapphire substrate illustrating the reflectivity background present for the CaF_2/sapphire/ZnO system used for this study.

Chapter 5

Dysprosium doped cadmium oxide: A gateway material for mid-infrared plasmonics

Published in Nature Materials, 16 February (2015) AOP – DOI: 10.1038/nmat4203

Edward Sachet[1], Christopher T. Shelton[1], Joshua S. Harris[1], Benjamin E. Gaddy[1], Douglas L. Irving[1], Stefano Curtarolo[2], Brian F. Donovan[3], Patrick E. Hopkins[4], Peter A. Sharma[5], Ana Lima Sharma[5], Jon Ihlefeld[5], Stefan Franzen[6] and Jon-Paul Maria[1]

[1]Department of Materials Science, North Carolina State University, Raleigh, North Carolina 27695, USA
[2]Department of Mechanical Engineering and Materials Science and Dept. of Electrical Engineering, Duke University, Durham, North Carolina 27708, USA
[3]Deptartment of Materials Science and Engineering, University of Virginia, Charlottesville, Virginia 22904, USA
[4]Deptartment of Mechanical and Aerospace Engineering, University of Virginia, Charlottesville, Virginia 22904, USA
[5]Sandia National Laboratories, Albuquerque, New Mexico 87185, USA
[6]Department of Chemistry, North Carolina State University, Raleigh, North Carolina 27695, USA

5.1 Abstract

The interest in plasmonic technologies surrounds many emergent optoelectronic applications, such as plasmon lasers, transistors, sensors, and information storage. While plasmonic materials for UV-VIS and near infrared wavelengths have been found, the mid-infrared range remains a challenge to address: few known systems can achieve subwavelength optical confinement with low loss in this range. With a combination of experiments and *ab-initio* modeling, here we demonstrate an extreme peak of electron mobility in Dy-doped CdO that is achieved through accurate "defect equilibrium engineering". In so doing, we create a tunable plasmon host that satisfies the criteria for mid-infrared spectrum plasmonics, and overcomes the losses seen in conventional plasmonic materials. In particular, extrinsic doping pins the CdO Fermi level above the conduction band minimum and it increases the formation energy of native oxygen vacancies, thus reducing their populations by several orders of magnitude. The substitutional lattice strain induced by Dy-doping is sufficiently small, allowing mobility values around 500 $cm^2V^{-1}s^{-1}$ for carrier densities above 10^{20} cm^{-3} . Our work shows that CdO:Dy is a model system for intrinsic and extrinsic manipulation of defects affecting electrical, optical, and thermal properties, that oxide conductors are ideal candidates for plasmonic devices and that the defect engineering approach for property optimization is generally applicable to other conducting metal oxides.

5.2 Main text

Plasmonic phenomena in the mid-IR offer an exciting complement to established plasmonic technologies that operate in the UV-VIS to near-IR energies. High value- added applications enabled by mid-IR operation range from targeted chemical sensing, thermography, heat harvesting, heat-assisted magnetic data recording and novel light emitters such as quantum cascade lasers. Gold and silver are the most common plasmonic conductors. However, they are lossy resonators in the mid-IR (due to their high electron concentration and inter-/intraband transitions[93]) and their carrier concentrations cannot be tuned. Consequently, they are not appropriate for this lower energy spectral range.

The urgency for a low loss, easy-to-manufacture and abundant material exhibiting high-quality plasmon resonance in the mid-IR range has been raised with insistence[94–97]. Until now, a solution has not been found. In this work, we present the conductive metal oxide (CMO) dysprosium-doped cadmium oxide (CdO:Dy) as the first gateway material for IR plasmonics. While CMOs such as indium tin oxide (ITO) and aluminum doped zinc oxide (AZO) exhibit plasmon resonance in mid-IR energies and are tunable, their utility is limited by consistently low mobility values. Graphene and patterned graphene structures support various plasmon modes in the mid-IR[98,99]; however, performance is limited to wavelengths >6.5 μm due to scattering with optical phonons[63]. Highly doped semiconductors such as

n-InAs have been reported to support low-loss plasmons, but doping limits below 1x10^{20} cm^{-3} restrict such materials for longer wavelength applications (>5.4 μm)[100,101]. While semiconductor metasurfaces that couple to IR light are of interest for plasmonics, efforts to date are still nascent[102].

We demonstrate in CdO how defect equilibria can be actively manipulated to achieve a combination of mobility and carrier density in donor-doped crystals that is often considered mutually exclusive. This combination enables high quality factor plasmons in the mid IR. In addition, a comprehensive and self-consistent model explaining the electrical, optical, and thermal properties of CdO is introduced.

CMOs are an ideal class of materials for lower energy plasmonics as they do not exhibit interband transitions in the mid-IR. The optical properties can be described using a lossy Drude electron plasma model with a complex dielectric function[65,73,78–80].

$$\epsilon = \epsilon_1 + i\epsilon_2 = \epsilon_\infty - \frac{\omega_p^2}{\omega(\omega + i\gamma)} \tag{5.1}$$

Here, $\epsilon_1 + i\epsilon_2$ is the dielectric function, ϵ_∞ is the high- frequency limit of permittivity, ω_p is the plasma frequency (proportional to the free carrier concentration), and γ is the damping factor describing the scattering and ohmic losses (supplementary information). When mobility increases, losses (ϵ_2) are reduced, and the model predicts enhanced plasmonic performance. Following this relationship, one recognizes immediately the need for a high mobility material at carrier concentrations that establish plasma frequencies in the mid-IR (n_e > 10^{20} cm^{-3}), which is a recognized challenge for conventional semiconductors. In 1969, Koffyberg showed that combinations of mobility and carrier density approaching the needs of mid-IR plasmonics can be achieved in intrinsic CdO single crystals[103]. Vacant oxygen sites, the preferred native defect in CdO, were the source of carriers and were modulated by reducing anneals. However, precise and reproducible control of electrical transport by reduction is a challenge, particularly considering the proximity in temperature and pressure to conditions that destabilize the entire crystal. It is thus reasonable to expect that doping with the correct aliovalent cation may enable further optimization. To explore this hypothesis, we developed a plasma-assisted molecular-beam epitaxy (PAMBE) method to synthesize Dy-doped CdO. In a CdO host, Dy populates the Cd sublattice with a 3^+ charge, thus acts as an electron donor. The initial experiment produced four dopant series of epitaxial layers, each on a different substrate; thus offering a range of orientation and mismatch possibilities.

Room temperature transport properties for a doping series of CdO:Dy grown on MgO (100) substrates are shown in Figure 5.1(a). Two trends are of particular interest. First, the free electron concentration is directly proportional to the dysprosium content, and an n-type doping range spanning 5x10^{19}-1x10^{21} cm^{-3} is accessible. Second, the free carrier mobility increases with Dy doping, reaching a maximum of almost 500 cm^{2}V^{-1}s^{-1} at 5x10^{19} cm^{-3} . After this point, mobility falls steadily until the solubility limit is reached at 5x10^{21} cm^{-3} .

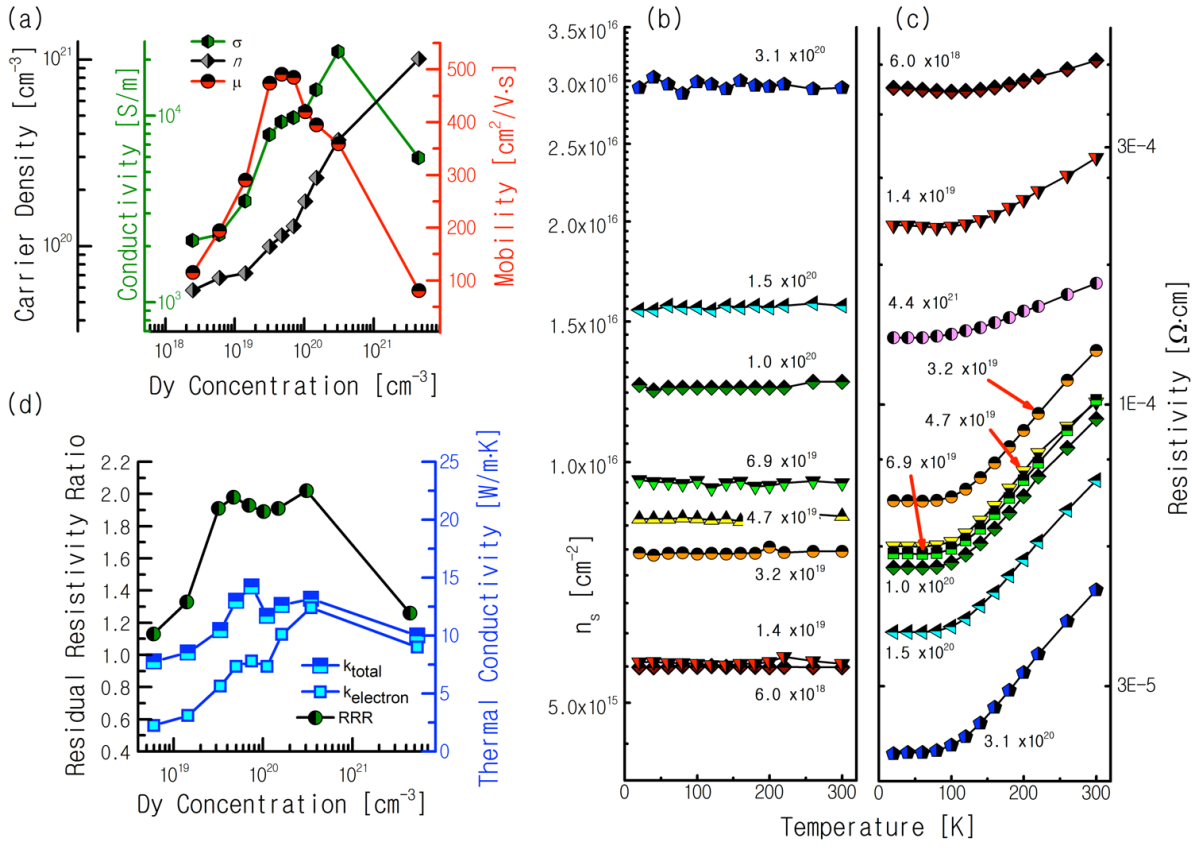

Figure 5.1 (a) Transport data for CdO:Dy grown on MgO (100) substrates summarizing carrier conc. (cm^{-3}), carrier mobility (μ) and conductivity (σ) as a function of dysprosium concentration. (b) Temperature dependent sheet carrier concentration (n_s) as a function of [Dy] for CdO:Dy grown on MgO (100) substrates; (c) Temperature dependent resistivity (Ω cm) as a function of [Dy] grown on MgO (100) substrates. (d) Residual resistance ratio (RRR), measured thermal conductivity (κ_t) and theoretical values for the electron contribution to thermal conductivity (κ_e) calculated vis Wiedemann-Franz law for CdO:Dy grown on MgO (100) substrates as a function of Dy concentration.

This mobility dependence was observed qualitatively on three additional substrates (MgO (111), GaN (002) and Al2O3 (006) - see extended data figures 5.6-5.8), and in each case the same 3-5x increase in mobility was found. X-ray diffraction analysis of CdO (002) rocking curves shows no dependence on Dy content until phase separation (see extended data figures 5.9-5.10). Consequently, crystalline disorder cannot explain this unusual mobility trend.
To understand this dependency, we consider the defect equilibria within the CdO-Dy system as described by the intrinsic and extrinsic defect reactions:

$$Cd_{Cd}^{\times} + O_O^{\times} \Leftrightarrow Cd_{Cd}^{\times} + V_O^{\bullet\bullet} + 2n + \frac{1}{2}O_2\ (g) \tag{5.2}$$

$$Dy_2O_3 \xrightarrow{CdO} 2Dy_{Cd}^{\bullet} + 2O_O^{\times} + 2n + \frac{1}{2}O_2\ (g) \tag{5.3}$$

CdO is an intrinsic n-type semiconductor, in which electrons originate from doubly ionized O-vacancies (equation 5.2). The carrier density depends upon the ratio of the O-vacancy formation energy to k_BT. Aliovalent cations, like Dy, populate the Cd sublattice and act as extrinsic donors (equation 5.3). The interplay between the two reactions and their cooperative equilibration is the key to understanding the present mobility trend. Dy doping pins the extrinsic electron concentration (n_e) in proportion to its molar fraction. This is established by flux ratios during growth. The intrinsic reaction is now forced to equilibrate in the presence of a potentially large n_e. By Le Chatelier's principle, the intrinsic defect reaction will be driven to the reactants side, which in turn lowers the concentration of O-vacancies.
Dysprosium on a Cd-site and an oxygen vacancy are both electron donors. However, since Dy and Cd have similar ionic radii (r_{Cd}^{2+} = 0.95 nm; r_{Dy}^{3+} = 0.92 nm [Ref.[104]]), we expect that their substitution will perturb the CdO lattice less than an oxygen vacancy. Consequently, Dy-doping creates carriers while reducing the concentration of vacant O-sites and the net lattice strain from point defects falls. Furthermore, the primary donor is now a singly positively charged cation, as opposed to a doubly positively charged vacancy. Since the impurity scattering potential scales with Z^2, at the same carrier density, there is less net scattering for $2n$ donors of charge e than for n donors of charge 2e [Ref.[105]]. Both effects will reduces carrier scattering and thus increases mobility.
This model has implications regarding additional properties, amongst them are low temperature resistivity and room temperature thermal conductivity, which must share parallel dependencies on Dy content. Figures 5.1(b) and 5.1(c) depict the temperature dependent sheet carrier concentration, n_s, and resistivity, and lead to three observations: 1) n_s is temperature independent, 2) the temperature coefficient of resistivity is positive, and 3) the residual resistivity ratio (RRR, ρ_{300K}/ρ_{20K}) increases with Dy doping. Overall, the data imply that CdO:Dy behaves as a metal and that mobility is inversely proportional to temperature; the doping level of $5x10^{19}$ cm^{-3} exhibits the highest mobility; and that adding impurity cations

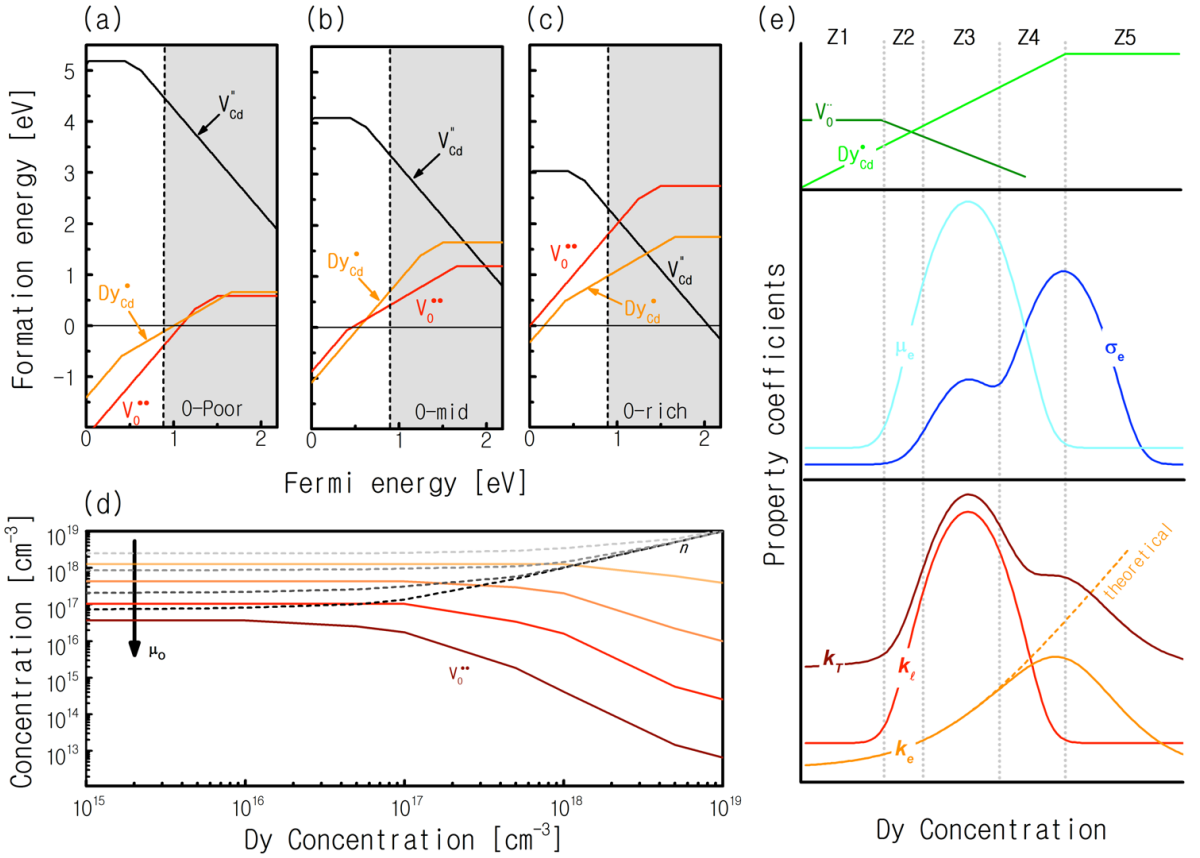

Figure 5.2 Defect formation energies as a function of Fermi level for oxygen vacancies (V_O), cadmium vacancies (V_{Cd}), and Dy substituents on the Cd site (Dy_{Cd}) in the (a) O-poor, (b) O-mid, and (c) O-rich limits. The slope of each line at a given Fermi level corresponds to the charge of the defect at that Fermi level. (d) $V_O^{\bullet\bullet}$ concentration and carrier concentration n as a function of $Dy_{Cd}^{\bullet}$ concentration for chemical potentials μ_0 in the middle range between the O-rich and O-poor extremes. (e) Idealized schematic summarizing the individual contributions of defects to the observed electronic transport in CdO:Dy. [V_O], measured thermal conductance (κ_{total}), conductivity (σ), electron mobility (μ) and the electronic contribution to the thermal conductivity (κ_e) are plotted vs. [Dy]. The Dy doping space is divided into 5 different zones, where within each zone the observed transport is regulated by a different mechanism.

reduces the number of — or/and the extent to which — lattice defects scatter electrons.
To disentangle the phenomena, thermal conductivity was measured for this film series using the thermoreflectance technique[106]. Total thermal conductivity (κ_t), and the electronic component of thermal conductivity (κ_e) are superimposed with the RRR data in Figure 5.1(d). Both κ_t and RRR exhibit two maxima. The first corresponds to [Dy] producing maximum mobility, and the second lies at a concentration approximately 10 times higher (more details later). As a final observation, all measured properties and trends degrade for the highest Dy concentration (4x10^{21} cm^{-3}) which approaches the Dy-solubility limit.
The equilibrium of defects was characterized with density functional theory (DFT) calculations to extract formation energies (at different charge states), for oxygen and cadmium vacancies (V_O,V_{Cd}), and dysprosium substituents (on the Cd site - Dy_{Cd})[107]. As an example, equation 5.4 expresses the formation energy for Dy substituted on a Cd site:

$$E_f|\mathrm{Dy}_{\mathrm{Cd}}^{q}| = E_{DFT}|\mathrm{Dy}_{\mathrm{Cd}}^{q}| - E_{DFT}|Bulk| + \mu_{Cd} - \mu_{Dy} + qE_f + E_{Corr} \tag{5.4}$$

Here, $E_{DFT}|\mathrm{Dy}_{\mathrm{Cd}}^{q}|$ is the total DFT energy of Dy on a Cd site in CdO in charge state q, and $E_{DFT}|Bulk|$ is the total DFT energy of the perfect bulk structure. The defect formation energies depend on the Fermi level, E_F, as well as the O, Cd, and Dy chemical potentials (μ_O, μ_{Cd}, and μ_{Dy}). This approach enables a particularly useful representation where defect formation energies are plotted versus E_F, as shown in Figure 5.2(a-c). Fermi energies are referenced to the valence band maximum.

The vertical dotted line at ≈0.9 eV represents the conduction band minimum (CBM), and the gray region corresponds to the energy range between the indirect and direct band gaps. The slope for each formation energy curve indicates the most energetically favorable charge state for a given E_F. For instance, Dy_{Cd} transitions from a doubly ionized ($Dy_{Cd}^{\bullet\bullet}$) to a singly ionized ($Dy_{Cd}^{\bullet}$) state in the mid-gap region, while V_O prefers a +2 charge state ($V_O^{\bullet\bullet}$) across the entire indirect band gap. At the O-poor limit, there is a substantial energy window where defect formation energies are negative, indicating CdO instability as a host.
Considering the high activity of atomic oxygen and that CdO is prepared under an oxygen plasma, it is sensible to assume defect equilibration under modest oxygen potentials (i.e., between the "O-Rich" and "O-Mid" scenarios of Figure 5.2(a-c)). Then, the implications are 1) formation energies for V_{Cd} are generally large and metal vacancies are unlikely to be the prevalent defect; 2) for all $E_F > Eg/2$ (the range of interest for n-type materials) the formation energy for Dy_{Cd} is less than that for V_O; and 3) Dy_{Cd} and V_O both increase E_F due to their donor behavior, and thus their formation energies increase with their concentration. Since oxygen vacancies prefer double- ionization, their formation energies increase twice faster than Dy_{Cd}. Consequently, doping with Dy to concentrations driving E_F to the CBM would increase the cost of electronically-compensated oxygen vacancies by more than 1 eV, dramatically reducing their concentrations.

Table 5.1 Calculated radial strains in CdO due to oxygen vacancies and dysprosium on cadmium sites

NN	# NN	$\epsilon(V_O^{\bullet\bullet})$	$\epsilon(Dy_{Cd}^{\bullet})$
1	6	0.041	-0.023
2	12	-0.023	0.011
3	8	0.004	-0.001

The CdO:Dy defect equilibrium can be calculated by self-consistently solving the mass balance equations[108]. Figure 5.2(d) shows [$V_O^{\bullet\bullet}$] and n versus [$Dy_{Cd}^{\bullet}$], for the pertinent range of μ_O keeping E_F within the indirect band gap. We restrict E_F to this range because the solver uses an effective density of states approximation — valid only for nondegenerate semiconductors. The solver predicts a reduction in V_O and an increase in n as [$Dy_{Cd}^{\bullet}$] exceeds the equilibrium [$V_O^{\bullet\bullet}$] for undoped CdO. While quantitative prediction is limited with respect to E_F (and thus carrier concentration), the trends are expected to persist in degenerate crystals considering that the Fermi level will continue to increase via the Moss-Burstein[109,110] effect (conduction band filling).

The radial strains up to the third-nearest neighbors (NN) for $V_O^{\bullet\bullet}$ and $Dy_{Cd}^{\bullet}$ were calculated by DFT to connect the reduction in [$V_O^{\bullet\bullet}$] with the hypothesized reduction in scattering and an increase in mobility. The results are reported in Table 5.1. $V_O^{\bullet\bullet}$ introduces approximately twice the radial strain on its NN as $Dy_{Cd}^{\bullet}$. Consequently, replacing oxygen vacancies with Dy as the predominant electron donor will reduce the electron and phonon scattering via reduced lattice distortion. As a premium, reducing the formal charge of the majority defect (replacing $V_O^{\bullet\bullet}$ with $Dy_{Cd}^{\bullet}$) will reduce the impurity scattering potential, thus increase electron mobility. An alternative explanation is that [V_O] remains constant, but association with Dy_{Cd} (existing in the opposite strain state) will relax the overall strain. Additional calculations showed that defect clustering was energetically unfavorable. This is reasonable: the mechanical strain relaxed by complex formation cannot overcome Coulombic repulsion between $V_O^{\bullet\bullet}$ and $Dy_{Cd}^{\bullet}$. One can now explain the trends observed in Figure 5.1(a) by considering how the population of each defect type depends on Dy, and how the changing populations of each will influence transport. The expected behavior is illustrated in Figure 5.2(e). Oxygen vacancies ($V_O^{\bullet\bullet}$), lattice thermal conductivity (κ_l), electronic thermal conductivity (κ_e) and mobility (μ_e) are represented by orange, red, green and cyan lines, respectively. Conductivity (σ) is plotted in blue, total thermal conductivity (κ_{total}) in black, and theoretical values for κ_e (from Wiedemann-Franz law) are plotted as a green-dotted line ($\kappa_{e,theory}$). We split [$Dy_{Cd}^{\bullet}$] space into five zones, each exhibiting a different mechanism to regulate transport.

ZONE 1 The population of oxygen vacancies - the majority defect - greatly exceeds [$Dy_{Cd}^{\bullet}$] and the material behaves as a n-type semiconductor.

ZONE 2 Conduction electrons from extrinsic Dy donors exceed the native value, and E_F

consequently increases. The formation energy for [$V_O^{\bullet\bullet}$] increases, [$V_O^{\bullet\bullet}$] falls sharply, and the overall radial strain falls. This leads to increased free carrier mobility and decreased phonon scattering. The conductivities rise accordingly.

ZONE 3 Electron and phonon transport reach a broad maximum. The maximum occurs because there is a diminishing reduction in overall strain and the replacement of doubly charge oxygen vacancy donors with singly charge Dy donors as the crystal lattice gets populated with additional $Dy_{Cd}^{\bullet}$. Reduced scattering in this zone is responsible for the first maxima in RRR and κ_{total} in Figure 5.1(d). At the higher end of this doping zone, the strain caused by additional $Dy_{Cd}^{\bullet}$ can no longer be compensated with a further reduction in $V_O^{\bullet\bullet}$. As a result, we observe a reduction in κ_l and μ_e with $Dy_{Cd}^{\bullet}$ concnetrations exceeding 5x10^{19} cm^{-3} .

ZONE 4 Strain, and therefore scattering, from $Dy_{Cd}^{\bullet}$ continues to increase. However, the observed properties are now governed by the steadily increasing number of free carriers. Electrical and thermal conductivity both increase to a second maximum wherein the amount of conduction electrons compensates for the decreasing carrier and phonon mobilities. As indicated by the theoretical curve ($\kappa_{e,theory}$), the electronic contribution to thermal conduction becomes increasingly important with rising $Dy_{Cd}^{\bullet}$ levels. The observed rise in RRR, κ_{total} and σ results from a steadily increasing free carrier concentration.

ZONE 5 The solubility limit of Dy in CdO is reached and Dy precipitation starts. Transport properties decrease as insulating secondary phases nucleate between highly disordered grain boundaries. The transport property trends deviate sharply from the classical semiconductor model.

The unique combination of high carrier density and high mobility makes CdO:Dy an ideal plasmonic host at mid-IR frequencies. Dielectric functions of CdO:Dy indicate that losses are low and that the plasma frequency ω_p is tunable through the entire mid-IR range (see extended data figure 5.11). To demonstrate experimentally the utility of CdO:Dy for plasmonic devices, epitaxial films were prepared on a MgO (100) substrate with Dy concentrations supporting surface plasmon polaritons (SPPs) that can be excited optically using an IR-Ellipsometer in the Kretschmann- Rather configuration. To visualize the response, the data are assembled into maps of reflected intensity against incident angle and energy. In such maps the SPP dispersion is represented by a band of minimum intensity where energy is coupling into the SPP. Figures 5.3(a) and 5.3(c) are reflectivity maps for CdO with 1x10^{20} and 3x10^{20} carriers cm^{-3} respectively. The shifting reflectivity minimum illustrates how carrier concentration can tune the SPP over the entire mid-IR range, *i.e.*, between 2500 cm^{-1} and 4000 cm^{-1}. Note that angle independent (vertical) absorption lines are caused by dark bands in the IR-elipsometers IR source (see supplementary material).

Figures 5.3(b) and 5.3(d) are companion simulations of reflectivity for the same CdO films where CdO optical properties are described by the Drude model. Close agreement is found at all angles and all energies, corroborating our approach and the theoretical treatment of the degenerate semiconductor CdO:Dy as a Drude metal. Having established the appropriateness

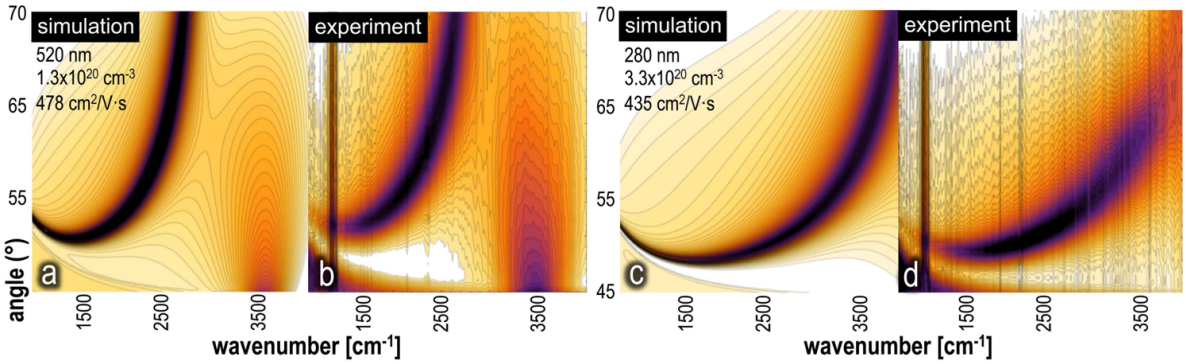

Figure 5.3 Reflectivity maps for CdO:Dy thin films recorded in the Kretschman configuration. Panels a) and c) show simulated reflectivity data using the tabulated properties as input, panels b) and d) show experimental data for CdO:Dy with $1.3x10^{20}$ and $3.3x10^{20}$ cm^{-3} respectively. In each map, the SPP dispersion can be seen as an angle dependent dip in the reflected light intensity (darker shades). The tunability of the SPP with changing carrier concentration can be seen as the shift of the reflectance dips towards higher energies. The high carrier mobility in CdO:Dy (low loss) results in the sharp absorption bands seen both in experimental and simulated data .

of treating CdO as a Drude metal, it is possible to evaluate its plasmonic performance using figures of merit based on propagation distance and field confinement. Such evaluations were demonstrated in a recent report by Naik[96] for noble metals, nitrides, and conventional transparent conducting oxides. An important conclusion of this (and other) reviews was a paucity of materials offering a combination of carrier density and mobility that yielded an appealing plasmonic response in the near-to mid-IR spectrum. The carrier density of elemental metals cannot reduced to sufficiently small densities to access the IR, while the carrier mobility of traditional CMOs are disappointingly modest. Figures 5.4(a) and 5.4(b) show the propagation distance and electric field confinement width for SPPs on CdO:Dy in air as a function of wavelength. The quotient of these values, M_1^{1D}, is the plasmonic figure of merit which accounts for the inexorable tradeoff between propagation distance and field confinement. Gold, which is the standard reference conductor for plasmonic applications, exhibits M values between 10 and 100 over its wavelength region of interest, the visible spectrum. In comparison the M values for CdO:Dy fall in the exact same range for its spectrum of interest, the near to mid-IR. In the case of CdO:Dy, the exceptionally small confinement width is responsible for this attractive performance.

Finally, Figure 5.4(d) shows calculated quality factors for 2D non-spherical CdO waveguides[111] (QLSPR) as a function of energy. The best CdO:Dy alloy presented here exceeds previously published values of nitrides and oxides by a substantial margin, and once again, QLSPR values (in their respective energy ranges) for Au and CdO are comparable. More generically, one can compare the real and imaginary components of the dielectric function in

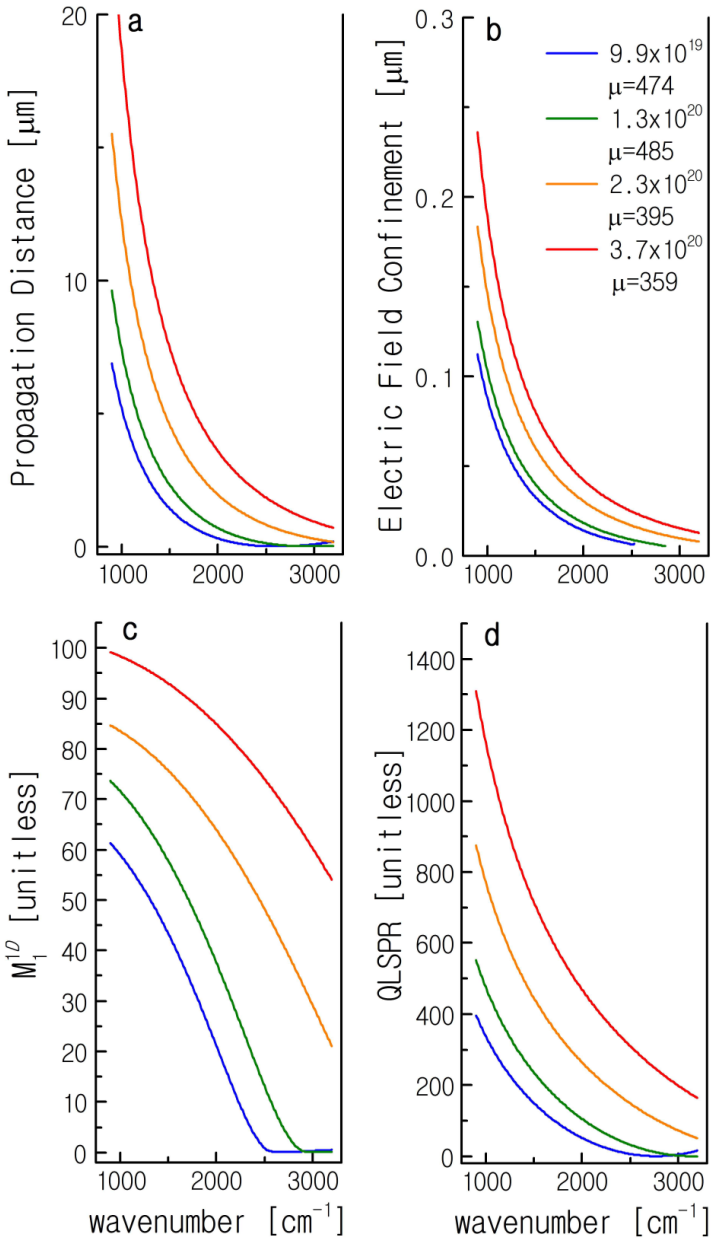

Figure 5.4 Calculated quality factors for four selected CdO:Dy alloys as a function of energy. (a) Calculated SPP propagation distances; (b) Calculated electric field confinement for the SPP; (c) Calculated M_1^{1D} figures of merit; and (d) Calculated quality factors for 2D non-spherical CdO waveguides (QLSPR).

the vicinity of the crossover frequency where ϵ_1=0. Ultimately, a small imaginary component is desirable in this range as it supports a low-loss plasma oscillation. Considering the dielectric data at crossover ensures a self-consistent comparison of materials with a range of carrier density values. The dielectric properties of CdO:Dy and other materials discussed in this article are compared in the extended data Table 5.2. In the range $-2 \leq \epsilon_1 \leq 0$ the imaginary component of CdO:Dy is substantially smaller.

Collectively, these metrics quantify CdO:Dy as a high performance plasmonic material with performance comparable to noble metals in a wavelength range that was previously inaccessible.
Optimal transport and optical properties are not the only attributes necessary for low loss plasmonics; a contributing factor for any wave guiding application is surface and interface quality. Plasmon propagation distance strongly correlates with surface roughness. A rough surface will change the dispersion relation of SPPs, and increase the loss function due to the emission of photons[16]. For Ag and Au, atomically flat surfaces are difficult to create. These elements tend to form islands in the thickness range of several nanometers required for optimal mid-IR interactions[112,113]. Furthermore, the grain size of thin metal films prepared under conditions that dissuade dewetting are typically comparable to film thickness. Consequently, thin noble metal films are populated by numerous grain boundaries and scattering polaritons, reducing the overall plasmonic performance[114,115]. In contrast, when assisted by an oxygen plasma, CdO:Dy can be grown with exceptional surface quality, even with thickness values of 400 nm. Thick films grown on MgO (100) substrates exhibit a RMS roughness of <150 pm (10 μm^2 measurement area) which translates to atomically flat surfaces. Figure 5.5 depicts a 10x10 μm atomic force microscopy (AFM) scan demonstrating the surface quality. Scanning electron microscope (SEM) images of the same surface (extended data figure 5.12) show over wider fields of view that a featureless surface morphology is sustained to thickness values exceeding 400 nm. This remarkable smoothness is attributed to the high-energy O species impacting the substrate during film growth[116].

5.3 Conclusion

In this article we introduced CdO:Dy as a promising new candidate for studying plasmonic phenomena in the mid- IR. The ability to understand and engineer coupled lattice defects leads to transport and optical properties that are IR-relevant and enabling. CdO:Dy can be reliably grown in an oxide-MBE environment, and the plasma frequency is tunable over a wide energy range in the mid-IR. The resulting losses are low due to very high (>300 $cm^2V^{-1}s^{-1}$) carrier mobility over the carrier concentration range of interest, and the surfaces are extremely smooth. This desirable collection of plasmonic properties in CdO:Dy can enable future generations of plasmonic devices operating in the mid-IR. In general, the results

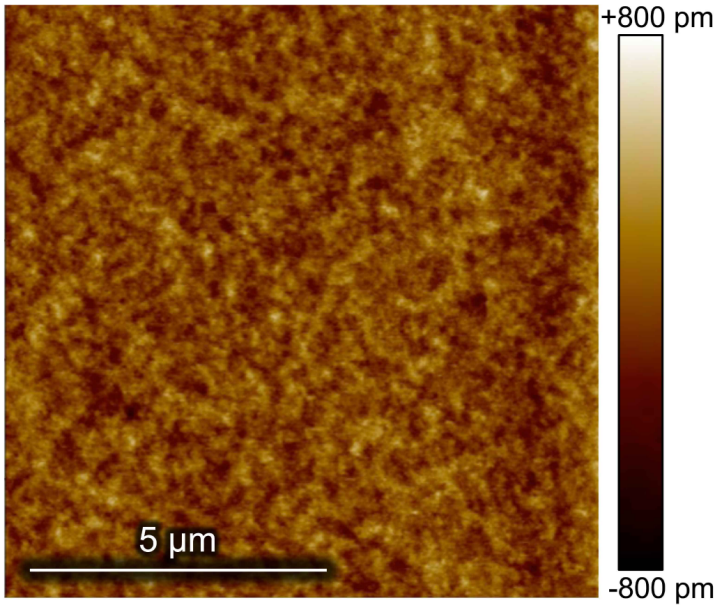

Figure 5.5 AFM topography scan of as-grown CdO:Dy demonstrating the atomically flat growth habit of CdO:Dy on MgO (100) substrates. The observed RMS roughness is <150 pm.

suggest that Fermi level pining can be used to optimize the transport properties in metal oxide systems and, potentially, other semiconductor materials.

5.4 Methods

CdO was grown in an oxide MBE system using a custom-built inductively coupled 300W RF oxygen plasma gun. Cd was deposited from a metal effusion cell and doping was achieved through evaporation of metallic Dy from a dopant cell. Employed Cd fluxes ranged from 2-5x10^{13}[at cm^{-2} s^{-2}] and the Dy flux was varied from 1x10^{8}-3.5x10^{12} [at cm^{-2} s^{-2}] for the doping series. A typical deposition process involves an O background pressure of 3x10-6 torr (230W oxygen plasma), substrate temperatures of 350°C and an atomic O flux of 1x10^{14} [at cm^{-2} s^{-2}] resulting in an average growth rate of 0.9nm/min.
Reflectivity data was recorded using a Woollam®IR-VASE ellipsometer with a custom built sample stage in the Kretschmann-Raether configuration. A calcium fluoride (CaF_2) prism was used to couple light into the samples, and good optical contact was ensured by applying an index matching fluid (Cargille Series M 1.720). Reflectivity data was recorded for p- and s-polarized light and is plotted as R=r_p/r_s.
Room temperature transport data was measured with the Van der Pauw technique using an Ecopia HMS-3000 Hall Measurement System. T-dependent transport measurements were

carried out using a custom built transport probe in a Quantum Design MPMS. Thermal conductivity data was acquired by TDTR measurements, an optical pump-probe experiment which utilizes a train of ultrashort laser pulses to induce a modulated heating event on the surface of the sample. For these measurements, the surface of the various CdO samples was coated with thin metal films. These act as a transducer to relate the absorbed pump energy to the temporal temperature change on the surface of the sample via the thermoreflectance change monitored in the time domain (see supplemental material for further details).
DFT calculations were performed with the Vienna Ab initio Simulation Package (VASP) with a plane-wave basis set, as implemented in VASP 5.3[117,118] using the hybrid exchange correlation functional of Heyd, Scuseria, and Ernzerhof (HSE06). The defect calculations were based on 64-atom supercells with a 2x2x2 k-point mesh, with a relaxation shell out to the third nearest neighbor around the defect site. Finite-size interactions for the charged defects were accounted for using the *sxdefectalign* code by Christoph Freysoldt. (see supplemental material for further details).
Although Cd interstitials have been previously considered as sources for carriers, recent theoretical work[119] demonstrates that these are energetically disfavorable, and therefore they have not been considered here. The HSE06 hybrid exchange-correlation functional[120,121] including a fraction (0.25) of short-range Hartree-Fock exact exchange, was employed in these calculations. This functional more accurately represents the structural and electronic properties of bulk CdO[119].
In one limiting condition (the O-rich extreme: the upper limit of μ_O and the lower limit of μ_{Cd}) μ_O is referenced to molecular O and μ_{Cd} is set such that $\mu_{Cd} = \mu_{CdO} - \mu_O$. In the opposite limiting condition (the O-poor extreme, the upper limit of μ_{Cd} and lower limit of μ_O) μ_{Cd} is referenced to metallic Cd, and μ_O is set such that $\mu_O = \mu_{CdO} - \mu_{Cd}$. μ_{Dy} accounts for the Dy_2O_3 solubility-limiting phase. E_{Corr} corrects for finite size effects of the unit cell and is determined through the method of Freysoldt et al[122,123].

5.5 Acknowldegments

SF and JPM gratefully acknowledge support of this work by NSF grant CHE-1112017. The NSF grant DMR-1151568 supported the DFT contributions. We would further like to acknowledge Dr. Efimenko and Dr. Genzer (NCSU, CBE) for granting us access to the IR-Ellipsometer. Sandia National Laboratories is a multi-program laboratory managed and operated by Sandia Corporation, a wholly owned subsidiary of Lockheed Martin Corporation, for the U.S. Department of Energy's National Nuclear Security Administration under contract DE-AC04-94AL85000. The thermal conductivity measurements were supported by Air Force Office of Scientific Research under AFOSR Award No. FA9550-14-1-0067 (Subaward No. 5010-UV-AFOSR-0067) and the ONR Young Investigator Program (N00014-13-4-0528). S.C. acknowledges the Duke Center for Materials Genomics and partial support by ONR (MURI

N00014-13-1-0635).

5.6 Author Contributions

E.S., S.F. and J-P. M. proposed the concept and experiments with support by S.C. C.T.S. and E.S developed the MBE deposition and doping technique for the growth of CdO:Dy. E.S. led the experimental/analytical efforts with support from C.T.S, B.F.D, P.E.H, P.A.S, A.L.S, and J.F.I. The DFT simulations and analysis of theoretical results were performed by D.L.I., B.E.G. and J.S.H. All authors mentioned above discussed and contributed to the paper.

5.7 Extended Data

Table 5.2 A comparison of plasmonic materials discussed in this article. The crossover frequency ϵ_1=0 describes the upper frequency limit for plasmonic phenomena in a material. The loss tangent ϵ_2 was summarized at and below (ϵ_1=-2) the crossover frequency to allow for a comparison of losses independent of the carrier concentrations and thus the supported plasmon wavelengths.

Material	Carriers [cm^{-3}]	mobility [$cm^2V^{-1}s^{-1}$]	ϵ_1=0 [cm^{-1}]	ϵ_2 at ϵ_1=0	ϵ_2 at ϵ_1=-2
CdO:Dy	9.94x10^{19}	474	2770	0.19	0.3
CdO:Dy	3.70x10^{20}	359	5350	0.13	0.2
AZO (2 wt%)[96]	7.2x10^{20}	47.6	6970	0.21	0.39
ITO (10 wt%)[96]	7.7x10^{20}	36	7122	0.69	1.29
GaAs[124]	1x10^{19}	1000	1005	1.26	1.63
InAs[100]	7.5x10^{19}	360	1785	2	2.6

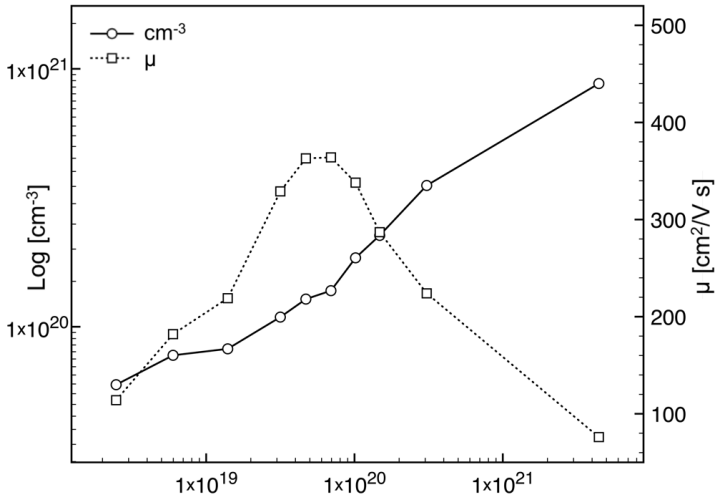

Figure 5.6 Transport data for CdO:Dy grown on MgO (111) substrates summarizing carrier conc. (cm^{-3}) and carrier mobility (μ) as a function of [Dy].

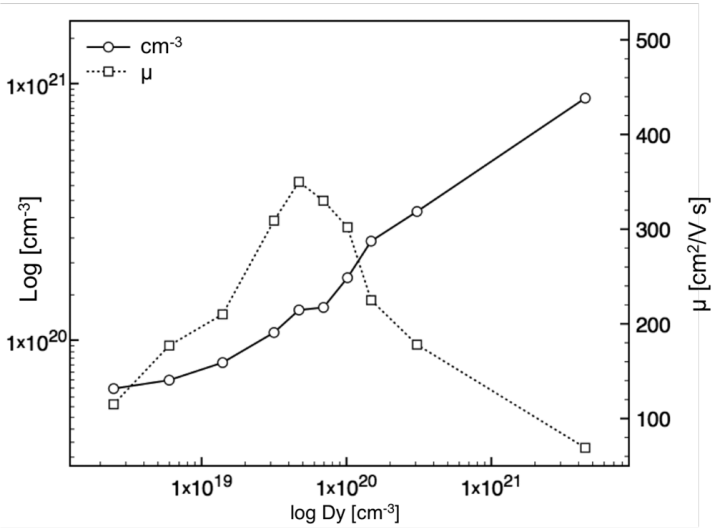

Figure 5.7 Transport data for CdO:Dy grown on GaN (002) substrates summarizing carrier conc. (cm^{-3}) and carrier mobility (μ) as a function of [Dy].

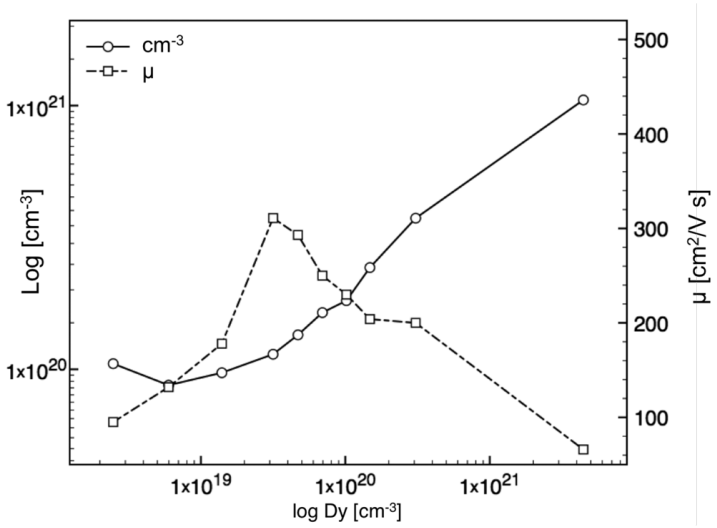

Figure 5.8 Transport data for CdO:Dy grown on Al_2O_3 (006) substrates summarizing carrier conc. (cm^{-3}) and carrier mobility (μ) as a function of [Dy].

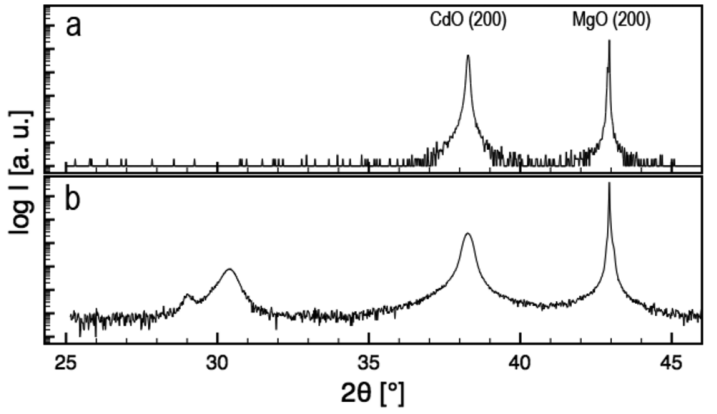

Figure 5.9 XRD diffraction patterns depicting heteroepitaxial growth of CdO on MgO (100) substrates. a) Diffraction pattern for single phase CdO:Dy samples. This growth habit is exemplary for Dy contents from 0-5x10^{21} cm^{-3} . b) Growth habit for samples with Dy content >5x10^{21} cm^{-3} . The precipitation of additional complex oxide phases can be seen around 30°2Θ.

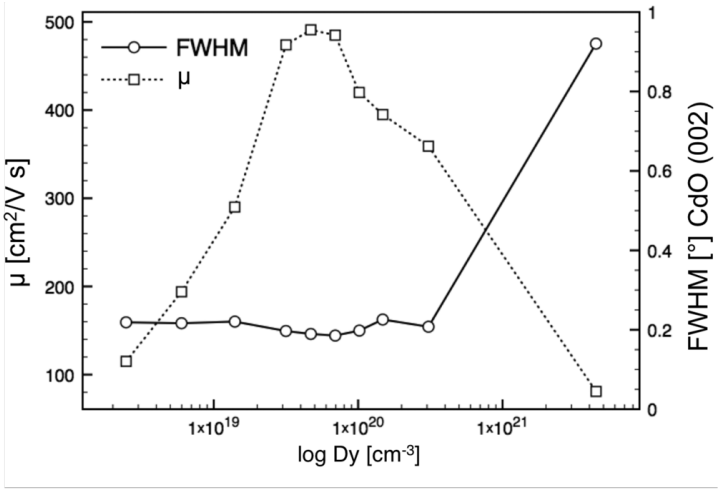

Figure 5.10 FWHM of X-ray omega rocking curves recorded for CdO:Dy grown on MgO (100) substrates compared to the measured carrier mobilities as a function of [Dy]. No significant change in crystal quality is observed over the high mobility range, the deteriorating FWHM and mobility at the highest [Dy] corresponds to the onset of phase separation as the solubility limit of Dy in CdO is reached

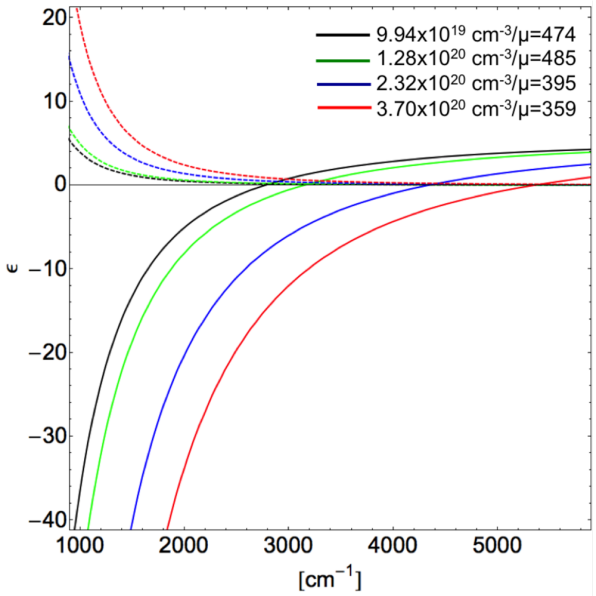

Figure 5.11 Calculated real (solid lines) and imaginary (dashed lines) dielectric functions for selected CdO:Dy alloys. The compositionally tunable SPR in CdO:Dy can be seen by the changing cross-over frequency of the real dielectric function (the energy at which the real part of ϵ becomes negative) for different carrier concentrations. In addition, the loss tangent (imaginary part of ϵ) exhibits very low values across the mid-IR energy range for all carrier concentrations depicted, indicating the potential for low loss plasmonic resonances in this material.

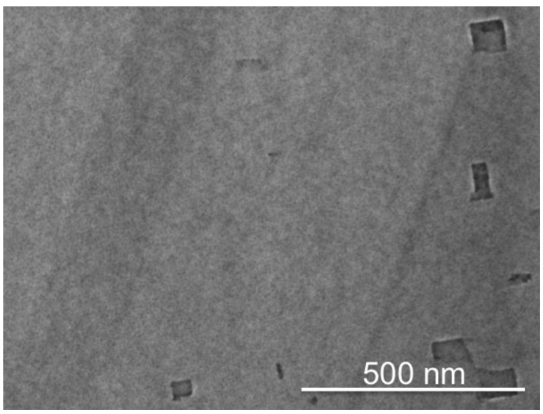

Figure 5.12 High resolution SEM surface image depicting the cubic growth habit in atomically smooth CdO:Dy films.

Chapter 6

SPR mode mixing for enhanced infrared absorption

Edward Sachet[1], Stefan Franzen[2] and Jon-Paul Maria[1]

[1]Department of Materials Science, North Carolina State University, Raleigh, North Carolina 27695, USA
[2]Department of Chemistry, North Carolina State University, Raleigh, North Carolina 27695, USA

6.1 Introduction

Surface Enhanced Infrared Absorption (SEIRA) has first been described by Harstein et al in a 1980 publication[125]. It was found that the infrared absorptions of thin organic films could be enhanced by evaporation of a noble metal such as silver or gold on top prior to the measurement. The phenomenon did not gain a lot of attraction until the end of the 1980's into the beginning of the 1990's when Osawa and Nishikawa commenced fundamental studies to explore the origin of this enhancement phenomenon[126–128]. It was found, that in particular small noble metal islands in the size range of tens of nanometers result in a significant SEIRA effect in their vicinity[129]. Subsequently, the technique was quickly established for surface analysis of semiconductors, glasses and polymers[130].

The significant enhancement of the obtainable IR signature of any adsorbed or chemisorbed organic substance allowed for very short sampling times, which enabled novel in-situ studies.

SEIRA enabled the in-situ study of self assembly and ordered orientation of organic molecules on metal surfaces[131–133], the in-situ study of chemical oxidation on metal surfaces[134,135] or time resolved studies of electrochemical reactions on metal electrodes[136–138]. Fundamentally, the SEIRA effect is attributed to two phenomena, an electromagnetic and a chemical enhancement mechanism. The electromagnetic effect can be attributed to the excitation of plasmon modes in the metallic particles. The strong electromagnetic field enhancement caused by LSPR (see chapter 1) can act as an amplifier for the electromagnetic absorption of the organic molecules investigated with SEIRA. The experimentally and theoretically established surface selection rules[139], as well as the influence of particle size, aspect ratio and continuity of the metal particles[129] agree well with EM-theory. Most of the experimentally found SEIRA features can be modeled with sufficient accuracy assuming electromagnetic interactions exclusively.

However, differences in enhancement power have been seen when comparing the SEIRA signals of chemisorbed and physisorbed molecules on metal surfaces. It is known, that the absorption cross section of chemisorbed molecules is significantly larger then those of purely condensed overlayers[140]. The chemical enhancement is theoretizised to involve charge transfer between the metal and the chemisorbed species[141,142] and subsequent resonances between molecular vibrations and electronic transitions within the metal[143–146].

As of now, it is still an active area of research which process dominates and to what extent they contribute to SEIRA[147]. One of the complications to resolve this question is the fact that neither of the mechanisms can be isolated. All fundamental studies of SEIRA involve condensed matter as analyte in direct physical contact with metal particles. Thus, a physi- or chemi-sorbtion of the analytes is always present. In the gas phase however, significant analyte surface interactions can be excluded and SEIRA studies of gas phase species would allow to study the electromagnetic contribution to SEIRA without any chemical effects present.

The development of a high mobility, low loss mid-IR plasmonic host material allows, for the first time, the study of gas phase molecules in the vicinity of the electromagnetic filed created by a SPR. By studying a single absorption mode, the interaction between the surface plasmon (thus the electromagnetic field) and the infrared absorber (gas molecule) can be studied. Furthermore, the gas phase allows for easy variation of analyte concentration via partial pressures and total pressure in the experiment.

6.2 Modeling an infrared absorption as a dielectric function

In order to simulate the interaction of SPPs with IR-absorption band using the simulation techniques described in this work, the absorption event has to be described as a dielectric function. Upon doing so, it can be used as background dielectric function for SPR simulations using the code described in chapter 3. The absorption event can be a gas phase absorption of polar, gaseous molecules such as CO_2 or N_2O.
Reference data for infrared absorption can be found in databases such as HITRAN[148]. The

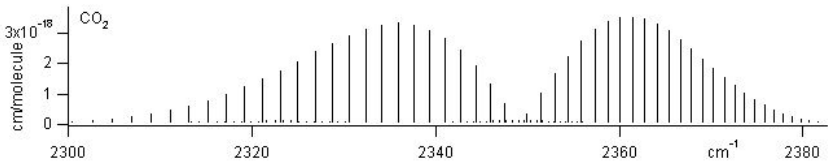

Figure 6.1 HITRAN data for CO_2

data recorded in these databases is typically comprised of energy vs. absorbance cross section for a given species in very high resolution, visualizing even the rotational components of the absorbance spectra (see figure 6.1 as example for the main (ν_3) absorption mode of CO_2 gas). Here, a method is derived to connect this absorbance cross section to a pressure dependent dielectric function that can be used for simulation purposes: We start by describing a single absorption event as a Lorentzian:

$$\epsilon(\omega) = \epsilon_1 - i\epsilon_2 = \epsilon_0 + \frac{A\omega_0\Gamma}{\omega_0^2 - \omega^2 - i\Gamma\omega} \tag{6.1}$$

with:

ϵ_1 Real part of the dielectric function

ϵ_2 Imaginary part of the dielectric function

ϵ_0 Background dielectric constant (e.g. 1.00054 in air)

ω_0 Resonance frequency of the Lorentzian

A Amplitude of the Lorentzian

Γ Damping term of the Lorentzian

On resonance (at ω_0) this can be reduced to:

$$\epsilon(\omega_0) = \epsilon_1 - i\epsilon_2 = \epsilon_0 + iA \tag{6.2}$$

Now we need to connect the Lorentzian amplitude factor A with a measured absorbance or molar absorptivity coefficient. This can be done through the optical constant k which relates to absorption through:

$$\alpha = \frac{4\pi k}{\lambda} \rightarrow k = \frac{\alpha\lambda}{4\pi} \tag{6.3}$$

with:

α Absorption coefficient

λ wavelength

k absorption loss

Assuming an ideal gas, the absorption coefficient can further be defined as:

$$\alpha = \frac{qP}{k_B T}\sigma_v \tag{6.4}$$

with:

q Mixing ratio

P Pressure

k_B Boltzmann constant

T Temperature

σ_v Absorption cross-section [cm^2/molecule]

The magnitude of σ_v can be found in absorbance databases, such as HITRAN. Now we can define k using the absorption cross-section and equation 6.3. Further we know the connection between k and the dielectric function with:

$$k = \sqrt{\frac{-\epsilon_1 + \sqrt{\epsilon_1^2 + \epsilon_2^2}}{2}} \tag{6.5}$$

On resonance (equation 6.3), this reduces to:

$$k = \sqrt{\frac{-\epsilon_0 + \sqrt{\epsilon_0^2 + A^2}}{2}} \tag{6.6}$$

Describing k with equation 6.3 we yield:

$$\frac{\alpha\lambda}{4\pi} = \sqrt{\frac{-\epsilon_0 + \sqrt{\epsilon_0^2 + A^2}}{2}} \tag{6.7}$$

This can be rearranged to calculate A:

$$A = \sqrt{(\frac{\alpha^2\lambda^2}{8\pi^2} + \epsilon_0)^2 - \epsilon_0^2} \tag{6.8}$$

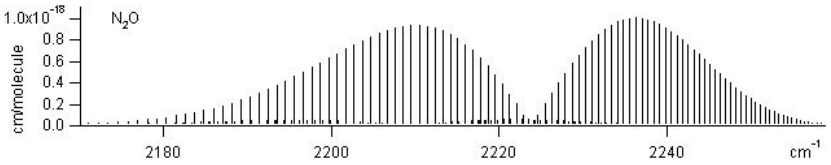

Figure 6.2 HITRAN N_2O absorption data of the ν_3 mode

This allows us to estimate the amplitude of a Lorentzian describing the absorption event using tabulated absorption cross-section data and the assumption of ideal gas behavior.

6.3 Modeling the bond-stretch (ν_3) mode of N_2O for SPR mode-mixing simulations

For practical reasons, N_2O gas has been used as test species for all mode mixing experiments. Due to the open beam path of the IR-VASE, common atmospheric gases such as CO_2 or H_2O are omnipresent in the background and the experimental background is constantly changing due to the presence of the operator in the same room. A dynamically changing background does severely interfere with high-resolution spectroscopy, especially if the species under investigation is part of the changing background. This is the reasons why initial experiments using CO_2 have been stopped and the species of interest has been replaced with N_2O. The N_2O ν_3 absorption does not overlap with any other atmospheric gases and thus is an excellent candidate to study SPR mode mixing with absorption bands. Figure 6.2 depicts the N_2O ν_3 absorption at 2220 cm^{-1} as recorded in the HITRAN database.

It can be seen that this data shows the typical line shape for gas absorption, with two absorbing maximums and pronounced asymmetry. The reference data is high-resolution, revealing the rotational energy levels within the absorption mode. For the purpose of this work, we will not simulate to this high resolution, rather we will try to describe the envelope of the absorption formed by all rotational transitions. Due to the two absorbance maxima, two overlapping Lorentzians will be used. To account for the asymmetry of the mode, a method outline by Stancik and Brauns will be modified for Lorentzians[149]. This method allows to break symmetry for the Lorentzian by replacing the constant width parameter with a smoothly varying function with energy dependency. The Mathematica code that has been written to model a dielectric function of N_2O and to use it for SPR reflectivity simulations can be found in the appendix B.

Using the method outlined above, a pressure (thus concentration) dependent dielectric function for the N_2O ν_3 mode can be calculated. Figures 6.3 and 6.4 depict the calculated functions for N_2O pressures of 20, 40, 60 and 80 psi above ambient. Assuming ideal gas behavior, this pressure series corresponds to a linear increase in N_2O concentration. The

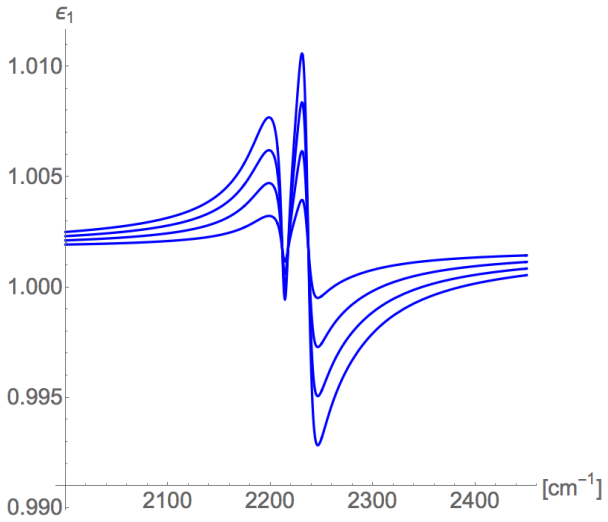

Figure 6.3 Real part of the pressure dependent N_2O dielectric function for pressures of 20, 40, 60 and 80 psi. An increasing amplitude with pressure (concentration) can be seen.

increasing amplitude with pressure in the real part, as well as the increasing loss tangent with increasing pressure can be clearly seen. These exact functions have been used in the modeling of the experimental data.

6.4 Interaction of absorption bands with the SPP dispersion

With the absorber in the dielectric environment of the SPR active material well-defined, the potential interaction of the SPP dispersion with this absorber can be theoretically investigated. First, the SPR host material has to be defined. Experimentally, measurements were carried out with CdO:Dy thin films, which therefore will be used in this theoretical description. Computationally, every Drude like material can be investigated with the procedure outline here. The films used have a free carrier concentration of 3.4x10^{20} cm^{-3} , a carrier mobility of 300 cm^{2}V^{-1}s^{-1} , high frequency dielectric constant of 5.5 and a relative electron mass of 0.21. Using the dispersion relation equation for the SPP dispersion and assuming a constant, dielectric environment with ϵ_d=1.00087 we can calculate the dispersion relation for SPPs supported by this particular CdO:Dy material. Using equation 6.9 we yield the dispersion depicted in figure 6.5.

$$k = k_{SPP} = \frac{\omega}{c}\sqrt{\frac{\epsilon_{Cdo:Dy} \cdot \epsilon_d}{\epsilon_{Cdo:Dy} + \epsilon_d}} \tag{6.9}$$

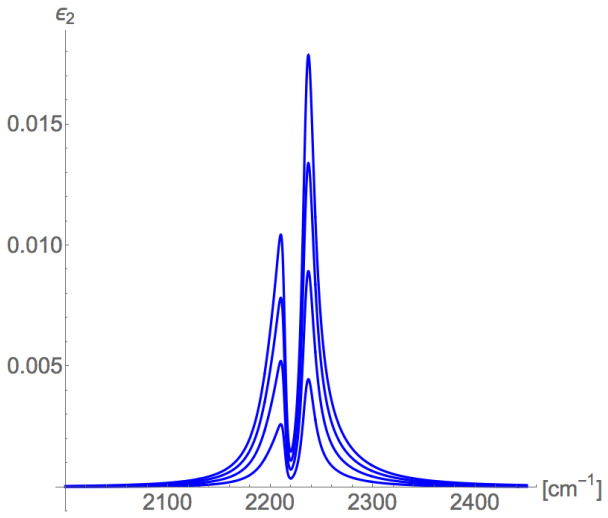

Figure 6.4 Imaginary part of the pressure dependent N_2O dielectric function for pressures of 20, 40, 60 and 80 psi. An increasing loss tangent with pressure (concentration) can be seen.

The typical dispersion shape for Drude metals as SPP materials can be found. As of now, the dielectric has always be considered as non-dispersive, with no frequency dependence of it's dielectric constant. However, for an absorption event, such as a gas absorption, this condition is no longer true, and a frequency dependence has to be accounted for. Replacing the constant ϵ_d with the dielectric function that were modeled for N_2O at various pressures (see figure 6.3), equation 6.9 now changes to:

$$k = k_{SPP} = \frac{\omega}{c}\sqrt{\frac{\epsilon_{Cdo:Dy} \cdot \epsilon_{N_2O}}{\epsilon_{Cdo:Dy} + \epsilon_{N_2O}}} \tag{6.10}$$

where ϵ_{N_2O} is now a function of frequency $\epsilon_{N_2O} \mapsto \epsilon_{N_2O}(\omega)$. Figure 6.6 depicts a comparison between the CdO:Dy SPP dispersion resulting from a static ϵ_d and the dispersive $\epsilon_{N_2O}(\omega)$, assuming a N_2O pressure of 20 psi above ambient. It can clearly be seen, that the dispersive $\epsilon_{N_2O}(\omega)$ strongly modifies the resulting SPP dispersion. Furthermore, we can study the influence of N_2O pressure (concentration) on the modification of the predicted real part of the SPP dispersion. Figure 6.7 depicts an analogous calculation for 20, 40 and 60 psi of N_2O pressure in comparison to the unmodified SPP dispersion. The dielectric functions for N_2O depicted in figures 6.3 and 6.4 directly map onto the SPP dispersion relation as expected from equation 6.10. This implies, that from a theoretical standpoint, a coupling (mode mixing)

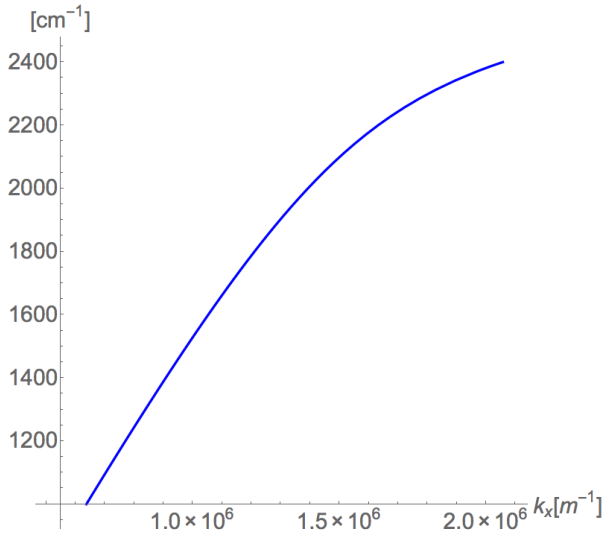

Figure 6.5 SPP dispersion for CdO:Dy in air; The assumed CdO:Dy Drude parameters are: n=3.4x10^{20} cm^{-3} , μ=300 cm^{2}V^{-1}s^{-1} , ϵ_∞=5.5 and m_e=0.21

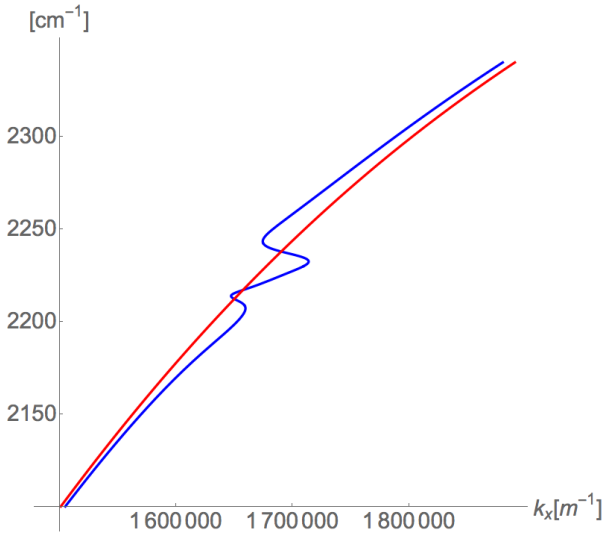

Figure 6.6 SPP dispersions for CdO:Dy in a static and dispersive environments ; The red trace assumes a dispersive $\epsilon_{N_2O}(\omega)$ compared to the static case in blue. A strong warping of the SPP dispersion can be found

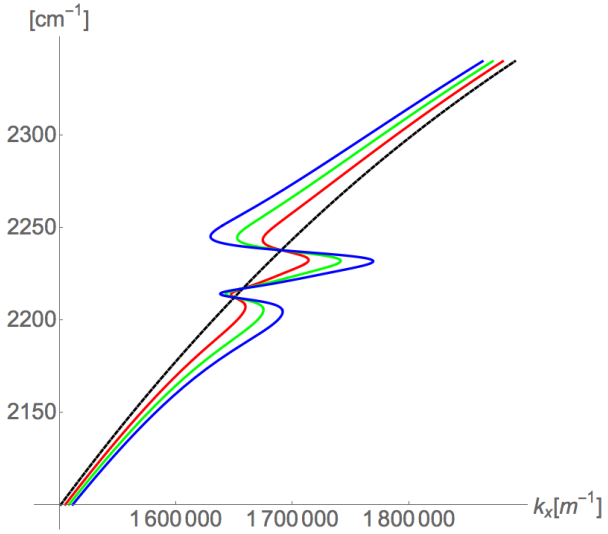

Figure 6.7 SPP dispersion (real part) with varying N_2O pressure; 20 (red), 40 (green) and 60 (blue) psi of N_2O pressure and the effects on the SPP dispersion in comparison to the SPP in a static (black, dashed) dielectric environment ϵ_d

between the SPP dispersion and the N_2O absorption band is expected. The magnitude of this coupling scales with the magnitude of the absorption amplitude, thus the concentration of the N_2O in the immediate environment of the CdO:Dy film. If we consider the imaginary (loss tangent) part of the SPP dispersion, we can see that the SPP loss tangent too is being modified by the absorption band. Figure 6.8 depicts calculated loss tangents for the same pressure series of N_2O. The SPPs loss tangent increases at the absorption energies of N_2O, and the magnitude scales with the assumed N_2O pressure, thus concentration.

Assuming no chemical interaction between N_2O and the CdO:Dy surface, this system is an ideal candidate to study the purely electromagnetic interaction between a SPP and an absorption medium in the vicinity of the interface.

6.5 Experimental

To record data of potential mode mixing, the IR-VASE setup described in chapter 2.3.6 has been used with certain modifications: Samples have been mounted on the flow cell sample holder (see appendix A) with the output gas line closed off. The input gas line was connected to a portable N_2O tank. This allowed to flood the flow cell sampling chamber with controlled, static pressures of N_2O while the SPR-samples active surface was exposed to this controlled

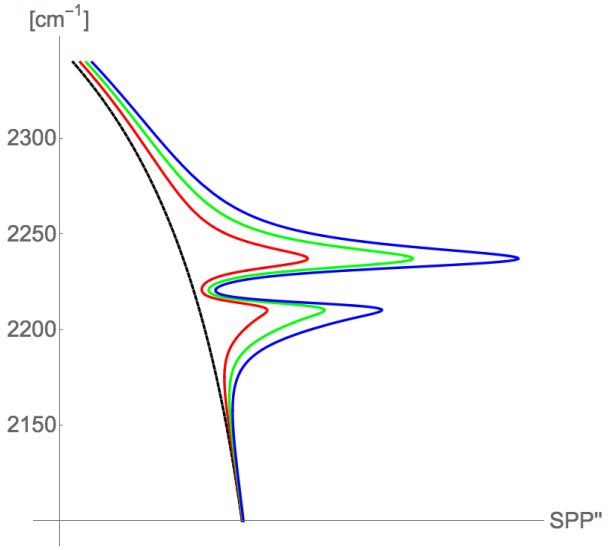

Figure 6.8 SPP dispersion (loss tangent) with varying N_2O pressure; 20 (red), 40 (green) and 60 (blue) psi of N_2O pressure and the effects on the SPP loss tangent in comparison to the SPP loss in a static dielectric environment ϵ_d (black, dashed)

atmosphere. Despite a slightly more complicated setup, the remaining procedure to record SPR maps was carried out using the automation features of the IR-VASE, as for all other SPR map scans in this work.

The SPR active thin film grown for this work uses a CdO:Dy composition with the following properties: n=3.4x10^{20} cm^{-3} , μ=300 cm^{2}V^{-1}s^{-1} , ϵ_∞=5.5, m_e=0.21 and thickness of 175 nm. The resulting SPR map (without gas sample present), spanning incidence angles of 45-50°can be seen in figure 6.9 . Since the potential mode mixing only occurs around the energies of the N_2O absorption mode (see figure 6.2), all further maps will be represented in a narrow energy range from 2100-2350 cm^{-1}. Figure 6.10 depicts a zoomed in SPR map of the same sample (no N_2O present) in the narrow energy band of interest. It can be seen that the SPP dispersion in this energy window is smooth, follows the predicted SPP dispersion and does not exhibit any interactions with the surrounding dielectric. This represents the baseline for all mode mixing experiments. Once N_2O is introduced in the flow cell, theory predicts the observed SPP dispersion to warp and change significantly with pressure.

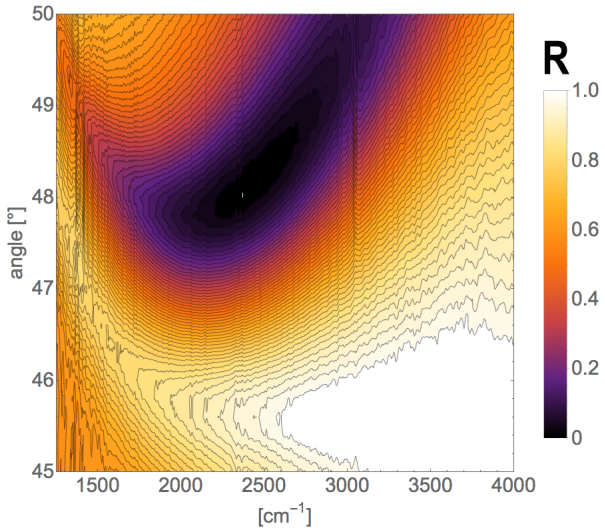

Figure 6.9 SPR map of the CdO:Dy thin film for mode-mixing experiments; properties: n=3.4x10^{20} cm^{-3} , μ=300 cm^{2}V^{-1}s^{-1} , ϵ_∞=5.5, m_e=0.21 and thickness of 175 nm.

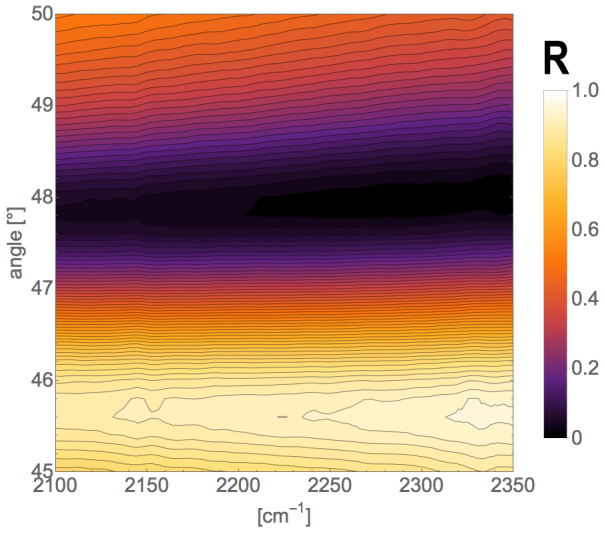

Figure 6.10 SPR map of the CdO:Dy thin film for mode-mixing experiments, zoomed to the energy range of interest; properties: n=3.4x10^{20} cm^{-3} , μ=300 cm^{2}V^{-1}s^{-1} , ϵ_∞=5.5, m_e=0.21 and thickness of 175 nm.

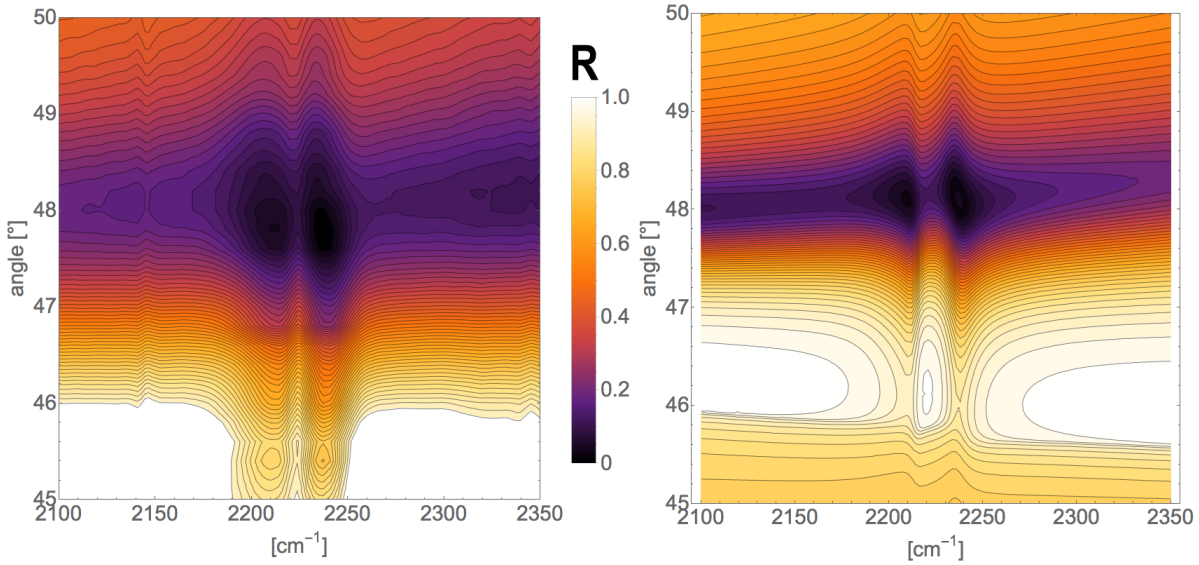

Figure 6.11 Low resolution (4 cm^{-1}) comparison SPR maps for 20 psi N_2O exposure; experimental reflectivity data (left), compared to simulated data (right)

6.6 Results

The initial experiment exposed the CdO:Dy film to 20 and 40 psi of N_2O pressure. The maps were recorded with the standard resolution settings of 4 cm^{-1} energy resolution and an angular resolution of 0.2°. Companion simulations were calculated using the calculated N_2O dispersion and the CdO:Dy film properties used in the actual experiments. Figures 6.11 and 6.11 show a comparison of theory to experiment, for 20 and 40 psi of N_2O pressure. The initial experimental data revealed the limitations of the standard map recording settings. A strong, pressure dependent interaction between the SPP dispersion and the N_2O absorption band is revealed.

However, the angle and energy granularity of the recorded data, in combination with the applied contouring function creates data that potentially alters line shapes (the data is only recorded every 0.2°, the intervals are interpolated by the contouring function) and prevents a thorough comparison to simulated mode-mixing effects. In consequence, the angle resolution was increased to 0.1°and the energy resolution was set to 1 cm^{-1}. Unfortunately, this imposes an extra constraint on the experimentally acquired data sets: The absolute time for a single map recording can not exceed 60 minutes. After one hour, the index matching fluid that ensures good optical connection between the prism and the backside of the sample will evaporate, thus the optical connection is lost. The higher resolution scans take significantly longer (4x per linescan) with an overall increase of line density. Due to the very fine angular

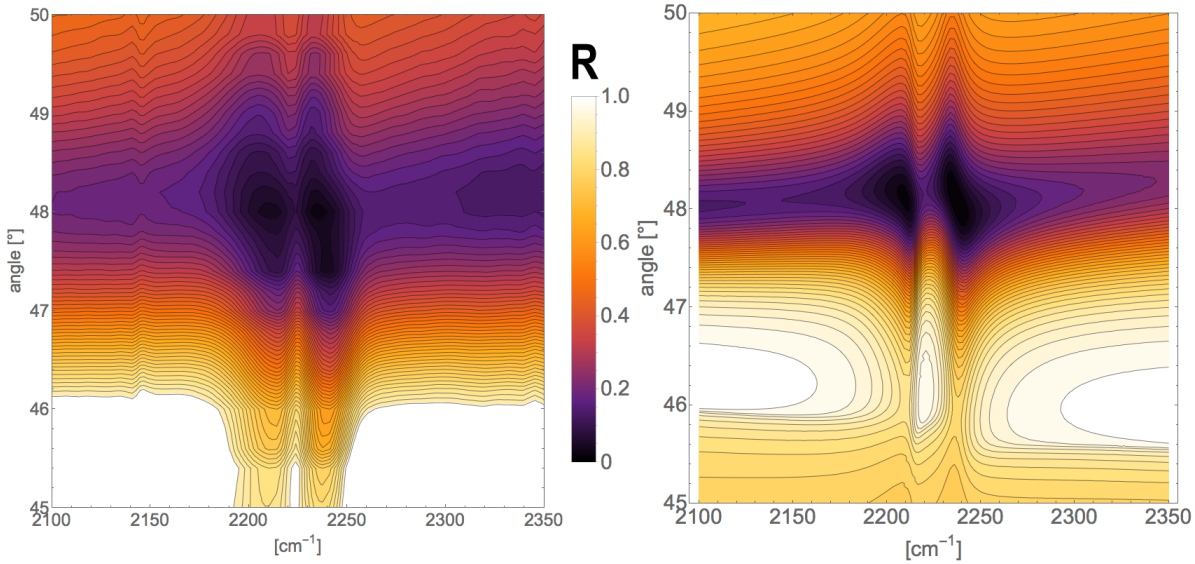

Figure 6.12 Low resolution (4 cm^{-1}) comparison SPR maps for 40 psi N_2O exposure; experimental reflectivity data (left), compared to simulated data (right)

and energy resolution, a re-application of the matching fluid and continuation of a map scan would result in data that cannot be stitched without creating significant artifacts.

Therefore, the mapped area had to be limited between 47-49.5°in order to not exceed the maximum measurement time. The following series of images (figures 6.13 - 6.13) depicts the results of the high resolution map scans over a narrower angular range in comparison to simulated data. The applied N_2O pressures range from 20-80 psi. The simulation parameter space was held constant. Increasing the angular and energy resolution clearly results in a sharper representation of the mode-mixing effect. A strong dependence with N_2O pressure can be found.

6.6.1 Comparison to conventional gold based ATR-SEIRA

To enable a comparison to established SEIRA technologies, a gold reference sample was prepared. 5 nm of gold have been deposited on a MgO (100) substrate. This allows for a comparative measurement using the exact same experimental details and measurement procedure, with the only change being the CdO film replaced by a gold layer.

Figure 6.17 depicts a 2 μm^2 AFM surface scan of the gold film. The film depicts a granular structure (RMS roughness 1.4 nm), which is typical for thin gold films. From a SEIRA perspective, the roughness and the overall grain size are suitable for strong absorption enhancement[129]. ATR-reflectivity data was recorded from this thin film using the flow cell sample stage, while the gold film was exposed to 60 psi of N_2O. Figure 6.18 depicts the

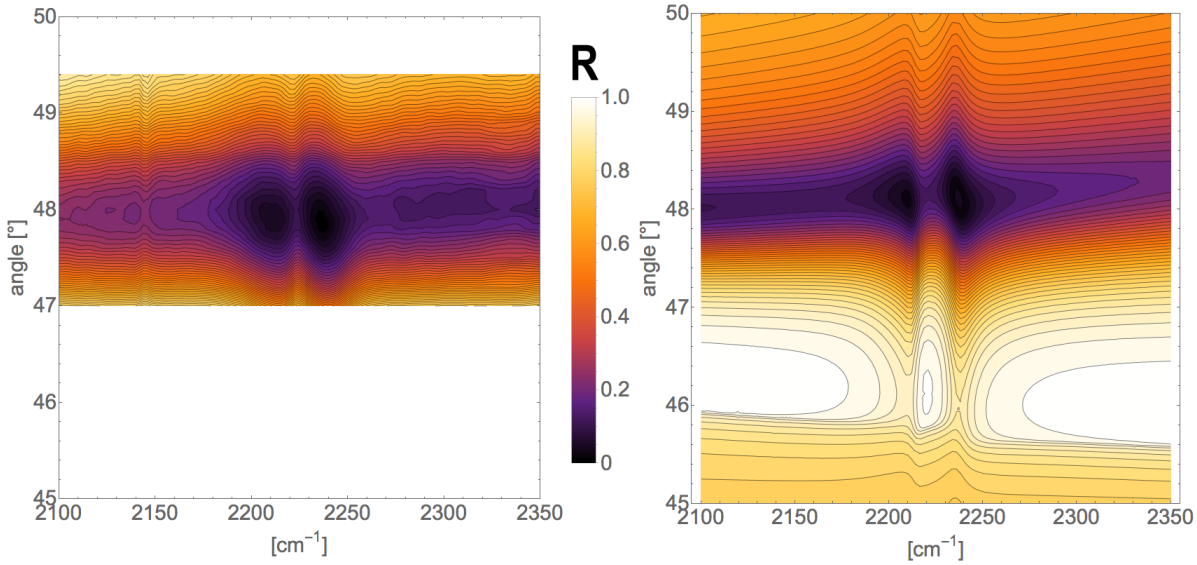

Figure 6.13 High resolution (1 cm^{-1}) SPR map comparison between measurement and theory for 20 psi of N_2O exposure; experimental reflectivity data (left), compared to simulated data (right)

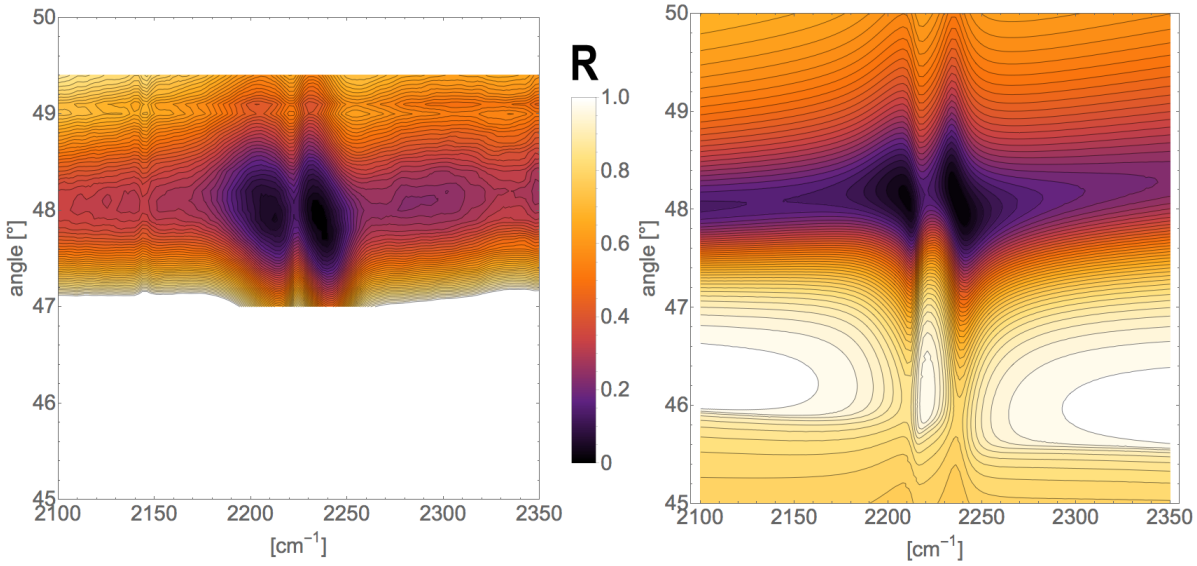

Figure 6.14 High resolution (1 cm^{-1}) SPR map comparison between measurement and theory for 40 psi of N_2O exposure; experimental reflectivity data (left), compared to simulated data (right)

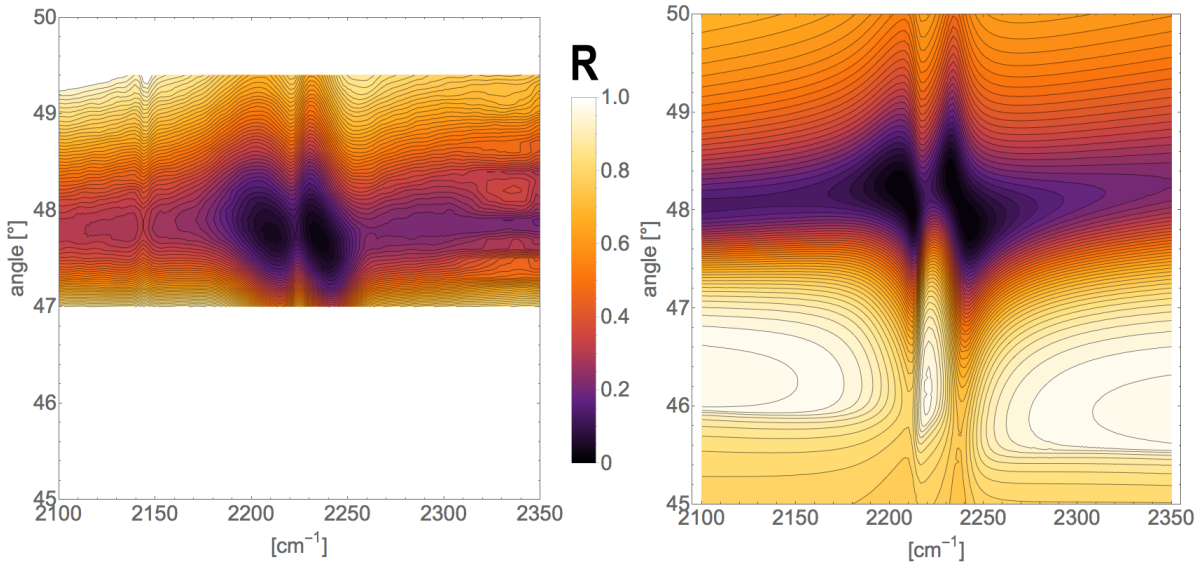

Figure 6.15 High resolution (1 cm^{-1}) SPR map comparison between measurement and theory for 60 psi of N_2O exposure; experimental reflectivity data (left), compared to simulated data (right)

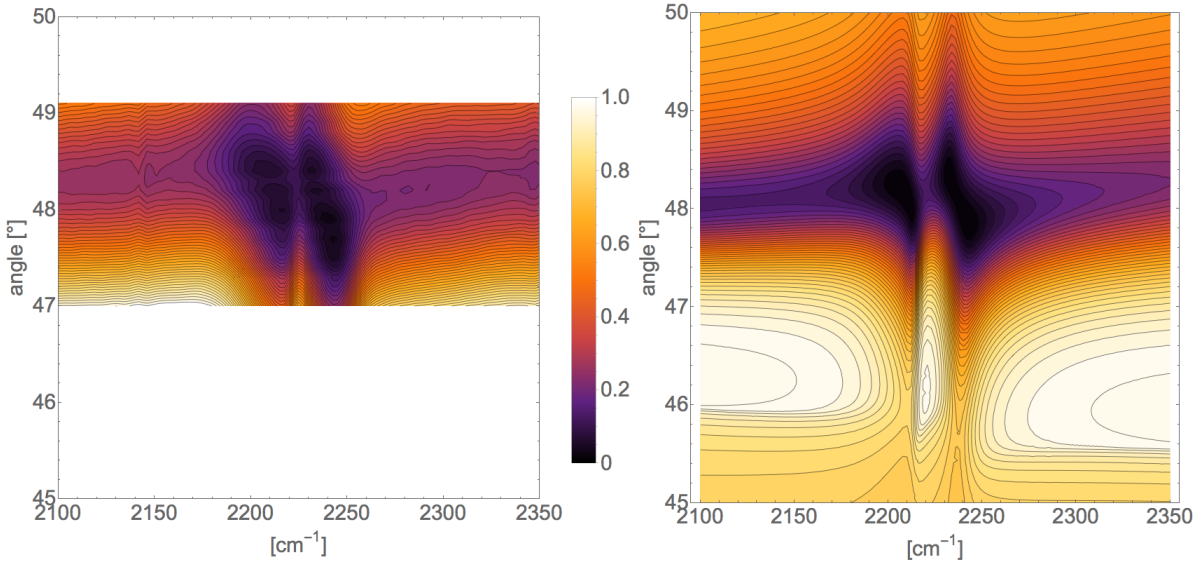

Figure 6.16 High resolution (1 cm^{-1}) SPR map comparison between measurement and theory for 80 psi of N_2O exposure; experimental reflectivity data (left), compared to simulated data (right)

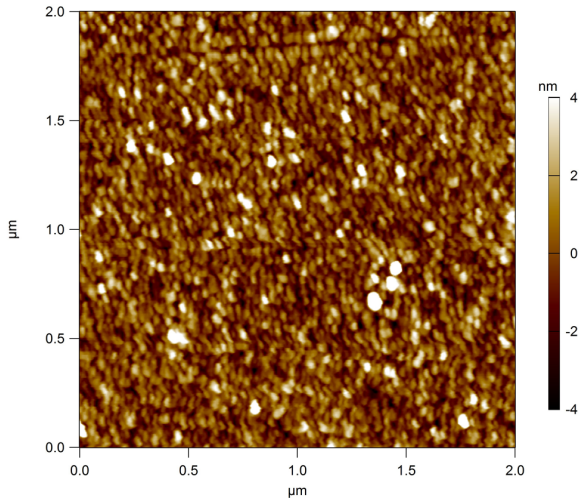

Figure 6.17 [AFM topography scan of 5 nm gold film sputter deposited on MgO (100); the film exhibits a RMS roughness of 1.4 nm

recorded reflectivity map. A small signature of the N_2O ν_3 mode can be found. No dispersion arc indicating coupling to a SPP can be seen, since gold does not support a SPP at these energies.

6.7 Discussion

The experimental data clearly reveals an interaction between the SPP dispersion and the N_2O ν_3 mode. A pressure (concentration) dependence can be found as well. To understand the results, it helps to go back to the modified SPP dispersion picture. Assuming the warping of the SPP dispersion due to the mode mixing occurs, it has implications on the experimentally observable coupling to the SPP using the Kretschmann configuration.

If the N_2O pressure modified SPP dispersion as depicted in figure 6.7 is correct, added lightlines for various incidence angles around the SPP resonance will help visualizing how the observed warping of the SPP in the plasmonic map can be interpreted. Figure 6.19 depicts the pressure modified dispersions, with added lightlines. From this picture we can make several predictions about the observed mode-mixing, *assuming the interaction is purely based on electromagnetic phenomena and no chemical interactions between the CdO:Dy film and the N_2O film take place*.

1) In the regions around the absorption band, (e.g. 2100 and 2350 cm^{-1}) the N_2O pressure modified dispersion is shifted to higher/lower in plane wave-vectors. Experimentally, this will result in the SPP branch coupling at a slightly increased/decreased resonance angle, when

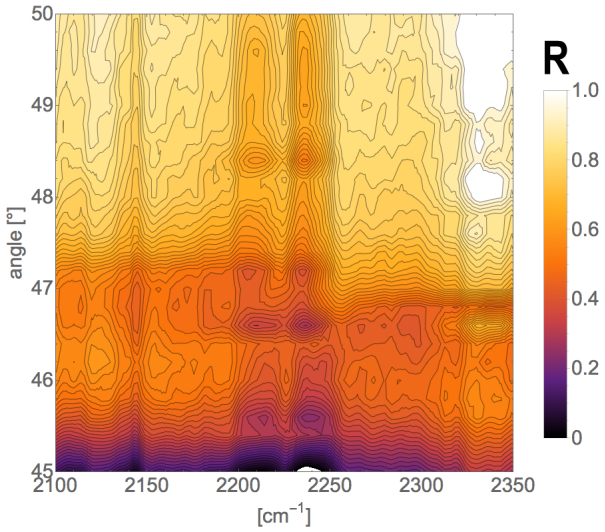

Figure 6.18 ATR reflectivity map for a 5 nm gold film exposed to 60 psi of N_2O; a weak signature of the N_2O ν_3 mode can be seen.

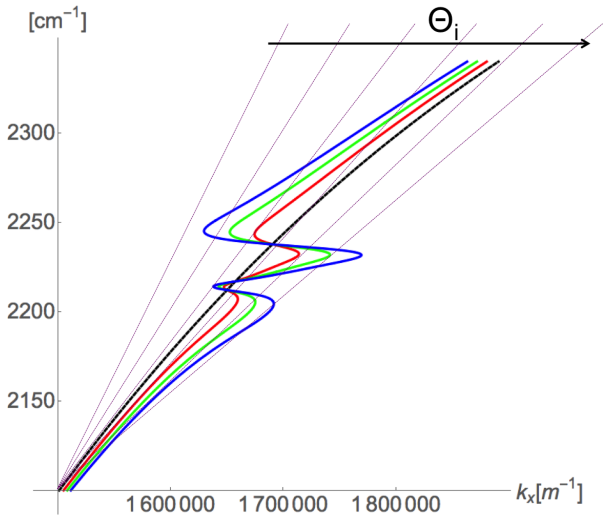

Figure 6.19 N_2O pressure modified SPP dispersion with added light lines; the complex coupling phenomena to the modified SPP dispersion are revealed. Every intersection of a lightline with a dispersion curve represents a coupling energy to light, which should be visible in SPR maps as dark bands.

compared to the bare (no N_2O) SPP dispersion. Furthermore, there should be a scaling of this effect with applied N_2O pressure (concentration). The experimental data reveals exactly that. Throughout the pressure series, the observed SPP branch is shifted to higher resonance angles for energies $<N_2O$ resonance energy and to lower angles for energies $>N_2O$ resonance energy. As predicted from the pressure modified dispersion calculations, this effect becomes more pronounced with higher N_2O pressures, thus higher N_2O concentration and absorption amplitude. For the 80 psi N_2O experiment, this angular split reaches a value of about 0.3°.

2) Due to the assumed line shape of the Lorentzian absorption events, there must be incidence angles around the resonance angle, that allow for coupling to the modified SPP dispersion at multiple energies. In the dispersion picture (figure 6.19) this is described by a single light line that crosses the modified SPP dispersion at more than one energy value.

Again, the experimental data verifies this picture. At incidence angles around the central SPP dispersion arc, we find a doublet of absorptions (for higher and lower angle values). These doublets become more intense and extend to higher absolute angles away from the central resonance angle, with increasing N_2O pressure. This behavior is perfectly predicted by the modified SPP dispersion assumption, assuming exclusively electromagnetic interaction between the SPP and the N_2O.

3) If the gas phase of N_2O does not interact with the CdO surface, and no adsorption or chemisorption events take place, the signal should increase linearly with pressure. By using the method outline in 6.2, amplitudes for the Lorentzian absorption have been calculated that follow this linearity. Since the simulated data (using the calculated amplitudes) depict agreement with the experimentally derived data set, this assumption seems to hold and the system can be treated as not interacting chemically with the surface.

The series of experiments further revealed an important aspect of the mode mixing phenomenon: Assuming ideal gas behavior, we can find 0.16 particles per nm^3 at 300K and 80 psi pressure above ambient (94.5 psi total, 655 001 pa). The electric field confinement for CdO:Dy is known to be strong, and for the CdO:Dy film used to record the mode mixing data we can calculate that 95 % of the field's energy are confined within 300 nm normal to the film surface (see chapter 5). This implies, that in a 300 nm tall, 1 nm^2 base column we would expect 48 particles. Despite this low density of atoms (especially when compared to condensed matter), the experiments revealed a strong signal from the N_2O.

The assumption of ideal gas behavior has to been seen as approximation, due to the strong dipole in the N_2O molecule so the actual concentration might divert from this calculation. Nevertheless, the data implies remarkable sensitivity towards absorption in the gas phase, when amplified by the effect of mode-mixing with a SPP dispersion.

To clarify the importance of mode mixing to achieve this enhancement, we can extract

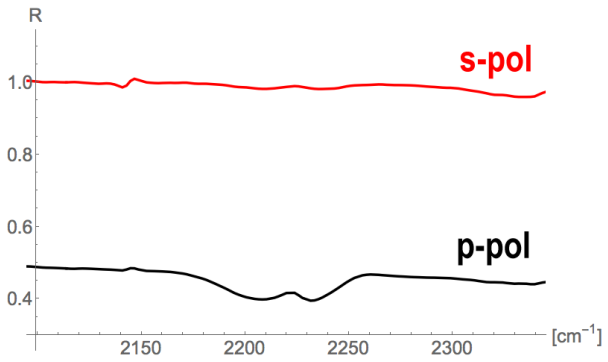

Figure 6.20 Comparison of the effect of incident light polarization on SPP mode mixing; the s-pol trace (red) does not exhibit any plasmonic resonance, and no interaction with N_2O mode the can be seen. The p-polarized trace (black) depicts coupling with the SPP *and* an increased absorption of the N_2O band.

energy dependent data from a SPR map and compare the p-polarized to the s-polarized measurement at a single angle. Figure 6.20 depicts this for 40 psi of N_2O at an incidence angle of 48.2°. The figure highlights two phenomena. For p-polarized light a significantly lower reflectivity R can be seen. This corresponds to coupling with the SPP, along a horizontal line at 48.2°when compared to the full map scan depicted in figure 6.14. Additionally, a strong coupling with the N_2O ν_3 mode can be seen, recognizable by the two local R minima around 2250 cm^{-1}. The s-polarized trace, does not exhibit any of these two characteristics. This supports the hypothesis, that the increased sensitivity towards the N_2O ν_3 mode results from the interaction (the mode mixing) of the SPP mode and the N_2O ν_3 mode. Since the SPP can only be coupled to using p-polarized light, the enhancement can only be measured when using p-polarized light.

The comparison to the ATR-SEIRA data recorded using a reference gold film supports the notion, that it is the mode mixing effect that results in this unusually strong absorbing behavior. In the gold reflectance data, a small signature of the N_2O mode can be found, however, under identical measurement conditions, the absorbance is significantly weaker when compared to CdO:Dy based data. To emphasize this result, figure 6.21 compares normalized reflectance data for identical measurement conditions, using CdO:Dy and gold films in the flow cell respectively. The data corresponds to an incidence angle of 48.2°and 60 psi N_2O pressure. An estimated increase in absorption of 5-7x can be found.

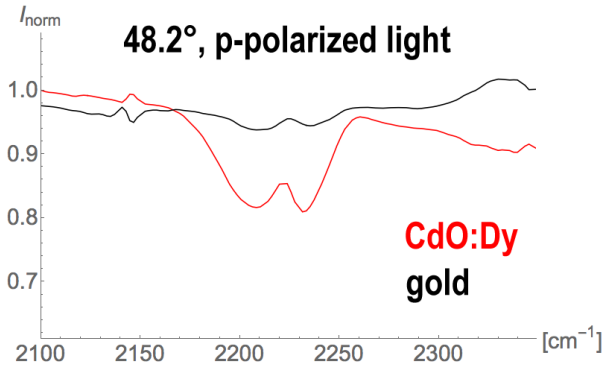

Figure 6.21 Comparison between gold ATR-SEIRA and CdO:Dy mode mixing data; normalized reflectance data at 48.2°incidence for both substrates (gold and CdO:Dy) using p-polarized light.

6.8 Conclusion

The set of experiments presented here represent the first demonstration of gas phase SEIRA utilizing mode mixing off a SPP and the analytes absorption in the mid-IR. Due to practical reasons N_2O was chosen as an absorber, however the conclusions presented here are valid for any gas phase absorption.

It was shown experimentally, that electromagnetic coupling between the surface confined SPP mode, supported by CdO:Dy thin films, and absorption bands in the environment of the CdO:Dy film can occur. The absorption was described purely by its dielectric function, where the gas phase ν_3 band of N_2O was modeled using two Lorentzians with an asymmetric line shape modification. These dielectric functions where used to calculate the effects of the absorption event on the SPP dispersion relation.

A pressure (concentration) variation of the N_2O and subsequent recording of reflectivity data in the Kretschmann configuration revealed a linear increase of the strength of the mode mixing. Experimentally, the predicted angular splitting of the SPR, as well as the intensity variations with pressure (concentration) have been confirmed and a remarkable sensitivity towards the presence of the analyte species (N_2O) was revealed. By comparing polarization depended results, this sensitivity was linked to the mode mixing between the SPP and the absorption band. Albeit not fully quantified, a comparison experiment to conventional ATR-SEIRA using a gold film revealed 5-7x stronger signals when comparing mode mixing data to the reference ATR-SEIRA gold data at identical measurement conditions.

The amplification of the enhancement can be understood as too communication resonators. In conventional ATR-SEIRA, the noble metal field acts as an antenna, focusing the incoming IR light into hot spot. Analytes in those hot spots are exposed to higher electromagnetic field strengths and an overall increase in the analytes characteristic absorption can be observed.

In the case of SPR mode mixing, a different mechanism is proposed. The isotopic, yet absorbing medium in the environment of the plasmonic thin film, in this example the N_2O gas, modifies the SPP dispersion by coupling to it. The SPP dispersion is highly sensitive towards changes in the dielectric environment, and an absorption band represents a significant perturbation in the dielectric function. The sensitivity of the SPP mode mixing can now be understood as measuring a SPP dispersion (modified by the presence and subsequent coupling to the dielectric function of N_2O), rather then measuring the N_2O absorption. The increase in sensitivity arises from the coupling of two resonant phenomena, rather then the local increase in electromagnetic field strength, when compared to conventional ATR-SEIRA based on gold.

Chapter 7

Conclusions and Future Work

The work presented in this thesis demonstrates a low loss plasmonic host material for mid-infrared energies, dysprosium doped cadmium oxide (CdO:Dy). Parts of this thesis present an initial exploration of the application space for a plasmonic material with previously inaccessible IR optical properties. This summary gives a brief overview of the techniques used and the material systems developed.

7.1 Conclusions

Development of a robust modeling technique for mid-IR SPR

Throughout this work, it was of great importance to model and predict the plasmonic behavior of any given material. Being able to theoretically screen potential materials for their applicability towards SPR is of enormous value and greatly accelerated the pace of this program. The multiple versions of the modeling code (see Appendix B) have been tailored for various task, such as deposition optimization (determine the optimal film parameters e.g. doping concentration/thickness) or theoretical studies of property-SPR relations. In general, the ability to readily compute maps of the SPR response in angle and energy space helped to visualize and thoroughly understand the SPR phenomena in the materials studied in this work and provided an understandable and visually pleasing way of communicating the complex optical phenomena described in this work.

Development of an advanced mid-IR SPR spectroscopy technique

Thanks to generous access to an IR-VASE spectroscopic ellipsometer, a refined spectroscopy technique could be developed. Based on multiple custom designed sample stages (see appendix A), the high angular and energy resolution of the IR-VASE system could be applied to mapping the SPR properties of thin films in angle and energy space. Further additions, such as a SPR flow cell, added versatility to the sample system and allowed to start exploring SPR application space using the materials created for this thesis. In general, excellent agreement between simulations and experimental data has been found throughout this work, highlighting the accuracy of the developed spectroscopy and modeling technique.

In combination with the companion simulation code, a powerful set of techniques to characterize infrared SPR materials has been created.

Proof of concept, mid-IR SPR in Zinc Oxide thin films

Although already predicted theoretically, the first experimental demonstration of thin film, mid-IR SPR in a wide bandgap material was of utmost importance. The occurrence of mid-IR SPR in heavily doped, epitaxial zinc oxide thin films revealed the limitations of most wide bandgap materials in the context of mid-IR SPR and highlighted the need for a rare combination of transport properties in order to achieve low loss SPR at infrared energies. Without the results from the ZnO study, we would not have moved on to materials such as CdO, which ultimately turned out to be the key to low loss mid-IR plasmonics.

Design and construction of a ICP-Oxygen source

The initial experiments for growing CdO thin films were carried out using PLD techniques. Despite the advantages, such as short deposition times which allow to efficiently screen a large parameter space, accurate doping in the sub 1% range is challenging when using pulsed laser deposition. Upon realizing that accurately doping the CdO system will be the key to achieve low optical losses in the material, the growth of CdO was continued using MBE techniques. Unfortunately, to grow CdO from a metal effusion source at MBE oxygen partial pressures (typically 1-5x10^{-6} torr) a higher oxygen activity is needed than can be achieved using molecular oxygen (O_2). This led to the development of an inductively coupled plasma source that provided a flux of atomic oxygen. Atomic oxygen has significantly higher activity then molecular O_2 (at identical partial pressures) and thus enabled the oxidation and depositions of CdO:Dy using MBE techniques. Furthermore, it is a versatile addition to the oxide MBE system of the Electronic Oxides group.

A publication in a collaboration with NCSU's nuclear engineering department that summarized the construction and use of the ICP-source and analyzes it's plasma characteristics

computationally is in preparation and soon to be submitted to the journal *Review of Scientific Instruments*.

Dysprosium doped Cadmium Oxide

The thorough study of the structure/property relationships in CdO and an extensive doping study revealed a very rare combination of transport properties. In CdO:Dy, an unusually high doping range, up to 1x10^{19}-1x10^{21} cm^{-3} can be accessed while maintaining extremely high electron mobilities of up to 500 $cm^2V^{-1}s^{-1}$. This transport behavior supports low loss plasmonics over the entire mid-IR range and represents a sought after material in the plasmonic community.

The material has been thoroughly characterized in its structural, transport, optical, and thermal properties. Alongside experimental characterization, DFT *ab initio* calculations were used to test and verify a defect based structure-property model that explained the unusual behavior of CdO:Dy upon doping.

7.2 Proposed future work

The development of CdO:Dy opens up opportunities to explore previously inaccessible plasmonic phenomena and applications. Furthermore, the processing of CdO:Dy can still be optimized and transferred to other film thin deposition techniques. Several possibilities, either works in progress or proposed work, include:

Development of a CdO:Dy sputtering process

Despite the many advantages of MBE deposition in terms of thin film growth, it is a very time consuming technique that requires advanced users for reliable performance and film quality. Developing a sputtering process that produces comparable film qualities could help to produce more CdO:Dy for distribution to collaborators, to allow for larger sample size experiments and to save time and cost. Furthermore it would open up access to CdO:Dy for research groups without plasma assisted oxide-MBE capabilities.

The proposed sputtering process could be based on a dual magnetron sputtering system, to co-sputter off-axis, onto a heated, rotating sample stage. Off axis sputtering is known for excellent uniformity and could allow to grow samples >2 inch in diameter in one deposition run. To control the doping levels, two different CdO targets could be used, one undoped CdO target and one doped to e.g. 2% Dy content. By varying the relative powers (thus the deposition rates) for the individual magnetrons, the entire doping range from 0-2 % should be accessible with a high level of control.

SPR mode mixing for chemical sensing

The experiments in chapter 6 revealed a remarkable sensitivity of the SPR mode towards interaction with absorption bands present close to the CdO:Dy/environment interface. Several avenues to explore this phenomenon further and to advance towards applications are:

- Use of the the mode mixing effect to study the chemistry of self assembled monolayers (SAMs) deposited onto CdO:Dy. SPR is well known for its sensitivity towards the existence of SAMs on the SPR chip's surface. However, combining this well known property with the SPR mode mixing presented in this work could lead to a combination of traditional SPR, where in addition to measuring the existence of a SAM, it's chemistry could be probed spectroscopically.

- The increased absorption observed due to mode mixing allows for shorter measurement times. This can enable novel *in situ* studies based on CdO:Dy substrates. For example, the fact that CdO:Dy is highly conductive could be used in electrochemical studies where the CdO:Dy could serve as electrode and to enhance the IR signatures of redox reaction in order to monitor them and measure their kinetics *in situ*.

- Using the SPR mode mixing effect for chemical detection: by depositing a thin film of a porous collecting polymer onto a CdO:Dy SPR chip, mode mixing might be useful to extract chemical information about the environment this film has been exposed to. A successful implementation of such a technology could have widespread uses from environmental monitoring to threat prevention. An initial set of experiments will be commenced in collaboration with the Naval Research Laboratories.

CdO:Dy for optoelectronic applications

The main motivation behind the development of CdO:Dy was the need of the optoelectronics community for an access to a low loss plasmonic material for the infrared. IR imaging, detection and information processing using infrared radiation are research topics of high impact due to current technological demand. Now that such a sought after material becomes available, avenues to explore include:

- CdO:Dy for infrared detection: by exploiting a phenomenon called "hot carrier generation", which is the result of non-radiative plasmon decay, it becomes feasible to design a sub-bandgap infrared detector. Such a structure could be comprised entirely of wide bandgap materials and thus be insensitive to thermal noise. The optical response is based

on an electronic transition within the device, therefore such a technology could combine high speed with a high stability of measurement, even in an uncooled environment.

- CdO:Dy for energy harvesting: By exploiting the creation of hot electrons, driven by infrared absorption within CdO:Dy, the efficiency of solar cells could be improved. The bandwidth of light a solar cell could access for current generation would be extended towards the infrared, a previously inaccessible energy range for silicon based solar cells. By additionally absorbing longer wavelengths of light, the overall efficiency of solar cells could be improved.

- Heat scavenging and thermal cloaks: Infrared radiation carries most of the heat radiated by the environment. A low loss plasmonic material for the mid-IR allows for wave guiding and focusing this radiation. Being able to selectively absorb and guide certain infrared wavelengths could lead to the development of thermal cloaking, where certain bands of infrared radiation could be prevented from emission.

  Alternatively, infrared radiation from hot environments could be focused to a single point where the high intensity of heat could be used for energy generation, for example by using a thermoelectric device.

- Sub wavelength diffraction of infrared radiation: Utilizing plasmonic wave guides it becomes possible to focus IR radiation into sub wavelength dimensions. Since IR radiation can transfer heat effectively, a CdO:Dy based wave guide could be implemented as data write element in future heat assisted data recording schemes where the fast, focused delivery of heat will be needed to record data.

Bibliography

[1] R. W. Wood. On a Remarkable Case of Uneven Distribution of Light in a Diffraction Grating Spectrum. *Proceedings of the Physical Society of London*, 18(1):269, June 1902.

[2] Lord Rayleigh. On the Dynamical Theory of Gratings. *Proceedings of the Royal Society of London A: Mathematical, Physical and Engineering Sciences*, 79(532):399–416, August 1907.

[3] R.W. Wood. XXVII. Diffraction gratings with controlled groove form and abnormal distribution of intensity. *Philosophical Magazine Series 6*, 23(134):310–317, February 1912.

[4] R. W. Wood. Anomalous Diffraction Gratings. *Physical Review*, 48(12):928–936, December 1935.

[5] JR. PALMER, C. HARVEY. Diffraction Grating Anomalies. II. Coarse Gratings. *Journal of the Optical Society of America*, 46(1):50–53, January 1956.

[6] JR. PALMER, C. HARVEY. Parallel Diffraction Grating Anomalies. *Journal of the Optical Society of America*, 42(4):269–273, April 1952.

[7] R. H. Ritchie. Plasma Losses by Fast Electrons in Thin Films. *Physical Review*, 106:874–881, June 1957.

[8] C. J. Powell and J. B. Swan. Effect of Oxidation on the Characteristic Loss Spectra of Aluminum and Magnesium. *Physical Review*, 118(3):640–643, May 1960.

[9] David Bohm and David Pines. A Collective Description of Electron Interactions. I. Magnetic Interactions. *Physical Review*, 82(5):625–634, June 1951.

[10] David Pines and David Bohm. A Collective Description of Electron Interactions: 2. Collective vs Individual Particle Aspects of the Interactions. *Phys.Rev.*, 85:338–353, 1952.

[11] David Bohm and David Pines. A Collective Description of Electron Interactions: 3. Coulomb Interactions in a Degenerate Electron Gas. *Phys.Rev.*, 92:609–625, 1953.

[12] E. Burstein, W. P. Chen, Y. J. Chen, and A. Hartstein. Surface polaritons—propagating electromagnetic modes at interfaces. *Journal of Vacuum Science & Technology*, 11(6):1004–1019, November 1974.

[13] E Kretschmann and H Raether. Radiative decay of nonradiative surface plasmons excited by light. *Z. Naturforsch. A*, 23:2135, 1968.

[14] E. Kretschmann. The angular dependence and the polarisation of light emitted by surface plasmons on metals due to roughness. *Optics Communications*, 5(5):331–336, August 1972.

[15] Erwin Kretschmann. Die Bestimmung optischer Konstanten von Metallen durch Anregung von Oberflächenplasmaschwingungen. *Zeitschrift fur Physik*, 241:313–324, August 1971.

[16] Heinz Raether. *Surface plasmons on smooth and rough surfaces and on gratings*. Springer, 1988.

[17] Andreas Otto. Excitation of nonradiative surface plasma waves in silver by the method of frustrated total reflection. *Zeitschrift für Physik*, 216(4):398–410, August 1968.

[18] P. Drude. Zur Elektronentheorie der Metalle. *Annalen der Physik*, 306(3):566–613, 1900.

[19] P. Drude. Zur Elektronentheorie der Metalle; II. Teil. Galvanomagnetische und thermomagnetische Effecte. *Annalen der Physik*, 308(11):369–402, 1900.

[20] F. Goos and H. Hänchen. Ein neuer und fundamentaler Versuch zur Totalreflexion. *Annalen der Physik*, 436(7-8):333–346, 1947.

[21] Frederique de Fornel. *Evanescent Waves: From Newtonian Optics to Atomic Optics*. Springer Science & Business Media, January 2001.

[22] Matthew A. Cooper. Optical biosensors in drug discovery. *Nat Rev Drug Discov*, 1(7):515–528, July 2002.

[23] D. Kambhampati, P. E. Nielsen, and W. Knoll. Investigating the kinetics of DNA-DNA and PNA-DNA interactions using surface plasmon resonance-enhanced fluorescence spectroscopy. *Biosensors & Bioelectronics*, 16(9-12):1109–1118, December 2001.

[24] Hui Li, Dafu Cui, Haoyuan Cai, Lulu Zhang, Xing Chen, Jianhai Sun, and Yapeng Chao. Use of surface plasmon resonance to investigate lateral wall deposition kinetics and properties of polydopamine films. *Biosensors & Bioelectronics*, 41:809–814, March 2013.

[25] Phinikoula S. Katsamba, Sungmin Park, and Ite A. Laird-Offringa. Kinetic studies of RNA-protein interactions using surface plasmon resonance. *Methods (San Diego, Calif.)*, 26(2):95–104, February 2002.

[26] Ding-Wei Huang, Yao-Feng Ma, Ming-Je Sung, and Chiao-Pan Huang. Approach the angular sensitivity limit in surface plasmon resonance sensors with low index prism and large resonant angle. *Optical Engineering*, 49(5):054403–054403–6, 2010.

[27] Ariel Lipson, Stephen G. Lipson, and Henry Lipson. *Optical Physics*. Cambridge University Press, Cambridge ; New York, 4 edition edition, November 2010.

[28] Satoshi Kawata, Yasushi Inouye, and Prabhat Verma. Plasmonics for near-field nano-imaging and superlensing. *Nature Photonics*, 3(7):388–394, July 2009.

[29] Igor I. Smolyaninov, ChristopherC. Davis, Jill Elliott, and Anatoly V. Zayats. Resolution enhancement of a surface immersion microscope near the plasmonresonance. *Optics Letters*, 30(4):382–384, February 2005.

[30] Hiromitsu Furukawa and Satoshi Kawata. Local field enhancement with an apertureless near-field-microscope probe. *Optics Communications*, 148(4–6):221–224, March 1998.

[31] Wei Bao, M. Melli, N. Caselli, F. Riboli, D. S. Wiersma, M. Staffaroni, H. Choo, D. F. Ogletree, S. Aloni, J. Bokor, S. Cabrini, F. Intonti, M. B. Salmeron, E. Yablonovitch, P. J. Schuck, and A. Weber-Bargioni. Mapping Local Charge Recombination Heterogeneity by Multidimensional Nanospectroscopic Imaging. *Science*, 338(6112):1317–1321, December 2012.

[32] Lukas Novotny and Stephan J. Stranick. Near-Field Optical Microscopy and Spectroscopy with Pointed Probes*. *Annual Review of Physical Chemistry*, 57(1):303–331, 2006.

[33] Hyuck Choo, Myung-Ki Kim, Matteo Staffaroni, Tae Joon Seok, Jeffrey Bokor, Stefano Cabrini, P. James Schuck, Ming C. Wu, and Eli Yablonovitch. Nanofocusing in a metal-insulator-metal gap plasmon waveguide with a three-dimensional linear taper. *Nature Photonics*, 6(12):838–844, December 2012.

[34] Wei Bao, Matteo Staffaroni, Jeffrey Bokor, Miquel B. Salmeron, Eli Yablonovitch, Stefano Cabrini, Alexander Weber-Bargioni, and P. James Schuck. Plasmonic near-field probes: a comparison of the campanile geometry with other sharp tips. *Optics Express*, 21(7):8166, April 2013.

[35] P. Mühlschlegel, H.-J. Eisler, O. J. F. Martin, B. Hecht, and D. W. Pohl. Resonant Optical Antennas. *Science*, 308(5728):1607–1609, June 2005.

[36] P. J. Schuck, D. P. Fromm, A. Sundaramurthy, G. S. Kino, and W. E. Moerner. Improving the Mismatch between Light and Nanoscale Objects with Gold Bowtie Nanoantennas. *Physical Review Letters*, 94(1):017402, January 2005.

[37] Javad N. Farahani, Hans-Jürgen Eisler, Dieter W. Pohl, Michaël Pavius, Philippe Flückiger, Philippe Gasser, and Bert Hecht. Bow-tie optical antenna probes for single-emitter scanning near-field optical microscopy. *Nanotechnology*, 18(12):125506, March 2007.

[38] Erik J. Sánchez, Lukas Novotny, and X. Sunney Xie. Near-Field Fluorescence Microscopy Based on Two-Photon Excitation with Metal Tips. *Physical Review Letters*, 82(20):4014–4017, May 1999.

[39] Jordan M. Gerton, Lawrence A. Wade, Guillaume A. Lessard, Z. Ma, and Stephen R. Quake. Tip-Enhanced Fluorescence Microscopy at 10 Nanometer Resolution. *Physical Review Letters*, 93(18):180801, October 2004.

[40] Joseph R. Lakowicz, Chris D. Geddes, Ignacy Gryczynski, Joanna Malicka, Zygmunt Gryczynski, Kadir Aslan, Joanna Lukomska, Evgenia Matveeva, Jian Zhang, Ramachandram Badugu, and Jun Huang. Advances in Surface-Enhanced Fluorescence. *Journal of Fluorescence*, 14(4):425–441, July 2004.

[41] Fu Min Huang, Frederic Festy, and David Richards. Tip-enhanced fluorescence imaging of quantum dots. *Applied Physics Letters*, 87(18):183101, October 2005.

[42] Shuming Nie and Steven R. Emory. Probing Single Molecules and Single Nanoparticles by Surface-Enhanced Raman Scattering. *Science*, 275(5303):1102–1106, February 1997.

[43] Saumyakanti Khatua, Pedro M. R. Paulo, Haifeng Yuan, Ankur Gupta, Peter Zijlstra, and Michel Orrit. Resonant Plasmonic Enhancement of Single-Molecule Fluorescence by Individual Gold Nanorods. *ACS Nano*, 8(5):4440–4449, 2014.

[44] Harry A. Atwater and Albert Polman. Plasmonics for improved photovoltaic devices. *Nature Materials*, 9(3):205–213, March 2010.

[45] Vivian E. Ferry, Luke A. Sweatlock, Domenico Pacifici, and Harry A. Atwater. Plasmonic Nanostructure Design for Efficient Light Coupling into Solar Cells. *Nano Letters*, 8(12):4391–4397, 2008.

[46] D. Derkacs, S. H. Lim, P. Matheu, W. Mar, and E. T. Yu. Improved performance of amorphous silicon solar cells via scattering from surface plasmon polaritons in nearby metallic nanoparticles. *Applied Physics Letters*, 89(9):093103, August 2006.

[47] P. Matheu, S. H. Lim, D. Derkacs, C. McPheeters, and E. T. Yu. Metal and dielectric nanoparticle scattering for improved optical absorption in photovoltaic devices. *Applied Physics Letters*, 93(11):113108, September 2008.

[48] David Duche, Philippe Torchio, Ludovic Escoubas, Florent Monestier, Jean-Jacques Simon, François Flory, and Gérard Mathian. Improving light absorption in organic solar cells by plasmonic contribution. *Solar Energy Materials and Solar Cells*, 93(8):1377–1382, August 2009.

[49] K. R. Catchpole and A. Polman. Design principles for particle plasmon enhanced solar cells. *Applied Physics Letters*, 93(19):191113, November 2008.

[50] Ronny Kirste, Marc P. Hoffmann, Edward Sachet, Milena Bobea, Zachary Bryan, Isaac Bryan, Christian Nenstiel, Axel Hoffmann, Jon-Paul Maria, Ramón Collazo, and Zlatko Sitar. Ge doped GaN with controllable high carrier concentration for plasmonic applications. *Applied Physics Letters*, 103(24):242107, December 2013.

[51] Jeffrey M. McMahon, George C. Schatz, and Stephen K. Gray. Plasmonics in the ultraviolet with the poor metals Al, Ga, In, Sn, Tl, Pb, and Bi. *Physical Chemistry Chemical Physics*, 15(15):5415, 2013.

[52] Pae C. Wu, Tong-Ho Kim, April S. Brown, Maria Losurdo, Giovanni Bruno, and Henry O. Everitt. Real-time plasmon resonance tuning of liquid Ga nanoparticles by in situ spectroscopic ellipsometry. *Applied Physics Letters*, 90(10):103119, March 2007.

[53] Gururaj V. Naik, Jeremy L. Schroeder, Xingjie Ni, Alexander V. Kildishev, Timothy D. Sands, and Alexandra Boltasseva. Titanium nitride as a plasmonic material for visible and near-infrared wavelengths. *Optical Materials Express*, 2(4):478–489, April 2012.

[54] Gururaj V. Naik, Bivas Saha, Jing Liu, Sammy M. Saber, Eric A. Stach, Joseph M. K. Irudayaraj, Timothy D. Sands, Vladimir M. Shalaev, and Alexandra Boltasseva. Epitaxial superlattices with titanium nitride as a plasmonic component for optical hyperbolic metamaterials. *Proceedings of the National Academy of Sciences*, 111(21):7546–7551, May 2014.

[55] J. B. Pendry, L. Martín-Moreno, and F. J. Garcia-Vidal. Mimicking Surface Plasmons with Structured Surfaces. *Science*, 305(5685):847–848, August 2004.

[56] Anastasia Rusina, Maxim Durach, and Mark I. Stockman. Theory of spoof plasmons in real metals. *Applied Physics A*, 100(2):375–378, August 2010.

[57] Víctor Torres, Rubén Ortuño, Pablo Rodríguez-Ulibarri, Amadeu Griol, Alejandro Martínez, Miguel Navarro-Cía, Miguel Beruete, and Mario Sorolla. Mid-infrared plasmonic inductors: Enhancing inductance with meandering lines. *Scientific Reports*, 4, January 2014.

[58] Pengyu Chen, Qiaoqiang Gan, Filbert J. Bartoli, and Lin Zhu. Spoof-surface-plasmon assisted light beaming in mid-infrared. *Journal of the Optical Society of America B*, 27(4):685–689, April 2010.

[59] Yimin Kang, Sina Najmaei, Zheng Liu, Yanjun Bao, Yumin Wang, Xing Zhu, Naomi J. Halas, Peter Nordlander, Pulickel M. Ajayan, Jun Lou, and Zheyu Fang. Plasmonic Hot Electron Induced Structural Phase Transition in a MoS2 Monolayer. *Advanced Materials*, 26(37):6467–6471, 2014.

[60] Stefan A. Maier. Graphene plasmonics: All eyes on flatland. *Nature Physics*, 8(8):581–582, August 2012.

[61] F. Javier Garcia de Abajo. Graphene Plasmonics: Challenges and Opportunities. *ACS Photonics*, 1(3):135–152, March 2014. arXiv: 1402.1969.

[62] Tony Low and Phaedon Avouris. Graphene Plasmonics for Terahertz to Mid-Infrared Applications. *ACS Nano*, 8(2):1086–1101, 2014.

[63] Hugen Yan, Tony Low, Wenjuan Zhu, Yanqing Wu, Marcus Freitag, Xuesong Li, Francisco Guinea, Phaedon Avouris, and Fengnian Xia. Damping pathways of mid-infrared plasmons in graphene nanostructures. *Nature Photonics*, 7(5):394–399, May 2013.

[64] Fengnian Xia, Han Wang, Di Xiao, Madan Dubey, and Ashwin Ramasubramaniam. Two-dimensional material nanophotonics. *Nature Photonics*, 8(12):899–907, December 2014.

[65] Crissy Rhodes, Stefan Franzen, Jon-Paul Maria, Mark Losego, Donovan N. Leonard, Brian Laughlin, Gerd Duscher, and Stephen Weibel. Surface plasmon resonance in conducting metal oxides. *Journal of Applied Physics*, 100(5):054905, 2006.

[66] C. Rhodes, M. Cerruti, A. Efremenko, M. Losego, D. E. Aspnes, J.-P. Maria, and S. Franzen. Dependence of plasmon polaritons on the thickness of indium tin oxide thin films. *Journal of Applied Physics*, 103(9):093108, 2008.

[67] Stefan Franzen. Surface Plasmon Polaritons and Screened Plasma Absorption in Indium Tin Oxide Compared to Silver and Gold. *The Journal of Physical Chemistry C*, 112(15):6027–6032, April 2008.

[68] A. K. Pradhan, R. M. Mundle, Kevin Santiago, J. R. Skuza, Bo Xiao, K. D. Song, M. Bahoura, Ramez Cheaito, and Patrick E. Hopkins. Extreme tunability in aluminum doped Zinc Oxide plasmonic materials for near-infrared applications. *Scientific Reports*, 4, September 2014.

[69] Conor T. Riley, Tien A. Kieu, Joseph S. T. Smalley, Si Hui Athena Pan, Sung Joo Kim, Kirk W. Post, Alireza Kargar, Dimitri N. Basov, Xiaoqing Pan, Yeshaiahu Fainman, Deli Wang, and Donald J. Sirbuly. Plasmonic tuning of aluminum doped zinc oxide nanostructures by atomic layer deposition. *physica status solidi (RRL) – Rapid Research Letters*, 8(11):948–952, 2014.

[70] Jongbum Kim, Gururaj V. Naik, Alexander V. Gavrilenko, Krishnaveni Dondapati, Vladimir I. Gavrilenko, S. M. Prokes, Orest J. Glembocki, Vladimir M. Shalaev, and Alexandra Boltasseva. Optical Properties of Gallium-Doped Zinc Oxide\char22{}A Low-Loss Plasmonic Material: First-Principles Theory and Experiment. *Physical Review X*, 3(4):041037, December 2013.

[71] Gururaj V. Naik, Jongbum Kim, and Alexandra Boltasseva. Oxides and nitrides as alternative plasmonic materials in the optical range [Invited]. *Optical Materials Express*, 1(6):1090, October 2011.

[72] Joshua T. Guske, Jeff Brown, Alex Welsh, and Stefan Franzen. Infrared surface plasmon resonance of AZO-Ag-AZO sandwich thin films. *Optics Express*, 20(21):23215–23226, October 2012.

[73] Mark D. Losego, Alina Y. Efremenko, Crissy L. Rhodes, Marta G. Cerruti, Stefan Franzen, and Jon-Paul Maria. Conductive oxide thin films: Model systems for understanding and controlling surface plasmon resonance. *Journal of Applied Physics*, 106(2):024903, 2009.

[74] M. Warzecha, J. I. Owen, M. Wimmer, F. Ruske, J. Hotovy, and J. Hüpkes. High mobility annealing of Transparent Conductive Oxides. *IOP Conference Series: Materials Science and Engineering*, 34(1):012004, April 2012.

[75] Stefan Alexander Maier. *Plasmonics: Fundamentals and Applications*. Springer, New York, 2007 edition edition, May 2007.

[76] Joshua Travis Guske. *Modeling and Prediction of Surface Plasmon Resonance Spectroscopy*. PhD thesis, NORTH CAROLINA STATE UNIVERSITY, 2013.

[77] Lukas Novotny and Bert Hecht. *Principles of Nano-Optics*. Cambridge University Press, September 2012.

[78] Rueben J. Mendelsberg, Guillermo Garcia, and Delia J. Milliron. Extracting reliable electronic properties from transmission spectra of indium tin oxide thin films and nanocrystal films by careful application of the Drude theory. *Journal of Applied Physics*, 111(6):063515, March 2012.

[79] M. A. Noginov, Lei Gu, J. Livenere, G. Zhu, A. K. Pradhan, R. Mundle, M. Bahoura, Yu A. Barnakov, and V. A. Podolskiy. Transparent conductive oxides: Plasmonic materials for telecom wavelengths. *Applied Physics Letters*, 99(2):021101, July 2011.

[80] Edward Sachet, Mark D. Losego, Joshua Guske, Stefan Franzen, and Jon-Paul Maria. Mid-infrared surface plasmon resonance in zinc oxide semiconductor thin films. *Applied Physics Letters*, 102(5):051111–051111–4, February 2013.

[81] Max Born and Emil Wolf. *Principles of Optics: Electromagnetic Theory of Propagation, Interference and Diffraction of Light*. CUP Archive, February 2000.

[82] Bo Liedberg, Claes Nylander, and Ingemar Lundström. Biosensing with surface plasmon resonance — how it all started. *Biosensors and Bioelectronics*, 10(8):i–ix, 1995.

[83] Jiří Homola. Present and future of surface plasmon resonance biosensors. *Analytical and Bioanalytical Chemistry*, 377(3):528–539, 2003.

[84] L. Wu, H. S. Chu, W. S. Koh, and E. P. Li. Highly sensitive graphene biosensors based on surface plasmon resonance. *Optics Express*, 18(14):14395–14400, July 2010.

[85] Julia M. Bingham, Jeffrey N. Anker, Lauren E. Kreno, and Richard P. Van Duyne. Gas Sensing with High-Resolution Localized Surface Plasmon Resonance Spectroscopy. *J. Am. Chem. Soc.*, 132(49):17358–17359, 2010.

[86] T Allsop, R Neal, E M Davies, C Mou, P Bond, S Rehman, K Kalli, D J Webb, P Calverhouse, and I Bennion. Low refractive index gas sensing using a surface plasmon resonance fibre device. *Measurement Science and Technology*, 21(9):094029, September 2010.

[87] William L Barnes. Surface plasmon–polariton length scales: a route to sub-wavelength optics. *Journal of Optics A: Pure and Applied Optics*, 8(4):S87–S93, April 2006.

[88] Jiři? Homola, Sinclair S. Yee, and Günter Gauglitz. Surface plasmon resonance sensors: review. *Sensors and Actuators B: Chemical*, 54(1–2):3–15, January 1999.

[89] Lukas Schmidt-Mende and Judith L. MacManus-Driscoll. ZnO – nanostructures, defects, and devices. *Materials Today*, 10(5):40–48, May 2007.

[90] Hadis Morkoç and Ümit Özgür. General Properties of ZnO. In *Zinc Oxide*, pages 1–76. Wiley-VCH Verlag GmbH & Co. KGaA, 2009.

[91] Hadis Morkoç and Ümit Özgür. *Zinc Oxide: Fundamentals, Materials and Device Technology*. Wiley-VCH, March 2009.

[92] T. J. Johnson, T. Masiello, and S. W. Sharpe. The quantitative infrared and NIR spectrum of CH2i2 vapor: vibrational assignments and potential for atmospheric monitoring. *Atmos. Chem. Phys.*, 6(9):2581–2591, July 2006.

[93] P. B. Johnson and R. W. Christy. Optical Constants of the Noble Metals. *Physical Review B*, 6(12):4370–4379, December 1972.

[94] P.r. West, S. Ishii, G.v. Naik, N.k. Emani, V.m. Shalaev, and A. Boltasseva. Searching for better plasmonic materials. *Laser & Photonics Reviews*, 4(6):795–808, 2010.

[95] Stephanie Law, Viktor Podolskiy, and Daniel Wasserman. Towards nano-scale photonics with micro-scale photons: the opportunities and challenges of mid-infrared plasmonics. *Nanophotonics*, 2(2):103–130, April 2013.

[96] Gururaj V. Naik, Vladimir M. Shalaev, and Alexandra Boltasseva. Alternative Plasmonic Materials: Beyond Gold and Silver. *Advanced Materials*, 25(24):3264–3294, 2013.

[97] Ross Stanley. Plasmonics in the mid-infrared. *Nature Photonics*, 6(7):409–411, July 2012.

[98] Victor W. Brar, Min Seok Jang, Michelle Sherrott, Josue J. Lopez, and Harry A. Atwater. Highly Confined Tunable Mid-Infrared Plasmonics in Graphene Nanoresonators. *Nano Letters*, 13(6):2541–2547, June 2013.

[99] Zheyu Fang, Sukosin Thongrattanasiri, Andrea Schlather, Zheng Liu, Lulu Ma, Yumin Wang, Pulickel M. Ajayan, Peter Nordlander, Naomi J. Halas, and F. Javier García de Abajo. Gated Tunability and Hybridization of Localized Plasmons in Nanostructured Graphene. *ACS Nano*, 7(3):2388–2395, March 2013.

[100] S. Law, D. C. Adams, A. M. Taylor, and D. Wasserman. Mid-infrared designer metals. *Optics Express*, 20(11):12155, May 2012.

[101] Stephanie Law, Lan Yu, and Daniel Wasserman. Epitaxial growth of engineered metals for mid-infrared plasmonics. *Journal of Vacuum Science & Technology B*, 31(3):03C121, May 2013.

[102] Aaron Rosenberg, Joshua Surya, Runyu Liu, William Streyer, Stephanie Law, L. Suzanne Leslie, Rohit Bhargava, and Daniel Wasserman. Flat mid-infrared composite plasmonic materials using lateral doping-patterned semiconductors. *Journal of Optics*, 16(9):094012, September 2014.

[103] F. P. Koffyberg. Carrier concentration in oxygen deficient CdO single crystals. *Physics Letters A - PHYS LETT A*, 30:37–38, 1969.

[104] R. D. Shannon. Revised effective ionic radii and systematic studies of interatomic distances in halides and chalcogenides. *Acta Crystallographica Section A*, 32(5):751–767, September 1976.

[105] B. K. Ridley. Reconciliation of the Conwell-Weisskopf and Brooks-Herring formulae for charged-impurity scattering in semiconductors: Third-body interference. *Journal of Physics C: Solid State Physics*, 10(10):1589, May 1977.

[106] David G. Cahill. Analysis of heat flow in layered structures for time-domain thermoreflectance. *Review of Scientific Instruments*, 75(12):5119–5122, December 2004.

[107] Chris G. Van de Walle and Jörg Neugebauer. First-principles calculations for defects and impurities: Applications to III-nitrides. *Journal of Applied Physics*, 95(8):3851–3879, April 2004.

[108] Benjamin E. Gaddy, Zachary Bryan, Isaac Bryan, Ronny Kirste, Jinqiao Xie, Rafael Dalmau, Baxter Moody, Yoshinao Kumagai, Toru Nagashima, Yuki Kubota, Toru Kinoshita, Akinori Koukitu, Zlatko Sitar, Ramón Collazo, and Douglas L. Irving. Vacancy compensation and related donor-acceptor pair recombination in bulk AlN. *Applied Physics Letters*, 103(16):161901, October 2013.

[109] Elias Burstein. Anomalous Optical Absorption Limit in InSb. *Physical Review*, 93(3):632–633, February 1954.

[110] T. S. Moss. The Interpretation of the Properties of Indium Antimonide. *Proceedings of the Physical Society. Section B*, 67(10):775, October 1954.

[111] Pierre Berini. Figures of merit for surface plasmon waveguides. *Optics Express*, 14(26):13030–13042, December 2006.

[112] Sylvain Herminjard, Lorenzo Sirigu, Hans Peter Herzig, Eric Studemann, Andrea Crottini, Jean-Paul Pellaux, Tobias Gresch, Milan Fischer, and Jérôme Faist. Surface Plasmon Resonance sensor showing enhanced sensitivity for CO_2 detection in the mid-infrared range. *Optics Express*, 17(1):293, January 2009.

[113] L. L. Kazmerski and Diane M. Racine. Growth, environmental, and electrical properties of ultrathin metal films. *Journal of Applied Physics*, 46(2):791–795, September 2008.

[114] W. A. Kraus and George C. Schatz. Plasmon resonance broadening in small metal particles. *The Journal of Chemical Physics*, 79(12):6130–6139, December 1983.

[115] H. Hövel, S. Fritz, A. Hilger, U. Kreibig, and M. Vollmer. Width of cluster plasmon resonances: Bulk dielectric functions and chemical interface damping. *Physical Review B*, 48(24):18178–18188, December 1993.

[116] M. H. Sohn, D. Kim, S. J. Kim, N. W. Paik, and S. Gupta. Super-smooth indium–tin oxide thin films by negative sputter ion beam technology. *Journal of Vacuum Science & Technology A*, 21(4):1347–1350, July 2003.

[117] G. Kresse and J. Hafner. Ab initio molecular dynamics for liquid metals. *Physical Review B*, 47(1):558–561, January 1993.

[118] G. Kresse and J. Hafner. Ab initio molecular-dynamics simulation of the liquid-metal–amorphous-semiconductor transition in germanium. *Physical Review B*, 49(20):14251–14269, May 1994.

[119] Mario Burbano, David O. Scanlon, and Graeme W. Watson. Sources of Conductivity and Doping Limits in CdO from Hybrid Density Functional Theory. *Journal of the American Chemical Society*, 133(38):15065–15072, September 2011.

[120] Jochen Heyd, Gustavo E. Scuseria, and Matthias Ernzerhof. Hybrid functionals based on a screened Coulomb potential. *The Journal of Chemical Physics*, 118(18):8207–8215, May 2003.

[121] Jochen Heyd, Gustavo E. Scuseria, and Matthias Ernzerhof. Erratum: "Hybrid functionals based on a screened Coulomb potential" [J. Chem. Phys.118, 8207 (2003)]. *The Journal of Chemical Physics*, 124(21):219906, June 2006.

[122] Christoph Freysoldt, Jörg Neugebauer, and Chris G. Van de Walle. Fully Ab Initio Finite-Size Corrections for Charged-Defect Supercell Calculations. *Physical Review Letters*, 102(1):016402, January 2009.

[123] Christoph Freysoldt, Jörg Neugebauer, and Chris G. Van de Walle. Electrostatic interactions between charged defects in supercells. *physica status solidi (b)*, 248(5):1067–1076, May 2011.

[124] D. M Szmyd, M. C Hanna, and A. Majerfeld. Heavily doped GaAs:Se. II. Electron mobility. *Journal of Applied Physics*, 68(5):2376–2381, September 1990.

[125] A. Hartstein, J. R. Kirtley, and J. C. Tsang. Enhancement of the Infrared Absorption from Molecular Monolayers with Thin Metal Overlayers. *Physical Review Letters*, 45(3):201–204, July 1980.

[126] Yuji Nishikawa, Kunihiro Fujiwara, and Tetsuo Shima. A Study on the Qualitative and Quantitative Analysis of Nanogram Samples by Transmission Infrared Spectroscopy with the Use of Silver Island Films. *Applied Spectroscopy*, 45(5):747–751, May 1991.

[127] M. Osawa, M. Kuramitsu, A. Hatta, W. Suëtaka, and H. Seki. Electromagnetic effect in enhanced infrared absorption of adsorbed molecules on thin metal films. *Surface Science Letters*, 175:L787–L793, 1986.

[128] Masatoshi Osawa and Masahiko Ikeda. Surface-enhanced infrared absorption of p-nitrobenzoic acid deposited on silver island films: contributions of electromagnetic and chemical mechanisms. *The Journal of Physical Chemistry*, 95(24):9914–9919, November 1991.

[129] Yuji Nishikawa, Tadahiro Nagasawa, Kunihiro Fujiwara, and Masatoshi Osawa. Silver island films for surface-enhanced infrared absorption spectroscopy: effect of island morphology on the absorption enhancement. *Vibrational Spectroscopy*, 6(1):43–53, October 1993.

[130] Yuji Nishikawa, Kunihiro Fujiwara, Kenichi Ataka, and Masatoshi Osawa. Surface-enhanced infrared external reflection spectroscopy at low reflective surfaces and its application to surface analysis of semiconductors, glasses, and polymers. *Analytical Chemistry*, 65(5):556–562, March 1993.

[131] Wen-Bin Cai, Li-Jun Wan, Hiroyuki Noda, Yuichi Hibino, Kenichi Ataka, and Masatoshi Osawa. Orientational Phase Transition in a Pyridine Adlayer on Gold(111) in Aqueous Solution Studied by in Situ Infrared Spectroscopy and Scanning Tunneling Microscopy. *Langmuir*, 14(24):6992–6998, November 1998.

[132] Li-Jun Wan, Mimi Terashima, Hiroyuki Noda, and Masatoshi Osawa. Molecular Orientation and Ordered Structure of Benzenethiol Adsorbed on Gold(111). *The Journal of Physical Chemistry B*, 104(15):3563–3569, April 2000.

[133] H. Noda, T. Minoha, L. Wan, and M. Osawa. Adsorption and ordered phase formation of 2,2'-bypyridine on Au(111): a combined surface-enhanced infrared and STM study. *Journal of Electroanalytical Chemistry*, 481(1):62–68, January 2000.

[134] Yimin Zhu, Hiroyuki Uchida, and Masahiro Watanabe. Oxidation of Carbon Monoxide at a Platinum Film Electrode Studied by Fourier Transform Infrared Spectroscopy with Attenuated Total Reflection Technique. *Langmuir*, 15(25):8757–8764, December 1999.

[135] Masahiro Watanabe, Yimin Zhu, and Hiroyuki Uchida. Oxidation of CO on a Pt-Fe Alloy Electrode Studied by Surface Enhanced Infrared Reflection-Absorption Spectroscopy. *The Journal of Physical Chemistry B*, 104(8):1762–1768, March 2000.

[136] Zhi Qiang. Feng, Takamasa. Sagara, and Katsumi. Niki. Application of potential-modulated UV-visible reflectance spectroscopy to electron transfer rate measurements for adsorbed species on electrode surfaces. *Analytical Chemistry*, 67(19):3564–3570, October 1995.

[137] Peter R. Griffiths Christine M. Pharr. Step-Scan FT-IR Spectroelectrochemical Analysis of Surface and Solution Species in the Ferricyanide/Ferrocyanide Redox Couple. *Analytical Chemistry - ANAL CHEM*, 69(22), 1997.

[138] Shi-Gang Sun, Wen-Bin Cai, Li-Jun Wan, and Masatoshi Osawa. Infrared Absorption Enhancement for CO Adsorbed on Au Films in Perchloric Acid Solutions and Effects of Surface Structure Studied by Cyclic Voltammetry, Scanning Tunneling Microscopy, and Surface-Enhanced IR Spectroscopy. *The Journal of Physical Chemistry B*, 103(13):2460–2466, April 1999.

[139] Masatoshi Osawa, Ken-Ichi Ataka, Katsumasa Yoshii, and Yuji Nishikawa. Surface-Enhanced Infrared Spectroscopy: The Origin of the Absorption Enhancement and Band Selection Rule in the Infrared Spectra of Molecules Adsorbed on Fine Metal Particles. *Applied Spectroscopy*, 47(9):1497–1502, September 1993.

[140] P. Dumas, R. G. Tobin, and P. L. Richards. Study of adsorption states and interactions of CO on evaporated noble metal surfaces by infrared absorption spectroscopy: I. Silver. *Surface Science*, 171(3):555–578, June 1986.

[141] Jarosław J. Panek, Aneta Jezierska-Mazzarello, Aleksander Koll, Galina Dovbeshko, and Olena Fesenko. p-Nitrobenzoic acid adsorption on nanostructured gold surfaces investigated by combined experimental and computational approaches. *Chemphyschem: A European Journal of Chemical Physics and Physical Chemistry*, 12(13):2485–2495, September 2011.

[142] Sunjie Ye, Li Fang, and Yun Lu. Contribution of charge-transfer effect to surface-enhanced IR for Ag@PPy nanoparticles. *Physical Chemistry Chemical Physics*, 11(14):2480–2484, March 2009.

[143] J. Paul Devlin and Keith Consani. Metal surface spectroscopy. Charge transfer and totally symmetric mode activity. *The Journal of Physical Chemistry*, 85(18):2597–2598, September 1981.

[144] T. Wadayama, T. Sakurai, S. Ichikawa, and W. Suëtaka. Charge-transfer enhancement in infrared absorption of thiocyanate ions adsorbed on a gold electrode in the Kretschmann ATR configuration. *Surface Science*, 198(3):L359–L364, 1988.

[145] T. Wadayama, M. Takada, K. Sugiyama, and A. Hatta. Infrared absorption enhancement of ${\mathrm{C}}_{60}$ on silver islands: Contribution of charge transfer and collective electron resonance. *Physical Review B*, 66(19):193401, November 2002.

[146] G. Fahsold O. Krauth. Asymmetric line shapes and surface enhanced infrared absorption of CO adsorbed on thin iron films on MgO(001). *The Journal of Chemical Physics*, 110(6):3113–3117, 1999.

[147] P. Alonso-González, P. Albella, M. Schnell, J. Chen, F. Huth, A. García-Etxarri, F. Casanova, F. Golmar, L. Arzubiaga, L. E. Hueso, J. Aizpurua, and R. Hillenbrand. Resolving the electromagnetic mechanism of surface-enhanced light scattering at single hot spots. *Nature Communications*, 3:684, February 2012.

[148] L. S. Rothman, I. E. Gordon, Y. Babikov, A. Barbe, D. Chris Benner, P. F. Bernath, M. Birk, L. Bizzocchi, V. Boudon, L. R. Brown, A. Campargue, K. Chance, E. A. Cohen, L. H. Coudert, V. M. Devi, B. J. Drouin, A. Fayt, J. M. Flaud, R. R. Gamache, J. J. Harrison, J. M. Hartmann, C. Hill, J. T. Hodges, D. Jacquemart, A. Jolly, J. Lamouroux, R. J. Le Roy, G. Li, D. A. Long, O. M. Lyulin, C. J. Mackie, S. T. Massie, S. Mikhailenko, H. S. P. Müller, O. V. Naumenko, A. V. Nikitin, J. Orphal, V. Perevalov, A. Perrin, E. R. Polovtseva, C. Richard, M. A. H. Smith, E. Starikova, K. Sung, S. Tashkun, J. Tennyson, G. C. Toon, Vl. G. Tyuterev, and G. Wagner. The HITRAN2012 molecular spectroscopic database. *Journal of Quantitative Spectroscopy and Radiative Transfer*, 130:4–50, November 2013.

[149] Aaron L. Stancik and Eric B. Brauns. A simple asymmetric lineshape for fitting infrared absorption spectra. *Vibrational Spectroscopy*, 47(1):66–69, May 2008.

Appendices

Appendix A

Technical Drawings

This part of the Appendix contains all technical drawings that were used to machine the various parts used in this work. These drawings were all information needed to machine the parts in question.

A.1 SPR sample holders for the IR-VASE

The sample holders are designed to accommodate 1x1 cm samples in the Kretschmann configuration.

A.1.1 SPR sample holder for air measurements

This design has been used for all measurements where the plasmonic film was measured against the room atmosphere, thus air.

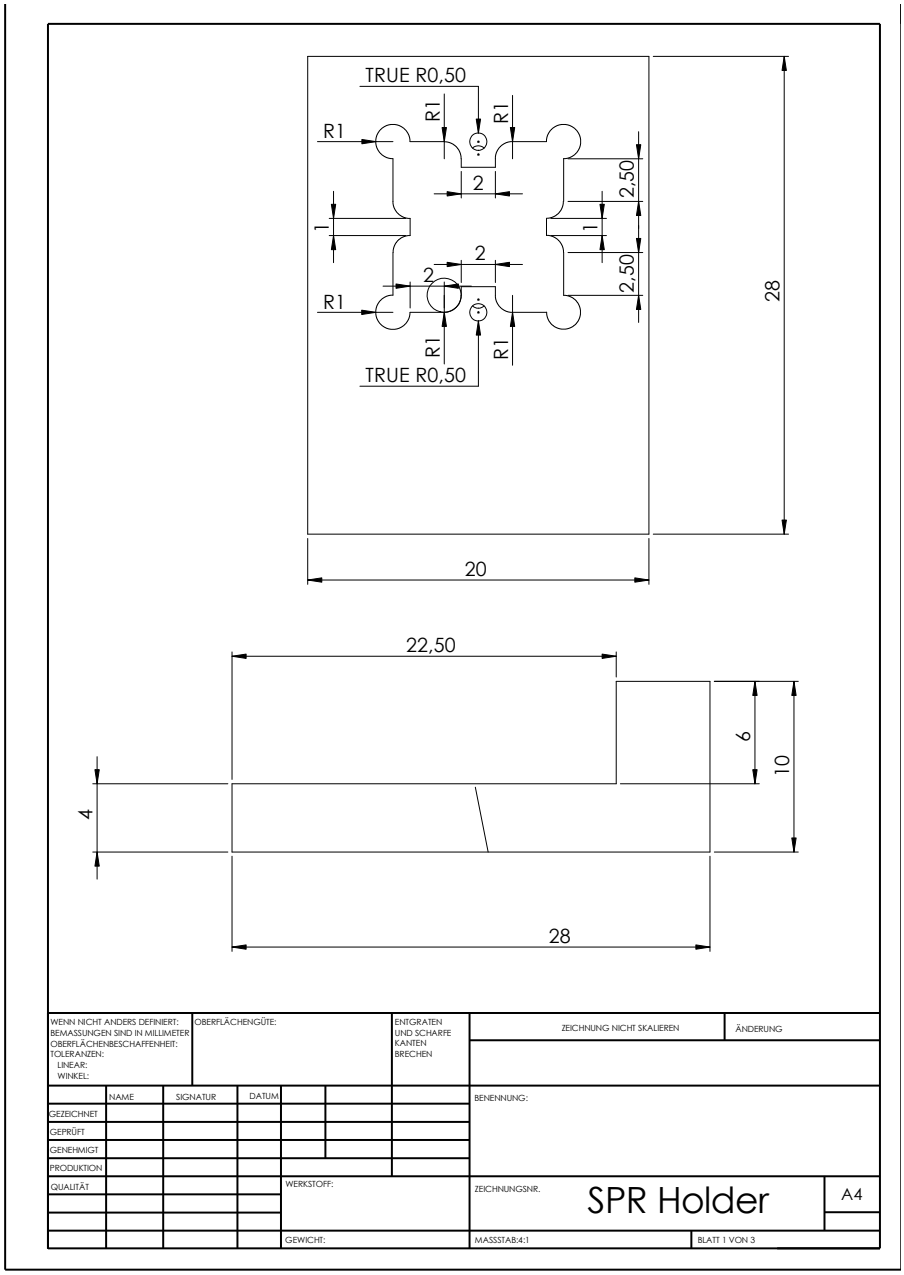
TRUE R0,50
R1
R1
R1
2
2,50
1
1
2
2
2,50
R1
R1
R1
TRUE R0,50
28
20
22,50
6
10
4
28
WENN NICHT ANDERS DEFINIERT:
BEMASSUNGEN SIND IN MILLIMETER
OBERFLÄCHENBESCHAFFENHEIT:
TOLERANZEN:
LINEAR:
WINKEL:
OBERFLÄCHENGÜTE:
ENTGRATEN UND SCHARFE KANTEN BRECHEN
ZEICHNUNG NICHT SKALIEREN
ÄNDERUNG
NAME
SIGNATUR
DATUM
GEZEICHNET
GEPRÜFT
GENEHMIGT
PRODUKTION
QUALITÄT
BENENNUNG:
WERKSTOFF:
ZEICHNUNGSNR.
SPR Holder
A4
GEWICHT:
MASSSTAB:4:1
BLATT 1 VON 3

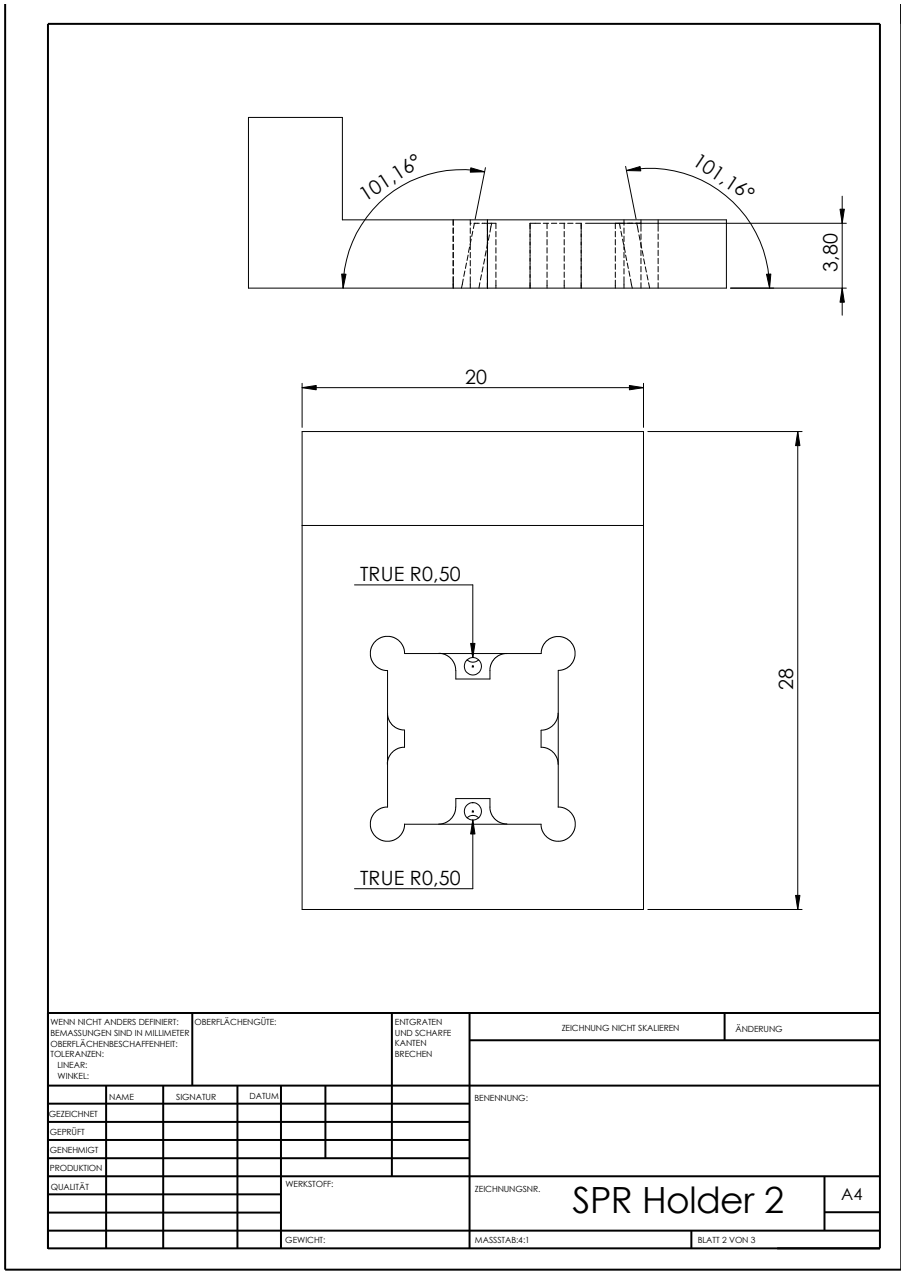
101,16°
101,16°
3,80
20
TRUE R0,50
28
TRUE R0,50
WENN NICHT ANDERS DEFINIERT:
BEMASSUNGEN SIND IN MILLIMETER
OBERFLÄCHENBESCHAFFENHEIT:
TOLERANZEN:
LINEAR:
WINKEL:
OBERFLÄCHENGÜTE:
ENTGRATEN UND SCHARFE KANTEN BRECHEN
ZEICHNUNG NICHT SKALIEREN
ÄNDERUNG
NAME
SIGNATUR
DATUM
GEZEICHNET
GEPRÜFT
GENEHMIGT
PRODUKTION
QUALITÄT
BENENNUNG:
WERKSTOFF:
ZEICHNUNGSNR.
SPR Holder 2
A4
GEWICHT:
MASSSTAB:4:1
BLATT 2 VON 3

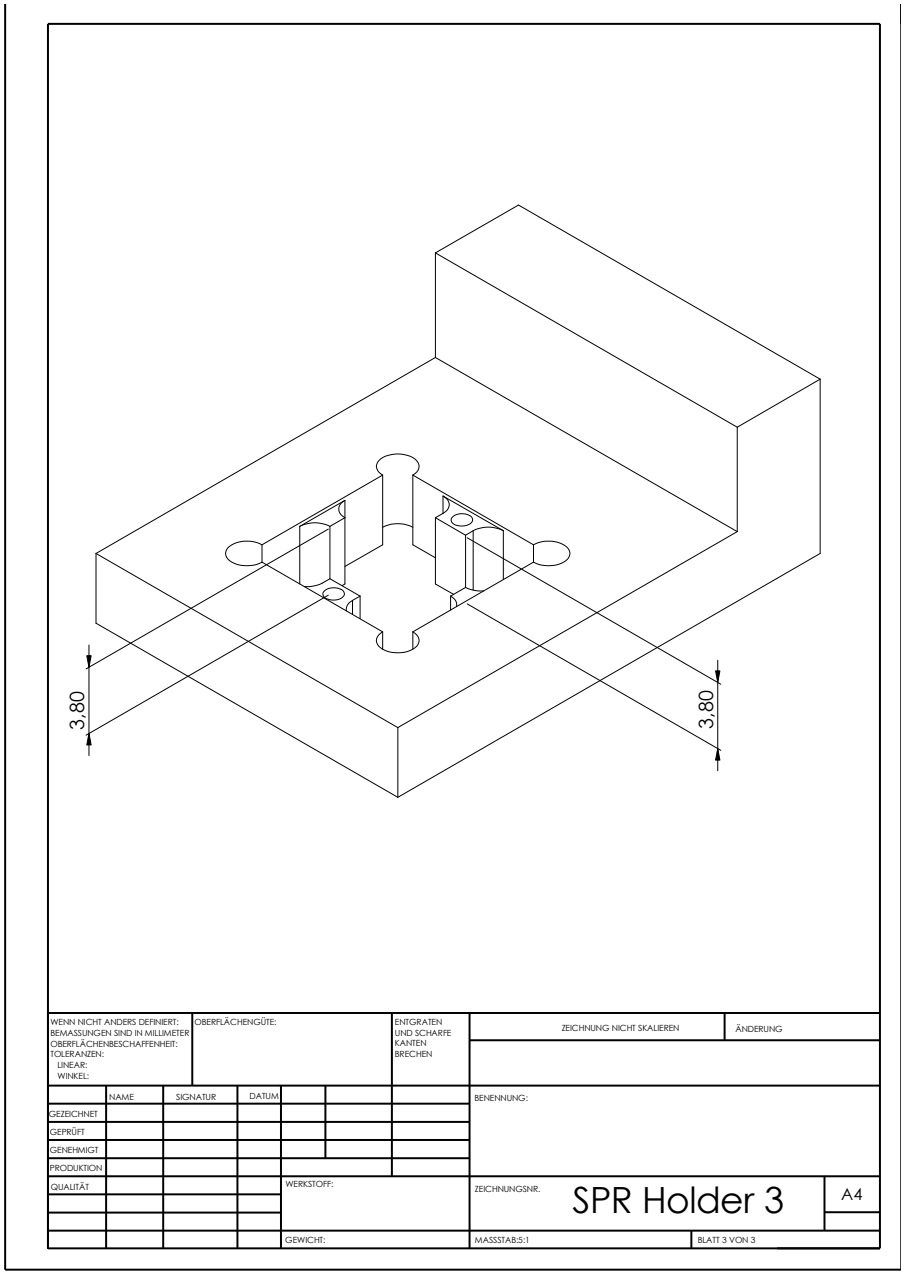
3,80
3,80
WENN NICHT ANDERS DEFINIERT:
BEMASSUNGEN SIND IN MILLIMETER
OBERFLÄCHENBESCHAFFENHEIT:
TOLERANZEN:
LINEAR:
WINKEL:
OBERFLÄCHENGÜTE:
ENTGRATEN UND SCHARFE KANTEN BRECHEN
ZEICHNUNG NICHT SKALIEREN
ÄNDERUNG
NAME
SIGNATUR
DATUM
GEZEICHNET
GEPRÜFT
GENEHMIGT
PRODUKTION
QUALITÄT
BENENNUNG:
WERKSTOFF:
ZEICHNUNGSNR.
SPR Holder 3
A4
GEWICHT:
MASSSTAB:5:1
BLATT 3 VON 3

A.1.2 SPR flow cell

This design allows to measure SPR of thin films samples in controlled atmospheres:

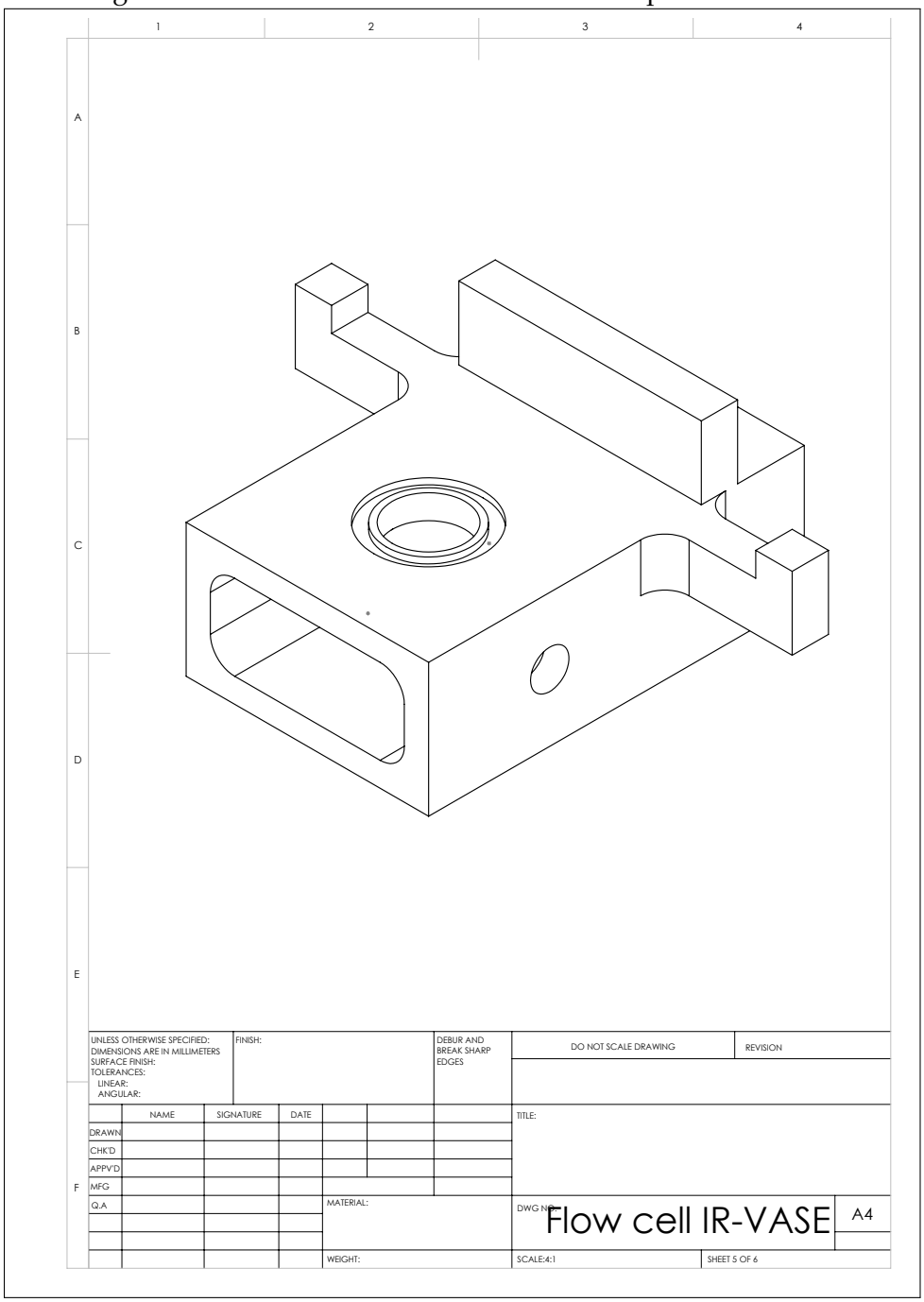

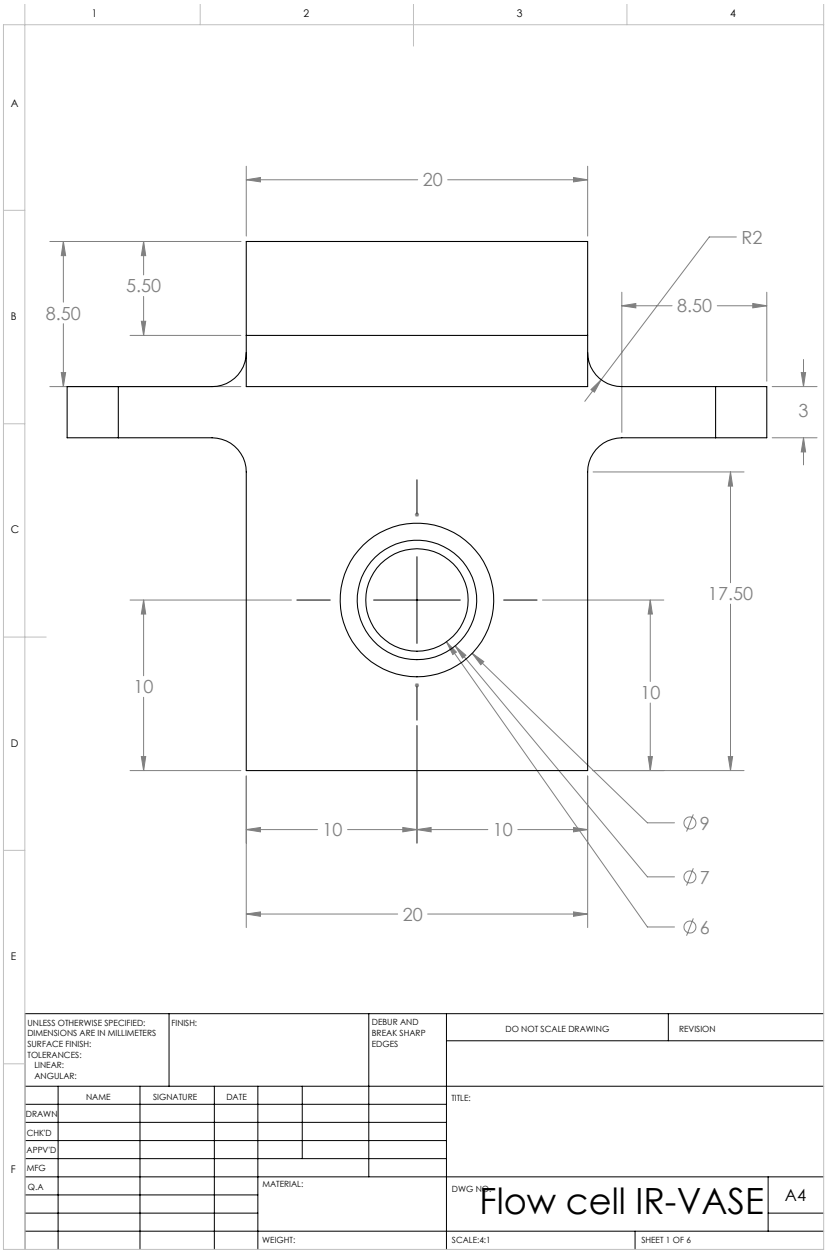
1
2
3
4
A
B
C
D
E
F
20
R2
5.50
8.50
8.50
3
17.50
10
10
10
10
20
Ø9
Ø7
Ø6
UNLESS OTHERWISE SPECIFIED:
DIMENSIONS ARE IN MILLIMETERS
SURFACE FINISH:
TOLERANCES:
LINEAR:
ANGULAR:
FINISH:
DEBUR AND BREAK SHARP EDGES
DO NOT SCALE DRAWING
REVISION
NAME
SIGNATURE
DATE
DRAWN
CHK'D
APPV'D
MFG
Q.A
TITLE:
MATERIAL:
DWG NO.
Flow cell IR-VASE
A4
WEIGHT:
SCALE:4:1
SHEET 1 OF 6

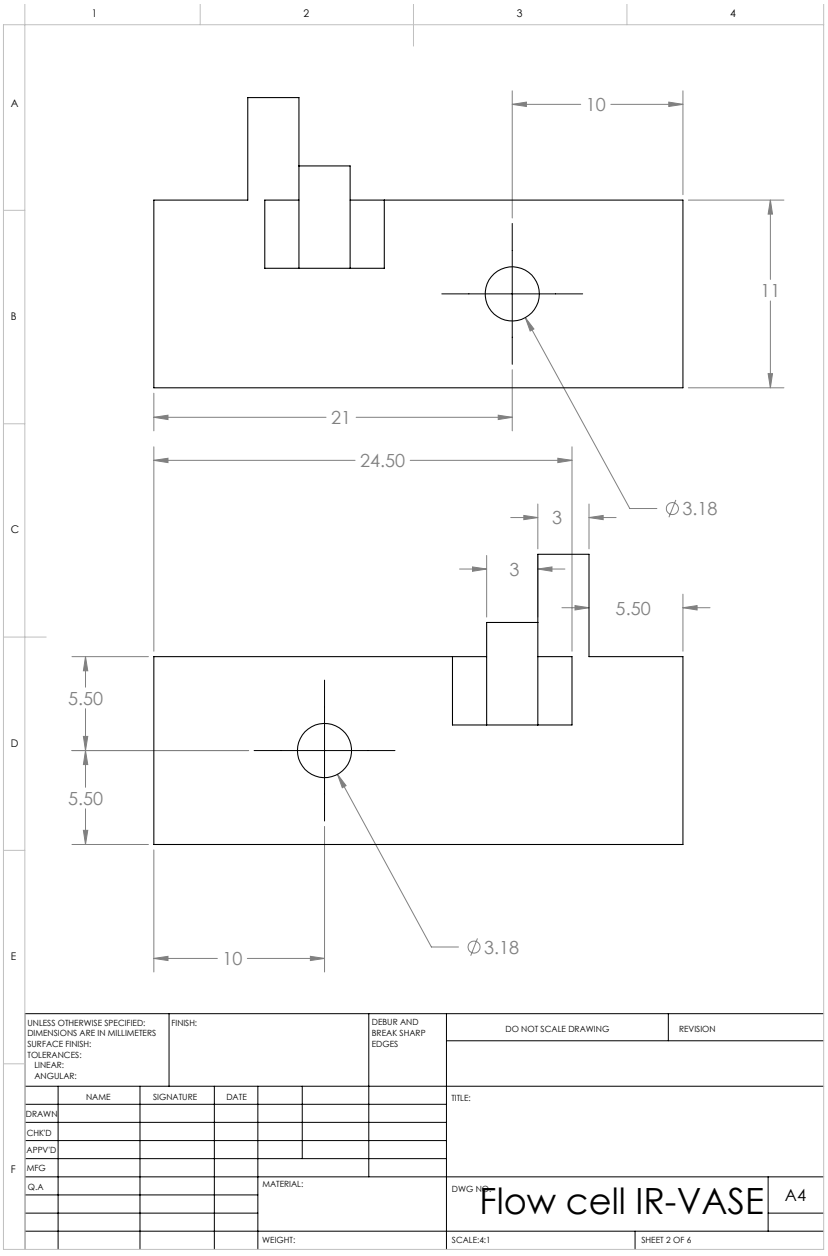
1
2
3
4
A
B
C
D
E
F
10
11
21
24.50
3
3
5.50
5.50
5.50
∅3.18
∅3.18
10
UNLESS OTHERWISE SPECIFIED:
DIMENSIONS ARE IN MILLIMETERS
SURFACE FINISH:
TOLERANCES:
LINEAR:
ANGULAR:
FINISH:
DEBUR AND BREAK SHARP EDGES
DO NOT SCALE DRAWING
REVISION
NAME
SIGNATURE
DATE
DRAWN
CHK'D
APPV'D
MFG
Q.A
TITLE:
MATERIAL:
DWG NO.
Flow cell IR-VASE
A4
WEIGHT:
SCALE:4:1
SHEET 2 OF 6

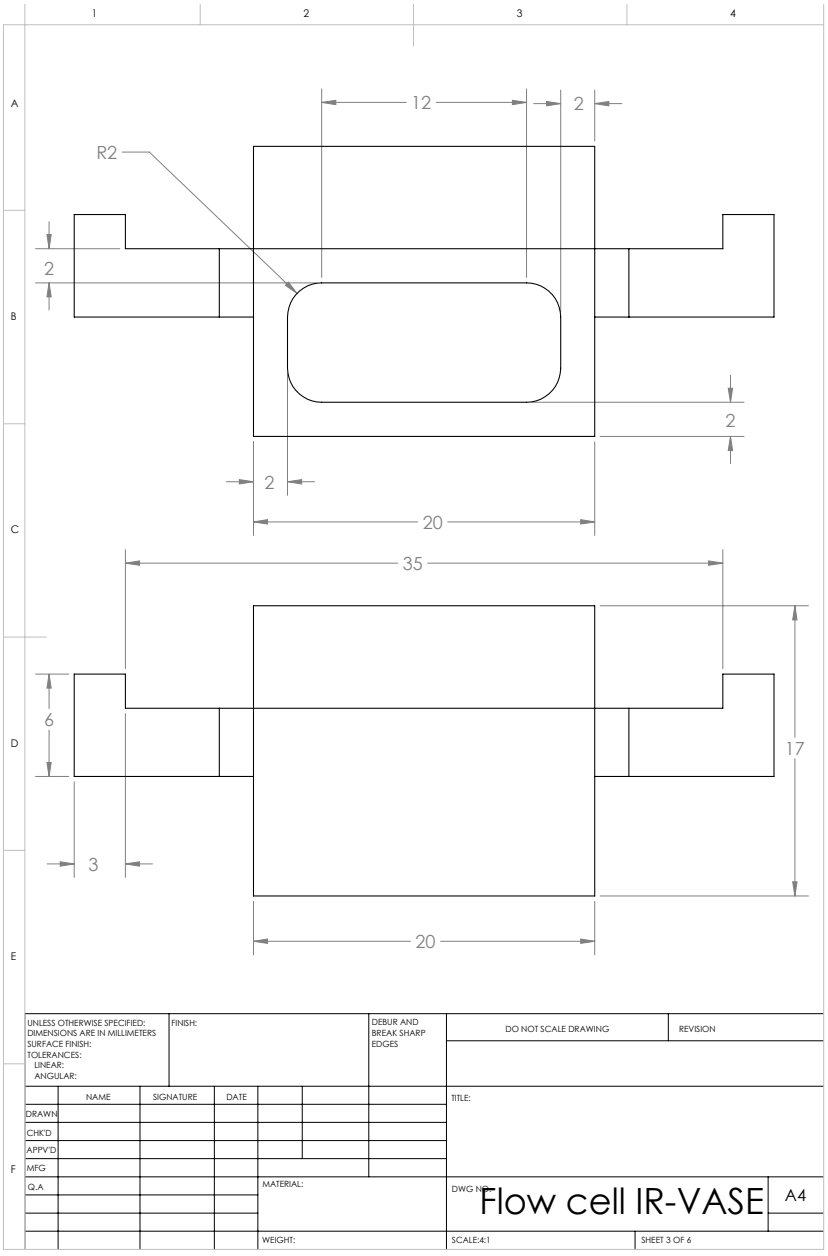
1
2
3
4
A
B
C
D
E
F
12
2
R2
2
2
2
20
35
6
17
3
20
UNLESS OTHERWISE SPECIFIED:
DIMENSIONS ARE IN MILLIMETERS
SURFACE FINISH:
TOLERANCES:
LINEAR:
ANGULAR:
FINISH:
DEBUR AND BREAK SHARP EDGES
DO NOT SCALE DRAWING
REVISION
NAME
SIGNATURE
DATE
DRAWN
CHK'D
APPV'D
MFG
Q.A
TITLE:
MATERIAL:
DWG NO.
Flow cell IR-VASE
A4
WEIGHT:
SCALE:4:1
SHEET 3 OF 6

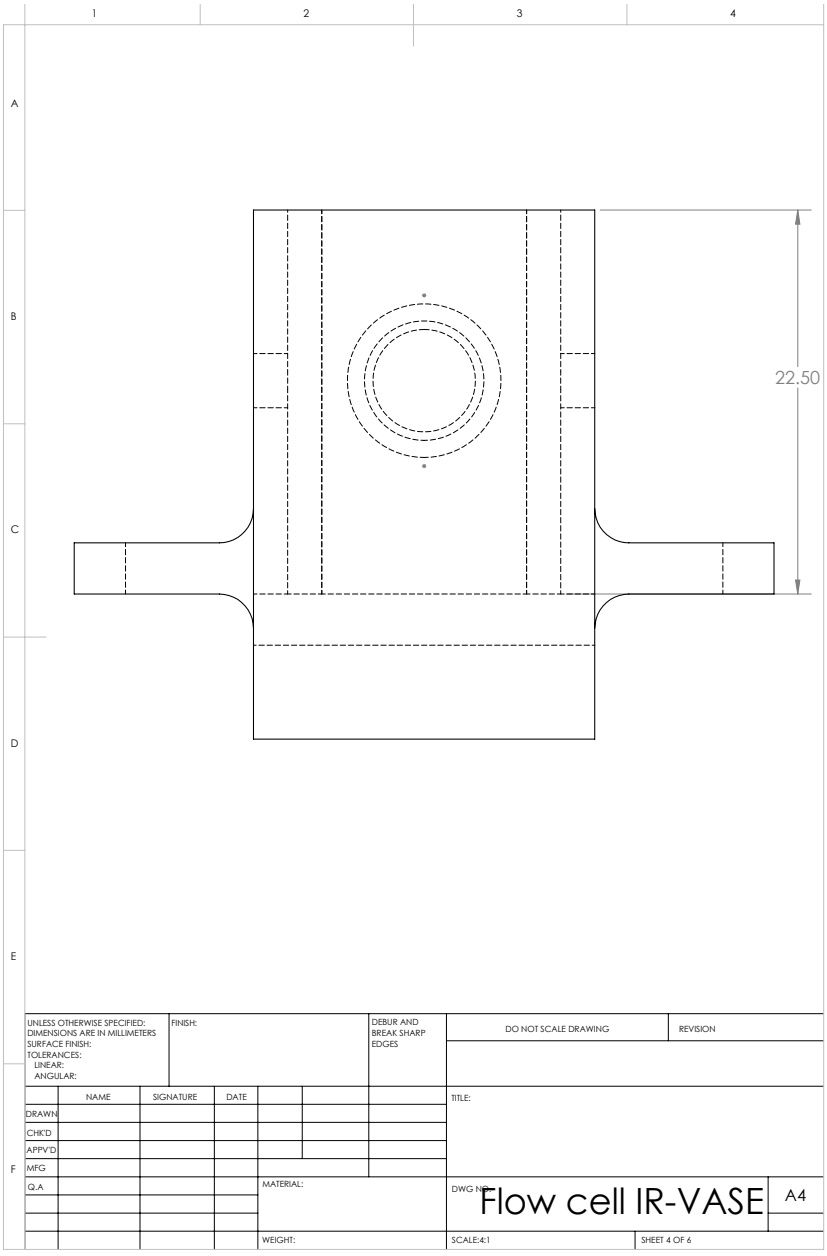
1
2
3
4
A
B
C
D
E
F
22.50
UNLESS OTHERWISE SPECIFIED:
DIMENSIONS ARE IN MILLIMETERS
SURFACE FINISH:
TOLERANCES:
LINEAR:
ANGULAR:
FINISH:
DEBUR AND BREAK SHARP EDGES
DO NOT SCALE DRAWING
REVISION
NAME
SIGNATURE
DATE
DRAWN
CHK'D
APPV'D
MFG
Q.A
TITLE:
MATERIAL:
DWG NO.
Flow cell IR-VASE
A4
WEIGHT:
SCALE:4:1
SHEET 4 OF 6

A.2 ICP-Plasma Source

The glass body that directly attaches to one of the MBE source flanges has been manufactured by Larson Electronic Glass:

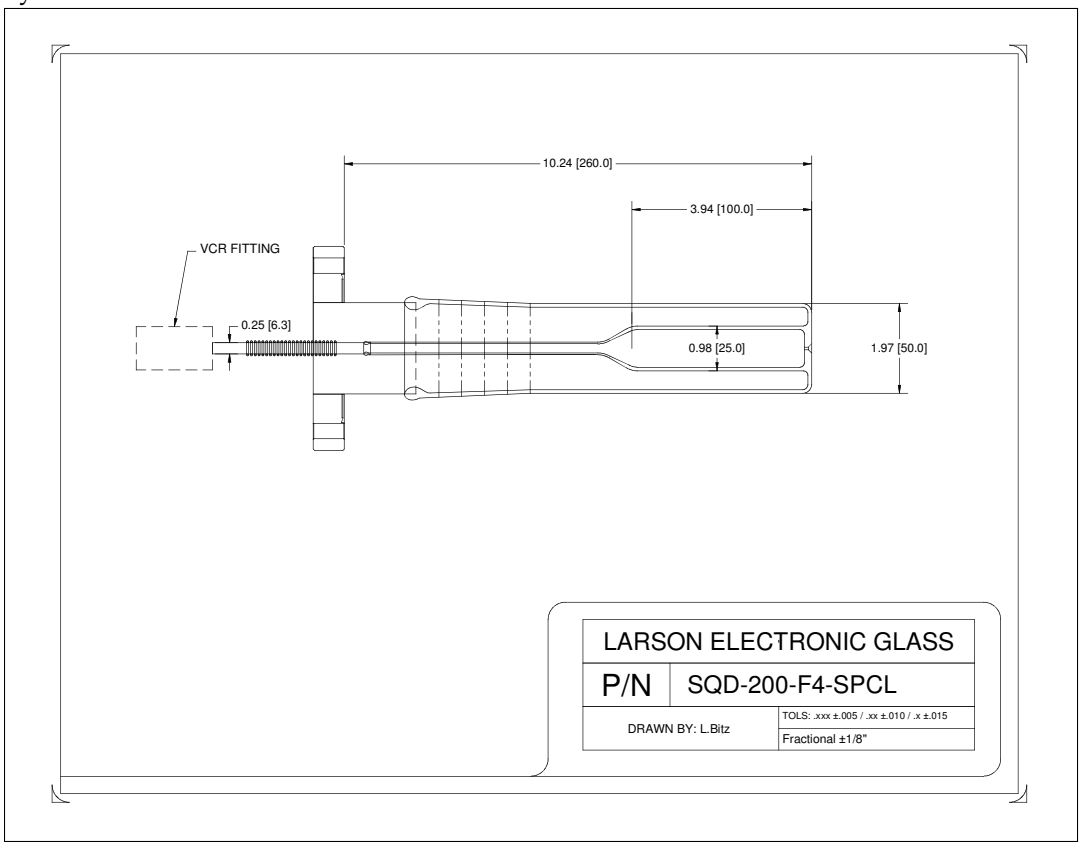

In order to keep the VCR fitting supported to not stress the bellows (those are directly connected to the main MBE chamber), a special clamping holder was designed to support the VCR nut and to secure it against the necessary torque needed for assembly of the gas line. The following three figures depict the use of the parts as well as the full assembly. Additionally, the technical drawing is also included. 2 identical parts are needed for installation.

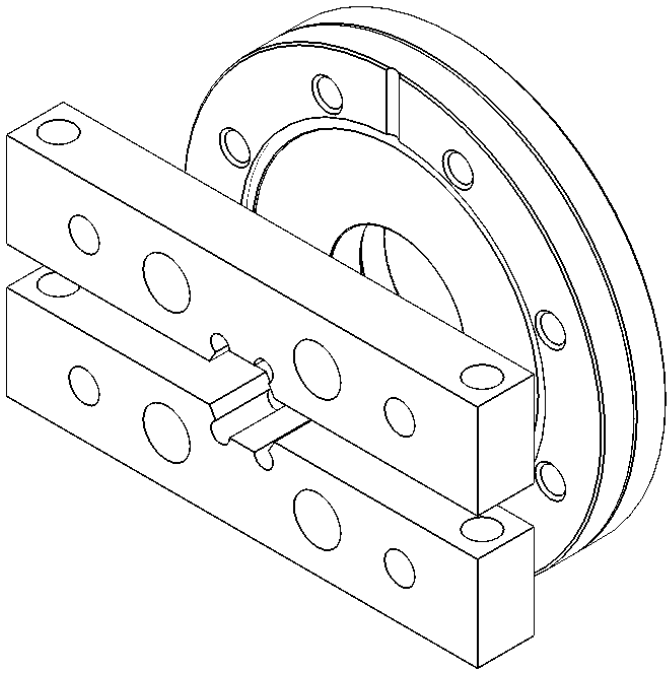

Figure A.1 Isometric view of the ICP source support

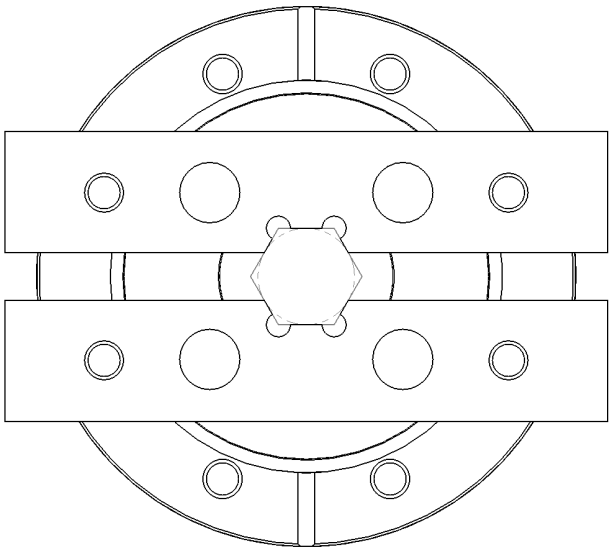

Figure A.2 Frontal view of the ICP source support

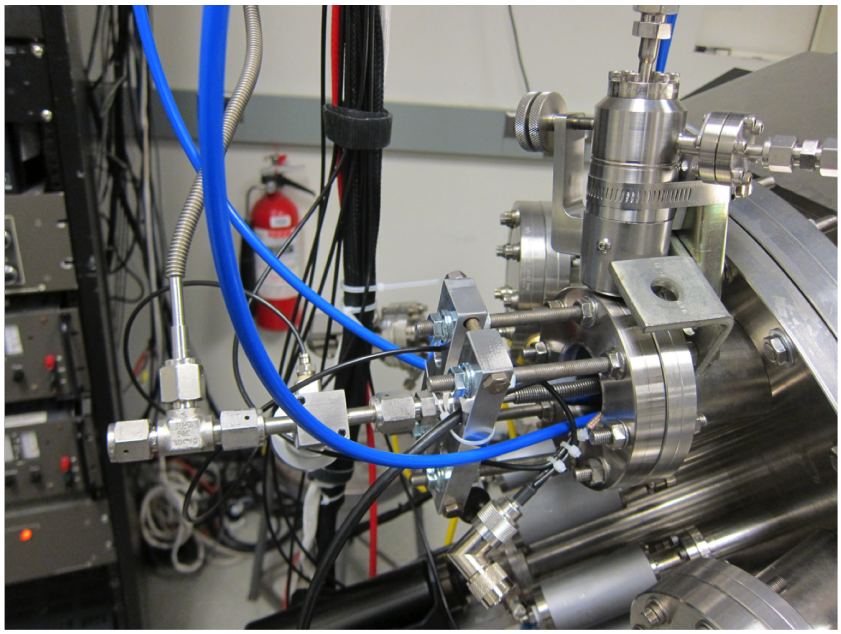

Figure A.3 Assembled ICP source mounted to a MBE source flange with all connections in place

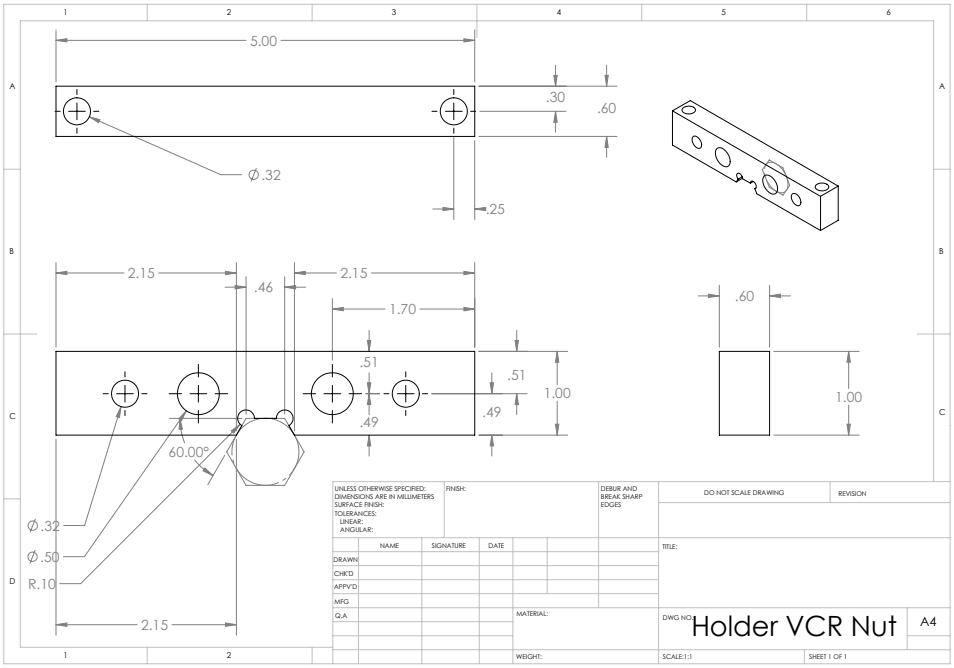
5.00
.30
.60
Ø .32
.25
2.15
.46
2.15
1.70
.51
.51
1.00
.49
.49
60.00°
.60
1.00
Ø .32
Ø .50
R.10
2.15
UNLESS OTHERWISE SPECIFIED:
DIMENSIONS ARE IN MILLIMETERS
SURFACE FINISH:
TOLERANCES:
LINEAR:
ANGULAR:
FINISH:
DEBUR AND BREAK SHARP EDGES
DO NOT SCALE DRAWING
REVISION
NAME
SIGNATURE
DATE
DRAWN
CHK'D
APPV'D
MFG
Q.A
TITLE:
MATERIAL:
DWG NO.
Holder VCR Nut
A4
WEIGHT:
SCALE:1:1
SHEET 1 OF 1

Additional renderings of the design to illustrate the assembly of the water cooled induction coil:

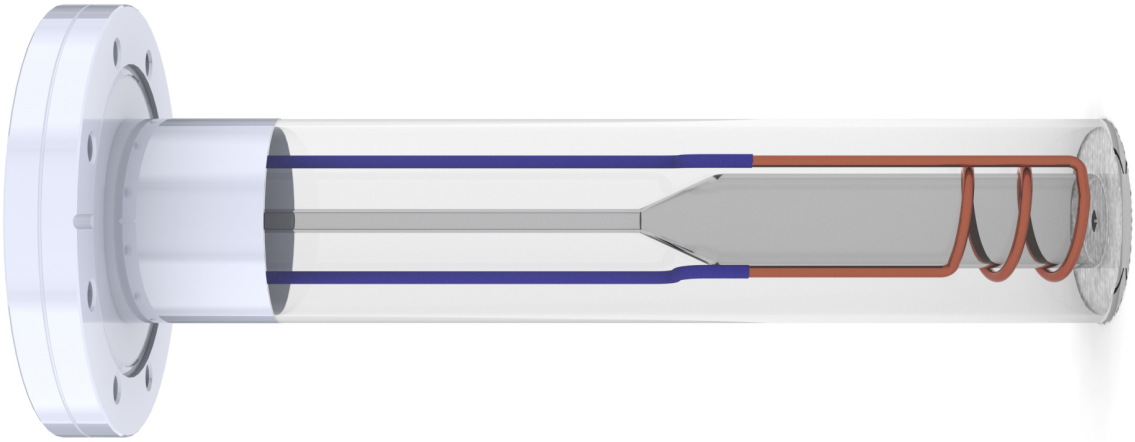

Figure A.4 Side view rendering of the ICP source internals

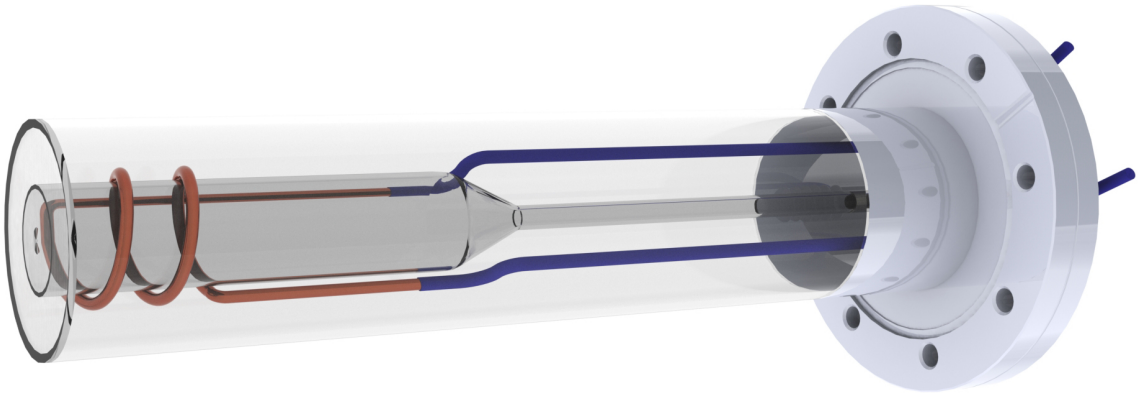

Figure A.5 Isometric view rendering of the ICP source internals

Appendix B

Mathematica Code

In this Appendix all of the Wolfram Mathematica code used for this work will be printed as a reference. This is not a manual, existing Mathematica knowledge will be necessary to use the code. Each code is included in two versions. The first being completely verbatim, which allows the code to be copied directly from the pdf-version of this thesis into Mathematica. This will result in working code that can be compiled (tested with OS X 10.9.2 and Mathematica 10). Unfortunately the cell formating will be lost, which is why a second version of the code will be provided to help the prospective user to set up the cell divisions as intended by the author. This code will be depicted exactly how it looks within the Mathematica editor.
Most code will rely on optical reference data for substrate and prism materials. This data will be supplied only once, code that relies on the data will be marked with an *. I recommend to include this code in an initialization cell at the start of each respective program.

B.1 Optical Constants

This data lists the optical properties of materials used in Mathematica simulations. The data is collected as a Mathematica list and then interpolated as a function that the simulations can call.

```
(* Dipsersion Data *)

(* Options: al2o3, caf2, si, znse, ge, gaas, inp, mgo, h2o (water) *)

(* Al2O3 *)
```

al2o3raw={{7876.71, 2.44386}, {7845.85, 2.44336}, {7814.99, 2.44285}, {7784.13, 2.44234}, {7753.27, 2.44183}, {7722.41, 2.44132}, {7695.41, 2.44087}, {7664.55, 2.44036}, {7633.69, 2.43984}, {7606.69, 2.43939}, {7575.83, 2.43887}, {7548.83, 2.43842}, {7521.83, 2.43796}, {7490.97, 2.43743}, {7463.97, 2.43697}, {7436.97, 2.43651}, {7409.97, 2.43605}, {7382.97, 2.43558}, {7355.96, 2.43511}, {7328.96, 2.43464}, {7301.96, 2.43417}, {7274.96, 2.4337}, {7247.96, 2.43322}, {7220.96, 2.43274}, {7197.81, 2.43233}, {7170.81, 2.43185}, {7143.81, 2.43137}, {7120.67, 2.43095}, {7093.66, 2.43046}, {7070.52, 2.43004}, {7043.52, 2.42955}, {7020.38, 2.42912}, {6993.37, 2.42862}, {6970.23, 2.42819}, {6947.09, 2.42776}, {6923.94, 2.42733}, {6896.94, 2.42682}, {6873.8, 2.42639}, {6850.65, 2.42595}, {6827.51, 2.4255}, {6804.36, 2.42506}, {6781.22, 2.42461}, {6758.08, 2.42416}, {6734.93, 2.42371}, {6711.79, 2.42326}, {6692.5, 2.42288}, {6669.36, 2.42242}, {6646.21, 2.42196}, {6623.07, 2.42149}, {6603.78, 2.4211}, {6580.64, 2.42063}, {6557.49, 2.42016}, {6538.21, 2.41976}, {6515.06, 2.41929}, {6495.78, 2.41888}, {6472.63, 2.4184}, {6453.34, 2.41799}, {6434.06, 2.41759}, {6410.91, 2.41709}, {6391.63, 2.41668}, {6372.34, 2.41626}, {6353.05, 2.41584}, {6329.91, 2.41534}, {6310.62, 2.41492}, {6291.34, 2.41449}, {6272.05, 2.41406}, {6252.76, 2.41363}, {6233.48, 2.41319}, {6214.19, 2.41275}, {6194.9, 2.41231}, {6175.62, 2.41187}, {6156.33, 2.41142}, {6137.04, 2.41097}, {6117.76, 2.41052}, {6098.47, 2.41006}, {6079.18, 2.4096}, {6063.75, 2.40923}, {6044.47, 2.40876}, {6025.18, 2.40829}, {6009.75, 2.40792}, {5990.46, 2.40744}, {5971.18, 2.40696}, {5955.75, 2.40657}, {5936.46, 2.40609}, {5917.17, 2.4056}, {5901.74, 2.4052}, {5882.46, 2.4047}, {5867.03, 2.4043}, {5851.6, 2.4039}, {5832.31, 2.40339}, {5816.88, 2.40298}, {5797.6, 2.40246}, {5782.17, 2.40204}, {5766.74, 2.40162}, {5747.45, 2.40109}, {5732.02, 2.40066}, {5716.59, 2.40023}, {5701.16, 2.3998}, {5681.88, 2.39925}, {5666.45, 2.39881}, {5651.02, 2.39837}, {5635.59, 2.39792}, {5620.16, 2.39747}, {5604.73, 2.39701}, {5589.3, 2.39655}, {5573.87, 2.39609}, {5558.44, 2.39563}, {5543.01, 2.39516}, {5527.58, 2.39468}, {5512.15, 2.3942}, {5496.72, 2.39372}, {5481.29, 2.39323}, {5465.86, 2.39274}, {5450.43, 2.39225}, {5435, 2.39175}, {5423.43, 2.39137}, {5408, 2.39086}, {5392.57, 2.39035}, {5377.14, 2.38983}, {5365.57, 2.38944}, {5350.14, 2.38891}, {5334.71, 2.38838}, {5319.28, 2.38784}, {5307.71, 2.38744}, {5292.28, 2.38689}, {5280.71, 2.38648}, {5265.28, 2.38592}, {5249.85, 2.38536}, {5238.28, 2.38494}, {5222.85, 2.38436}, {5211.28, 2.38393}, {5195.85, 2.38335}, {5184.28, 2.38291}, {5168.85, 2.38231}, {5157.28, 2.38186}, {5141.85, 2.38126}, {5130.27, 2.3808}, {5118.7, 2.38034}, {5103.27, 2.37971}, {5091.7, 2.37924}, {5076.27, 2.3786}, {5064.7, 2.37812}, {5053.13, 2.37764}, {5041.56, 2.37715}, {5026.13, 2.37648}, {5014.55, 2.37598}, {5002.98, 2.37548}, {4987.55, 2.37479}, {4975.98, 2.37428}, {4964.41, 2.37375}, {4952.84, 2.37323}, {4941.26, 2.37269}, {4929.69, 2.37216}, {4914.26, 2.37143}, {4902.69, 2.37088}, {4891.12, 2.37032}, {4879.55, 2.36976}, {4867.97, 2.36919}, {4856.4, 2.36862}, {4844.83, 2.36804}, {4833.26, 2.36745}, {4821.69, 2.36685}, {4810.11, 2.36625}, {4798.54, 2.36565}, {4786.97, 2.36503}, {4775.4, 2.36441}, {4763.83, 2.36378}, {4752.25, 2.36315}, {4740.68, 2.3625}, {4729.11, 2.36185}, {4717.54, 2.36119}, {4705.97, 2.36053}, {4698.25, 2.36008}, {4686.68, 2.3594}, {4675.11, 2.35871}, {4663.54, 2.35801}, {4651.96, 2.3573}, {4640.39, 2.35658}, {4632.68, 2.3561}, {4621.1, 2.35537}, {4609.53, 2.35462}, {4597.96, 2.35387}, {4590.25, 2.35336}, {4578.67, 2.35259}, {4567.1, 2.35181}, {4559.39, 2.35128}, {4547.81, 2.35048}, {4536.24, 2.34966}, {4528.53, 2.34911}, {4516.96, 2.34828}, {4505.38, 2.34743}, {4497.67, 2.34686}, {4486.1, 2.34599}, {4474.52, 2.3451}, {4466.81, 2.34451}, {4455.24, 2.3436}, {4447.52, 2.34298}, {4435.95, 2.34205}, {4428.24, 2.34142}, {4416.66, 2.34045}, {4408.95, 2.3398}, {4397.38, 2.33881}, {4389.66, 2.33814}, {4378.09, 2.33712}, {4370.38, 2.33643}, {4358.8, 2.33537}, {4351.09, 2.33466}, {4339.52, 2.33357}, {4331.8, 2.33283}, {4320.23, 2.3317}, {4312.52, 2.33094}, {4304.8, 2.33016}, {4293.23, 2.32898}, {4285.51, 2.32818}, {4273.94, 2.32695}, {4266.23, 2.32612}, {4258.51, 2.32527}, {4246.94, 2.32398}, {4239.23, 2.3231}, {4231.51, 2.32221}, {4219.94, 2.32084}, {4212.23, 2.31991}, {4204.51, 2.31896}, {4192.94, 2.31751}, {4185.22, 2.31652}, {4177.51, 2.31551}, {4169.79, 2.31449}, {4158.22, 2.31291}, {4150.51, 2.31184}, {4142.79, 2.31075}, {4135.08, 2.30963}, {4127.36, 2.30849}, {4115.79, 2.30674}, {4108.08, 2.30554}, {4100.36, 2.30432}, {4092.65, 2.30307}, {4084.93, 2.30179}, {4073.36, 2.29982}, {4065.65, 2.29846}, {4057.93, 2.29708}, {4050.22, 2.29566}, {4042.5, 2.29421}, {4034.79, 2.29272}, {4027.07, 2.29119}, {4019.36, 2.28963}, {4011.64, 2.28802}, {4000.07, 2.28553}, {3992.36, 2.28381}, {3984.64, 2.28205}, {3976.93, 2.28023}, {3969.21, 2.27837}, {3961.5, 2.27645}, {3953.78, 2.27448}, {3946.07, 2.27245}, {3938.35, 2.27036}, {3930.64, 2.26821}, {3922.92, 2.266}, {3915.21, 2.26373}, {3907.49, 2.26139}, {3899.78, 2.25898}, {3892.07, 2.2565}, {3884.35, 2.25395}, {3876.64, 2.25133}, {3868.92, 2.24864}, {3861.21, 2.24588}, {3857.35, 2.24447}, {3849.63, 2.2416}, {3841.92, 2.23866}, {3834.21, 2.23565}, {3826.49, 2.23257}, {3818.78, 2.22942}, {3811.06, 2.22622}, {3803.35, 2.22296}, {3795.63, 2.21964}, {3787.92, 2.21628}, {3784.06, 2.21458}, {3776.34, 2.21115}, {3768.63, 2.2077}, {3760.92, 2.20422}, {3753.2, 2.20074}, {3745.49, 2.19725}, {3741.63, 2.19551}, {3733.91, 2.19204}, {3726.2, 2.18861}, {3718.48, 2.18522}, {3710.77, 2.18189}, {3706.91, 2.18025}, {3699.2, 2.17704}, {3691.48, 2.17393}, {3683.77, 2.17095}, {3679.91, 2.1695}, {3672.2, 2.16674}, {3664.48, 2.16414}, {3656.77, 2.16173}, {3652.91, 2.1606}, {3645.2, 2.15851}, {3637.48, 2.15667}, {3629.77, 2.15508}, {3625.91, 2.15439}, {3618.19, 2.15323}, {3610.48, 2.15238}, {3606.62, 2.15208}, {3598.91, 2.15172}, {3591.19, 2.15172}, {3587.33, 2.15186}, {3579.62, 2.15241}, {3571.91, 2.15335}, {3568.05, 2.15397}, {3560.33, 2.1555}, {3552.62, 2.15745}, {3548.76, 2.15857}, {3541.05, 2.16114}, {3537.19, 2.16258}, {3529.47, 2.16577}, {3521.76, 2.16938}, {3517.9, 2.17134}, {3510.19, 2.17556}, {3506.33, 2.17782}, {3498.62, 2.18263}, {3490.9, 2.18782}, {3487.04, 2.19056}, {3479.33, 2.19629}, {3475.47, 2.19928}, {3467.76, 2.20551}, {3463.9, 2.20874}, {3456.18, 2.21542}, {3448.47, 2.22236}, {3444.61, 2.22592}, {3436.9, 2.23321}, {3433.04, 2.23693}, {3425.33, 2.2445}, {3421.47, 2.24835}, {3413.75, 2.25613}, {3409.9, 2.26006}, {3402.18, 2.26797}, {3398.32, 2.27196}, {3390.61, 2.27994}, {3386.75, 2.28393}, {3379.04, 2.29191}, {3375.18, 2.29588}, {3367.47, 2.30377}, {3363.61, 2.30768}, {3355.89, 2.31543}, {3352.04, 2.31925}, {3348.18, 2.32304}, {3340.46, 2.33049}, {3336.61, 2.33414}, {3328.89, 2.3413}, {3325.04, 2.3448}, {3317.32, 2.35163}, {3313.46, 2.35495}, {3309.61, 2.3582}, {3301.89, 2.36452}, {3298.03, 2.36757}, {3290.32, 2.37346}, {3286.46, 2.3763}, {3278.75, 2.38175}, {3274.89, 2.38436}, {3271.03, 2.3869}, {3263.32, 2.39174}, {3259.46, 2.39405}, {3255.6, 2.39628}, {3247.89, 2.40051}, {3244.03, 2.40251}, {3236.32, 2.40629}, {3232.46, 2.40807}, {3228.6, 2.40977}, {3220.89, 2.41297}, {3217.03, 2.41446}, {3213.17, 2.41589}, {3205.46, 2.41854}, {3201.6, 2.41977}, {3197.74, 2.42093}, {3190.03, 2.42309}, {3186.17, 2.42408}, {3182.31, 2.42502}, {3178.46, 2.4259}, {3170.74, 2.42751}, {3166.88, 2.42825}, {3163.03, 2.42894}, {3155.31, 2.43019}, {3151.45, 2.43075}, {3147.6, 2.43127}, {3139.88, 2.43222}, {3136.02, 2.43264}, {3132.17, 2.43303}, {3128.31, 2.43339}, {3120.6, 2.43404}, {3116.74, 2.43433}, {3112.88, 2.43459}, {3109.02, 2.43484}, {3101.31, 2.43527}, {3097.45, 2.43546}, {3093.59, 2.43564}, {3089.74, 2.4358}, {3082.02, 2.4361}, {3078.16, 2.43623}, {3074.31, 2.43635}, {3070.45, 2.43647}, {3066.59, 2.43658}, {3058.88, 2.43678}, {3055.02, 2.43687}, {3051.16, 2.43696}, {3047.31, 2.43705}, {3039.59, 2.43722}, {3035.73, 2.43731}, {3031.88, 2.43739}, {3028.02, 2.43748}, {3024.16, 2.43756}, {3020.3, 2.43765}, {3012.59, 2.43782}, {3008.73, 2.43791}, {3004.88, 2.43799}, {3001.02, 2.43808}, {2997.16, 2.43817}, {2993.3, 2.43827}, {2985.59, 2.43845}, {2981.73, 2.43855}, {2977.87, 2.43864}, {2974.02, 2.43874}, {2970.16, 2.43884}, {2966.3, 2.43893}, {2958.59, 2.43913}, {2954.73, 2.43922}, {2950.87, 2.43931}, {2947.01, 2.4394}, {2943.16, 2.43949}, {2939.3, 2.43958}, {2935.44, 2.43967}, {2931.59, 2.43975}, {2927.73, 2.43983}, {2920.01, 2.43997}, {2916.16, 2.44003}, {2912.3, 2.44009}, {2908.44, 2.44014}, {2904.58, 2.44019}, {2900.73, 2.44023}, {2896.87, 2.44026}, {2893.01, 2.44029}, {2889.15, 2.44031}, {2885.3, 2.44032}, {2881.44, 2.44032}, {2873.73, 2.44029}, {2869.87, 2.44026}, {2866.01, 2.44022}, {2862.15, 2.44017}, {2858.3, 2.44011}, {2854.44, 2.44003}, {2850.58, 2.43995}, {2846.72, 2.43985}, {2842.87, 2.43974}, {2839.01, 2.43962}, {2835.15, 2.43948}, {2831.29, 2.43933}, {2827.44, 2.43917}, {2823.58, 2.43899}, {2819.72, 2.4388}, {2815.87, 2.43859}, {2812.01, 2.43837}, {2808.15, 2.43814}, {2804.29, 2.43789}, {2800.44, 2.43762}, {2796.58, 2.43734}, {2792.72, 2.43704}, {2788.86, 2.43673}, {2785.01, 2.4364}, {2781.15, 2.43605}, {2777.29, 2.43569}, {2773.43, 2.43531}, {2769.58, 2.43492}, {2765.72, 2.43451}, {2761.86, 2.43408}, {2758, 2.43364}, {2754.15, 2.43318}, {2750.29, 2.43271}, {2746.43, 2.43222}, {2742.58, 2.43171}, {2738.72, 2.43118}, {2734.86, 2.43064}, {2731, 2.43009}, {2727.15, 2.42951}, {2723.29, 2.42892}, {2719.43, 2.42832}, {2715.57, 2.4277}, {2711.72, 2.42706}, {2707.86, 2.42641}, {2704, 2.42574}, {2700.14, 2.42505}, {2696.29, 2.42436}, {2692.43, 2.42364}, {2688.57, 2.42291}, {2684.72, 2.42217}, {2680.86, 2.42141}, {2677, 2.42063}, {2673.14, 2.41985}, {2669.29, 2.41904}, {2665.43, 2.41823}, {2661.57, 2.4174}, {2657.71, 2.41655}, {2653.86, 2.41569}, {2650, 2.41482}, {2646.14, 2.41394}, {2642.28, 2.41304}, {2638.43, 2.41213}, {2634.57, 2.41121}, {2630.71, 2.41028}, {2626.85, 2.40933}, {2623, 2.40838}, {2619.14, 2.40741}, {2615.28,

2.40643}, {2611.43, 2.40543}, {2607.57, 2.40443}, {2603.71, 2.40342}, {2599.85, 2.4024}, {2596, 2.40136}, {2592.14, 2.40032}, {2588.28, 2.39927}, {2584.42, 2.39821}, {2580.57, 2.39713}, {2576.71, 2.39605}, {2572.85, 2.39497}, {2568.99, 2.39387}, {2565.14, 2.39276}, {2561.28, 2.39165}, {2557.42, 2.39053}, {2553.57, 2.3894}, {2549.71, 2.38826}, {2545.85, 2.38712}, {2541.99, 2.38597}, {2538.14, 2.38481}, {2534.28, 2.38365}, {2530.42, 2.38248}, {2526.56, 2.3813}, {2522.71, 2.38012}, {2518.85, 2.37894}, {2514.99, 2.37774}, {2511.13, 2.37655}, {2507.28, 2.37534}, {2503.42, 2.37414}, {2499.56, 2.37293}, {2495.71, 2.37171}, {2491.85, 2.37049}, {2487.99, 2.36927}, {2484.13, 2.36804}, {2480.28, 2.36681}, {2476.42, 2.36557}, {2472.56, 2.36433}, {2468.7, 2.36309}, {2464.85, 2.36185}, {2460.99, 2.3606}, {2457.13, 2.35935}, {2453.27, 2.3581}, {2449.42, 2.35684}, {2445.56, 2.35559}, {2441.7, 2.35433}, {2437.84, 2.35307}, {2433.99, 2.3518}, {2430.13, 2.35054}, {2426.27, 2.34927}, {2422.42, 2.34801}, {2418.56, 2.34674}, {2414.7, 2.34547}, {2410.84, 2.3442}, {2406.99, 2.34292}, {2403.13, 2.34165}, {2399.27, 2.34038}, {2395.41, 2.3391}, {2391.56, 2.33783}, {2387.7, 2.33655}, {2383.84, 2.33528}, {2379.98, 2.334}, {2376.13, 2.33272}, {2372.27, 2.33145}, {2368.41, 2.33017}, {2364.56, 2.32889}, {2360.7, 2.32762}, {2356.84, 2.32634}, {2352.98, 2.32506}, {2349.13, 2.32379}, {2345.27, 2.32251}, {2341.41, 2.32124}, {2337.55, 2.31996}, {2333.7, 2.31869}, {2329.84, 2.31741}, {2325.98, 2.31614}, {2322.12, 2.31486}, {2318.27, 2.31359}, {2314.41, 2.31232}, {2310.55, 2.31105}, {2306.7, 2.30977}, {2302.84, 2.3085}, {2298.98, 2.30723}, {2295.12, 2.30596}, {2291.27, 2.30469}, {2287.41, 2.30343}, {2283.55, 2.30216}, {2279.69, 2.30089}, {2275.84, 2.29962}, {2271.98, 2.29836}, {2268.12, 2.29709}, {2264.26, 2.29583}, {2260.41, 2.29456}, {2256.55, 2.2933}, {2252.69, 2.29204}, {2248.83, 2.29078}, {2244.98, 2.28951}, {2241.12, 2.28825}, {2237.26, 2.28699}, {2233.41, 2.28573}, {2229.55, 2.28447}, {2225.69, 2.28322}, {2221.83, 2.28196}, {2217.98, 2.2807}, {2214.12, 2.27944}, {2210.26, 2.27819}, {2206.4, 2.27693}, {2202.55, 2.27567}, {2198.69, 2.27442}, {2194.83, 2.27316}, {2190.97, 2.27191}, {2187.12, 2.27065}, {2183.26, 2.26939}, {2179.4, 2.26814}, {2175.55, 2.26689}, {2171.69, 2.26563}, {2167.83, 2.26438}, {2163.97, 2.26312}, {2160.12, 2.26187}, {2156.26, 2.26061}, {2152.4, 2.25936}, {2148.54, 2.2581}, {2144.69, 2.25684}, {2140.83, 2.25559}, {2136.97, 2.25433}, {2133.11, 2.25307}, {2129.26, 2.25182}, {2125.4, 2.25056}, {2121.54, 2.2493}, {2117.68, 2.24804}, {2113.83, 2.24678}, {2109.97, 2.24552}, {2106.11, 2.24426}, {2102.26, 2.243}, {2098.4, 2.24174}, {2094.54, 2.24047}, {2090.68, 2.23921}, {2086.83, 2.23794}, {2082.97, 2.23668}, {2079.11, 2.23541}, {2075.25, 2.23414}, {2071.4, 2.23287}, {2067.54, 2.2316}, {2063.68, 2.23033}, {2059.82, 2.22905}, {2055.97, 2.22778}, {2052.11, 2.2265}, {2048.25, 2.22522}, {2044.4, 2.22394}, {2040.54, 2.22266}, {2036.68, 2.22138}, {2032.82, 2.22009}, {2028.97, 2.2188}, {2025.11, 2.21751}, {2021.25, 2.21622}, {2017.39, 2.21493}, {2013.54, 2.21363}, {2009.68, 2.21234}, {2005.82, 2.21103}, {2001.96, 2.20973}, {1998.11, 2.20843}, {1994.25, 2.20712}, {1990.39, 2.20581}, {1986.54, 2.2045}, {1982.68, 2.20318}, {1978.82, 2.20187}, {1974.96, 2.20055}, {1971.11, 2.19922}, {1967.25, 2.1979}, {1963.39, 2.19657}, {1959.53, 2.19524}, {1955.68, 2.1939}, {1951.82, 2.19256}, {1947.96, 2.19122}, {1944.1, 2.18988}, {1940.25, 2.18853}, {1936.39, 2.18718}, {1932.53, 2.18582}, {1928.67, 2.18446}, {1924.82, 2.1831}, {1920.96, 2.18173}, {1917.1, 2.18036}, {1913.25, 2.17899}, {1909.39, 2.17761}, {1905.53, 2.17623}, {1901.67, 2.17484}, {1897.82, 2.17345}, {1893.96, 2.17206}, {1890.1, 2.17066}, {1886.24, 2.16925}, {1882.39, 2.16784}, {1878.53, 2.16643}, {1874.67, 2.16501}, {1870.81, 2.16359}, {1866.96, 2.16216}, {1863.1, 2.16073}, {1859.24, 2.15929}, {1855.39, 2.15785}, {1851.53, 2.1564}, {1847.67, 2.15495}, {1843.81, 2.15349}, {1839.96, 2.15202}, {1836.1, 2.15055}, {1832.24, 2.14908}, {1828.38, 2.14759}, {1824.53, 2.14611}, {1820.67, 2.14461}, {1816.81, 2.14311}, {1812.95, 2.14161}, {1809.1, 2.14009}, {1805.24, 2.13857}, {1801.38, 2.13705}, {1797.53, 2.13551}, {1793.67, 2.13397}, {1789.81, 2.13243}, {1785.95, 2.13087}, {1782.1, 2.12931}, {1778.24, 2.12774}, {1774.38, 2.12617}, {1770.52, 2.12458}, {1766.67, 2.12299}, {1762.81, 2.12139}, {1758.95, 2.11978}, {1755.09, 2.11817}, {1751.24, 2.11654}, {1747.38, 2.11491}, {1743.52, 2.11327}, {1739.66, 2.11162}, {1735.81, 2.10996}, {1731.95, 2.10829}, {1728.09, 2.10661}, {1724.24, 2.10493}, {1720.38, 2.10323}, {1716.52, 2.10153}, {1712.66, 2.09981}, {1708.81, 2.09808}, {1704.95, 2.09635}, {1701.09, 2.0946}, {1697.23, 2.09284}, {1693.38, 2.09108}, {1689.52, 2.0893}, {1685.66, 2.08751}, {1681.8, 2.08571}, {1677.95, 2.08389}, {1674.09, 2.08207}, {1670.23, 2.08023}, {1666.38, 2.07838}, {1662.52, 2.07652}, {1658.66, 2.07465}, {1654.8, 2.07276}, {1650.95, 2.07086}, {1647.09, 2.06894}, {1643.23, 2.06702}, {1639.37, 2.06508}, {1635.52, 2.06312}, {1631.66, 2.06115}, {1627.8, 2.05917}, {1623.94, 2.05717}, {1620.09, 2.05515}, {1616.23, 2.05313}, {1612.37, 2.05108}, {1608.51, 2.04902}, {1604.66, 2.04694}, {1600.8, 2.04485}, {1596.94, 2.04274}, {1593.09, 2.04061}, {1589.23, 2.03846}, {1585.37, 2.0363}, {1581.51, 2.03411}, {1577.66, 2.03191}, {1573.8, 2.02969}, {1569.94, 2.02746}, {1566.08, 2.0252}, {1562.23, 2.02292}, {1558.37, 2.02062}, {1554.51, 2.0183}, {1550.65, 2.01596}, {1546.8, 2.01359}, {1542.94, 2.01121}, {1539.08, 2.0088}, {1535.23, 2.00637}, {1531.37, 2.00391}, {1527.51, 2.00144}, {1523.65, 1.99893}, {1519.8, 1.9964}, {1515.94, 1.99385}, {1512.08, 1.99127}, {1508.22, 1.98867}, {1504.37, 1.98603}, {1500.51, 1.98337}, {1496.65, 1.98068}, {1492.79, 1.97797}, {1488.94, 1.97522}, {1485.08, 1.97244}, {1481.22, 1.96963}, {1477.37, 1.96679}, {1473.51, 1.96392}, {1469.65, 1.96102}, {1465.79, 1.95808}, {1461.94, 1.9551}, {1458.08, 1.9521}, {1454.22, 1.94905}, {1450.36, 1.94597}, {1446.51, 1.94285}, {1442.65, 1.9397}, {1438.79, 1.9365}, {1434.93, 1.93326}, {1431.08, 1.92998}, {1427.22, 1.92666}, {1423.36, 1.9233}, {1419.5, 1.91989}, {1415.65, 1.91644}, {1411.79, 1.91293}, {1407.93, 1.90938}, {1404.08, 1.90578}, {1400.22, 1.90213}, {1396.36, 1.89843}, {1392.5, 1.89467}, {1388.65, 1.89086}, {1384.79, 1.88699}, {1380.93, 1.88307}, {1377.07, 1.87908}, {1373.22, 1.87503}, {1369.36, 1.87091}, {1365.5, 1.86673}, {1361.64, 1.86249}, {1357.79, 1.85817}, {1353.93, 1.85377}, {1350.07, 1.8493}, {1346.22, 1.84476}, {1342.36, 1.84013}, {1338.5, 1.83542}, {1334.64, 1.83062}, {1330.79, 1.82573}, {1326.93, 1.82074}, {1323.07, 1.81566}, {1319.21, 1.81048}, {1315.36, 1.80519}, {1311.5, 1.79979}, {1307.64, 1.79427}, {1303.78, 1.78863}, {1299.93, 1.78287}, {1296.07, 1.77698}, {1292.21, 1.77096}, {1288.35, 1.76479}, {1284.5, 1.75848}, {1280.64, 1.75202}, {1276.78, 1.7454}, {1272.93, 1.73862}, {1269.07, 1.73168}, {1265.21, 1.72456}, {1261.35, 1.71726}, {1257.5, 1.70979}, {1253.64, 1.70213}, {1249.78, 1.69428}, {1245.92, 1.68624}, {1242.07, 1.67801}, {1238.21, 1.66959}, {1234.35, 1.66098}, {1230.49, 1.65218}, {1226.64, 1.6432}, {1222.78, 1.63404}, {1218.92, 1.62471}, {1215.07, 1.61521}, {1211.21, 1.60556}, {1207.35, 1.59577}, {1203.49, 1.58585}, {1199.64, 1.57583}, {1195.78, 1.56571}, {1191.92, 1.55553}, {1188.06, 1.54529}, {1184.21, 1.53504}, {1180.35, 1.52478}, {1176.49, 1.51454}, {1172.63, 1.50436}, {1168.78, 1.49426}, {1164.92, 1.48425}, {1161.06, 1.47438}, {1157.21, 1.46467}, {1153.35, 1.45512}, {1149.49, 1.44578}, {1145.63, 1.43666}, {1141.78, 1.42776}, {1137.92, 1.41911}, {1134.06, 1.41071}, {1130.2, 1.40257}, {1126.35, 1.39468}, {1122.49, 1.38704}, {1118.63, 1.37964}, {1114.77, 1.37246}, {1110.92, 1.36548}, {1107.06, 1.35867}, {1103.2, 1.352}, {1099.34, 1.34544}, {1095.49, 1.33894}, {1091.63, 1.33246}, {1087.77, 1.32596}, {1083.92, 1.31937}, {1080.06, 1.31266}, {1076.2, 1.30576}, {1072.34, 1.29864}, {1068.49, 1.29122}, {1064.63, 1.28346}, {1060.77, 1.27531}, {1056.91, 1.26674}, {1053.06, 1.25768}, {1049.2, 1.24811}, {1045.34, 1.23799}, {1041.48, 1.22729}, {1037.63, 1.21601}, {1033.77, 1.20411}, {1029.91, 1.19159}, {1026.06, 1.17845}, {1022.2, 1.1647}, {1018.34, 1.15035}, {1014.48, 1.13541}, {1010.63, 1.11992}, {1006.77, 1.1039}, {1002.91, 1.08739}, {999.053, 1.07043}, {995.196, 1.05308}, {991.339, 1.03537}, {987.481, 1.01736}, {983.624, 0.999119}, {979.767, 0.980696}, {975.909, 0.96215}, {972.052, 0.94355}, {968.195, 0.924955}, {964.337, 0.906421}, {960.48, 0.888019}, {956.622, 0.8698}, {952.765, 0.851833}, {948.908, 0.834169}, {945.05, 0.816857}, {941.193, 0.79996}, {937.336, 0.783522}, {933.478, 0.767583}, {929.621, 0.752195}, {925.764, 0.737394}, {921.906, 0.723211}, {918.049, 0.709686}, {914.192, 0.696843}, {910.334, 0.684704}, {906.477, 0.673296}, {902.62, 0.662633}, {898.762, 0.652727}, {894.905, 0.643593}, {891.048, 0.635233}, {887.19, 0.627649}, {883.333, 0.620844}, {879.476, 0.614811}, {875.618, 0.609541}, {871.761, 0.605027}, {867.903, 0.601252}, {864.046, 0.598202}, {860.189, 0.595854}, {856.331, 0.594187}, {852.474, 0.593176}, {848.617, 0.592794}, {844.759, 0.593011}, {840.902, 0.593798}, {837.045, 0.59512}, {833.187, 0.596946}, {829.33, 0.599239}, {825.473, 0.601964}, {821.615, 0.605088}, {817.758, 0.608574}, {813.901, 0.612386}, {810.043, 0.616494}, {806.186, 0.620861}, {802.329, 0.625459}, {798.471, 0.630261}, {794.614, 0.635237}, {790.756, 0.640369}, {786.899, 0.645635}, {783.042, 0.65102}, {779.184, 0.656515}, {775.327, 0.662112}, {771.47, 0.667812}, {767.612, 0.673621}, {763.755, 0.679546}, {759.898, 0.685606}, {756.04, 0.691826}, {752.183, 0.698233}, {748.326, 0.704865}, {744.468, 0.711769}, {740.611, 0.718991}, {736.754, 0.726591}, {732.896, 0.734636}, {729.039, 0.743194}, {725.182, 0.752345}, {721.324, 0.762176}, {717.467, 0.772775}, {713.609, 0.784242}, {709.752, 0.796673}, {705.895, 0.810178}, {702.037, 0.824873}, {698.18, 0.840863}, {694.323, 0.858269}, {690.465, 0.877216}, {686.608, 0.897814}, {682.751, 0.920188}, {678.893, 0.944465}, {675.036, 0.97075}, {671.179, 0.999166}, {667.321, 1.02983}, {663.464, 1.06284}, {659.607, 1.09831}, {655.749, 1.13633}, {651.892, 1.17698}, {648.035, 1.22035}, {644.177, 1.26651}, {640.32, 1.31551}, {636.463, 1.36741}, {632.605, 1.42226},

{628.748, 1.48004}, {624.891, 1.54079}, {621.033, 1.60453}, {617.176, 1.67119}, {613.318, 1.74078}, {609.461, 1.81321}, {605.604, 1.88844}, {601.746, 1.96642}, {597.889, 2.04699}, {594.032, 2.13008}, {590.174, 2.21558}, {586.317, 2.30331}, {582.46, 2.39313}, {578.602, 2.48489}, {574.745, 2.57837}, {570.888, 2.6734}, {567.03, 2.7698}, {563.173, 2.8673}, {559.316, 2.96569}, {555.458, 3.06478}, {551.601, 3.16427}, {547.744, 3.26393}, {543.886, 3.36354}, {540.029, 3.46279}, {536.171, 3.56148}, {532.314, 3.6593}, {528.457, 3.75601}, {524.599, 3.85139}, {520.742, 3.94512}, {516.885, 4.037}, {513.027, 4.1268}, {509.17, 4.21424}, {505.313, 4.29912}, {501.455, 4.38124}, {497.598, 4.46036}, {493.741, 4.53629}, {489.883, 4.60889}, {486.026, 4.67794}, {482.169, 4.7433}, {478.311, 4.80485}, {474.454, 4.86243}, {470.597, 4.91594}, {466.739, 4.96531}, {462.882, 5.01043}, {459.025, 5.05123}, {455.167, 5.08769}, {451.31, 5.11975}, {447.452, 5.14741}, {443.595, 5.17064}, {439.738, 5.18947}, {435.88, 5.20392}, {432.023, 5.21401}, {428.166, 5.2198}, {424.308, 5.22135}, {420.451, 5.21873}, {416.594, 5.21201}, {412.736, 5.20129}, {408.879, 5.18666}, {405.022, 5.16823}, {401.164, 5.14609}, {397.307, 5.12039}, {393.45, 5.09122}, {389.592, 5.0587}, {385.735, 5.02297}, {381.878, 4.98416}, {378.02, 4.94237}, {374.163, 4.89774}, {370.305, 4.85039}, {366.448, 4.80046}, {362.591, 4.74804}, {358.733, 4.69325}, {354.876, 4.63621}, {351.019, 4.57702}, {347.161, 4.51576}, {343.304, 4.45254}, {339.447, 4.38745}, {335.589, 4.32053}, {331.732, 4.25189}, {327.875, 4.18157}, {324.017, 4.10959}, {320.16, 4.03605}, {316.303, 3.96094}, {312.445, 3.88426}, {308.588, 3.80607}, {304.731, 3.72634}, {300.873, 3.64504}, {297.016, 3.56219}, {293.159, 3.47772}, {289.301, 3.39156}, {285.444, 3.3037}, {281.586, 3.21401}, {277.729, 3.12246}, {273.872, 3.02891}, {270.014, 2.93322}, {266.157, 2.8353}, {262.3, 2.735}, {258.442, 2.6321}, {254.585, 2.52648}, {250.728, 2.41791}, {246.87, 2.30613}, {243.013, 2.19097}, {239.156, 2.07213}, {235.298, 1.94927}, {231.441, 1.82215}, {227.584, 1.69038}, {223.726, 1.55355}, {219.869, 1.41132}, {216.012, 1.2632}, {212.154, 1.10865}, {208.297, 0.947214}, {204.439, 0.778215}, {200.582, 0.60109}, {196.725, 0.415084}, {192.867, 0.219361}, {189.01, 0.0131579}, {185.153, −0.204528}, {181.295, −0.434814}, {177.438, −0.678752}, {173.581, −0.9377}, {169.723, −1.21318}, {165.866, −1.50667}, {162.009, −1.82004}, {158.151, −2.15543}, {154.294, −2.51494}, {150.437, −2.90126}, {146.579, −3.31742}, {142.722, −3.76654}, {138.865, −4.25254}, {135.007, −4.77991}, {131.15, −5.35338}, {127.293, −5.97888}, {123.435, −6.66329}, {119.578, −7.41407}, {115.72, −8.24077}, {111.863, −9.15371}, {108.006, −10.1658}, {104.148, −11.2926}, {100.291, −12.5517}};

al2o3=Interpolation[al2o3raw];

al2o3rawn={{7876.71, 1.56329}, {7845.85, 1.56312}, {7814.99, 1.56296}, {7784.13, 1.5628}, {7753.27, 1.56264}, {7722.41, 1.56247}, {7695.41, 1.56233}, {7664.55, 1.56217}, {7633.69, 1.562}, {7606.69, 1.56186}, {7575.83, 1.56169}, {7548.83, 1.56154}, {7521.83, 1.5614}, {7490.97, 1.56123}, {7463.97, 1.56108}, {7436.97, 1.56093}, {7409.97, 1.56078}, {7382.97, 1.56063}, {7355.96, 1.56048}, {7328.96, 1.56033}, {7301.96, 1.56018}, {7274.96, 1.56003}, {7247.96, 1.55988}, {7220.96, 1.55973}, {7197.81, 1.55959}, {7170.81, 1.55944}, {7143.81, 1.55928}, {7120.67, 1.55915}, {7093.66, 1.55899}, {7070.52, 1.55886}, {7043.52, 1.5587}, {7020.38, 1.55856}, {6993.37, 1.5584}, {6970.23, 1.55827}, {6947.09, 1.55813}, {6923.94, 1.55799}, {6896.94, 1.55783}, {6873.8, 1.55769}, {6850.65, 1.55754}, {6827.51, 1.5574}, {6804.36, 1.55726}, {6781.22, 1.55712}, {6758.08, 1.55697}, {6734.93, 1.55683}, {6711.79, 1.55668}, {6692.5, 1.55656}, {6669.36, 1.55641}, {6646.21, 1.55626}, {6623.07, 1.55611}, {6603.78, 1.55599}, {6580.64, 1.55584}, {6557.49, 1.55569}, {6538.21, 1.55556}, {6515.06, 1.55541}, {6495.78, 1.55528}, {6472.63, 1.55512}, {6453.34, 1.55499}, {6434.06, 1.55486}, {6410.91, 1.5547}, {6391.63, 1.55457}, {6372.34, 1.55443}, {6353.05, 1.5543}, {6329.91, 1.55414}, {6310.62, 1.554}, {6291.34, 1.55386}, {6272.05, 1.55372}, {6252.76, 1.55359}, {6233.48, 1.55344}, {6214.19, 1.5533}, {6194.9, 1.55316}, {6175.62, 1.55302}, {6156.33, 1.55288}, {6137.04, 1.55273}, {6117.76, 1.55258}, {6098.47, 1.55244}, {6079.18, 1.55229}, {6063.75, 1.55217}, {6044.47, 1.55202}, {6025.18, 1.55187}, {6009.75, 1.55175}, {5990.46, 1.55159}, {5971.18, 1.55144}, {5955.75, 1.55131}, {5936.46, 1.55116}, {5917.17, 1.551}, {5901.74, 1.55087}, {5882.46, 1.55071}, {5867.03, 1.55058}, {5851.6, 1.55045}, {5832.31, 1.55029}, {5816.88, 1.55015}, {5797.6, 1.54999}, {5782.17, 1.54985}, {5766.74, 1.54972}, {5747.45, 1.54955}, {5732.02, 1.54941}, {5716.59, 1.54927}, {5701.16, 1.54913}, {5681.88, 1.54895}, {5666.45, 1.54881}, {5651.02, 1.54867}, {5635.59, 1.54852}, {5620.16, 1.54838}, {5604.73, 1.54823}, {5589.3, 1.54808}, {5573.87, 1.54793}, {5558.44, 1.54778}, {5543.01, 1.54763}, {5527.58, 1.54748}, {5512.15, 1.54732}, {5496.72, 1.54717}, {5481.29, 1.54701}, {5465.86, 1.54685}, {5450.43, 1.54669}, {5435, 1.54653}, {5423.43, 1.5464}, {5408, 1.54624}, {5392.57, 1.54607}, {5377.14, 1.54591}, {5365.57, 1.54578}, {5350.14, 1.54561}, {5334.71, 1.54544}, {5319.28, 1.54526}, {5307.71, 1.54513}, {5292.28, 1.54496}, {5280.71, 1.54482}, {5265.28, 1.54464}, {5249.85, 1.54446}, {5238.28, 1.54432}, {5222.85, 1.54414}, {5211.28, 1.544}, {5195.85, 1.54381}, {5184.28, 1.54367}, {5168.85, 1.54347}, {5157.28, 1.54333}, {5141.85, 1.54313}, {5130.27, 1.54298}, {5118.7, 1.54283}, {5103.27, 1.54263}, {5091.7, 1.54248}, {5076.27, 1.54227}, {5064.7, 1.54212}, {5053.13, 1.54196}, {5041.56, 1.5418}, {5026.13, 1.54159}, {5014.55, 1.54142}, {5002.98, 1.54126}, {4987.55, 1.54104}, {4975.98, 1.54087}, {4964.41, 1.5407}, {4952.84, 1.54053}, {4941.26, 1.54036}, {4929.69, 1.54018}, {4914.26, 1.53994}, {4902.69, 1.53977}, {4891.12, 1.53958}, {4879.55, 1.5394}, {4867.97, 1.53922}, {4856.4, 1.53903}, {4844.83, 1.53884}, {4833.26, 1.53865}, {4821.69, 1.53846}, {4810.11, 1.53826}, {4798.54, 1.53807}, {4786.97, 1.53787}, {4775.4, 1.53766}, {4763.83, 1.53746}, {4752.25, 1.53725}, {4740.68, 1.53704}, {4729.11, 1.53683}, {4717.54, 1.53662}, {4705.97, 1.5364}, {4698.25, 1.53625}, {4686.68, 1.53603}, {4675.11, 1.53581}, {4663.54, 1.53558}, {4651.96, 1.53535}, {4640.39, 1.53512}, {4632.68, 1.53496}, {4621.1, 1.53472}, {4609.53, 1.53448}, {4597.96, 1.53423}, {4590.25, 1.53407}, {4578.67, 1.53382}, {4567.1, 1.53356}, {4559.39, 1.53339}, {4547.81, 1.53313}, {4536.24, 1.53286}, {4528.53, 1.53268}, {4516.96, 1.53241}, {4505.38, 1.53213}, {4497.67, 1.53195}, {4486.1, 1.53166}, {4474.52, 1.53137}, {4466.81, 1.53118}, {4455.24, 1.53088}, {4447.52, 1.53068}, {4435.95, 1.53038}, {4428.24, 1.53017}, {4416.66, 1.52985}, {4408.95, 1.52964}, {4397.38, 1.52932}, {4389.66, 1.5291}, {4378.09, 1.52876}, {4370.38, 1.52854}, {4358.8, 1.52819}, {4351.09, 1.52796}, {4339.52, 1.5276}, {4331.8, 1.52736}, {4320.23, 1.52699}, {4312.52, 1.52674}, {4304.8, 1.52649}, {4293.23, 1.5261}, {4285.51, 1.52584}, {4273.94, 1.52543}, {4266.23, 1.52516}, {4258.51, 1.52488}, {4246.94, 1.52446}, {4239.23, 1.52417}, {4231.51, 1.52388}, {4219.94, 1.52343}, {4212.23, 1.52312}, {4204.51, 1.52281}, {4192.94, 1.52234}, {4185.22, 1.52201}, {4177.51, 1.52168}, {4169.79, 1.52134}, {4158.22, 1.52083}, {4150.51, 1.52047}, {4142.79, 1.52011}, {4135.08, 1.51975}, {4127.36, 1.51937}, {4115.79, 1.5188}, {4108.08, 1.5184}, {4100.36, 1.518}, {4092.65, 1.51759}, {4084.93, 1.51716}, {4073.36, 1.51651}, {4065.65, 1.51607}, {4057.93, 1.51561}, {4050.22, 1.51514}, {4042.5, 1.51466}, {4034.79, 1.51417}, {4027.07, 1.51367}, {4019.36, 1.51315}, {4011.64, 1.51262}, {4000.07, 1.5118}, {3992.36, 1.51123}, {3984.64, 1.51064}, {3976.93, 1.51004}, {3969.21, 1.50943}, {3961.5, 1.50879}, {3953.78, 1.50814}, {3946.07, 1.50747}, {3938.35, 1.50677}, {3930.64, 1.50606}, {3922.92, 1.50533}, {3915.21, 1.50457}, {3907.49, 1.50379}, {3899.78, 1.50299}, {3892.07, 1.50216}, {3884.35, 1.50132}, {3876.64, 1.50044}, {3868.92, 1.49955}, {3861.21, 1.49862}, {3857.35, 1.49815}, {3849.63, 1.4972}, {3841.92, 1.49621}, {3834.21, 1.49521}, {3826.49, 1.49418}, {3818.78, 1.49313}, {3811.06, 1.49205}, {3803.35, 1.49096}, {3795.63, 1.48985}, {3787.92, 1.48872}, {3784.06, 1.48815}, {3776.34, 1.48699}, {3768.63, 1.48583}, {3760.92, 1.48466}, {3753.2, 1.48349}, {3745.49, 1.48231}, {3741.63, 1.48172}, {3733.91, 1.48055}, {3726.2, 1.47939}, {3718.48, 1.47825}, {3710.77, 1.47712}, {3706.91, 1.47657}, {3699.2, 1.47548}, {3691.48, 1.47443}, {3683.77, 1.47341}, {3679.91, 1.47292}, {3672.2, 1.47198}, {3664.48, 1.4711}, {3656.77, 1.47028}, {3652.91, 1.4699}, {3645.2, 1.46919}, {3637.48, 1.46856}, {3629.77, 1.46802}, {3625.91, 1.46778}, {3618.19, 1.46739}, {3610.48, 1.4671}, {3606.62, 1.467}, {3598.91, 1.46688}, {3591.19, 1.46687}, {3587.33, 1.46692}, {3579.62, 1.46711}, {3571.91, 1.46743}, {3568.05, 1.46764}, {3560.33, 1.46816}, {3552.62, 1.46883}, {3548.76, 1.46921}, {3541.05, 1.47008}, {3537.19, 1.47057}, {3529.47, 1.47166}, {3521.76, 1.47288}, {3517.9, 1.47355}, {3510.19, 1.47498}, {3506.33, 1.47574}, {3498.62, 1.47737}, {3490.9, 1.47913}, {3487.04, 1.48005}, {3479.33, 1.48199}, {3475.47, 1.483}, {3467.76, 1.4851}, {3463.9, 1.48618}, {3456.18, 1.48843}, {3448.47, 1.49076}, {3444.61, 1.49195}, {3436.9, 1.49439}, {3433.04, 1.49564}, {3425.33, 1.49817}, {3421.47, 1.49945}, {3413.75, 1.50204}, {3409.9, 1.50335}, {3402.18, 1.50598}, {3398.32, 1.5073}, {3390.61, 1.50995}, {3386.75, 1.51127}, {3379.04, 1.5139}, {3375.18, 1.51522}, {3367.47, 1.51782}, {3363.61, 1.51911}, {3355.89, 1.52165}, {3352.04, 1.52291}, {3348.18, 1.52415}, {3340.46, 1.52659}, {3336.61, 1.52779}, {3328.89, 1.53013}, {3325.04, 1.53127}, {3317.32, 1.5335}, {3313.46, 1.53458}, {3309.61, 1.53564}, {3301.89, 1.5377}, {3298.03, 1.53869}, {3290.32, 1.5406}, {3286.46, 1.54153}, {3278.75, 1.54329}, {3274.89, 1.54414}, {3271.03, 1.54496}, {3263.32, 1.54653}, {3259.46, 1.54727}, {3255.6, 1.54799},

{3247.89, 1.54936}, {3244.03, 1.55}, {3236.32, 1.55122}, {3232.46, 1.55179}, {3228.6, 1.55234}, {3220.89, 1.55337}, {3217.03, 1.55385}, {3213.17, 1.55431}, {3205.46, 1.55516}, {3201.6, 1.55556}, {3197.74, 1.55593}, {3190.03, 1.55663}, {3186.17, 1.55695}, {3182.31, 1.55725}, {3178.46, 1.55753}, {3170.74, 1.55805}, {3166.88, 1.55828}, {3163.03, 1.5585}, {3155.31, 1.55891}, {3151.45, 1.55909}, {3147.6, 1.55925}, {3139.88, 1.55956}, {3136.02, 1.55969}, {3132.17, 1.55982}, {3128.31, 1.55993}, {3120.6, 1.56014}, {3116.74, 1.56023}, {3112.88, 1.56032}, {3109.02, 1.5604}, {3101.31, 1.56054}, {3097.45, 1.5606}, {3093.59, 1.56065}, {3089.74, 1.56071}, {3082.02, 1.5608}, {3078.16, 1.56084}, {3074.31, 1.56088}, {3070.45, 1.56092}, {3066.59, 1.56095}, {3058.88, 1.56102}, {3055.02, 1.56105}, {3051.16, 1.56108}, {3047.31, 1.56111}, {3039.59, 1.56116}, {3035.73, 1.56119}, {3031.88, 1.56122}, {3028.02, 1.56124}, {3024.16, 1.56127}, {3020.3, 1.5613}, {3012.59, 1.56135}, {3008.73, 1.56138}, {3004.88, 1.56141}, {3001.02, 1.56144}, {2997.16, 1.56147}, {2993.3, 1.56149}, {2985.59, 1.56155}, {2981.73, 1.56159}, {2977.87, 1.56162}, {2974.02, 1.56165}, {2970.16, 1.56168}, {2966.3, 1.56171}, {2958.59, 1.56177}, {2954.73, 1.5618}, {2950.87, 1.56183}, {2947.01, 1.56186}, {2943.16, 1.56189}, {2939.3, 1.56192}, {2935.44, 1.56194}, {2931.59, 1.56197}, {2927.73, 1.56199}, {2920.01, 1.56204}, {2916.16, 1.56206}, {2912.3, 1.56208}, {2908.44, 1.5621}, {2904.58, 1.56211}, {2900.73, 1.56212}, {2896.87, 1.56213}, {2893.01, 1.56214}, {2889.15, 1.56215}, {2885.3, 1.56215}, {2881.44, 1.56215}, {2873.73, 1.56214}, {2869.87, 1.56213}, {2866.01, 1.56212}, {2862.15, 1.5621}, {2858.3, 1.56208}, {2854.44, 1.56206}, {2850.58, 1.56203}, {2846.72, 1.562}, {2842.87, 1.56197}, {2839.01, 1.56193}, {2835.15, 1.56188}, {2831.29, 1.56184}, {2827.44, 1.56178}, {2823.58, 1.56173}, {2819.72, 1.56167}, {2815.87, 1.5616}, {2812.01, 1.56153}, {2808.15, 1.56145}, {2804.29, 1.56137}, {2800.44, 1.56129}, {2796.58, 1.5612}, {2792.72, 1.5611}, {2788.86, 1.561}, {2785.01, 1.5609}, {2781.15, 1.56079}, {2777.29, 1.56067}, {2773.43, 1.56055}, {2769.58, 1.56042}, {2765.72, 1.56029}, {2761.86, 1.56016}, {2758, 1.56001}, {2754.15, 1.55987}, {2750.29, 1.55971}, {2746.43, 1.55956}, {2742.58, 1.55939}, {2738.72, 1.55923}, {2734.86, 1.55905}, {2731, 1.55887}, {2727.15, 1.55869}, {2723.29, 1.5585}, {2719.43, 1.55831}, {2715.57, 1.55811}, {2711.72, 1.5579}, {2707.86, 1.55769}, {2704, 1.55748}, {2700.14, 1.55726}, {2696.29, 1.55703}, {2692.43, 1.5568}, {2688.57, 1.55657}, {2684.72, 1.55633}, {2680.86, 1.55609}, {2677, 1.55584}, {2673.14, 1.55559}, {2669.29, 1.55533}, {2665.43, 1.55506}, {2661.57, 1.5548}, {2657.71, 1.55453}, {2653.86, 1.55425}, {2650, 1.55397}, {2646.14, 1.55369}, {2642.28, 1.5534}, {2638.43, 1.5531}, {2634.57, 1.55281}, {2630.71, 1.55251}, {2626.85, 1.5522}, {2623, 1.55189}, {2619.14, 1.55158}, {2615.28, 1.55127}, {2611.43, 1.55095}, {2607.57, 1.55062}, {2603.71, 1.5503}, {2599.85, 1.54997}, {2596, 1.54963}, {2592.14, 1.5493}, {2588.28, 1.54896}, {2584.42, 1.54861}, {2580.57, 1.54827}, {2576.71, 1.54792}, {2572.85, 1.54757}, {2568.99, 1.54721}, {2565.14, 1.54686}, {2561.28, 1.5465}, {2557.42, 1.54613}, {2553.57, 1.54577}, {2549.71, 1.5454}, {2545.85, 1.54503}, {2541.99, 1.54466}, {2538.14, 1.54428}, {2534.28, 1.54391}, {2530.42, 1.54353}, {2526.56, 1.54315}, {2522.71, 1.54276}, {2518.85, 1.54238}, {2514.99, 1.54199}, {2511.13, 1.54161}, {2507.28, 1.54122}, {2503.42, 1.54082}, {2499.56, 1.54043}, {2495.71, 1.54004}, {2491.85, 1.53964}, {2487.99, 1.53924}, {2484.13, 1.53884}, {2480.28, 1.53844}, {2476.42, 1.53804}, {2472.56, 1.53764}, {2468.7, 1.53724}, {2464.85, 1.53683}, {2460.99, 1.53642}, {2457.13, 1.53602}, {2453.27, 1.53561}, {2449.42, 1.5352}, {2445.56, 1.53479}, {2441.7, 1.53438}, {2437.84, 1.53397}, {2433.99, 1.53356}, {2430.13, 1.53315}, {2426.27, 1.53273}, {2422.42, 1.53232}, {2418.56, 1.53191}, {2414.7, 1.53149}, {2410.84, 1.53108}, {2406.99, 1.53066}, {2403.13, 1.53025}, {2399.27, 1.52983}, {2395.41, 1.52941}, {2391.56, 1.529}, {2387.7, 1.52858}, {2383.84, 1.52816}, {2379.98, 1.52774}, {2376.13, 1.52733}, {2372.27, 1.52691}, {2368.41, 1.52649}, {2364.56, 1.52607}, {2360.7, 1.52565}, {2356.84, 1.52523}, {2352.98, 1.52482}, {2349.13, 1.5244}, {2345.27, 1.52398}, {2341.41, 1.52356}, {2337.55, 1.52314}, {2333.7, 1.52272}, {2329.84, 1.5223}, {2325.98, 1.52189}, {2322.12, 1.52147}, {2318.27, 1.52105}, {2314.41, 1.52063}, {2310.55, 1.52021}, {2306.7, 1.51979}, {2302.84, 1.51938}, {2298.98, 1.51896}, {2295.12, 1.51854}, {2291.27, 1.51812}, {2287.41, 1.5177}, {2283.55, 1.51729}, {2279.69, 1.51687}, {2275.84, 1.51645}, {2271.98, 1.51603}, {2268.12, 1.51562}, {2264.26, 1.5152}, {2260.41, 1.51478}, {2256.55, 1.51436}, {2252.69, 1.51395}, {2248.83, 1.51353}, {2244.98, 1.51311}, {2241.12, 1.5127}, {2237.26, 1.51228}, {2233.41, 1.51186}, {2229.55, 1.51145}, {2225.69, 1.51103}, {2221.83, 1.51061}, {2217.98, 1.5102}, {2214.12, 1.50978}, {2210.26, 1.50937}, {2206.4, 1.50895}, {2202.55, 1.50853}, {2198.69, 1.50812}, {2194.83, 1.5077}, {2190.97, 1.50728}, {2187.12, 1.50687}, {2183.26, 1.50645}, {2179.4, 1.50603}, {2175.55, 1.50562}, {2171.69, 1.5052}, {2167.83, 1.50478}, {2163.97, 1.50437}, {2160.12, 1.50395}, {2156.26, 1.50353}, {2152.4, 1.50312}, {2148.54, 1.5027}, {2144.69, 1.50228}, {2140.83, 1.50186}, {2136.97, 1.50144}, {2133.11, 1.50102}, {2129.26, 1.50061}, {2125.4, 1.50019}, {2121.54, 1.49977}, {2117.68, 1.49935}, {2113.83, 1.49893}, {2109.97, 1.49851}, {2106.11, 1.49809}, {2102.26, 1.49766}, {2098.4, 1.49724}, {2094.54, 1.49682}, {2090.68, 1.4964}, {2086.83, 1.49598}, {2082.97, 1.49555}, {2079.11, 1.49513}, {2075.25, 1.4947}, {2071.4, 1.49428}, {2067.54, 1.49385}, {2063.68, 1.49343}, {2059.82, 1.493}, {2055.97, 1.49257}, {2052.11, 1.49215}, {2048.25, 1.49172}, {2044.4, 1.49129}, {2040.54, 1.49086}, {2036.68, 1.49043}, {2032.82, 1.49}, {2028.97, 1.48956}, {2025.11, 1.48913}, {2021.25, 1.4887}, {2017.39, 1.48826}, {2013.54, 1.48783}, {2009.68, 1.48739}, {2005.82, 1.48695}, {2001.96, 1.48652}, {1998.11, 1.48608}, {1994.25, 1.48564}, {1990.39, 1.4852}, {1986.54, 1.48476}, {1982.68, 1.48431}, {1978.82, 1.48387}, {1974.96, 1.48342}, {1971.11, 1.48298}, {1967.25, 1.48253}, {1963.39, 1.48208}, {1959.53, 1.48163}, {1955.68, 1.48118}, {1951.82, 1.48073}, {1947.96, 1.48028}, {1944.1, 1.47982}, {1940.25, 1.47937}, {1936.39, 1.47891}, {1932.53, 1.47845}, {1928.67, 1.47799}, {1924.82, 1.47753}, {1920.96, 1.47707}, {1917.1, 1.47661}, {1913.25, 1.47614}, {1909.39, 1.47567}, {1905.53, 1.4752}, {1901.67, 1.47473}, {1897.82, 1.47426}, {1893.96, 1.47379}, {1890.1, 1.47331}, {1886.24, 1.47284}, {1882.39, 1.47236}, {1878.53, 1.47188}, {1874.67, 1.4714}, {1870.81, 1.47091}, {1866.96, 1.47043}, {1863.1, 1.46994}, {1859.24, 1.46945}, {1855.39, 1.46896}, {1851.53, 1.46847}, {1847.67, 1.46797}, {1843.81, 1.46748}, {1839.96, 1.46698}, {1836.1, 1.46648}, {1832.24, 1.46597}, {1828.38, 1.46547}, {1824.53, 1.46496}, {1820.67, 1.46445}, {1816.81, 1.46394}, {1812.95, 1.46342}, {1809.1, 1.46291}, {1805.24, 1.46239}, {1801.38, 1.46186}, {1797.53, 1.46134}, {1793.67, 1.46081}, {1789.81, 1.46028}, {1785.95, 1.45975}, {1782.1, 1.45922}, {1778.24, 1.45868}, {1774.38, 1.45814}, {1770.52, 1.45759}, {1766.67, 1.45705}, {1762.81, 1.4565}, {1758.95, 1.45595}, {1755.09, 1.45539}, {1751.24, 1.45483}, {1747.38, 1.45427}, {1743.52, 1.45371}, {1739.66, 1.45314}, {1735.81, 1.45257}, {1731.95, 1.452}, {1728.09, 1.45142}, {1724.24, 1.45084}, {1720.38, 1.45025}, {1716.52, 1.44966}, {1712.66, 1.44907}, {1708.81, 1.44848}, {1704.95, 1.44788}, {1701.09, 1.44727}, {1697.23, 1.44667}, {1693.38, 1.44606}, {1689.52, 1.44544}, {1685.66, 1.44482}, {1681.8, 1.4442}, {1677.95, 1.44357}, {1674.09, 1.44294}, {1670.23, 1.4423}, {1666.38, 1.44166}, {1662.52, 1.44101}, {1658.66, 1.44036}, {1654.8, 1.43971}, {1650.95, 1.43905}, {1647.09, 1.43838}, {1643.23, 1.43771}, {1639.37, 1.43704}, {1635.52, 1.43636}, {1631.66, 1.43567}, {1627.8, 1.43498}, {1623.94, 1.43428}, {1620.09, 1.43358}, {1616.23, 1.43287}, {1612.37, 1.43216}, {1608.51, 1.43144}, {1604.66, 1.43071}, {1600.8, 1.42998}, {1596.94, 1.42924}, {1593.09, 1.4285}, {1589.23, 1.42775}, {1585.37, 1.42699}, {1581.51, 1.42622}, {1577.66, 1.42545}, {1573.8, 1.42467}, {1569.94, 1.42389}, {1566.08, 1.42309}, {1562.23, 1.42229}, {1558.37, 1.42148}, {1554.51, 1.42067}, {1550.65, 1.41984}, {1546.8, 1.41901}, {1542.94, 1.41817}, {1539.08, 1.41732}, {1535.23, 1.41646}, {1531.37, 1.4156}, {1527.51, 1.41472}, {1523.65, 1.41384}, {1519.8, 1.41294}, {1515.94, 1.41204}, {1512.08, 1.41112}, {1508.22, 1.4102}, {1504.37, 1.40927}, {1500.51, 1.40832}, {1496.65, 1.40737}, {1492.79, 1.4064}, {1488.94, 1.40542}, {1485.08, 1.40444}, {1481.22, 1.40344}, {1477.37, 1.40242}, {1473.51, 1.4014}, {1469.65, 1.40036}, {1465.79, 1.39931}, {1461.94, 1.39825}, {1458.08, 1.39717}, {1454.22, 1.39608}, {1450.36, 1.39498}, {1446.51, 1.39386}, {1442.65, 1.39273}, {1438.79, 1.39158}, {1434.93, 1.39042}, {1431.08, 1.38924}, {1427.22, 1.38804}, {1423.36, 1.38683}, {1419.5, 1.3856}, {1415.65, 1.38435}, {1411.79, 1.38309}, {1407.93, 1.3818}, {1404.08, 1.3805}, {1400.22, 1.37918}, {1396.36, 1.37784}, {1392.5, 1.37647}, {1388.65, 1.37509}, {1384.79, 1.37368}, {1380.93, 1.37225}, {1377.07, 1.37079}, {1373.22, 1.36932}, {1369.36, 1.36781}, {1365.5, 1.36628}, {1361.64, 1.36473}, {1357.79, 1.36315}, {1353.93, 1.36153}, {1350.07, 1.35989}, {1346.22, 1.35822}, {1342.36, 1.35651}, {1338.5, 1.35478}, {1334.64, 1.353}, {1330.79, 1.3512}, {1326.93, 1.34935}, {1323.07, 1.34747}, {1319.21, 1.34554}, {1315.36, 1.34357}, {1311.5, 1.34156}, {1307.64, 1.3395}, {1303.78, 1.3374}, {1299.93, 1.33524}, {1296.07, 1.33304}, {1292.21, 1.33077}, {1288.35, 1.32846}, {1284.5, 1.32608}, {1280.64, 1.32364}, {1276.78, 1.32114}, {1272.93, 1.31857}, {1269.07, 1.31593}, {1265.21, 1.31322}, {1261.35, 1.31044}, {1257.5, 1.30759}, {1253.64, 1.30466}, {1249.78, 1.30165}, {1245.92, 1.29855}, {1242.07, 1.29538}, {1238.21, 1.29213}, {1234.35, 1.28879}, {1230.49, 1.28537}, {1226.64, 1.28187}, {1222.78, 1.2783}, {1218.92, 1.27464}, {1215.07, 1.27091}, {1211.21, 1.26711}, {1207.35, 1.26324}, {1203.49, 1.25931}, {1199.64, 1.25532}, {1195.78, 1.25128}, {1191.92, 1.24721}, {1188.06, 1.2431}, {1184.21, 1.23897}, {1180.35, 1.23482}, {1176.49, 1.23067}, {1172.63, 1.22652},

```
{1168.78, 1.2224}, {1164.92, 1.2183}, {1161.06, 1.21424}, {1157.21, 1.21023}, {1153.35, 1.20629}, {1149.49, 1.20241}, {1145.63, 1.19861}, {1141.78, 1.19489},
{1137.92, 1.19126}, {1134.06, 1.18774}, {1130.2, 1.1843}, {1126.35, 1.18097}, {1122.49, 1.17773}, {1118.63, 1.17458}, {1114.77, 1.17152}, {1110.92, 1.16854},
{1107.06, 1.16562}, {1103.2, 1.16276}, {1099.34, 1.15993}, {1095.49, 1.15713}, {1091.63, 1.15432}, {1087.77, 1.1515}, {1083.92, 1.14864}, {1080.06, 1.14571},
{1076.2, 1.1427}, {1072.34, 1.13958}, {1068.49, 1.13632}, {1064.63, 1.1329}, {1060.77, 1.1293}, {1056.91, 1.12549}, {1053.06, 1.12146}, {1049.2, 1.11719},
{1045.34, 1.11265}, {1041.48, 1.10783}, {1037.63, 1.10273}, {1033.77, 1.09732}, {1029.91, 1.0916}, {1026.06, 1.08557}, {1022.2, 1.07921}, {1018.34, 1.07254},
{1014.48, 1.06556}, {1010.63, 1.05826}, {1006.77, 1.05067}, {1002.91, 1.04278}, {999.053, 1.03462}, {995.196, 1.02619}, {991.339, 1.01753}, {987.481,
1.00864}, {983.624, 0.999559}, {979.767, 0.990301}, {975.909, 0.980892}, {972.052, 0.971365}, {968.195, 0.961746}, {964.337, 0.952061}, {960.48, 0.942348},
{956.622, 0.932631}, {952.765, 0.922948}, {948.908, 0.913328}, {945.05, 0.903802}, {941.193, 0.894405}, {937.336, 0.885168}, {933.478, 0.876118}, {929.621,
0.867292}, {925.764, 0.858717}, {921.906, 0.850418}, {918.049, 0.842428}, {914.192, 0.834771}, {910.334, 0.827468}, {906.477, 0.820546}, {902.62, 0.814023},
{898.762, 0.807915}, {894.905, 0.802242}, {891.048, 0.797015}, {887.19, 0.792243}, {883.333, 0.787936}, {879.476, 0.784099}, {875.618, 0.780731}, {871.761,
0.777835}, {867.903, 0.775405}, {864.046, 0.773435}, {860.189, 0.771916}, {856.331, 0.770835}, {852.474, 0.770179}, {848.617, 0.769931}, {844.759, 0.770072},
{840.902, 0.770583}, {837.045, 0.77144}, {833.187, 0.772623}, {829.33, 0.774105}, {825.473, 0.775864}, {821.615, 0.777874}, {817.758, 0.780111}, {813.901,
0.782551}, {810.043, 0.785171}, {806.186, 0.787947}, {802.329, 0.79086}, {798.471, 0.79389}, {794.614, 0.797018}, {790.756, 0.800231}, {786.899, 0.803514},
{783.042, 0.806858}, {779.184, 0.810256}, {775.327, 0.813703}, {771.47, 0.817198}, {767.612, 0.820744}, {763.755, 0.824346}, {759.898, 0.828013}, {756.04,
0.831761}, {752.183, 0.835603}, {748.326, 0.839562}, {744.468, 0.843664}, {740.611, 0.847933}, {736.754, 0.852403}, {732.896, 0.857109}, {729.039, 0.862087},
{725.182, 0.867378}, {721.324, 0.873027}, {717.467, 0.879076}, {713.609, 0.885574}, {709.752, 0.892565}, {705.895, 0.900099}, {702.037, 0.908225}, {698.18,
0.916986}, {694.323, 0.926428}, {690.465, 0.936598}, {686.608, 0.947531}, {682.751, 0.959264}, {678.893, 0.971836}, {675.036, 0.985267}, {671.179, 0.999583},
{667.321, 1.01481}, {663.464, 1.03094}, {659.607, 1.048}, {655.749, 1.06599}, {651.892, 1.08489}, {648.035, 1.10469}, {644.177, 1.12539}, {640.32, 1.14696},
{636.463, 1.16936}, {632.605, 1.19258}, {628.748, 1.21657}, {624.891, 1.24129}, {621.033, 1.2667}, {617.176, 1.29274}, {613.318, 1.31938}, {609.461, 1.34656},
{605.604, 1.37421}, {601.746, 1.40229}, {597.889, 1.43073}, {594.032, 1.45948}, {590.174, 1.48848}, {586.317, 1.51767}, {582.46, 1.54697}, {578.602,
1.57635}, {574.745, 1.60573}, {570.888, 1.63505}, {567.03, 1.66427}, {563.173, 1.69331}, {559.316, 1.72212}, {555.458, 1.75065}, {551.601, 1.77884}, {547.744,
1.80663}, {543.886, 1.834}, {540.029, 1.86086}, {536.171, 1.88719}, {532.314, 1.91293}, {528.457, 1.93804}, {524.599, 1.96249}, {520.742, 1.98623}, {516.885,
2.00923}, {513.027, 2.03145}, {509.17, 2.05286}, {505.313, 2.07343}, {501.455, 2.09314}, {497.598, 2.11196}, {493.741, 2.12986}, {489.883, 2.14683},
{486.026, 2.16285}, {482.169, 2.17791}, {478.311, 2.192}, {474.454, 2.20509}, {470.597, 2.21719}, {466.739, 2.2283}, {462.882, 2.2384}, {459.025, 2.2475},
{455.167, 2.25559}, {451.31, 2.26269}, {447.452, 2.26879}, {443.595, 2.27391}, {439.738, 2.27804}, {435.88, 2.28121}, {432.023, 2.28342}, {428.166, 2.28469},
{424.308, 2.28503}, {420.451, 2.28445}, {416.594, 2.28298}, {412.736, 2.28063}, {408.879, 2.27742}, {405.022, 2.27337}, {401.164, 2.2685}, {397.307, 2.26283},
{393.45, 2.25637}, {389.592, 2.24915}, {385.735, 2.2412}, {381.878, 2.23252}, {378.02, 2.22314}, {374.163, 2.21308}, {370.305, 2.20236}, {366.448, 2.19099},
{362.591, 2.179}, {358.733, 2.16639}, {354.876, 2.15319}, {351.019, 2.1394}, {347.161, 2.12503}, {343.304, 2.11011}, {339.447, 2.09462}, {335.589, 2.07859},
{331.732, 2.06201}, {327.875, 2.04489}, {324.017, 2.02721}, {320.16, 2.00899}, {316.303, 1.99021}, {312.445, 1.97085}, {308.588, 1.95092}, {304.731, 1.93037},
{300.873, 1.9092}, {297.016, 1.88738}, {293.159, 1.86486}, {289.301, 1.84162}, {285.444, 1.81761}, {281.586, 1.79277}, {277.729, 1.76705}, {273.872,
1.74038}, {270.014, 1.71266}, {266.157, 1.68384}, {262.3, 1.65378}, {258.442, 1.62237}, {254.585, 1.58949}, {250.728, 1.55496}, {246.87, 1.5186}, {243.013,
1.48019}, {239.156, 1.43949}, {235.298, 1.39616}, {231.441, 1.34987}, {227.584, 1.30015}, {223.726, 1.24642}, {219.869, 1.18799}, {216.012, 1.12392},
{212.154, 1.05292}, {208.297, 0.973249}, {204.439, 0.882165}, {200.582, 0.7753}, {196.725, 0.64427}, {192.867, 0.46836}, {189.01, 0.114708}, {185.153, 0.
+0.452248 I}, {181.295, 0. +0.659404 I}, {177.438, 0. +0.823864 I}, {173.581, 0. +0.968349 I}, {169.723, 0. +1.10144 I}, {165.866, 0. +1.22746 I}, {162.009,
0. +1.34909 I}, {158.151, 0. +1.46814 I}, {154.294, 0. +1.58586 I}, {150.437, 0. +1.70331 I}, {146.579, 0. +1.82138 I}, {142.722, 0. +1.94076 I}, {138.865, 0.
+2.06217 I}, {135.007, 0. +2.1863 I}, {131.15, 0. +2.31374 I}, {127.293, 0. +2.44518 I}, {123.435, 0. +2.58134 I}, {119.578, 0. +2.72288 I}, {115.72, 0.
+2.87067 I}, {111.863, 0. +3.02551 I}, {108.006, 0. +3.18839 I}, {104.148, 0. +3.36045 I}, {100.291, 0. +3.54283 I}};

al2o3n=Interpolation[al2o3rawn];

(* CaF2 65000−300cm^−1*)

caf2raw={{7876.71, 2.02752}, {7845.85, 2.02748}, {7814.99, 2.02744}, {7784.13, 2.0274}, {7753.27, 2.02735}, {7722.41, 2.02731}, {7695.41, 2.02727}, {7664.55,
2.02723}, {7633.69, 2.02719}, {7606.69, 2.02715}, {7575.83, 2.0271}, {7548.83, 2.02706}, {7521.83, 2.02702}, {7490.97, 2.02697}, {7463.97, 2.02693}, {7436.97,
2.02689}, {7409.97, 2.02685}, {7382.97, 2.0268}, {7355.96, 2.02676}, {7328.96, 2.02672}, {7301.96, 2.02667}, {7274.96, 2.02663}, {7247.96, 2.02658},
{7220.96, 2.02654}, {7197.81, 2.0265}, {7170.81, 2.02645}, {7143.81, 2.0264}, {7120.67, 2.02636}, {7093.66, 2.02631}, {7070.52, 2.02627}, {7043.52, 2.02622},
{7020.38, 2.02618}, {6993.37, 2.02613}, {6970.23, 2.02608}, {6947.09, 2.02604}, {6923.94, 2.026}, {6896.94, 2.02594}, {6873.8, 2.0259}, {6850.65, 2.02585},
{6827.51, 2.0258}, {6804.36, 2.02576}, {6781.22, 2.02571}, {6758.08, 2.02566}, {6734.93, 2.02561}, {6711.79, 2.02556}, {6692.5, 2.02552}, {6669.36, 2.02547},
{6646.21, 2.02542}, {6623.07, 2.02537}, {6603.78, 2.02533}, {6580.64, 2.02528}, {6557.49, 2.02522}, {6538.21, 2.02518}, {6515.06, 2.02513}, {6495.78,
2.02508}, {6472.63, 2.02503}, {6453.34, 2.02498}, {6434.06, 2.02493}, {6410.91, 2.02488}, {6391.63, 2.02483}, {6372.34, 2.02478}, {6353.05, 2.02473},
{6329.91, 2.02467}, {6310.62, 2.02463}, {6291.34, 2.02458}, {6272.05, 2.02453}, {6252.76, 2.02448}, {6233.48, 2.02442}, {6214.19, 2.02437}, {6194.9, 2.02432},
{6175.62, 2.02427}, {6156.33, 2.02422}, {6137.04, 2.02416}, {6117.76, 2.02411}, {6098.47, 2.02405}, {6079.18, 2.024}, {6063.75, 2.02395}, {6044.47, 2.0239},
{6025.18, 2.02384}, {6009.75, 2.0238}, {5990.46, 2.02374}, {5971.18, 2.02368}, {5955.75, 2.02363}, {5936.46, 2.02357}, {5917.17, 2.02351}, {5901.74, 2.02347},
{5882.46, 2.0234}, {5867.03, 2.02336}, {5851.6, 2.02331}, {5832.31, 2.02324}, {5816.88, 2.02319}, {5797.6, 2.02313}, {5782.17, 2.02308}, {5766.74, 2.02303},
{5747.45, 2.02296}, {5732.02, 2.02291}, {5716.59, 2.02286}, {5701.16, 2.0228}, {5681.88, 2.02274}, {5666.45, 2.02268}, {5651.02, 2.02263}, {5635.59, 2.02257},
{5620.16, 2.02251}, {5604.73, 2.02246}, {5589.3, 2.0224}, {5573.87, 2.02234}, {5558.44, 2.02229}, {5543.01, 2.02223}, {5527.58, 2.02217}, {5512.15, 2.02211},
{5496.72, 2.02205}, {5481.29, 2.02199}, {5465.86, 2.02193}, {5450.43, 2.02187}, {5435, 2.02181}, {5423.43, 2.02176}, {5408, 2.0217}, {5392.57, 2.02163},
{5377.14, 2.02157}, {5365.57, 2.02152}, {5350.14, 2.02146}, {5334.71, 2.02139}, {5319.28, 2.02133}, {5307.71, 2.02128}, {5292.28, 2.02121}, {5280.71,
2.02116}, {5265.28, 2.02109}, {5249.85, 2.02102}, {5238.28, 2.02097}, {5222.85, 2.0209}, {5211.28, 2.02085}, {5195.85, 2.02078}, {5184.28, 2.02072}, {5168.85,
2.02065}, {5157.28, 2.0206}, {5141.85, 2.02053}, {5130.27, 2.02047}, {5118.7, 2.02041}, {5103.27, 2.02034}, {5091.7, 2.02028}, {5076.27, 2.02021}, {5064.7,
2.02015}, {5053.13, 2.02009}, {5041.56, 2.02003}, {5026.13, 2.01996}, {5014.55, 2.0199}, {5002.98, 2.01984}, {4987.55, 2.01976}, {4975.98, 2.0197}, {4964.41,
2.01964}, {4952.84, 2.01958}, {4941.26, 2.01951}, {4929.69, 2.01945}, {4914.26, 2.01937}, {4902.69, 2.0193}, {4891.12, 2.01924}, {4879.55, 2.01918}, {4867.97,
2.01911}, {4856.4, 2.01905}, {4844.83, 2.01898}, {4833.26, 2.01892}, {4821.69, 2.01885}, {4810.11, 2.01878}, {4798.54, 2.01871}, {4786.97, 2.01865}, {4775.4,
2.01858}, {4763.83, 2.01851}, {4752.25, 2.01844}, {4740.68, 2.01837}, {4729.11, 2.0183}, {4717.54, 2.01823}, {4705.97, 2.01816}, {4698.25, 2.01811},
{4686.68, 2.01804}, {4675.11, 2.01796}, {4663.54, 2.01789}, {4651.96, 2.01782}, {4640.39, 2.01774}, {4632.68, 2.01769}, {4621.1, 2.01762}, {4609.53, 2.01754},
{4597.96, 2.01746}, {4590.25, 2.01741}, {4578.67, 2.01733}, {4567.1, 2.01726}, {4559.39, 2.0172}, {4547.81, 2.01712}, {4536.24, 2.01704}, {4528.53, 2.01699},
```

{4516.96, 2.01691}, {4505.38, 2.01683}, {4497.67, 2.01677}, {4486.1, 2.01669}, {4474.52, 2.01661}, {4466.81, 2.01655}, {4455.24, 2.01647}, {4447.52, 2.01641}, {4435.95, 2.01633}, {4428.24, 2.01627}, {4416.66, 2.01618}, {4408.95, 2.01612}, {4397.38, 2.01604}, {4389.66, 2.01598}, {4378.09, 2.01589}, {4370.38, 2.01583}, {4358.8, 2.01574}, {4351.09, 2.01568}, {4339.52, 2.01559}, {4331.8, 2.01553}, {4320.23, 2.01543}, {4312.52, 2.01537}, {4304.8, 2.01531}, {4293.23, 2.01521}, {4285.51, 2.01515}, {4273.94, 2.01506}, {4266.23, 2.01499}, {4258.51, 2.01493}, {4246.94, 2.01483}, {4239.23, 2.01476}, {4231.51, 2.0147}, {4219.94, 2.0146}, {4212.23, 2.01453}, {4204.51, 2.01447}, {4192.94, 2.01436}, {4185.22, 2.0143}, {4177.51, 2.01423}, {4169.79, 2.01416}, {4158.22, 2.01405}, {4150.51, 2.01399}, {4142.79, 2.01392}, {4135.08, 2.01384}, {4127.36, 2.01377}, {4115.79, 2.01367}, {4108.08, 2.01359}, {4100.36, 2.01352}, {4092.65, 2.01345}, {4084.93, 2.01338}, {4073.36, 2.01327}, {4065.65, 2.01319}, {4057.93, 2.01312}, {4050.22, 2.01304}, {4042.5, 2.01297}, {4034.79, 2.01289}, {4027.07, 2.01281}, {4019.36, 2.01274}, {4011.64, 2.01266}, {4000.07, 2.01254}, {3992.36, 2.01247}, {3984.64, 2.01239}, {3976.93, 2.01231}, {3969.21, 2.01223}, {3961.5, 2.01215}, {3953.78, 2.01207}, {3946.07, 2.01199}, {3938.35, 2.0119}, {3930.64, 2.01182}, {3922.92, 2.01174}, {3915.21, 2.01166}, {3907.49, 2.01157}, {3899.78, 2.01149}, {3892.07, 2.0114}, {3884.35, 2.01132}, {3876.64, 2.01123}, {3868.92, 2.01115}, {3861.21, 2.01106}, {3857.35, 2.01102}, {3849.63, 2.01093}, {3841.92, 2.01084}, {3834.21, 2.01075}, {3826.49, 2.01066}, {3818.78, 2.01057}, {3811.06, 2.01048}, {3803.35, 2.01039}, {3795.63, 2.0103}, {3787.92, 2.01021}, {3784.06, 2.01016}, {3776.34, 2.01007}, {3768.63, 2.00998}, {3760.92, 2.00988}, {3753.2, 2.00979}, {3745.49, 2.00969}, {3741.63, 2.00965}, {3733.91, 2.00955}, {3726.2, 2.00945}, {3718.48, 2.00936}, {3710.77, 2.00926}, {3706.91, 2.00921}, {3699.2, 2.00911}, {3691.48, 2.00901}, {3683.77, 2.00891}, {3679.91, 2.00886}, {3672.2, 2.00876}, {3664.48, 2.00866}, {3656.77, 2.00856}, {3652.91, 2.00851}, {3645.2, 2.0084}, {3637.48, 2.0083}, {3629.77, 2.0082}, {3625.91, 2.00814}, {3618.19, 2.00804}, {3610.48, 2.00793}, {3606.62, 2.00788}, {3598.91, 2.00777}, {3591.19, 2.00766}, {3587.33, 2.00761}, {3579.62, 2.0075}, {3571.91, 2.00739}, {3568.05, 2.00733}, {3560.33, 2.00722}, {3552.62, 2.00711}, {3548.76, 2.00706}, {3541.05, 2.00694}, {3537.19, 2.00689}, {3529.47, 2.00677}, {3521.76, 2.00666}, {3517.9, 2.0066}, {3510.19, 2.00649}, {3506.33, 2.00643}, {3498.62, 2.00631}, {3490.9, 2.00619}, {3487.04, 2.00613}, {3479.33, 2.00602}, {3475.47, 2.00596}, {3467.76, 2.00584}, {3463.9, 2.00578}, {3456.18, 2.00566}, {3448.47, 2.00553}, {3444.61, 2.00547}, {3436.9, 2.00535}, {3433.04, 2.00529}, {3425.33, 2.00516}, {3421.47, 2.0051}, {3413.75, 2.00497}, {3409.9, 2.00491}, {3402.18, 2.00478}, {3398.32, 2.00472}, {3390.61, 2.00459}, {3386.75, 2.00453}, {3379.04, 2.0044}, {3375.18, 2.00433}, {3367.47, 2.0042}, {3363.61, 2.00414}, {3355.89, 2.004}, {3352.04, 2.00394}, {3348.18, 2.00387}, {3340.46, 2.00374}, {3336.61, 2.00367}, {3328.89, 2.00353}, {3325.04, 2.00346}, {3317.32, 2.00333}, {3313.46, 2.00326}, {3309.61, 2.00319}, {3301.89, 2.00305}, {3298.03, 2.00298}, {3290.32, 2.00284}, {3286.46, 2.00277}, {3278.75, 2.00263}, {3274.89, 2.00255}, {3271.03, 2.00248}, {3263.32, 2.00234}, {3259.46, 2.00227}, {3255.6, 2.00219}, {3247.89, 2.00205}, {3244.03, 2.00197}, {3236.32, 2.00183}, {3232.46, 2.00175}, {3228.6, 2.00168}, {3220.89, 2.00153}, {3217.03, 2.00145}, {3213.17, 2.00138}, {3205.46, 2.00122}, {3201.6, 2.00115}, {3197.74, 2.00107}, {3190.03, 2.00092}, {3186.17, 2.00084}, {3182.31, 2.00076}, {3178.46, 2.00068}, {3170.74, 2.00053}, {3166.88, 2.00045}, {3163.03, 2.00037}, {3155.31, 2.00021}, {3151.45, 2.00013}, {3147.6, 2.00005}, {3139.88, 1.99989}, {3136.02, 1.9998}, {3132.17, 1.99972}, {3128.31, 1.99964}, {3120.6, 1.99948}, {3116.74, 1.99939}, {3112.88, 1.99931}, {3109.02, 1.99923}, {3101.31, 1.99906}, {3097.45, 1.99897}, {3093.59, 1.99889}, {3089.74, 1.9988}, {3082.02, 1.99863}, {3078.16, 1.99854}, {3074.31, 1.99846}, {3070.45, 1.99837}, {3066.59, 1.99828}, {3058.88, 1.99811}, {3055.02, 1.99802}, {3051.16, 1.99793}, {3047.31, 1.99784}, {3039.59, 1.99767}, {3035.73, 1.99758}, {3031.88, 1.99748}, {3028.02, 1.99739}, {3024.16, 1.9973}, {3020.3, 1.99721}, {3012.59, 1.99703}, {3008.73, 1.99694}, {3004.88, 1.99684}, {3001.02, 1.99675}, {2997.16, 1.99666}, {2993.3, 1.99656}, {2985.59, 1.99637}, {2981.73, 1.99628}, {2977.87, 1.99618}, {2974.02, 1.99609}, {2970.16, 1.99599}, {2966.3, 1.9959}, {2958.59, 1.9957}, {2954.73, 1.9956}, {2950.87, 1.99551}, {2947.01, 1.99541}, {2943.16, 1.99531}, {2939.3, 1.99521}, {2935.44, 1.99511}, {2931.59, 1.99501}, {2927.73, 1.99491}, {2920.01, 1.99471}, {2916.16, 1.99461}, {2912.3, 1.99451}, {2908.44, 1.9944}, {2904.58, 1.9943}, {2900.73, 1.9942}, {2896.87, 1.99409}, {2893.01, 1.99399}, {2889.15, 1.99389}, {2885.3, 1.99378}, {2881.44, 1.99368}, {2873.73, 1.99346}, {2869.87, 1.99336}, {2866.01, 1.99325}, {2862.15, 1.99314}, {2858.3, 1.99303}, {2854.44, 1.99293}, {2850.58, 1.99282}, {2846.72, 1.99271}, {2842.87, 1.9926}, {2839.01, 1.99249}, {2835.15, 1.99238}, {2831.29, 1.99227}, {2827.44, 1.99216}, {2823.58, 1.99204}, {2819.72, 1.99193}, {2815.87, 1.99182}, {2812.01, 1.9917}, {2808.15, 1.99159}, {2804.29, 1.99148}, {2800.44, 1.99136}, {2796.58, 1.99125}, {2792.72, 1.99113}, {2788.86, 1.99101}, {2785.01, 1.9909}, {2781.15, 1.99078}, {2777.29, 1.99066}, {2773.43, 1.99054}, {2769.58, 1.99043}, {2765.72, 1.99031}, {2761.86, 1.99019}, {2758, 1.99007}, {2754.15, 1.98995}, {2750.29, 1.98982}, {2746.43, 1.9897}, {2742.58, 1.98958}, {2738.72, 1.98946}, {2734.86, 1.98933}, {2731, 1.98921}, {2727.15, 1.98909}, {2723.29, 1.98896}, {2719.43, 1.98883}, {2715.57, 1.98871}, {2711.72, 1.98858}, {2707.86, 1.98846}, {2704, 1.98833}, {2700.14, 1.9882}, {2696.29, 1.98807}, {2692.43, 1.98794}, {2688.57, 1.98781}, {2684.72, 1.98768}, {2680.86, 1.98755}, {2677, 1.98742}, {2673.14, 1.98729}, {2669.29, 1.98715}, {2665.43, 1.98702}, {2661.57, 1.98689}, {2657.71, 1.98675}, {2653.86, 1.98662}, {2650, 1.98648}, {2646.14, 1.98634}, {2642.28, 1.98621}, {2638.43, 1.98607}, {2634.57, 1.98593}, {2630.71, 1.98579}, {2626.85, 1.98565}, {2623, 1.98551}, {2619.14, 1.98537}, {2615.28, 1.98523}, {2611.43, 1.98509}, {2607.57, 1.98494}, {2603.71, 1.9848}, {2599.85, 1.98466}, {2596, 1.98451}, {2592.14, 1.98437}, {2588.28, 1.98422}, {2584.42, 1.98408}, {2580.57, 1.98393}, {2576.71, 1.98378}, {2572.85, 1.98363}, {2568.99, 1.98348}, {2565.14, 1.98333}, {2561.28, 1.98318}, {2557.42, 1.98303}, {2553.57, 1.98288}, {2549.71, 1.98273}, {2545.85, 1.98257}, {2541.99, 1.98242}, {2538.14, 1.98226}, {2534.28, 1.98211}, {2530.42, 1.98195}, {2526.56, 1.98179}, {2522.71, 1.98164}, {2518.85, 1.98148}, {2514.99, 1.98132}, {2511.13, 1.98116}, {2507.28, 1.981}, {2503.42, 1.98084}, {2499.56, 1.98067}, {2495.71, 1.98051}, {2491.85, 1.98035}, {2487.99, 1.98018}, {2484.13, 1.98002}, {2480.28, 1.97985}, {2476.42, 1.97968}, {2472.56, 1.97952}, {2468.7, 1.97935}, {2464.85, 1.97918}, {2460.99, 1.97901}, {2457.13, 1.97884}, {2453.27, 1.97867}, {2449.42, 1.97849}, {2445.56, 1.97832}, {2441.7, 1.97815}, {2437.84, 1.97797}, {2433.99, 1.97779}, {2430.13, 1.97762}, {2426.27, 1.97744}, {2422.42, 1.97726}, {2418.56, 1.97708}, {2414.7, 1.9769}, {2410.84, 1.97672}, {2406.99, 1.97654}, {2403.13, 1.97636}, {2399.27, 1.97617}, {2395.41, 1.97599}, {2391.56, 1.9758}, {2387.7, 1.97561}, {2383.84, 1.97543}, {2379.98, 1.97524}, {2376.13, 1.97505}, {2372.27, 1.97486}, {2368.41, 1.97467}, {2364.56, 1.97447}, {2360.7, 1.97428}, {2356.84, 1.97409}, {2352.98, 1.97389}, {2349.13, 1.9737}, {2345.27, 1.9735}, {2341.41, 1.9733}, {2337.55, 1.9731}, {2333.7, 1.9729}, {2329.84, 1.9727}, {2325.98, 1.9725}, {2322.12, 1.9723}, {2318.27, 1.97209}, {2314.41, 1.97189}, {2310.55, 1.97168}, {2306.7, 1.97147}, {2302.84, 1.97126}, {2298.98, 1.97105}, {2295.12, 1.97084}, {2291.27, 1.97063}, {2287.41, 1.97042}, {2283.55, 1.97021}, {2279.69, 1.96999}, {2275.84, 1.96977}, {2271.98, 1.96956}, {2268.12, 1.96934}, {2264.26, 1.96912}, {2260.41, 1.9689}, {2256.55, 1.96868}, {2252.69, 1.96845}, {2248.83, 1.96823}, {2244.98, 1.968}, {2241.12, 1.96778}, {2237.26, 1.96755}, {2233.41, 1.96732}, {2229.55, 1.96709}, {2225.69, 1.96686}, {2221.83, 1.96663}, {2217.98, 1.96639}, {2214.12, 1.96616}, {2210.26, 1.96592}, {2206.4, 1.96568}, {2202.55, 1.96545}, {2198.69, 1.96521}, {2194.83, 1.96496}, {2190.97, 1.96472}, {2187.12, 1.96448}, {2183.26, 1.96423}, {2179.4, 1.96398}, {2175.55, 1.96374}, {2171.69, 1.96349}, {2167.83, 1.96324}, {2163.97, 1.96298}, {2160.12, 1.96273}, {2156.26, 1.96248}, {2152.4, 1.96222}, {2148.54, 1.96196}, {2144.69, 1.9617}, {2140.83, 1.96144}, {2136.97, 1.96118}, {2133.11, 1.96092}, {2129.26, 1.96065}, {2125.4, 1.96038}, {2121.54, 1.96012}, {2117.68, 1.95985}, {2113.83, 1.95958}, {2109.97, 1.9593}, {2106.11, 1.95903}, {2102.26, 1.95875}, {2098.4, 1.95848}, {2094.54, 1.9582}, {2090.68, 1.95792}, {2086.83, 1.95764}, {2082.97, 1.95735}, {2079.11, 1.95707}, {2075.25, 1.95678}, {2071.4, 1.95649}, {2067.54, 1.9562}, {2063.68, 1.95591}, {2059.82, 1.95562}, {2055.97, 1.95532}, {2052.11, 1.95502}, {2048.25, 1.95473}, {2044.4, 1.95443}, {2040.54, 1.95412}, {2036.68, 1.95382}, {2032.82, 1.95351}, {2028.97, 1.95321}, {2025.11, 1.9529}, {2021.25, 1.95259}, {2017.39, 1.95227}, {2013.54, 1.95196}, {2009.68, 1.95164}, {2005.82, 1.95132}, {2001.96, 1.951}, {1998.11, 1.95068}, {1994.25, 1.95036}, {1990.39, 1.95003}, {1986.54, 1.9497}, {1982.68, 1.94937}, {1978.82, 1.94904}, {1974.96, 1.94871}, {1971.11, 1.94837}, {1967.25, 1.94803}, {1963.39, 1.94769}, {1959.53, 1.94735}, {1955.68, 1.94701}, {1951.82, 1.94666}, {1947.96, 1.94631}, {1944.1, 1.94596}, {1940.25, 1.94561}, {1936.39, 1.94525}, {1932.53, 1.9449}, {1928.67, 1.94454}, {1924.82, 1.94418}, {1920.96, 1.94381}, {1917.1, 1.94345}, {1913.25, 1.94308}, {1909.39, 1.94271}, {1905.53, 1.94233}, {1901.67, 1.94196}, {1897.82, 1.94158}, {1893.96, 1.9412}, {1890.1, 1.94082}, {1886.24, 1.94043}, {1882.39, 1.94005}, {1878.53, 1.93966}, {1874.67, 1.93926}, {1870.81, 1.93887}, {1866.96, 1.93847}, {1863.1, 1.93807}, {1859.24, 1.93767}, {1855.39, 1.93726}, {1851.53, 1.93686}, {1847.67,

```
1.93645}, {1843.81, 1.93603}, {1839.96, 1.93562}, {1836.1, 1.9352}, {1832.24, 1.93478}, {1828.38, 1.93435}, {1824.53, 1.93393}, {1820.67, 1.9335}, {1816.81,
1.93307}, {1812.95, 1.93263}, {1809.1, 1.93219}, {1805.24, 1.93175}, {1801.38, 1.93131}, {1797.53, 1.93086}, {1793.67, 1.93041}, {1789.81, 1.92996}, {1785.95,
1.9295}, {1782.1, 1.92904}, {1778.24, 1.92858}, {1774.38, 1.92812}, {1770.52, 1.92765}, {1766.67, 1.92718}, {1762.81, 1.9267}, {1758.95, 1.92622}, {1755.09,
1.92574}, {1751.24, 1.92526}, {1747.38, 1.92477}, {1743.52, 1.92428}, {1739.66, 1.92378}, {1735.81, 1.92329}, {1731.95, 1.92279}, {1728.09, 1.92228},
{1724.24, 1.92177}, {1720.38, 1.92126}, {1716.52, 1.92074}, {1712.66, 1.92023}, {1708.81, 1.9197}, {1704.95, 1.91918}, {1701.09, 1.91865}, {1697.23, 1.91811},
{1693.38, 1.91757}, {1689.52, 1.91703}, {1685.66, 1.91649}, {1681.8, 1.91594}, {1677.95, 1.91538}, {1674.09, 1.91483}, {1670.23, 1.91426}, {1666.38, 1.9137},
{1662.52, 1.91313}, {1658.66, 1.91256}, {1654.8, 1.91198}, {1650.95, 1.9114}, {1647.09, 1.91081}, {1643.23, 1.91022}, {1639.37, 1.90962}, {1635.52, 1.90902},
{1631.66, 1.90842}, {1627.8, 1.90781}, {1623.94, 1.9072}, {1620.09, 1.90658}, {1616.23, 1.90596}, {1612.37, 1.90533}, {1608.51, 1.9047}, {1604.66, 1.90406},
{1600.8, 1.90342}, {1596.94, 1.90278}, {1593.09, 1.90213}, {1589.23, 1.90147}, {1585.37, 1.90081}, {1581.51, 1.90014}, {1577.66, 1.89947}, {1573.8, 1.8988},
{1569.94, 1.89812}, {1566.08, 1.89743}, {1562.23, 1.89674}, {1558.37, 1.89604}, {1554.51, 1.89534}, {1550.65, 1.89463}, {1546.8, 1.89391}, {1542.94, 1.8932},
{1539.08, 1.89247}, {1535.23, 1.89174}, {1531.37, 1.891}, {1527.51, 1.89026}, {1523.65, 1.88951}, {1519.8, 1.88876}, {1515.94, 1.888}, {1512.08, 1.88723},
{1508.22, 1.88646}, {1504.37, 1.88568}, {1500.51, 1.88489}, {1496.65, 1.8841}, {1492.79, 1.8833}, {1488.94, 1.8825}, {1485.08, 1.88168}, {1481.22, 1.88087},
{1477.37, 1.88004}, {1473.51, 1.87921}, {1469.65, 1.87837}, {1465.79, 1.87753}, {1461.94, 1.87667}, {1458.08, 1.87581}, {1454.22, 1.87495}, {1450.36,
1.87407}, {1446.51, 1.87319}, {1442.65, 1.8723}, {1438.79, 1.8714}, {1434.93, 1.8705}, {1431.08, 1.86959}, {1427.22, 1.86867}, {1423.36, 1.86774}, {1419.5,
1.8668}, {1415.65, 1.86586}, {1411.79, 1.8649}, {1407.93, 1.86394}, {1404.08, 1.86297}, {1400.22, 1.862}, {1396.36, 1.86101}, {1392.5, 1.86002}, {1388.65,
1.85901}, {1384.79, 1.858}, {1380.93, 1.85698}, {1377.07, 1.85595}, {1373.22, 1.85491}, {1369.36, 1.85386}, {1365.5, 1.8528}, {1361.64, 1.85173}, {1357.79,
1.85065}, {1353.93, 1.84956}, {1350.07, 1.84846}, {1346.22, 1.84736}, {1342.36, 1.84624}, {1338.5, 1.84511}, {1334.64, 1.84397}, {1330.79, 1.84282}, {1326.93,
1.84166}, {1323.07, 1.84049}, {1319.21, 1.8393}, {1315.36, 1.83811}, {1311.5, 1.83691}, {1307.64, 1.83569}, {1303.78, 1.83446}, {1299.93, 1.83322}, {1296.07,
1.83197}, {1292.21, 1.83071}, {1288.35, 1.82943}, {1284.5, 1.82814}, {1280.64, 1.82684}, {1276.78, 1.82553}, {1272.93, 1.8242}, {1269.07, 1.82286}, {1265.21,
1.82151}, {1261.35, 1.82014}, {1257.5, 1.81876}, {1253.64, 1.81737}, {1249.78, 1.81596}, {1245.92, 1.81454}, {1242.07, 1.81311}, {1238.21, 1.81166},
{1234.35, 1.81019}, {1230.49, 1.80871}, {1226.64, 1.80722}, {1222.78, 1.80571}, {1218.92, 1.80418}, {1215.07, 1.80264}, {1211.21, 1.80108}, {1207.35,
1.79951}, {1203.49, 1.79792}, {1199.64, 1.79631}, {1195.78, 1.79468}, {1191.92, 1.79304}, {1188.06, 1.79138}, {1184.21, 1.78971}, {1180.35, 1.78801},
{1176.49, 1.7863}, {1172.63, 1.78457}, {1168.78, 1.78282}, {1164.92, 1.78105}, {1161.06, 1.77926}, {1157.21, 1.77746}, {1153.35, 1.77563}, {1149.49, 1.77378},
{1145.63, 1.77191}, {1141.78, 1.77002}, {1137.92, 1.76811}, {1134.06, 1.76618}, {1130.2, 1.76423}, {1126.35, 1.76225}, {1122.49, 1.76026}, {1118.63,
1.75823}, {1114.77, 1.75619}, {1110.92, 1.75412}, {1107.06, 1.75203}, {1103.2, 1.74992}, {1099.34, 1.74778}, {1095.49, 1.74561}, {1091.63, 1.74342}, {1087.77,
1.7412}, {1083.92, 1.73896}, {1080.06, 1.73669}, {1076.2, 1.73439}, {1072.34, 1.73207}, {1068.49, 1.72972}, {1064.63, 1.72734}, {1060.77, 1.72493}, {1056.91,
1.72249}, {1053.06, 1.72002}, {1049.2, 1.71752}, {1045.34, 1.71499}, {1041.48, 1.71242}, {1037.63, 1.70983}, {1033.77, 1.7072}, {1029.91, 1.70454}, {1026.06,
1.70185}, {1022.2, 1.69912}, {1018.34, 1.69635}, {1014.48, 1.69355}, {1010.63, 1.69072}, {1006.77, 1.68784}, {1002.91, 1.68493}, {999.053, 1.68198},
{995.196, 1.679}, {991.339, 1.67597}, {987.481, 1.6729}, {983.624, 1.66979}, {979.767, 1.66664}, {975.909, 1.66344}, {972.052, 1.6602}, {968.195, 1.65692},
{964.337, 1.65359}, {960.48, 1.65022}, {956.622, 1.64679}, {952.765, 1.64332}, {948.908, 1.63981}, {945.05, 1.63624}, {941.193, 1.63262}, {937.336, 1.62894},
{933.478, 1.62522}, {929.621, 1.62144}, {925.764, 1.6176}, {921.906, 1.61371}, {918.049, 1.60976}, {914.192, 1.60575}, {910.334, 1.60168}, {906.477, 1.59755},
{902.62, 1.59336}, {898.762, 1.5891}, {894.905, 1.58478}, {891.048, 1.58039}, {887.19, 1.57593}, {883.333, 1.57141}, {879.476, 1.56681}, {875.618, 1.56214},
{871.761, 1.55739}, {867.903, 1.55257}, {864.046, 1.54767}, {860.189, 1.5427}, {856.331, 1.53764}, {852.474, 1.5325}, {848.617, 1.52727}, {844.759, 1.52196},
{840.902, 1.51656}, {837.045, 1.51107}, {833.187, 1.50549}, {829.33, 1.49981}, {825.473, 1.49404}, {821.615, 1.48817}, {817.758, 1.4822}, {813.901, 1.47612},
{810.043, 1.46994}, {806.186, 1.46366}, {802.329, 1.45726}, {798.471, 1.45075}, {794.614, 1.44413}, {790.756, 1.43739}, {786.899, 1.43053}, {783.042,
1.42356}, {779.184, 1.41645}, {775.327, 1.40922}, {771.47, 1.40186}, {767.612, 1.39436}, {763.755, 1.38673}, {759.898, 1.37897}, {756.04, 1.37105}, {752.183,
1.363}, {748.326, 1.3548}, {744.468, 1.34645}, {740.611, 1.33794}, {736.754, 1.32928}, {732.896, 1.32045}, {729.039, 1.31147}, {725.182, 1.30231}, {721.324,
1.29299}, {717.467, 1.28349}, {713.609, 1.27381}, {709.752, 1.26395}, {705.895, 1.25391}, {702.037, 1.24367}, {698.18, 1.23324}, {694.323, 1.22261}, {690.465,
1.21178}, {686.608, 1.20074}, {682.751, 1.1895}, {678.893, 1.17803}, {675.036, 1.16634}, {671.179, 1.15443}, {667.321, 1.14228}, {663.464, 1.1299}, {659.607,
1.11727}, {655.749, 1.10439}, {651.892, 1.09126}, {648.035, 1.07787}, {644.177, 1.0642}, {640.32, 1.05026}, {636.463, 1.03604}, {632.605, 1.02152}, {628.748,
1.00671}, {624.891, 0.991584}, {621.033, 0.976139}, {617.176, 0.96037}, {613.318, 0.944258}, {609.461, 0.927802}, {605.604, 0.910984}, {601.746, 0.893789},
{597.889, 0.876213}, {594.032, 0.858236}, {590.174, 0.83984}, {586.317, 0.821017}, {582.46, 0.801747}, {578.602, 0.782007}, {574.745, 0.761787}, {570.888,
0.741062}, {567.03, 0.719803}, {563.173, 0.698}, {559.316, 0.675621}, {555.458, 0.652632}, {551.601, 0.629017}, {547.744, 0.60474}, {543.886, 0.579759},
{540.029, 0.554052}, {536.171, 0.527568}, {532.314, 0.500278}, {528.457, 0.472132}, {524.599, 0.443075}, {520.742, 0.413072}, {516.885, 0.38206}, {513.027,
0.349974}, {509.17, 0.316768}, {505.313, 0.28237}, {501.455, 0.246699}, {497.598, 0.209701}, {493.741, 0.171287}, {489.883, 0.131368}, {486.026, 0.0898746},
{482.169, 0.0467085}, {478.311, 0.00176241}, {474.454, −0.0450378}, {470.597, −0.0938054}, {466.739, −0.144658}, {462.882, −0.197679}, {459.025, −0.252989},
{455.167, −0.310717}, {451.31, −0.370948}, {447.452, −0.433828}, {443.595, −0.499441}, {439.738, −0.567922}, {435.88, −0.639408}, {432.023, −0.713983},
{428.166, −0.791788}, {424.308, −0.87297}, {420.451, −0.957614}, {416.594, −1.04588}, {412.736, −1.13793}, {408.879, −1.23388}, {405.022, −1.33393}, {401.164,
−1.43829}, {397.307, −1.54714}, {393.45, −1.66076}, {389.592, −1.77949}, {385.735, −1.90363}, {381.878, −2.03365}, {378.02, −2.17011}, {374.163, −2.31356},
{370.305, −2.46484}, {366.448, −2.6248}, {362.591, −2.79458}, {358.733, −2.97557}, {354.876, −3.16929}, {351.019, −3.37774}, {347.161, −3.60334}, {343.304,
−3.84886}, {339.447, −4.11782}, {335.589, −4.41457}, {331.732, −4.7442}, {327.875, −5.11324}, {324.017, −5.52989}, {320.16, −6.00414}, {316.303, −6.5491},
{312.445, −7.18185}, {308.588, −7.92437}, {304.731, −8.80691}, {300.873, −9.87137}, {297.016, −11.1764}, {293.159, −12.8098}, {289.301, −14.9067}, {285.444,
−17.6855}, {281.586, −21.5304}, {277.729, −27.1737}, {273.872, −36.2249}, {270.014, −53.0317}, {266.157, −94.7605}, {262.3, −372.755}, {258.442, 209.723},
{254.585, 84.6657}, {250.728, 54.1551}, {246.87, 40.4007}, {243.013, 32.5859}, {239.156, 27.5508}, {235.298, 24.0381}, {231.441, 21.4506}, {227.584, 19.4653},
{223.726, 17.8933}, {219.869, 16.6182}, {216.012, 15.5622}, {212.154, 14.6727}, {208.297, 13.9129}, {204.439, 13.2556}, {200.582, 12.681}, {196.725,
12.1741}, {192.867, 11.723}, {189.01, 11.319}, {185.153, 10.9547}, {181.295, 10.6243}, {177.438, 10.3234}, {173.581, 10.0481}, {169.723, 9.79525}, {165.866,
9.56232}, {162.009, 9.3471}, {158.151, 9.14769}, {154.294, 8.96263}, {150.437, 8.79052}, {146.579, 8.63015}, {142.722, 8.48061}, {138.865, 8.34095}, {135.007,
8.21036}, {131.15, 8.08822}, {127.293, 7.97386}, {123.435, 7.86671}, {119.578, 7.76632}, {115.72, 7.67219}, {111.863, 7.58395}, {108.006, 7.5012}, {104.148,
7.42359}, {100.291, 7.35084}};
caf2=Interpolation[caf2raw];

siraw={{7876.71, 12.3379}, {7845.85, 12.3325}, {7814.99, 12.3272}, {7784.13, 12.3218}, {7753.27, 12.3165}, {7722.41, 12.3112}, {7695.41, 12.3066}, {7664.55,
12.3014}, {7633.69, 12.2962}, {7606.69, 12.2917}, {7575.83, 12.2865}, {7548.83, 12.282}, {7521.83, 12.2775}, {7490.97, 12.2724}, {7463.97, 12.268}, {7436.97,
12.2636}, {7409.97, 12.2592}, {7382.97, 12.2548}, {7355.96, 12.2505}, {7328.96, 12.2461}, {7301.96, 12.2418}, {7274.96, 12.2375}, {7247.96, 12.2333},
{7220.96, 12.229}, {7197.81, 12.2254}, {7170.81, 12.2211}, {7143.81, 12.2169}, {7120.67, 12.2134}, {7093.66, 12.2092}, {7070.52, 12.2056}, {7043.52, 12.2015},
{7020.38, 12.198}, {6993.37, 12.1939}, {6970.23, 12.1904}, {6947.09, 12.1869}, {6923.94, 12.1834}, {6896.94, 12.1794}, {6873.8, 12.176}, {6850.65, 12.1725},
```

{6827.51, 12.1691}, {6804.36, 12.1657}, {6781.22, 12.1624}, {6758.08, 12.159}, {6734.93, 12.1556}, {6711.79, 12.1523}, {6692.5, 12.1495}, {6669.36, 12.1462}, {6646.21, 12.1429}, {6623.07, 12.1396}, {6603.78, 12.1369}, {6580.64, 12.1336}, {6557.49, 12.1303}, {6538.21, 12.1276}, {6515.06, 12.1244}, {6495.78, 12.1217}, {6472.63, 12.1185}, {6453.34, 12.1159}, {6434.06, 12.1132}, {6410.91, 12.1101}, {6391.63, 12.1074}, {6372.34, 12.1048}, {6353.05, 12.1022}, {6329.91, 12.0991}, {6310.62, 12.0965}, {6291.34, 12.0939}, {6272.05, 12.0913}, {6252.76, 12.0888}, {6233.48, 12.0862}, {6214.19, 12.0837}, {6194.9, 12.0811}, {6175.62, 12.0786}, {6156.33, 12.0761}, {6137.04, 12.0736}, {6117.76, 12.0711}, {6098.47, 12.0686}, {6079.18, 12.0661}, {6063.75, 12.0641}, {6044.47, 12.0617}, {6025.18, 12.0592}, {6009.75, 12.0572}, {5990.46, 12.0548}, {5971.18, 12.0524}, {5955.75, 12.0504}, {5936.46, 12.048}, {5917.17, 12.0456}, {5901.74, 12.0437}, {5882.46, 12.0413}, {5867.03, 12.0394}, {5851.6, 12.0375}, {5832.31, 12.0351}, {5816.88, 12.0332}, {5797.6, 12.0309}, {5782.17, 12.029}, {5766.74, 12.0271}, {5747.45, 12.0248}, {5732.02, 12.023}, {5716.59, 12.0211}, {5701.16, 12.0193}, {5681.88, 12.017}, {5666.45, 12.0151}, {5651.02, 12.0133}, {5635.59, 12.0115}, {5620.16, 12.0097}, {5604.73, 12.0079}, {5589.3, 12.0061}, {5573.87, 12.0043}, {5558.44, 12.0025}, {5543.01, 12.0007}, {5527.58, 11.9989}, {5512.15, 11.9971}, {5496.72, 11.9953}, {5481.29, 11.9936}, {5465.86, 11.9918}, {5450.43, 11.9901}, {5435, 11.9883}, {5423.43, 11.987}, {5408, 11.9853}, {5392.57, 11.9835}, {5377.14, 11.9818}, {5365.57, 11.9805}, {5350.14, 11.9788}, {5334.71, 11.9771}, {5319.28, 11.9754}, {5307.71, 11.9741}, {5292.28, 11.9724}, {5280.71, 11.9711}, {5265.28, 11.9694}, {5249.85, 11.9678}, {5238.28, 11.9665}, {5222.85, 11.9648}, {5211.28, 11.9636}, {5195.85, 11.9619}, {5184.28, 11.9607}, {5168.85, 11.959}, {5157.28, 11.9578}, {5141.85, 11.9561}, {5130.27, 11.9549}, {5118.7, 11.9537}, {5103.27, 11.952}, {5091.7, 11.9508}, {5076.27, 11.9492}, {5064.7, 11.948}, {5053.13, 11.9468}, {5041.56, 11.9456}, {5026.13, 11.944}, {5014.55, 11.9428}, {5002.98, 11.9416}, {4987.55, 11.94}, {4975.98, 11.9388}, {4964.41, 11.9376}, {4952.84, 11.9364}, {4941.26, 11.9352}, {4929.69, 11.9341}, {4914.26, 11.9325}, {4902.69, 11.9313}, {4891.12, 11.9302}, {4879.55, 11.929}, {4867.97, 11.9278}, {4856.4, 11.9267}, {4844.83, 11.9255}, {4833.26, 11.9244}, {4821.69, 11.9232}, {4810.11, 11.9221}, {4798.54, 11.9209}, {4786.97, 11.9198}, {4775.4, 11.9187}, {4763.83, 11.9175}, {4752.25, 11.9164}, {4740.68, 11.9153}, {4729.11, 11.9141}, {4717.54, 11.913}, {4705.97, 11.9119}, {4698.25, 11.9112}, {4686.68, 11.91}, {4675.11, 11.9089}, {4663.54, 11.9078}, {4651.96, 11.9067}, {4640.39, 11.9056}, {4632.68, 11.9049}, {4621.1, 11.9038}, {4609.53, 11.9027}, {4597.96, 11.9016}, {4590.25, 11.9009}, {4578.67, 11.8998}, {4567.1, 11.8987}, {4559.39, 11.898}, {4547.81, 11.8969}, {4536.24, 11.8958}, {4528.53, 11.8951}, {4516.96, 11.8941}, {4505.38, 11.893}, {4497.67, 11.8923}, {4486.1, 11.8912}, {4474.52, 11.8902}, {4466.81, 11.8894}, {4455.24, 11.8884}, {4447.52, 11.8877}, {4435.95, 11.8866}, {4428.24, 11.8859}, {4416.66, 11.8849}, {4408.95, 11.8842}, {4397.38, 11.8832}, {4389.66, 11.8825}, {4378.09, 11.8814}, {4370.38, 11.8807}, {4358.8, 11.8797}, {4351.09, 11.879}, {4339.52, 11.878}, {4331.8, 11.8773}, {4320.23, 11.8763}, {4312.52, 11.8756}, {4304.8, 11.875}, {4293.23, 11.8739}, {4285.51, 11.8733}, {4273.94, 11.8723}, {4266.23, 11.8716}, {4258.51, 11.8709}, {4246.94, 11.8699}, {4239.23, 11.8692}, {4231.51, 11.8686}, {4219.94, 11.8676}, {4212.23, 11.8669}, {4204.51, 11.8663}, {4192.94, 11.8653}, {4185.22, 11.8646}, {4177.51, 11.864}, {4169.79, 11.8633}, {4158.22, 11.8623}, {4150.51, 11.8617}, {4142.79, 11.861}, {4135.08, 11.8604}, {4127.36, 11.8597}, {4115.79, 11.8588}, {4108.08, 11.8581}, {4100.36, 11.8575}, {4092.65, 11.8568}, {4084.93, 11.8562}, {4073.36, 11.8552}, {4065.65, 11.8546}, {4057.93, 11.854}, {4050.22, 11.8533}, {4042.5, 11.8527}, {4034.79, 11.8521}, {4027.07, 11.8514}, {4019.36, 11.8508}, {4011.64, 11.8502}, {4000.07, 11.8492}, {3992.36, 11.8486}, {3984.64, 11.848}, {3976.93, 11.8474}, {3969.21, 11.8467}, {3961.5, 11.8461}, {3953.78, 11.8455}, {3946.07, 11.8449}, {3938.35, 11.8443}, {3930.64, 11.8437}, {3922.92, 11.843}, {3915.21, 11.8424}, {3907.49, 11.8418}, {3899.78, 11.8412}, {3892.07, 11.8406}, {3884.35, 11.84}, {3876.64, 11.8394}, {3868.92, 11.8388}, {3861.21, 11.8382}, {3857.35, 11.8379}, {3849.63, 11.8373}, {3841.92, 11.8367}, {3834.21, 11.8361}, {3826.49, 11.8355}, {3818.78, 11.8349}, {3811.06, 11.8343}, {3803.35, 11.8337}, {3795.63, 11.8331}, {3787.92, 11.8325}, {3784.06, 11.8322}, {3776.34, 11.8316}, {3768.63, 11.831}, {3760.92, 11.8304}, {3753.2, 11.8299}, {3745.49, 11.8293}, {3741.63, 11.829}, {3733.91, 11.8284}, {3726.2, 11.8278}, {3718.48, 11.8272}, {3710.77, 11.8267}, {3706.91, 11.8264}, {3699.2, 11.8258}, {3691.48, 11.8252}, {3683.77, 11.8246}, {3679.91, 11.8244}, {3672.2, 11.8238}, {3664.48, 11.8232}, {3656.77, 11.8226}, {3652.91, 11.8224}, {3645.2, 11.8218}, {3637.48, 11.8212}, {3629.77, 11.8207}, {3625.91, 11.8204}, {3618.19, 11.8198}, {3610.48, 11.8193}, {3606.62, 11.819}, {3598.91, 11.8184}, {3591.19, 11.8179}, {3587.33, 11.8176}, {3579.62, 11.817}, {3571.91, 11.8165}, {3568.05, 11.8162}, {3560.33, 11.8156}, {3552.62, 11.8151}, {3548.76, 11.8148}, {3541.05, 11.8143}, {3537.19, 11.814}, {3529.47, 11.8134}, {3521.76, 11.8129}, {3517.9, 11.8126}, {3510.19, 11.8121}, {3506.33, 11.8118}, {3498.62, 11.8112}, {3490.9, 11.8107}, {3487.04, 11.8104}, {3479.33, 11.8099}, {3475.47, 11.8096}, {3467.76, 11.8091}, {3463.9, 11.8088}, {3456.18, 11.8083}, {3448.47, 11.8077}, {3444.61, 11.8075}, {3436.9, 11.8069}, {3433.04, 11.8067}, {3425.33, 11.8061}, {3421.47, 11.8059}, {3413.75, 11.8053}, {3409.9, 11.8051}, {3402.18, 11.8046}, {3398.32, 11.8043}, {3390.61, 11.8038}, {3386.75, 11.8035}, {3379.04, 11.803}, {3375.18, 11.8027}, {3367.47, 11.8022}, {3363.61, 11.8019}, {3355.89, 11.8014}, {3352.04, 11.8012}, {3348.18, 11.8009}, {3340.46, 11.8004}, {3336.61, 11.8001}, {3328.89, 11.7996}, {3325.04, 11.7993}, {3317.32, 11.7988}, {3313.46, 11.7986}, {3309.61, 11.7983}, {3301.89, 11.7978}, {3298.03, 11.7975}, {3290.32, 11.797}, {3286.46, 11.7968}, {3278.75, 11.7963}, {3274.89, 11.796}, {3271.03, 11.7958}, {3263.32, 11.7953}, {3259.46, 11.795}, {3255.6, 11.7948}, {3247.89, 11.7942}, {3244.03, 11.794}, {3236.32, 11.7935}, {3232.46, 11.7932}, {3228.6, 11.793}, {3220.89, 11.7925}, {3217.03, 11.7922}, {3213.17, 11.792}, {3205.46, 11.7915}, {3201.6, 11.7913}, {3197.74, 11.791}, {3190.03, 11.7905}, {3186.17, 11.7903}, {3182.31, 11.79}, {3178.46, 11.7898}, {3170.74, 11.7893}, {3166.88, 11.789}, {3163.03, 11.7888}, {3155.31, 11.7883}, {3151.45, 11.7881}, {3147.6, 11.7878}, {3139.88, 11.7873}, {3136.02, 11.7871}, {3132.17, 11.7868}, {3128.31, 11.7866}, {3120.6, 11.7861}, {3116.74, 11.7859}, {3112.88, 11.7856}, {3109.02, 11.7854}, {3101.31, 11.7849}, {3097.45, 11.7847}, {3093.59, 11.7844}, {3089.74, 11.7842}, {3082.02, 11.7837}, {3078.16, 11.7835}, {3074.31, 11.7833}, {3070.45, 11.783}, {3066.59, 11.7828}, {3058.88, 11.7823}, {3055.02, 11.7821}, {3051.16, 11.7818}, {3047.31, 11.7816}, {3039.59, 11.7811}, {3035.73, 11.7809}, {3031.88, 11.7807}, {3028.02, 11.7804}, {3024.16, 11.7802}, {3020.3, 11.78}, {3012.59, 11.7795}, {3008.73, 11.7793}, {3004.88, 11.779}, {3001.02, 11.7788}, {2997.16, 11.7786}, {2993.3, 11.7783}, {2985.59, 11.7779}, {2981.73, 11.7776}, {2977.87, 11.7774}, {2974.02, 11.7772}, {2970.16, 11.777}, {2966.3, 11.7767}, {2958.59, 11.7763}, {2954.73, 11.776}, {2950.87, 11.7758}, {2947.01, 11.7756}, {2943.16, 11.7754}, {2939.3, 11.7751}, {2935.44, 11.7749}, {2931.59, 11.7747}, {2927.73, 11.7745}, {2920.01, 11.774}, {2916.16, 11.7738}, {2912.3, 11.7735}, {2908.44, 11.7733}, {2904.58, 11.7731}, {2900.73, 11.7729}, {2896.87, 11.7727}, {2893.01, 11.7724}, {2889.15, 11.7722}, {2885.3, 11.772}, {2881.44, 11.7718}, {2873.73, 11.7713}, {2869.87, 11.7711}, {2866.01, 11.7709}, {2862.15, 11.7707}, {2858.3, 11.7704}, {2854.44, 11.7702}, {2850.58, 11.77}, {2846.72, 11.7698}, {2842.87, 11.7696}, {2839.01, 11.7693}, {2835.15, 11.7691}, {2831.29, 11.7689}, {2827.44, 11.7687}, {2823.58, 11.7685}, {2819.72, 11.7682}, {2815.87, 11.768}, {2812.01, 11.7678}, {2808.15, 11.7676}, {2804.29, 11.7674}, {2800.44, 11.7672}, {2796.58, 11.767}, {2792.72, 11.7667}, {2788.86, 11.7665}, {2785.01, 11.7663}, {2781.15, 11.7661}, {2777.29, 11.7659}, {2773.43, 11.7657}, {2769.58, 11.7655}, {2765.72, 11.7652}, {2761.86, 11.765}, {2758, 11.7648}, {2754.15, 11.7646}, {2750.29, 11.7644}, {2746.43, 11.7642}, {2742.58, 11.764}, {2738.72, 11.7638}, {2734.86, 11.7635}, {2731, 11.7633}, {2727.15, 11.7631}, {2723.29, 11.7629}, {2719.43, 11.7627}, {2715.57, 11.7625}, {2711.72, 11.7623}, {2707.86, 11.7621}, {2704, 11.7619}, {2700.14, 11.7617}, {2696.29, 11.7615}, {2692.43, 11.7612}, {2688.57, 11.761}, {2684.72, 11.7608}, {2680.86, 11.7606}, {2677, 11.7604}, {2673.14, 11.7602}, {2669.29, 11.76}, {2665.43, 11.7598}, {2661.57, 11.7596}, {2657.71, 11.7594}, {2653.86, 11.7592}, {2650, 11.759}, {2646.14, 11.7588}, {2642.28, 11.7586}, {2638.43, 11.7584}, {2634.57, 11.7582}, {2630.71, 11.758}, {2626.85, 11.7578}, {2623, 11.7576}, {2619.14, 11.7574}, {2615.28, 11.7572}, {2611.43, 11.757}, {2607.57, 11.7568}, {2603.71, 11.7566}, {2599.85, 11.7564}, {2596, 11.7562}, {2592.14, 11.756}, {2588.28, 11.7558}, {2584.42, 11.7556}, {2580.57, 11.7554}, {2576.71, 11.7552}, {2572.85, 11.755}, {2568.99, 11.7548}, {2565.14, 11.7546}, {2561.28, 11.7544}, {2557.42, 11.7542}, {2553.57, 11.754}, {2549.71, 11.7538}, {2545.85, 11.7536}, {2541.99, 11.7534}, {2538.14, 11.7532}, {2534.28, 11.753}, {2530.42, 11.7528}, {2526.56, 11.7526}, {2522.71, 11.7524}, {2518.85, 11.7522}, {2514.99, 11.752}, {2511.13, 11.7518}, {2507.28, 11.7517}, {2503.42, 11.7515}, {2499.56, 11.7513}, {2495.71, 11.7511}, {2491.85, 11.7509}, {2487.99, 11.7507}, {2484.13, 11.7505}, {2480.28, 11.7503}, {2476.42, 11.7501}, {2472.56, 11.7499}, {2468.7, 11.7497}, {2464.85, 11.7496}, {2460.99, 11.7494}, {2457.13, 11.7492}, {2453.27, 11.749}, {2449.42, 11.7488}, {2445.56, 11.7486}, {2441.7, 11.7484}, {2437.84, 11.7482}, {2433.99, 11.7481}, {2430.13, 11.7479}, {2426.27, 11.7477}, {2422.42,

11.7475}, {2418.56, 11.7473}, {2414.7, 11.7471}, {2410.84, 11.7469}, {2406.99, 11.7468}, {2403.13, 11.7466}, {2399.27, 11.7464}, {2395.41, 11.7462}, {2391.56, 11.746}, {2387.7, 11.7458}, {2383.84, 11.7456}, {2379.98, 11.7455}, {2376.13, 11.7453}, {2372.27, 11.7451}, {2368.41, 11.7449}, {2364.56, 11.7447}, {2360.7, 11.7446}, {2356.84, 11.7444}, {2352.98, 11.7442}, {2349.13, 11.744}, {2345.27, 11.7438}, {2341.41, 11.7437}, {2337.55, 11.7435}, {2333.7, 11.7433}, {2329.84, 11.7431}, {2325.98, 11.7429}, {2322.12, 11.7428}, {2318.27, 11.7426}, {2314.41, 11.7424}, {2310.55, 11.7422}, {2306.7, 11.7421}, {2302.84, 11.7419}, {2298.98, 11.7417}, {2295.12, 11.7415}, {2291.27, 11.7413}, {2287.41, 11.7412}, {2283.55, 11.741}, {2279.69, 11.7408}, {2275.84, 11.7406}, {2271.98, 11.7405}, {2268.12, 11.7403}, {2264.26, 11.7401}, {2260.41, 11.74}, {2256.55, 11.7398}, {2252.69, 11.7396}, {2248.83, 11.7394}, {2244.98, 11.7393}, {2241.12, 11.7391}, {2237.26, 11.7389}, {2233.41, 11.7387}, {2229.55, 11.7386}, {2225.69, 11.7384}, {2221.83, 11.7382}, {2217.98, 11.7381}, {2214.12, 11.7379}, {2210.26, 11.7377}, {2206.4, 11.7376}, {2202.55, 11.7374}, {2198.69, 11.7372}, {2194.83, 11.737}, {2190.97, 11.7369}, {2187.12, 11.7367}, {2183.26, 11.7365}, {2179.4, 11.7364}, {2175.55, 11.7362}, {2171.69, 11.736}, {2167.83, 11.7359}, {2163.97, 11.7357}, {2160.12, 11.7355}, {2156.26, 11.7354}, {2152.4, 11.7352}, {2148.54, 11.7351}, {2144.69, 11.7349}, {2140.83, 11.7347}, {2136.97, 11.7346}, {2133.11, 11.7344}, {2129.26, 11.7342}, {2125.4, 11.7341}, {2121.54, 11.7339}, {2117.68, 11.7337}, {2113.83, 11.7336}, {2109.97, 11.7334}, {2106.11, 11.7333}, {2102.26, 11.7331}, {2098.4, 11.7329}, {2094.54, 11.7328}, {2090.68, 11.7326}, {2086.83, 11.7325}, {2082.97, 11.7323}, {2079.11, 11.7321}, {2075.25, 11.732}, {2071.4, 11.7318}, {2067.54, 11.7317}, {2063.68, 11.7315}, {2059.82, 11.7313}, {2055.97, 11.7312}, {2052.11, 11.731}, {2048.25, 11.7309}, {2044.4, 11.7307}, {2040.54, 11.7306}, {2036.68, 11.7304}, {2032.82, 11.7303}, {2028.97, 11.7301}, {2025.11, 11.7299}, {2021.25, 11.7298}, {2017.39, 11.7296}, {2013.54, 11.7295}, {2009.68, 11.7293}, {2005.82, 11.7292}, {2001.96, 11.729}, {1998.11, 11.7289}, {1994.25, 11.7287}, {1990.39, 11.7286}, {1986.54, 11.7284}, {1982.68, 11.7283}, {1978.82, 11.7281}, {1974.96, 11.7279}, {1971.11, 11.7278}, {1967.25, 11.7276}, {1963.39, 11.7275}, {1959.53, 11.7273}, {1955.68, 11.7272}, {1951.82, 11.727}, {1947.96, 11.7269}, {1944.1, 11.7268}, {1940.25, 11.7266}, {1936.39, 11.7265}, {1932.53, 11.7263}, {1928.67, 11.7262}, {1924.82, 11.726}, {1920.96, 11.7259}, {1917.1, 11.7257}, {1913.25, 11.7256}, {1909.39, 11.7254}, {1905.53, 11.7253}, {1901.67, 11.7251}, {1897.82, 11.725}, {1893.96, 11.7248}, {1890.1, 11.7247}, {1886.24, 11.7246}, {1882.39, 11.7244}, {1878.53, 11.7243}, {1874.67, 11.7241}, {1870.81, 11.724}, {1866.96, 11.7238}, {1863.1, 11.7237}, {1859.24, 11.7235}, {1855.39, 11.7234}, {1851.53, 11.7233}, {1847.67, 11.7231}, {1843.81, 11.723}, {1839.96, 11.7228}, {1836.1, 11.7227}, {1832.24, 11.7226}, {1828.38, 11.7224}, {1824.53, 11.7223}, {1820.67, 11.7221}, {1816.81, 11.722}, {1812.95, 11.7219}, {1809.1, 11.7217}, {1805.24, 11.7216}, {1801.38, 11.7214}, {1797.53, 11.7213}, {1793.67, 11.7212}, {1789.81, 11.721}, {1785.95, 11.7209}, {1782.1, 11.7208}, {1778.24, 11.7206}, {1774.38, 11.7205}, {1770.52, 11.7204}, {1766.67, 11.7202}, {1762.81, 11.7201}, {1758.95, 11.72}, {1755.09, 11.7198}, {1751.24, 11.7197}, {1747.38, 11.7195}, {1743.52, 11.7194}, {1739.66, 11.7193}, {1735.81, 11.7191}, {1731.95, 11.719}, {1728.09, 11.7189}, {1724.24, 11.7188}, {1720.38, 11.7186}, {1716.52, 11.7185}, {1712.66, 11.7184}, {1708.81, 11.7182}, {1704.95, 11.7181}, {1701.09, 11.718}, {1697.23, 11.7178}, {1693.38, 11.7177}, {1689.52, 11.7176}, {1685.66, 11.7174}, {1681.8, 11.7173}, {1677.95, 11.7172}, {1674.09, 11.7171}, {1670.23, 11.7169}, {1666.38, 11.7168}, {1662.52, 11.7167}, {1658.66, 11.7166}, {1654.8, 11.7164}, {1650.95, 11.7163}, {1647.09, 11.7162}, {1643.23, 11.716}, {1639.37, 11.7159}, {1635.52, 11.7158}, {1631.66, 11.7157}, {1627.8, 11.7155}, {1623.94, 11.7154}, {1620.09, 11.7153}, {1616.23, 11.7152}, {1612.37, 11.7151}, {1608.51, 11.7149}, {1604.66, 11.7148}, {1600.8, 11.7147}, {1596.94, 11.7146}, {1593.09, 11.7144}, {1589.23, 11.7143}, {1585.37, 11.7142}, {1581.51, 11.7141}, {1577.66, 11.714}, {1573.8, 11.7138}, {1569.94, 11.7137}, {1566.08, 11.7136}, {1562.23, 11.7135}, {1558.37, 11.7134}, {1554.51, 11.7132}, {1550.65, 11.7131}, {1546.8, 11.713}, {1542.94, 11.7129}, {1539.08, 11.7128}, {1535.23, 11.7126}, {1531.37, 11.7125}, {1527.51, 11.7124}, {1523.65, 11.7123}, {1519.8, 11.7122}, {1515.94, 11.7121}, {1512.08, 11.7119}, {1508.22, 11.7118}, {1504.37, 11.7117}, {1500.51, 11.7116}, {1496.65, 11.7115}, {1492.79, 11.7114}, {1488.94, 11.7113}, {1485.08, 11.7111}, {1481.22, 11.711}, {1477.37, 11.7109}, {1473.51, 11.7108}, {1469.65, 11.7107}, {1465.79, 11.7106}, {1461.94, 11.7105}, {1458.08, 11.7104}, {1454.22, 11.7102}, {1450.36, 11.7101}, {1446.51, 11.71}, {1442.65, 11.7099}, {1438.79, 11.7098}, {1434.93, 11.7097}, {1431.08, 11.7096}, {1427.22, 11.7095}, {1423.36, 11.7094}, {1419.5, 11.7093}, {1415.65, 11.7091}, {1411.79, 11.709}, {1407.93, 11.7089}, {1404.08, 11.7088}, {1400.22, 11.7087}, {1396.36, 11.7086}, {1392.5, 11.7085}, {1388.65, 11.7084}, {1384.79, 11.7083}, {1380.93, 11.7082}, {1377.07, 11.7081}, {1373.22, 11.708}, {1369.36, 11.7079}, {1365.5, 11.7078}, {1361.64, 11.7077}, {1357.79, 11.7076}, {1353.93, 11.7074}, {1350.07, 11.7073}, {1346.22, 11.7072}, {1342.36, 11.7071}, {1338.5, 11.707}, {1334.64, 11.7069}, {1330.79, 11.7068}, {1326.93, 11.7067}, {1323.07, 11.7066}, {1319.21, 11.7065}, {1315.36, 11.7064}, {1311.5, 11.7063}, {1307.64, 11.7062}, {1303.78, 11.7061}, {1299.93, 11.706}, {1296.07, 11.7059}, {1292.21, 11.7058}, {1288.35, 11.7057}, {1284.5, 11.7056}, {1280.64, 11.7055}, {1276.78, 11.7054}, {1272.93, 11.7053}, {1269.07, 11.7052}, {1265.21, 11.7051}, {1261.35, 11.705}, {1257.5, 11.7049}, {1253.64, 11.7048}, {1249.78, 11.7048}, {1245.92, 11.7047}, {1242.07, 11.7046}, {1238.21, 11.7045}, {1234.35, 11.7044}, {1230.49, 11.7043}, {1226.64, 11.7042}, {1222.78, 11.7041}, {1218.92, 11.704}, {1215.07, 11.7039}, {1211.21, 11.7038}, {1207.35, 11.7037}, {1203.49, 11.7036}, {1199.64, 11.7035}, {1195.78, 11.7034}, {1191.92, 11.7033}, {1188.06, 11.7033}, {1184.21, 11.7032}, {1180.35, 11.7031}, {1176.49, 11.703}, {1172.63, 11.7029}, {1168.78, 11.7028}, {1164.92, 11.7027}, {1161.06, 11.7026}, {1157.21, 11.7025}, {1153.35, 11.7024}, {1149.49, 11.7024}, {1145.63, 11.7023}, {1141.78, 11.7022}, {1137.92, 11.7021}, {1134.06, 11.702}, {1130.2, 11.7019}, {1126.35, 11.7018}, {1122.49, 11.7017}, {1118.63, 11.7017}, {1114.77, 11.7016}, {1110.92, 11.7015}, {1107.06, 11.7014}, {1103.2, 11.7013}, {1099.34, 11.7012}, {1095.49, 11.7011}, {1091.63, 11.7011}, {1087.77, 11.701}, {1083.92, 11.7009}, {1080.06, 11.7008}, {1076.2, 11.7007}, {1072.34, 11.7006}, {1068.49, 11.7006}, {1064.63, 11.7005}, {1060.77, 11.7004}, {1056.91, 11.7003}, {1053.06, 11.7002}, {1049.2, 11.7001}, {1045.34, 11.7001}, {1041.48, 11.7}, {1037.63, 11.6999}, {1033.77, 11.6998}, {1029.91, 11.6997}, {1026.06, 11.6997}, {1022.2, 11.6996}, {1018.34, 11.6995}, {1014.48, 11.6994}, {1010.63, 11.6994}, {1006.77, 11.6993}, {1002.91, 11.6992}, {999.053, 11.6991}, {995.196, 11.699}, {991.339, 11.699}, {987.481, 11.6989}, {983.624, 11.6988}, {979.767, 11.6987}, {975.909, 11.6987}, {972.052, 11.6986}, {968.195, 11.6985}, {964.337, 11.6984}, {960.48, 11.6984}, {956.622, 11.6983}, {952.765, 11.6982}, {948.908, 11.6981}, {945.05, 11.6981}, {941.193, 11.698}, {937.336, 11.6979}, {933.478, 11.6978}, {929.621, 11.6978}, {925.764, 11.6977}, {921.906, 11.6976}, {918.049, 11.6976}, {914.192, 11.6975}, {910.334, 11.6974}, {906.477, 11.6973}, {902.62, 11.6973}, {898.762, 11.6972}, {894.905, 11.6971}, {891.048, 11.6971}, {887.19, 11.697}, {883.333, 11.6969}, {879.476, 11.6969}, {875.618, 11.6968}, {871.761, 11.6967}, {867.903, 11.6967}, {864.046, 11.6966}, {860.189, 11.6965}, {856.331, 11.6964}, {852.474, 11.6964}, {848.617, 11.6963}, {844.759, 11.6962}, {840.902, 11.6962}, {837.045, 11.6961}, {833.187, 11.6961}, {829.33, 11.696}, {825.473, 11.6959}, {821.615, 11.6959}, {817.758, 11.6958}, {813.901, 11.6957}, {810.043, 11.6957}, {806.186, 11.6956}, {802.329, 11.6955}, {798.471, 11.6955}, {794.614, 11.6954}, {790.756, 11.6953}, {786.899, 11.6953}, {783.042, 11.6952}, {779.184, 11.6952}, {775.327, 11.6951}, {771.47, 11.695}, {767.612, 11.695}, {763.755, 11.6949}, {759.898, 11.6949}, {756.04, 11.6948}, {752.183, 11.6947}, {748.326, 11.6947}, {744.468, 11.6946}, {740.611, 11.6946}, {736.754, 11.6945}, {732.896, 11.6944}, {729.039, 11.6944}, {725.182, 11.6943}, {721.324, 11.6943}, {717.467, 11.6942}, {713.609, 11.6942}, {709.752, 11.6941}, {705.895, 11.694}, {702.037, 11.694}, {698.18, 11.6939}, {694.323, 11.6939}, {690.465, 11.6938}, {686.608, 11.6938}, {682.751, 11.6937}, {678.893, 11.6937}, {675.036, 11.6936}, {671.179, 11.6935}, {667.321, 11.6935}, {663.464, 11.6934}, {659.607, 11.6934}, {655.749, 11.6933}, {651.892, 11.6933}, {648.035, 11.6932}, {644.177, 11.6932}, {640.32, 11.6931}, {636.463, 11.6931}, {632.605, 11.693}, {628.748, 11.693}, {624.891, 11.6929}, {621.033, 11.6929}, {617.176, 11.6928}, {613.318, 11.6928}, {609.461, 11.6927}, {605.604, 11.6927}, {601.746, 11.6926}, {597.889, 11.6926}, {594.032, 11.6925}, {590.174, 11.6925}, {586.317, 11.6924}, {582.46, 11.6924}, {578.602, 11.6923}, {574.745, 11.6923}, {570.888, 11.6922}, {567.03, 11.6922}, {563.173, 11.6921}, {559.316, 11.6921}, {555.458, 11.692}, {551.601, 11.692}, {547.744, 11.692}, {543.886, 11.6919}, {540.029, 11.6919}, {536.171, 11.6918}, {532.314, 11.6918}, {528.457, 11.6917}, {524.599, 11.6917}, {520.742, 11.6916}, {516.885, 11.6916}, {513.027, 11.6916}, {509.17, 11.6915}, {505.313, 11.6915}, {501.455, 11.6914}, {497.598, 11.6914}, {493.741, 11.6913}, {489.883, 11.6913}, {486.026, 11.6913}, {482.169, 11.6912}, {478.311, 11.6912}, {474.454, 11.6911}, {470.597, 11.6911}, {466.739, 11.6911}, {462.882, 11.691}, {459.025, 11.691}, {455.167, 11.6909}, {451.31, 11.6909}, {447.452, 11.6909}, {443.595, 11.6908}, {439.738, 11.6908}, {435.88, 11.6907}, {432.023, 11.6907}, {428.166, 11.6907}, {424.308, 11.6906}, {420.451, 11.6906},

{416.594, 11.6906}, {412.736, 11.6905}, {408.879, 11.6905}, {405.022, 11.6904}, {401.164, 11.6904}, {397.307, 11.6904}, {393.45, 11.6903}, {389.592, 11.6903}, {385.735, 11.6903}, {381.878, 11.6902}, {378.02, 11.6902}, {374.163, 11.6902}, {370.305, 11.6901}, {366.448, 11.6901}, {362.591, 11.6901}, {358.733, 11.69}, {354.876, 11.69}, {351.019, 11.69}, {347.161, 11.6899}, {343.304, 11.6899}, {339.447, 11.6899}, {335.589, 11.6899}, {331.732, 11.6898}, {327.875, 11.6898}, {324.017, 11.6898}, {320.16, 11.6897}, {316.303, 11.6897}, {312.445, 11.6897}, {308.588, 11.6896}, {304.731, 11.6896}, {300.873, 11.6896}, {297.016, 11.6896}, {293.159, 11.6895}, {289.301, 11.6895}, {285.444, 11.6895}, {281.586, 11.6894}, {277.729, 11.6894}, {273.872, 11.6894}, {270.014, 11.6894}, {266.157, 11.6893}, {262.3, 11.6893}, {258.442, 11.6893}, {254.585, 11.6893}, {250.728, 11.6892}, {246.87, 11.6892}, {243.013, 11.6892}, {239.156, 11.6892}, {235.298, 11.6892}, {231.441, 11.6891}, {227.584, 11.6891}, {223.726, 11.6891}, {219.869, 11.6891}, {216.012, 11.689}, {212.154, 11.689}, {208.297, 11.689}, {204.439, 11.689}, {200.582, 11.689}, {196.725, 11.6889}, {192.867, 11.6889}, {189.01, 11.6889}, {185.153, 11.6889}, {181.295, 11.6889}, {177.438, 11.6888}, {173.581, 11.6888}, {169.723, 11.6888}, {165.866, 11.6888}, {162.009, 11.6888}, {158.151, 11.6888}, {154.294, 11.6887}, {150.437, 11.6887}, {146.579, 11.6887}, {142.722, 11.6887}, {138.865, 11.6887}, {135.007, 11.6887}, {131.15, 11.6887}, {127.293, 11.6886}, {123.435, 11.6886}, {119.578, 11.6886}, {115.72, 11.6886}, {111.863, 11.6886}, {108.006, 11.6886}, {104.148, 11.6886}, {100.291, 11.6886}};

si=Interpolation[siraw];

znseraw={{7876.71, 6.08512}, {7845.85, 6.08375}, {7814.99, 6.08238}, {7784.13, 6.08101}, {7753.27, 6.07966}, {7722.41, 6.0783}, {7695.41, 6.07713}, {7664.55, 6.07579}, {7633.69, 6.07446}, {7606.69, 6.07329}, {7575.83, 6.07197}, {7548.83, 6.07082}, {7521.83, 6.06967}, {7490.97, 6.06837}, {7463.97, 6.06723}, {7436.97, 6.0661}, {7409.97, 6.06497}, {7382.97, 6.06385}, {7355.96, 6.06273}, {7328.96, 6.06162}, {7301.96, 6.06051}, {7274.96, 6.0594}, {7247.96, 6.0583}, {7220.96, 6.0572}, {7197.81, 6.05627}, {7170.81, 6.05518}, {7143.81, 6.0541}, {7120.67, 6.05317}, {7093.66, 6.0521}, {7070.52, 6.05118}, {7043.52, 6.05011}, {7020.38, 6.0492}, {6993.37, 6.04814}, {6970.23, 6.04724}, {6947.09, 6.04634}, {6923.94, 6.04544}, {6896.94, 6.0444}, {6873.8, 6.04351}, {6850.65, 6.04262}, {6827.51, 6.04174}, {6804.36, 6.04086}, {6781.22, 6.03998}, {6758.08, 6.0391}, {6734.93, 6.03823}, {6711.79, 6.03736}, {6692.5, 6.03664}, {6669.36, 6.03578}, {6646.21, 6.03492}, {6623.07, 6.03406}, {6603.78, 6.03335}, {6580.64, 6.0325}, {6557.49, 6.03166}, {6538.21, 6.03095}, {6515.06, 6.03011}, {6495.78, 6.02941}, {6472.63, 6.02857}, {6453.34, 6.02788}, {6434.06, 6.02719}, {6410.91, 6.02636}, {6391.63, 6.02567}, {6372.34, 6.02498}, {6353.05, 6.0243}, {6329.91, 6.02348}, {6310.62, 6.0228}, {6291.34, 6.02213}, {6272.05, 6.02145}, {6252.76, 6.02078}, {6233.48, 6.02011}, {6214.19, 6.01944}, {6194.9, 6.01877}, {6175.62, 6.01811}, {6156.33, 6.01744}, {6137.04, 6.01678}, {6117.76, 6.01612}, {6098.47, 6.01547}, {6079.18, 6.01481}, {6063.75, 6.01429}, {6044.47, 6.01364}, {6025.18, 6.01299}, {6009.75, 6.01247}, {5990.46, 6.01183}, {5971.18, 6.01118}, {5955.75, 6.01067}, {5936.46, 6.01003}, {5917.17, 6.00939}, {5901.74, 6.00888}, {5882.46, 6.00825}, {5867.03, 6.00774}, {5851.6, 6.00724}, {5832.31, 6.00661}, {5816.88, 6.0061}, {5797.6, 6.00548}, {5782.17, 6.00498}, {5766.74, 6.00448}, {5747.45, 6.00386}, {5732.02, 6.00336}, {5716.59, 6.00287}, {5701.16, 6.00237}, {5681.88, 6.00176}, {5666.45, 6.00127}, {5651.02, 6.00078}, {5635.59, 6.00029}, {5620.16, 5.99981}, {5604.73, 5.99932}, {5589.3, 5.99884}, {5573.87, 5.99835}, {5558.44, 5.99787}, {5543.01, 5.99739}, {5527.58, 5.99691}, {5512.15, 5.99643}, {5496.72, 5.99595}, {5481.29, 5.99548}, {5465.86, 5.995}, {5450.43, 5.99453}, {5435, 5.99405}, {5423.43, 5.9937}, {5408, 5.99323}, {5392.57, 5.99276}, {5377.14, 5.99229}, {5365.57, 5.99194}, {5350.14, 5.99147}, {5334.71, 5.99101}, {5319.28, 5.99054}, {5307.71, 5.9902}, {5292.28, 5.98973}, {5280.71, 5.98939}, {5265.28, 5.98893}, {5249.85, 5.98847}, {5238.28, 5.98812}, {5222.85, 5.98767}, {5211.28, 5.98732}, {5195.85, 5.98687}, {5184.28, 5.98653}, {5168.85, 5.98607}, {5157.28, 5.98573}, {5141.85, 5.98528}, {5130.27, 5.98494}, {5118.7, 5.98461}, {5103.27, 5.98416}, {5091.7, 5.98382}, {5076.27, 5.98337}, {5064.7, 5.98304}, {5053.13, 5.9827}, {5041.56, 5.98237}, {5026.13, 5.98193}, {5014.55, 5.98159}, {5002.98, 5.98126}, {4987.55, 5.98082}, {4975.98, 5.98049}, {4964.41, 5.98016}, {4952.84, 5.97983}, {4941.26, 5.9795}, {4929.69, 5.97917}, {4914.26, 5.97874}, {4902.69, 5.97841}, {4891.12, 5.97808}, {4879.55, 5.97776}, {4867.97, 5.97743}, {4856.4, 5.97711}, {4844.83, 5.97678}, {4833.26, 5.97646}, {4821.69, 5.97614}, {4810.11, 5.97582}, {4798.54, 5.97549}, {4786.97, 5.97517}, {4775.4, 5.97485}, {4763.83, 5.97453}, {4752.25, 5.97421}, {4740.68, 5.97389}, {4729.11, 5.97357}, {4717.54, 5.97325}, {4705.97, 5.97294}, {4698.25, 5.97272}, {4686.68, 5.97241}, {4675.11, 5.97209}, {4663.54, 5.97177}, {4651.96, 5.97146}, {4640.39, 5.97114}, {4632.68, 5.97093}, {4621.1, 5.97062}, {4609.53, 5.97031}, {4597.96, 5.96999}, {4590.25, 5.96978}, {4578.67, 5.96947}, {4567.1, 5.96916}, {4559.39, 5.96895}, {4547.81, 5.96864}, {4536.24, 5.96833}, {4528.53, 5.96812}, {4516.96, 5.96781}, {4505.38, 5.9675}, {4497.67, 5.9673}, {4486.1, 5.96699}, {4474.52, 5.96668}, {4466.81, 5.96648}, {4455.24, 5.96617}, {4447.52, 5.96596}, {4435.95, 5.96566}, {4428.24, 5.96545}, {4416.66, 5.96515}, {4408.95, 5.96494}, {4397.38, 5.96464}, {4389.66, 5.96443}, {4378.09, 5.96413}, {4370.38, 5.96393}, {4358.8, 5.96362}, {4351.09, 5.96342}, {4339.52, 5.96312}, {4331.8, 5.96291}, {4320.23, 5.96261}, {4312.52, 5.96241}, {4304.8, 5.96221}, {4293.23, 5.96191}, {4285.51, 5.96171}, {4273.94, 5.96141}, {4266.23, 5.9612}, {4258.51, 5.961}, {4246.94, 5.9607}, {4239.23, 5.9605}, {4231.51, 5.9603}, {4219.94, 5.96}, {4212.23, 5.95981}, {4204.51, 5.95961}, {4192.94, 5.95931}, {4185.22, 5.95911}, {4177.51, 5.95891}, {4169.79, 5.95871}, {4158.22, 5.95841}, {4150.51, 5.95822}, {4142.79, 5.95802}, {4135.08, 5.95782}, {4127.36, 5.95762}, {4115.79, 5.95733}, {4108.08, 5.95713}, {4100.36, 5.95693}, {4092.65, 5.95673}, {4084.93, 5.95654}, {4073.36, 5.95624}, {4065.65, 5.95605}, {4057.93, 5.95585}, {4050.22, 5.95565}, {4042.5, 5.95546}, {4034.79, 5.95526}, {4027.07, 5.95506}, {4019.36, 5.95487}, {4011.64, 5.95467}, {4000.07, 5.95438}, {3992.36, 5.95418}, {3984.64, 5.95399}, {3976.93, 5.95379}, {3969.21, 5.9536}, {3961.5, 5.9534}, {3953.78, 5.95321}, {3946.07, 5.95301}, {3938.35, 5.95282}, {3930.64, 5.95262}, {3922.92, 5.95243}, {3915.21, 5.95224}, {3907.49, 5.95204}, {3899.78, 5.95185}, {3892.07, 5.95165}, {3884.35, 5.95146}, {3876.64, 5.95126}, {3868.92, 5.95107}, {3861.21, 5.95088}, {3857.35, 5.95078}, {3849.63, 5.95059}, {3841.92, 5.95039}, {3834.21, 5.9502}, {3826.49, 5.95001}, {3818.78, 5.94981}, {3811.06, 5.94962}, {3803.35, 5.94943}, {3795.63, 5.94923}, {3787.92, 5.94904}, {3784.06, 5.94894}, {3776.34, 5.94875}, {3768.63, 5.94856}, {3760.92, 5.94836}, {3753.2, 5.94817}, {3745.49, 5.94798}, {3741.63, 5.94788}, {3733.91, 5.94769}, {3726.2, 5.9475}, {3718.48, 5.9473}, {3710.77, 5.94711}, {3706.91, 5.94702}, {3699.2, 5.94682}, {3691.48, 5.94663}, {3683.77, 5.94644}, {3679.91, 5.94634}, {3672.2, 5.94615}, {3664.48, 5.94596}, {3656.77, 5.94577}, {3652.91, 5.94567}, {3645.2, 5.94548}, {3637.48, 5.94528}, {3629.77, 5.94509}, {3625.91, 5.945}, {3618.19, 5.9448}, {3610.48, 5.94461}, {3606.62, 5.94452}, {3598.91, 5.94432}, {3591.19, 5.94413}, {3587.33, 5.94403}, {3579.62, 5.94384}, {3571.91, 5.94365}, {3568.05, 5.94355}, {3560.33, 5.94336}, {3552.62, 5.94317}, {3548.76, 5.94307}, {3541.05, 5.94288}, {3537.19, 5.94279}, {3529.47, 5.94259}, {3521.76, 5.9424}, {3517.9, 5.9423}, {3510.19, 5.94211}, {3506.33, 5.94202}, {3498.62, 5.94182}, {3490.9, 5.94163}, {3487.04, 5.94153}, {3479.33, 5.94134}, {3475.47, 5.94125}, {3467.76, 5.94105}, {3463.9, 5.94096}, {3456.18, 5.94076}, {3448.47, 5.94057}, {3444.61, 5.94047}, {3436.9, 5.94028}, {3433.04, 5.94019}, {3425.33, 5.93999}, {3421.47, 5.9399}, {3413.75, 5.9397}, {3409.9, 5.93961}, {3402.18, 5.93941}, {3398.32, 5.93932}, {3390.61, 5.93912}, {3386.75, 5.93903}, {3379.04, 5.93883}, {3375.18, 5.93874}, {3367.47, 5.93854}, {3363.61, 5.93845}, {3355.89, 5.93825}, {3352.04, 5.93816}, {3348.18, 5.93806}, {3340.46, 5.93786}, {3336.61, 5.93777}, {3328.89, 5.93757}, {3325.04, 5.93748}, {3317.32, 5.93728}, {3313.46, 5.93718}, {3309.61, 5.93709}, {3301.89, 5.93689}, {3298.03, 5.9368}, {3290.32, 5.9366}, {3286.46, 5.9365}, {3278.75, 5.93631}, {3274.89, 5.93621}, {3271.03, 5.93611}, {3263.32, 5.93592}, {3259.46, 5.93582}, {3255.6, 5.93572}, {3247.89, 5.93553}, {3244.03, 5.93543}, {3236.32, 5.93523}, {3232.46, 5.93514}, {3228.6, 5.93504}, {3220.89, 5.93484}, {3217.03, 5.93474}, {3213.17, 5.93465}, {3205.46, 5.93445}, {3201.6, 5.93435}, {3197.74, 5.93425}, {3190.03, 5.93405}, {3186.17, 5.93396}, {3182.31, 5.93386}, {3178.46, 5.93376}, {3170.74, 5.93356}, {3166.88, 5.93346}, {3163.03, 5.93336}, {3155.31, 5.93317}, {3151.45, 5.93307}, {3147.6, 5.93297}, {3139.88, 5.93277}, {3136.02, 5.93267}, {3132.17, 5.93257}, {3128.31, 5.93247}, {3120.6, 5.93227}, {3116.74, 5.93217}, {3112.88, 5.93207}, {3109.02, 5.93197}, {3101.31, 5.93177}, {3097.45, 5.93167}, {3093.59, 5.93157}, {3089.74, 5.93147}, {3082.02, 5.93127}, {3078.16, 5.93117}, {3074.31, 5.93107}, {3070.45, 5.93097}, {3066.59, 5.93087}, {3058.88, 5.93067}, {3055.02, 5.93057}, {3051.16, 5.93047}, {3047.31, 5.93037}, {3039.59, 5.93017}, {3035.73, 5.93007}, {3031.88, 5.92997}, {3028.02, 5.92986}, {3024.16, 5.92976}, {3020.3, 5.92966}, {3012.59, 5.92946}, {3008.73, 5.92936}, {3004.88, 5.92926}, {3001.02, 5.92915},

{2997.16, 5.92905}, {2993.3, 5.92895}, {2985.59, 5.92875}, {2981.73, 5.92864}, {2977.87, 5.92854}, {2974.02, 5.92844}, {2970.16, 5.92834}, {2966.3, 5.92823}, {2958.59, 5.92803}, {2954.73, 5.92793}, {2950.87, 5.92782}, {2947.01, 5.92772}, {2943.16, 5.92762}, {2939.3, 5.92751}, {2935.44, 5.92741}, {2931.59, 5.92731}, {2927.73, 5.9272}, {2920.01, 5.92699}, {2916.16, 5.92689}, {2912.3, 5.92679}, {2908.44, 5.92668}, {2904.58, 5.92658}, {2900.73, 5.92647}, {2896.87, 5.92637}, {2893.01, 5.92626}, {2889.15, 5.92616}, {2885.3, 5.92606}, {2881.44, 5.92595}, {2873.73, 5.92574}, {2869.87, 5.92564}, {2866.01, 5.92553}, {2862.15, 5.92542}, {2858.3, 5.92532}, {2854.44, 5.92521}, {2850.58, 5.92511}, {2846.72, 5.925}, {2842.87, 5.92489}, {2839.01, 5.92479}, {2835.15, 5.92468}, {2831.29, 5.92458}, {2827.44, 5.92447}, {2823.58, 5.92436}, {2819.72, 5.92426}, {2815.87, 5.92415}, {2812.01, 5.92404}, {2808.15, 5.92393}, {2804.29, 5.92383}, {2800.44, 5.92372}, {2796.58, 5.92361}, {2792.72, 5.9235}, {2788.86, 5.9234}, {2785.01, 5.92329}, {2781.15, 5.92318}, {2777.29, 5.92307}, {2773.43, 5.92296}, {2769.58, 5.92285}, {2765.72, 5.92274}, {2761.86, 5.92263}, {2758, 5.92253}, {2754.15, 5.92242}, {2750.29, 5.92231}, {2746.43, 5.9222}, {2742.58, 5.92209}, {2738.72, 5.92198}, {2734.86, 5.92187}, {2731, 5.92176}, {2727.15, 5.92165}, {2723.29, 5.92154}, {2719.43, 5.92142}, {2715.57, 5.92131}, {2711.72, 5.9212}, {2707.86, 5.92109}, {2704, 5.92098}, {2700.14, 5.92087}, {2696.29, 5.92076}, {2692.43, 5.92064}, {2688.57, 5.92053}, {2684.72, 5.92042}, {2680.86, 5.92031}, {2677, 5.92019}, {2673.14, 5.92008}, {2669.29, 5.91997}, {2665.43, 5.91986}, {2661.57, 5.91974}, {2657.71, 5.91963}, {2653.86, 5.91951}, {2650, 5.9194}, {2646.14, 5.91929}, {2642.28, 5.91917}, {2638.43, 5.91906}, {2634.57, 5.91894}, {2630.71, 5.91883}, {2626.85, 5.91871}, {2623, 5.9186}, {2619.14, 5.91848}, {2615.28, 5.91836}, {2611.43, 5.91825}, {2607.57, 5.91813}, {2603.71, 5.91802}, {2599.85, 5.9179}, {2596, 5.91778}, {2592.14, 5.91767}, {2588.28, 5.91755}, {2584.42, 5.91743}, {2580.57, 5.91731}, {2576.71, 5.91719}, {2572.85, 5.91708}, {2568.99, 5.91696}, {2565.14, 5.91684}, {2561.28, 5.91672}, {2557.42, 5.9166}, {2553.57, 5.91648}, {2549.71, 5.91636}, {2545.85, 5.91624}, {2541.99, 5.91612}, {2538.14, 5.916}, {2534.28, 5.91588}, {2530.42, 5.91576}, {2526.56, 5.91564}, {2522.71, 5.91552}, {2518.85, 5.9154}, {2514.99, 5.91527}, {2511.13, 5.91515}, {2507.28, 5.91503}, {2503.42, 5.91491}, {2499.56, 5.91478}, {2495.71, 5.91466}, {2491.85, 5.91454}, {2487.99, 5.91441}, {2484.13, 5.91429}, {2480.28, 5.91416}, {2476.42, 5.91404}, {2472.56, 5.91391}, {2468.7, 5.91379}, {2464.85, 5.91366}, {2460.99, 5.91354}, {2457.13, 5.91341}, {2453.27, 5.91329}, {2449.42, 5.91316}, {2445.56, 5.91303}, {2441.7, 5.91291}, {2437.84, 5.91278}, {2433.99, 5.91265}, {2430.13, 5.91252}, {2426.27, 5.91239}, {2422.42, 5.91226}, {2418.56, 5.91214}, {2414.7, 5.91201}, {2410.84, 5.91188}, {2406.99, 5.91175}, {2403.13, 5.91162}, {2399.27, 5.91149}, {2395.41, 5.91135}, {2391.56, 5.91122}, {2387.7, 5.91109}, {2383.84, 5.91096}, {2379.98, 5.91083}, {2376.13, 5.91069}, {2372.27, 5.91056}, {2368.41, 5.91043}, {2364.56, 5.91029}, {2360.7, 5.91016}, {2356.84, 5.91003}, {2352.98, 5.90989}, {2349.13, 5.90976}, {2345.27, 5.90962}, {2341.41, 5.90948}, {2337.55, 5.90935}, {2333.7, 5.90921}, {2329.84, 5.90907}, {2325.98, 5.90894}, {2322.12, 5.9088}, {2318.27, 5.90866}, {2314.41, 5.90852}, {2310.55, 5.90838}, {2306.7, 5.90824}, {2302.84, 5.9081}, {2298.98, 5.90796}, {2295.12, 5.90782}, {2291.27, 5.90768}, {2287.41, 5.90754}, {2283.55, 5.9074}, {2279.69, 5.90726}, {2275.84, 5.90712}, {2271.98, 5.90697}, {2268.12, 5.90683}, {2264.26, 5.90668}, {2260.41, 5.90654}, {2256.55, 5.9064}, {2252.69, 5.90625}, {2248.83, 5.9061}, {2244.98, 5.90596}, {2241.12, 5.90581}, {2237.26, 5.90566}, {2233.41, 5.90552}, {2229.55, 5.90537}, {2225.69, 5.90522}, {2221.83, 5.90507}, {2217.98, 5.90492}, {2214.12, 5.90477}, {2210.26, 5.90462}, {2206.4, 5.90447}, {2202.55, 5.90432}, {2198.69, 5.90417}, {2194.83, 5.90402}, {2190.97, 5.90386}, {2187.12, 5.90371}, {2183.26, 5.90356}, {2179.4, 5.9034}, {2175.55, 5.90325}, {2171.69, 5.90309}, {2167.83, 5.90293}, {2163.97, 5.90278}, {2160.12, 5.90262}, {2156.26, 5.90246}, {2152.4, 5.90231}, {2148.54, 5.90215}, {2144.69, 5.90199}, {2140.83, 5.90183}, {2136.97, 5.90167}, {2133.11, 5.90151}, {2129.26, 5.90134}, {2125.4, 5.90118}, {2121.54, 5.90102}, {2117.68, 5.90086}, {2113.83, 5.90069}, {2109.97, 5.90053}, {2106.11, 5.90036}, {2102.26, 5.9002}, {2098.4, 5.90003}, {2094.54, 5.89986}, {2090.68, 5.8997}, {2086.83, 5.89953}, {2082.97, 5.89936}, {2079.11, 5.89919}, {2075.25, 5.89902}, {2071.4, 5.89885}, {2067.54, 5.89868}, {2063.68, 5.89851}, {2059.82, 5.89833}, {2055.97, 5.89816}, {2052.11, 5.89798}, {2048.25, 5.89781}, {2044.4, 5.89763}, {2040.54, 5.89746}, {2036.68, 5.89728}, {2032.82, 5.8971}, {2028.97, 5.89693}, {2025.11, 5.89675}, {2021.25, 5.89657}, {2017.39, 5.89639}, {2013.54, 5.8962}, {2009.68, 5.89602}, {2005.82, 5.89584}, {2001.96, 5.89566}, {1998.11, 5.89547}, {1994.25, 5.89529}, {1990.39, 5.8951}, {1986.54, 5.89491}, {1982.68, 5.89473}, {1978.82, 5.89454}, {1974.96, 5.89435}, {1971.11, 5.89416}, {1967.25, 5.89397}, {1963.39, 5.89378}, {1959.53, 5.89358}, {1955.68, 5.89339}, {1951.82, 5.8932}, {1947.96, 5.893}, {1944.1, 5.89281}, {1940.25, 5.89261}, {1936.39, 5.89241}, {1932.53, 5.89221}, {1928.67, 5.89201}, {1924.82, 5.89181}, {1920.96, 5.89161}, {1917.1, 5.89141}, {1913.25, 5.89121}, {1909.39, 5.891}, {1905.53, 5.8908}, {1901.67, 5.89059}, {1897.82, 5.89039}, {1893.96, 5.89018}, {1890.1, 5.88997}, {1886.24, 5.88976}, {1882.39, 5.88955}, {1878.53, 5.88934}, {1874.67, 5.88912}, {1870.81, 5.88891}, {1866.96, 5.8887}, {1863.1, 5.88848}, {1859.24, 5.88826}, {1855.39, 5.88805}, {1851.53, 5.88783}, {1847.67, 5.88761}, {1843.81, 5.88738}, {1839.96, 5.88716}, {1836.1, 5.88694}, {1832.24, 5.88671}, {1828.38, 5.88649}, {1824.53, 5.88626}, {1820.67, 5.88603}, {1816.81, 5.8858}, {1812.95, 5.88557}, {1809.1, 5.88534}, {1805.24, 5.88511}, {1801.38, 5.88488}, {1797.53, 5.88464}, {1793.67, 5.8844}, {1789.81, 5.88417}, {1785.95, 5.88393}, {1782.1, 5.88369}, {1778.24, 5.88345}, {1774.38, 5.8832}, {1770.52, 5.88296}, {1766.67, 5.88271}, {1762.81, 5.88247}, {1758.95, 5.88222}, {1755.09, 5.88197}, {1751.24, 5.88172}, {1747.38, 5.88147}, {1743.52, 5.88121}, {1739.66, 5.88096}, {1735.81, 5.8807}, {1731.95, 5.88044}, {1728.09, 5.88019}, {1724.24, 5.87992}, {1720.38, 5.87966}, {1716.52, 5.8794}, {1712.66, 5.87913}, {1708.81, 5.87887}, {1704.95, 5.8786}, {1701.09, 5.87833}, {1697.23, 5.87806}, {1693.38, 5.87779}, {1689.52, 5.87751}, {1685.66, 5.87724}, {1681.8, 5.87696}, {1677.95, 5.87668}, {1674.09, 5.8764}, {1670.23, 5.87611}, {1666.38, 5.87583}, {1662.52, 5.87554}, {1658.66, 5.87526}, {1654.8, 5.87497}, {1650.95, 5.87468}, {1647.09, 5.87438}, {1643.23, 5.87409}, {1639.37, 5.87379}, {1635.52, 5.87349}, {1631.66, 5.87319}, {1627.8, 5.87289}, {1623.94, 5.87259}, {1620.09, 5.87228}, {1616.23, 5.87197}, {1612.37, 5.87166}, {1608.51, 5.87135}, {1604.66, 5.87104}, {1600.8, 5.87072}, {1596.94, 5.87041}, {1593.09, 5.87009}, {1589.23, 5.86976}, {1585.37, 5.86944}, {1581.51, 5.86912}, {1577.66, 5.86879}, {1573.8, 5.86846}, {1569.94, 5.86812}, {1566.08, 5.86779}, {1562.23, 5.86745}, {1558.37, 5.86711}, {1554.51, 5.86677}, {1550.65, 5.86643}, {1546.8, 5.86608}, {1542.94, 5.86574}, {1539.08, 5.86539}, {1535.23, 5.86503}, {1531.37, 5.86468}, {1527.51, 5.86432}, {1523.65, 5.86396}, {1519.8, 5.8636}, {1515.94, 5.86323}, {1512.08, 5.86286}, {1508.22, 5.86249}, {1504.37, 5.86212}, {1500.51, 5.86175}, {1496.65, 5.86137}, {1492.79, 5.86099}, {1488.94, 5.8606}, {1485.08, 5.86022}, {1481.22, 5.85983}, {1477.37, 5.85944}, {1473.51, 5.85904}, {1469.65, 5.85864}, {1465.79, 5.85824}, {1461.94, 5.85784}, {1458.08, 5.85743}, {1454.22, 5.85702}, {1450.36, 5.85661}, {1446.51, 5.8562}, {1442.65, 5.85578}, {1438.79, 5.85536}, {1434.93, 5.85493}, {1431.08, 5.85451}, {1427.22, 5.85407}, {1423.36, 5.85364}, {1419.5, 5.8532}, {1415.65, 5.85276}, {1411.79, 5.85232}, {1407.93, 5.85187}, {1404.08, 5.85142}, {1400.22, 5.85096}, {1396.36, 5.8505}, {1392.5, 5.85004}, {1388.65, 5.84958}, {1384.79, 5.84911}, {1380.93, 5.84864}, {1377.07, 5.84816}, {1373.22, 5.84768}, {1369.36, 5.84719}, {1365.5, 5.84671}, {1361.64, 5.84621}, {1357.79, 5.84572}, {1353.93, 5.84522}, {1350.07, 5.84471}, {1346.22, 5.84421}, {1342.36, 5.84369}, {1338.5, 5.84318}, {1334.64, 5.84266}, {1330.79, 5.84213}, {1326.93, 5.8416}, {1323.07, 5.84107}, {1319.21, 5.84053}, {1315.36, 5.83999}, {1311.5, 5.83944}, {1307.64, 5.83889}, {1303.78, 5.83833}, {1299.93, 5.83777}, {1296.07, 5.8372}, {1292.21, 5.83663}, {1288.35, 5.83605}, {1284.5, 5.83547}, {1280.64, 5.83489}, {1276.78, 5.83429}, {1272.93, 5.8337}, {1269.07, 5.8331}, {1265.21, 5.83249}, {1261.35, 5.83188}, {1257.5, 5.83126}, {1253.64, 5.83063}, {1249.78, 5.83}, {1245.92, 5.82937}, {1242.07, 5.82873}, {1238.21, 5.82808}, {1234.35, 5.82743}, {1230.49, 5.82677}, {1226.64, 5.82611}, {1222.78, 5.82544}, {1218.92, 5.82476}, {1215.07, 5.82408}, {1211.21, 5.82339}, {1207.35, 5.82269}, {1203.49, 5.82199}, {1199.64, 5.82128}, {1195.78, 5.82056}, {1191.92, 5.81984}, {1188.06, 5.81911}, {1184.21, 5.81837}, {1180.35, 5.81763}, {1176.49, 5.81688}, {1172.63, 5.81612}, {1168.78, 5.81535}, {1164.92, 5.81458}, {1161.06, 5.8138}, {1157.21, 5.81301}, {1153.35, 5.81221}, {1149.49, 5.81141}, {1145.63, 5.8106}, {1141.78, 5.80977}, {1137.92, 5.80895}, {1134.06, 5.80811}, {1130.2, 5.80726}, {1126.35, 5.80641}, {1122.49, 5.80554}, {1118.63, 5.80467}, {1114.77, 5.80379}, {1110.92, 5.8029}, {1107.06, 5.802}, {1103.2, 5.80109}, {1099.34, 5.80017}, {1095.49, 5.79924}, {1091.63, 5.7983}, {1087.77, 5.79736}, {1083.92, 5.7964}, {1080.06, 5.79543}, {1076.2, 5.79445}, {1072.34, 5.79346}, {1068.49, 5.79246}, {1064.63, 5.79145}, {1060.77, 5.79042}, {1056.91, 5.78939}, {1053.06, 5.78835}, {1049.2, 5.78729}, {1045.34, 5.78622}, {1041.48, 5.78514}, {1037.63, 5.78405}, {1033.77, 5.78294}, {1029.91, 5.78182}, {1026.06, 5.78069}, {1022.2, 5.77955}, {1018.34, 5.77839}, {1014.48, 5.77722}, {1010.63, 5.77604}, {1006.77, 5.77484}, {1002.91, 5.77363}, {999.053, 5.7724}, {995.196, 5.77116}, {991.339, 5.76991}, {987.481, 5.76864}, {983.624, 5.76735}, {979.767, 5.76605}, {975.909,

```
5.76473}, {972.052, 5.7634}, {968.195, 5.76205}, {964.337, 5.76069}, {960.48, 5.7593}, {956.622, 5.7579}, {952.765, 5.75649}, {948.908, 5.75505}, {945.05,
5.7536}, {941.193, 5.75213}, {937.336, 5.75064}, {933.478, 5.74913}, {929.621, 5.7476}, {925.764, 5.74606}, {921.906, 5.74449}, {918.049, 5.7429}, {914.192,
5.74129}, {910.334, 5.73966}, {906.477, 5.73801}, {902.62, 5.73634}, {898.762, 5.73464}, {894.905, 5.73293}, {891.048, 5.73118}, {887.19, 5.72942}, {883.333,
5.72763}, {879.476, 5.72582}, {875.618, 5.72398}, {871.761, 5.72212}, {867.903, 5.72023}, {864.046, 5.71831}, {860.189, 5.71637}, {856.331, 5.7144}, {852.474,
5.7124}, {848.617, 5.71038}, {844.759, 5.70832}, {840.902, 5.70624}, {837.045, 5.70413}, {833.187, 5.70198}, {829.33, 5.6998}, {825.473, 5.6976}, {821.615,
5.69535}, {817.758, 5.69308}, {813.901, 5.69077}, {810.043, 5.68843}, {806.186, 5.68605}, {802.329, 5.68364}, {798.471, 5.68119}, {794.614, 5.6787}, {790.756,
5.67617}, {786.899, 5.6736}, {783.042, 5.671}, {779.184, 5.66835}, {775.327, 5.66566}, {771.47, 5.66293}, {767.612, 5.66015}, {763.755, 5.65733}, {759.898,
5.65447}, {756.04, 5.65155}, {752.183, 5.64859}, {748.326, 5.64558}, {744.468, 5.64253}, {740.611, 5.63942}, {736.754, 5.63625}, {732.896, 5.63304}, {729.039,
5.62977}, {725.182, 5.62644}, {721.324, 5.62306}, {717.467, 5.61961}, {713.609, 5.61611}, {709.752, 5.61255}, {705.895, 5.60892}, {702.037, 5.60522},
{698.18, 5.60147}, {694.323, 5.59764}, {690.465, 5.59374}, {686.608, 5.58978}, {682.751, 5.58574}, {678.893, 5.58163}, {675.036, 5.57744}, {671.179, 5.57317},
{667.321, 5.56882}, {663.464, 5.56439}, {659.607, 5.55987}, {655.749, 5.55527}, {651.892, 5.55058}, {648.035, 5.54579}, {644.177, 5.54092}, {640.32,
5.53595}, {636.463, 5.53088}, {632.605, 5.52572}, {628.748, 5.52045}, {624.891, 5.51508}, {621.033, 5.5096}, {617.176, 5.50401}, {613.318, 5.4983}, {609.461,
5.49247}, {605.604, 5.48651}, {601.746, 5.48042}, {597.889, 5.47419}, {594.032, 5.46782}, {590.174, 5.46131}, {586.317, 5.45466}, {582.46, 5.44785}, {578.602,
5.4409}, {574.745, 5.43379}, {570.888, 5.42653}, {567.03, 5.4191}, {563.173, 5.4115}, {559.316, 5.40372}, {555.458, 5.39575}, {551.601, 5.38758}, {547.744,
5.37919}, {543.886, 5.37058}, {540.029, 5.36175}, {536.171, 5.35268}, {532.314, 5.34337}, {528.457, 5.33383}, {524.599, 5.32403}, {520.742, 5.314}, {516.885,
5.30371}, {513.027, 5.29317}, {509.17, 5.28237}, {505.313, 5.27129}, {501.455, 5.25993}, {497.598, 5.24826}, {493.741, 5.23626}, {489.883, 5.22393}, {486.026,
5.21123}, {482.169, 5.19816}, {478.311, 5.18469}, {474.454, 5.17084}, {470.597, 5.1566}, {466.739, 5.14197}, {462.882, 5.12696}, {459.025, 5.11159},
{455.167, 5.09586}, {451.31, 5.07979}, {447.452, 5.06338}, {443.595, 5.04663}, {439.738, 5.02954}, {435.88, 5.01208}, {432.023, 4.99423}, {428.166, 4.97595},
{424.308, 4.95718}, {420.451, 4.93786}, {416.594, 4.91793}, {412.736, 4.8973}, {408.879, 4.8759}, {405.022, 4.85364}, {401.164, 4.83043}, {397.307, 4.80619},
{393.45, 4.78084}, {389.592, 4.75429}, {385.735, 4.7265}, {381.878, 4.69737}, {378.02, 4.66685}, {374.163, 4.63489}, {370.305, 4.60141}, {366.448, 4.56638},
{362.591, 4.52972}, {358.733, 4.49136}, {354.876, 4.45125}, {351.019, 4.40929}, {347.161, 4.36537}, {343.304, 4.31942}, {339.447, 4.27131}, {335.589,
4.22088}, {331.732, 4.168}, {327.875, 4.11251}, {324.017, 4.05418}, {320.16, 3.99285}, {316.303, 3.92825}, {312.445, 3.86012}, {308.588, 3.78821}, {304.731,
3.71217}, {300.873, 3.63164}, {297.016, 3.54626}, {293.159, 3.45557}, {289.301, 3.35905}, {285.444, 3.2562}, {281.586, 3.14633}, {277.729, 3.02881}, {273.872,
2.90278}, {270.014, 2.76731}, {266.157, 2.6214}, {262.3, 2.4638}, {258.442, 2.29307}, {254.585, 2.10763}, {250.728, 1.90553}, {246.87, 1.68443}, {243.013,
1.44174}, {239.156, 1.17416}, {235.298, 0.877691}, {231.441, 0.547708}, {227.584, 0.178241}, {223.726, −0.238179}, {219.869, −0.710629}, {216.012, −1.25112},
{212.154, −1.87537}, {208.297, −2.60366}, {204.439, −3.46442}, {200.582, −4.4962}, {196.725, −5.75521}, {192.867, −7.32527}, {189.01, −9.33536}, {185.153,
−11.9995}, {181.295, −15.6974}, {177.438, −21.1674}, {173.581, −30.0797}, {169.723, −47.1642}, {165.866, −93.0693}, {162.009, −631.883}, {158.151, 153.699},
{154.294, 73.0439}, {150.437, 49.7271}, {146.579, 38.6453}, {142.722, 32.1776}, {138.865, 27.9418}, {135.007, 24.9547}, {131.15, 22.7384}, {127.293, 21.0302},
{123.435, 19.6746}, {119.578, 18.5746}, {115.72, 17.665}, {111.863, 16.9017}, {108.006, 16.253}, {104.148, 15.6957}, {100.291, 15.2129}};
znse=Interpolation[znseraw];


geraw={{7876.71, 19.3251}, {7845.85, 19.2806}, {7814.99, 19.2367}, {7784.13, 19.1936}, {7753.27, 19.1511}, {7722.41, 19.1092}, {7695.41, 19.073}, {7664.55, 19.0322},
{7633.69, 18.992}, {7606.69, 18.9572}, {7575.83, 18.918}, {7548.83, 18.8841}, {7521.83, 18.8505}, {7490.97, 18.8126}, {7463.97, 18.7798}, {7436.97, 18.7474},
{7409.97, 18.7153}, {7382.97, 18.6835}, {7355.96, 18.652}, {7328.96, 18.6209}, {7301.96, 18.5901}, {7274.96, 18.5596}, {7247.96, 18.5294}, {7220.96,
18.4994}, {7197.81, 18.474}, {7170.81, 18.4447}, {7143.81, 18.4156}, {7120.67, 18.3909}, {7093.66, 18.3623}, {7070.52, 18.338}, {7043.52, 18.31}, {7020.38,
18.2862}, {6993.37, 18.2586}, {6970.23, 18.2352}, {6947.09, 18.2121}, {6923.94, 18.1891}, {6896.94, 18.1625}, {6873.8, 18.1399}, {6850.65, 18.1176}, {6827.51,
18.0954}, {6804.36, 18.0734}, {6781.22, 18.0516}, {6758.08, 18.03}, {6734.93, 18.0086}, {6711.79, 17.9874}, {6692.5, 17.9699}, {6669.36, 17.949}, {6646.21,
17.9284}, {6623.07, 17.9079}, {6603.78, 17.891}, {6580.64, 17.8708}, {6557.49, 17.8509}, {6538.21, 17.8344}, {6515.06, 17.8148}, {6495.78, 17.7986}, {6472.63,
17.7794}, {6453.34, 17.7635}, {6434.06, 17.7477}, {6410.91, 17.7289}, {6391.63, 17.7134}, {6372.34, 17.6981}, {6353.05, 17.6828}, {6329.91, 17.6647},
{6310.62, 17.6497}, {6291.34, 17.6349}, {6272.05, 17.6202}, {6252.76, 17.6056}, {6233.48, 17.5911}, {6214.19, 17.5768}, {6194.9, 17.5626}, {6175.62, 17.5485},
{6156.33, 17.5345}, {6137.04, 17.5206}, {6117.76, 17.5069}, {6098.47, 17.4932}, {6079.18, 17.4797}, {6063.75, 17.469}, {6044.47, 17.4557}, {6025.18,
17.4425}, {6009.75, 17.432}, {5990.46, 17.4191}, {5971.18, 17.4062}, {5955.75, 17.396}, {5936.46, 17.3833}, {5917.17, 17.3708}, {5901.74, 17.3608}, {5882.46,
17.3484}, {5867.03, 17.3386}, {5851.6, 17.3289}, {5832.31, 17.3168}, {5816.88, 17.3072}, {5797.6, 17.2953}, {5782.17, 17.2859}, {5766.74, 17.2765}, {5747.45,
17.2649}, {5732.02, 17.2557}, {5716.59, 17.2465}, {5701.16, 17.2374}, {5681.88, 17.2262}, {5666.45, 17.2172}, {5651.02, 17.2083}, {5635.59, 17.1995},
{5620.16, 17.1907}, {5604.73, 17.182}, {5589.3, 17.1734}, {5573.87, 17.1648}, {5558.44, 17.1563}, {5543.01, 17.1478}, {5527.58, 17.1394}, {5512.15, 17.1311},
{5496.72, 17.1228}, {5481.29, 17.1146}, {5465.86, 17.1064}, {5450.43, 17.0983}, {5435, 17.0903}, {5423.43, 17.0842}, {5408, 17.0763}, {5392.57, 17.0684},
{5377.14, 17.0605}, {5365.57, 17.0547}, {5350.14, 17.0469}, {5334.71, 17.0392}, {5319.28, 17.0316}, {5307.71, 17.0259}, {5292.28, 17.0183}, {5280.71,
17.0127}, {5265.28, 17.0052}, {5249.85, 16.9978}, {5238.28, 16.9923}, {5222.85, 16.9849}, {5211.28, 16.9795}, {5195.85, 16.9722}, {5184.28, 16.9668},
{5168.85, 16.9597}, {5157.28, 16.9544}, {5141.85, 16.9473}, {5130.27, 16.942}, {5118.7, 16.9368}, {5103.27, 16.9298}, {5091.7, 16.9246}, {5076.27, 16.9178},
{5064.7, 16.9126}, {5053.13, 16.9075}, {5041.56, 16.9025}, {5026.13, 16.8957}, {5014.55, 16.8907}, {5002.98, 16.8857}, {4987.55, 16.8791}, {4975.98, 16.8742},
{4964.41, 16.8693}, {4952.84, 16.8644}, {4941.26, 16.8596}, {4929.69, 16.8547}, {4914.26, 16.8483}, {4902.69, 16.8435}, {4891.12, 16.8388}, {4879.55,
16.8341}, {4867.97, 16.8294}, {4856.4, 16.8247}, {4844.83, 16.82}, {4833.26, 16.8154}, {4821.69, 16.8108}, {4810.11, 16.8062}, {4798.54, 16.8016}, {4786.97,
16.797}, {4775.4, 16.7925}, {4763.83, 16.788}, {4752.25, 16.7835}, {4740.68, 16.7791}, {4729.11, 16.7746}, {4717.54, 16.7702}, {4705.97, 16.7658}, {4698.25,
16.7629}, {4686.68, 16.7585}, {4675.11, 16.7542}, {4663.54, 16.7499}, {4651.96, 16.7456}, {4640.39, 16.7413}, {4632.68, 16.7385}, {4621.1, 16.7342}, {4609.53,
16.73}, {4597.96, 16.7258}, {4590.25, 16.723}, {4578.67, 16.7189}, {4567.1, 16.7147}, {4559.39, 16.7119}, {4547.81, 16.7078}, {4536.24, 16.7037}, {4528.53,
16.701}, {4516.96, 16.697}, {4505.38, 16.6929}, {4497.67, 16.6902}, {4486.1, 16.6862}, {4474.52, 16.6822}, {4466.81, 16.6796}, {4455.24, 16.6756}, {4447.52,
16.673}, {4435.95, 16.669}, {4428.24, 16.6664}, {4416.66, 16.6625}, {4408.95, 16.6599}, {4397.38, 16.6561}, {4389.66, 16.6535}, {4378.09, 16.6497}, {4370.38,
16.6471}, {4358.8, 16.6433}, {4351.09, 16.6408}, {4339.52, 16.637}, {4331.8, 16.6345}, {4320.23, 16.6307}, {4312.52, 16.6283}, {4304.8, 16.6258}, {4293.23,
16.6221}, {4285.51, 16.6196}, {4273.94, 16.6159}, {4266.23, 16.6135}, {4258.51, 16.611}, {4246.94, 16.6074}, {4239.23, 16.605}, {4231.51, 16.6026}, {4219.94,
16.599}, {4212.23, 16.5966}, {4204.51, 16.5942}, {4192.94, 16.5906}, {4185.22, 16.5883}, {4177.51, 16.5859}, {4169.79, 16.5836}, {4158.22, 16.5801}, {4150.51,
16.5777}, {4142.79, 16.5754}, {4135.08, 16.5731}, {4127.36, 16.5708}, {4115.79, 16.5673}, {4108.08, 16.565}, {4100.36, 16.5627}, {4092.65, 16.5605},
{4084.93, 16.5582}, {4073.36, 16.5548}, {4065.65, 16.5525}, {4057.93, 16.5503}, {4050.22, 16.548}, {4042.5, 16.5458}, {4034.79, 16.5436}, {4027.07, 16.5414},
{4019.36, 16.5392}, {4011.64, 16.537}, {4000.07, 16.5337}, {3992.36, 16.5315}, {3984.64, 16.5293}, {3976.93, 16.5271}, {3969.21, 16.5249}, {3961.5, 16.5228},
{3953.78, 16.5206}, {3946.07, 16.5185}, {3938.35, 16.5163}, {3930.64, 16.5142}, {3922.92, 16.5121}, {3915.21, 16.5099}, {3907.49, 16.5078}, {3899.78,
16.5057}, {3892.07, 16.5036}, {3884.35, 16.5015}, {3876.64, 16.4994}, {3868.92, 16.4973}, {3861.21, 16.4953}, {3857.35, 16.4942}, {3849.63, 16.4922},
```

{3841.92, 16.4901}, {3834.21, 16.488}, {3826.49, 16.486}, {3818.78, 16.4839}, {3811.06, 16.4819}, {3803.35, 16.4799}, {3795.63, 16.4779}, {3787.92, 16.4758}, {3784.06, 16.4748}, {3776.34, 16.4728}, {3768.63, 16.4708}, {3760.92, 16.4688}, {3753.2, 16.4668}, {3745.49, 16.4648}, {3741.63, 16.4639}, {3733.91, 16.4619}, {3726.2, 16.4599}, {3718.48, 16.4579}, {3710.77, 16.456}, {3706.91, 16.455}, {3699.2, 16.4531}, {3691.48, 16.4511}, {3683.77, 16.4492}, {3679.91, 16.4482}, {3672.2, 16.4463}, {3664.48, 16.4444}, {3656.77, 16.4425}, {3652.91, 16.4415}, {3645.2, 16.4396}, {3637.48, 16.4377}, {3629.77, 16.4358}, {3625.91, 16.4348}, {3618.19, 16.433}, {3610.48, 16.4311}, {3606.62, 16.4301}, {3598.91, 16.4283}, {3591.19, 16.4264}, {3587.33, 16.4255}, {3579.62, 16.4236}, {3571.91, 16.4218}, {3568.05, 16.4208}, {3560.33, 16.419}, {3552.62, 16.4171}, {3548.76, 16.4162}, {3541.05, 16.4144}, {3537.19, 16.4135}, {3529.47, 16.4117}, {3521.76, 16.4098}, {3517.9, 16.4089}, {3510.19, 16.4071}, {3506.33, 16.4062}, {3498.62, 16.4044}, {3490.9, 16.4026}, {3487.04, 16.4017}, {3479.33, 16.4}, {3475.47, 16.3991}, {3467.76, 16.3973}, {3463.9, 16.3964}, {3456.18, 16.3946}, {3448.47, 16.3929}, {3444.61, 16.392}, {3436.9, 16.3902}, {3433.04, 16.3893}, {3425.33, 16.3876}, {3421.47, 16.3867}, {3413.75, 16.385}, {3409.9, 16.3841}, {3402.18, 16.3824}, {3398.32, 16.3815}, {3390.61, 16.3798}, {3386.75, 16.3789}, {3379.04, 16.3772}, {3375.18, 16.3764}, {3367.47, 16.3746}, {3363.61, 16.3738}, {3355.89, 16.3721}, {3352.04, 16.3712}, {3348.18, 16.3704}, {3340.46, 16.3687}, {3336.61, 16.3679}, {3328.89, 16.3662}, {3325.04, 16.3653}, {3317.32, 16.3637}, {3313.46, 16.3628}, {3309.61, 16.362}, {3301.89, 16.3603}, {3298.03, 16.3595}, {3290.32, 16.3578}, {3286.46, 16.357}, {3278.75, 16.3554}, {3274.89, 16.3545}, {3271.03, 16.3537}, {3263.32, 16.3521}, {3259.46, 16.3512}, {3255.6, 16.3504}, {3247.89, 16.3488}, {3244.03, 16.348}, {3236.32, 16.3464}, {3232.46, 16.3455}, {3228.6, 16.3447}, {3220.89, 16.3431}, {3217.03, 16.3423}, {3213.17, 16.3415}, {3205.46, 16.3399}, {3201.6, 16.3391}, {3197.74, 16.3383}, {3190.03, 16.3367}, {3186.17, 16.3359}, {3182.31, 16.3351}, {3178.46, 16.3343}, {3170.74, 16.3327}, {3166.88, 16.332}, {3163.03, 16.3312}, {3155.31, 16.3296}, {3151.45, 16.3288}, {3147.6, 16.328}, {3139.88, 16.3265}, {3136.02, 16.3257}, {3132.17, 16.3249}, {3128.31, 16.3241}, {3120.6, 16.3226}, {3116.74, 16.3218}, {3112.88, 16.321}, {3109.02, 16.3203}, {3101.31, 16.3187}, {3097.45, 16.3179}, {3093.59, 16.3172}, {3089.74, 16.3164}, {3082.02, 16.3149}, {3078.16, 16.3141}, {3074.31, 16.3134}, {3070.45, 16.3126}, {3066.59, 16.3118}, {3058.88, 16.3103}, {3055.02, 16.3096}, {3051.16, 16.3088}, {3047.31, 16.3081}, {3039.59, 16.3065}, {3035.73, 16.3058}, {3031.88, 16.305}, {3028.02, 16.3043}, {3024.16, 16.3036}, {3020.3, 16.3028}, {3012.59, 16.3013}, {3008.73, 16.3006}, {3004.88, 16.2998}, {3001.02, 16.2991}, {2997.16, 16.2984}, {2993.3, 16.2976}, {2985.59, 16.2961}, {2981.73, 16.2954}, {2977.87, 16.2947}, {2974.02, 16.2939}, {2970.16, 16.2932}, {2966.3, 16.2925}, {2958.59, 16.291}, {2954.73, 16.2903}, {2950.87, 16.2896}, {2947.01, 16.2888}, {2943.16, 16.2881}, {2939.3, 16.2874}, {2935.44, 16.2867}, {2931.59, 16.2859}, {2927.73, 16.2852}, {2920.01, 16.2838}, {2916.16, 16.2831}, {2912.3, 16.2824}, {2908.44, 16.2816}, {2904.58, 16.2809}, {2900.73, 16.2802}, {2896.87, 16.2795}, {2893.01, 16.2788}, {2889.15, 16.2781}, {2885.3, 16.2774}, {2881.44, 16.2767}, {2873.73, 16.2753}, {2869.87, 16.2746}, {2866.01, 16.2738}, {2862.15, 16.2731}, {2858.3, 16.2724}, {2854.44, 16.2717}, {2850.58, 16.271}, {2846.72, 16.2703}, {2842.87, 16.2697}, {2839.01, 16.269}, {2835.15, 16.2683}, {2831.29, 16.2676}, {2827.44, 16.2669}, {2823.58, 16.2662}, {2819.72, 16.2655}, {2815.87, 16.2648}, {2812.01, 16.2641}, {2808.15, 16.2634}, {2804.29, 16.2627}, {2800.44, 16.262}, {2796.58, 16.2614}, {2792.72, 16.2607}, {2788.86, 16.26}, {2785.01, 16.2593}, {2781.15, 16.2586}, {2777.29, 16.258}, {2773.43, 16.2573}, {2769.58, 16.2566}, {2765.72, 16.2559}, {2761.86, 16.2552}, {2758, 16.2546}, {2754.15, 16.2539}, {2750.29, 16.2532}, {2746.43, 16.2525}, {2742.58, 16.2519}, {2738.72, 16.2512}, {2734.86, 16.2505}, {2731, 16.2499}, {2727.15, 16.2492}, {2723.29, 16.2485}, {2719.43, 16.2479}, {2715.57, 16.2472}, {2711.72, 16.2465}, {2707.86, 16.2459}, {2704, 16.2452}, {2700.14, 16.2446}, {2696.29, 16.2439}, {2692.43, 16.2432}, {2688.57, 16.2426}, {2684.72, 16.2419}, {2680.86, 16.2413}, {2677, 16.2406}, {2673.14, 16.24}, {2669.29, 16.2393}, {2665.43, 16.2387}, {2661.57, 16.238}, {2657.71, 16.2373}, {2653.86, 16.2367}, {2650, 16.2361}, {2646.14, 16.2354}, {2642.28, 16.2348}, {2638.43, 16.2341}, {2634.57, 16.2335}, {2630.71, 16.2328}, {2626.85, 16.2322}, {2623, 16.2315}, {2619.14, 16.2309}, {2615.28, 16.2303}, {2611.43, 16.2296}, {2607.57, 16.229}, {2603.71, 16.2283}, {2599.85, 16.2277}, {2596, 16.2271}, {2592.14, 16.2264}, {2588.28, 16.2258}, {2584.42, 16.2252}, {2580.57, 16.2245}, {2576.71, 16.2239}, {2572.85, 16.2233}, {2568.99, 16.2226}, {2565.14, 16.222}, {2561.28, 16.2214}, {2557.42, 16.2207}, {2553.57, 16.2201}, {2549.71, 16.2195}, {2545.85, 16.2189}, {2541.99, 16.2182}, {2538.14, 16.2176}, {2534.28, 16.217}, {2530.42, 16.2164}, {2526.56, 16.2158}, {2522.71, 16.2151}, {2518.85, 16.2145}, {2514.99, 16.2139}, {2511.13, 16.2133}, {2507.28, 16.2127}, {2503.42, 16.2121}, {2499.56, 16.2114}, {2495.71, 16.2108}, {2491.85, 16.2102}, {2487.99, 16.2096}, {2484.13, 16.209}, {2480.28, 16.2084}, {2476.42, 16.2078}, {2472.56, 16.2072}, {2468.7, 16.2065}, {2464.85, 16.2059}, {2460.99, 16.2053}, {2457.13, 16.2047}, {2453.27, 16.2041}, {2449.42, 16.2035}, {2445.56, 16.2029}, {2441.7, 16.2023}, {2437.84, 16.2017}, {2433.99, 16.2011}, {2430.13, 16.2005}, {2426.27, 16.1999}, {2422.42, 16.1993}, {2418.56, 16.1987}, {2414.7, 16.1981}, {2410.84, 16.1975}, {2406.99, 16.1969}, {2403.13, 16.1963}, {2399.27, 16.1957}, {2395.41, 16.1951}, {2391.56, 16.1945}, {2387.7, 16.194}, {2383.84, 16.1934}, {2379.98, 16.1928}, {2376.13, 16.1922}, {2372.27, 16.1916}, {2368.41, 16.191}, {2364.56, 16.1904}, {2360.7, 16.1898}, {2356.84, 16.1892}, {2352.98, 16.1887}, {2349.13, 16.1881}, {2345.27, 16.1875}, {2341.41, 16.1869}, {2337.55, 16.1863}, {2333.7, 16.1857}, {2329.84, 16.1852}, {2325.98, 16.1846}, {2322.12, 16.184}, {2318.27, 16.1834}, {2314.41, 16.1828}, {2310.55, 16.1823}, {2306.7, 16.1817}, {2302.84, 16.1811}, {2298.98, 16.1805}, {2295.12, 16.18}, {2291.27, 16.1794}, {2287.41, 16.1788}, {2283.55, 16.1782}, {2279.69, 16.1777}, {2275.84, 16.1771}, {2271.98, 16.1765}, {2268.12, 16.176}, {2264.26, 16.1754}, {2260.41, 16.1748}, {2256.55, 16.1742}, {2252.69, 16.1737}, {2248.83, 16.1731}, {2244.98, 16.1725}, {2241.12, 16.172}, {2237.26, 16.1714}, {2233.41, 16.1709}, {2229.55, 16.1703}, {2225.69, 16.1697}, {2221.83, 16.1692}, {2217.98, 16.1686}, {2214.12, 16.168}, {2210.26, 16.1675}, {2206.4, 16.1669}, {2202.55, 16.1664}, {2198.69, 16.1658}, {2194.83, 16.1652}, {2190.97, 16.1647}, {2187.12, 16.1641}, {2183.26, 16.1636}, {2179.4, 16.163}, {2175.55, 16.1625}, {2171.69, 16.1619}, {2167.83, 16.1613}, {2163.97, 16.1608}, {2160.12, 16.1602}, {2156.26, 16.1597}, {2152.4, 16.1591}, {2148.54, 16.1586}, {2144.69, 16.158}, {2140.83, 16.1575}, {2136.97, 16.1569}, {2133.11, 16.1564}, {2129.26, 16.1558}, {2125.4, 16.1553}, {2121.54, 16.1547}, {2117.68, 16.1542}, {2113.83, 16.1536}, {2109.97, 16.1531}, {2106.11, 16.1525}, {2102.26, 16.152}, {2098.4, 16.1515}, {2094.54, 16.1509}, {2090.68, 16.1504}, {2086.83, 16.1498}, {2082.97, 16.1493}, {2079.11, 16.1487}, {2075.25, 16.1482}, {2071.4, 16.1476}, {2067.54, 16.1471}, {2063.68, 16.1466}, {2059.82, 16.146}, {2055.97, 16.1455}, {2052.11, 16.1449}, {2048.25, 16.1444}, {2044.4, 16.1439}, {2040.54, 16.1433}, {2036.68, 16.1428}, {2032.82, 16.1423}, {2028.97, 16.1417}, {2025.11, 16.1412}, {2021.25, 16.1406}, {2017.39, 16.1401}, {2013.54, 16.1396}, {2009.68, 16.139}, {2005.82, 16.1385}, {2001.96, 16.138}, {1998.11, 16.1374}, {1994.25, 16.1369}, {1990.39, 16.1364}, {1986.54, 16.1358}, {1982.68, 16.1353}, {1978.82, 16.1348}, {1974.96, 16.1342}, {1971.11, 16.1337}, {1967.25, 16.1332}, {1963.39, 16.1326}, {1959.53, 16.1321}, {1955.68, 16.1316}, {1951.82, 16.1311}, {1947.96, 16.1305}, {1944.1, 16.13}, {1940.25, 16.1295}, {1936.39, 16.1289}, {1932.53, 16.1284}, {1928.67, 16.1279}, {1924.82, 16.1273}, {1920.96, 16.1268}, {1917.1, 16.1263}, {1913.25, 16.1258}, {1909.39, 16.1252}, {1905.53, 16.1247}, {1901.67, 16.1242}, {1897.82, 16.1237}, {1893.96, 16.1231}, {1890.1, 16.1226}, {1886.24, 16.1221}, {1882.39, 16.1216}, {1878.53, 16.121}, {1874.67, 16.1205}, {1870.81, 16.12}, {1866.96, 16.1195}, {1863.1, 16.1189}, {1859.24, 16.1184}, {1855.39, 16.1179}, {1851.53, 16.1174}, {1847.67, 16.1168}, {1843.81, 16.1163}, {1839.96, 16.1158}, {1836.1, 16.1153}, {1832.24, 16.1147}, {1828.38, 16.1142}, {1824.53, 16.1137}, {1820.67, 16.1132}, {1816.81, 16.1126}, {1812.95, 16.1121}, {1809.1, 16.1116}, {1805.24, 16.1111}, {1801.38, 16.1105}, {1797.53, 16.11}, {1793.67, 16.1095}, {1789.81, 16.109}, {1785.95, 16.1084}, {1782.1, 16.1079}, {1778.24, 16.1074}, {1774.38, 16.1069}, {1770.52, 16.1064}, {1766.67, 16.1058}, {1762.81, 16.1053}, {1758.95, 16.1048}, {1755.09, 16.1043}, {1751.24, 16.1037}, {1747.38, 16.1032}, {1743.52, 16.1027}, {1739.66, 16.1022}, {1735.81, 16.1016}, {1731.95, 16.1011}, {1728.09, 16.1006}, {1724.24, 16.1001}, {1720.38, 16.0995}, {1716.52, 16.099}, {1712.66, 16.0985}, {1708.81, 16.098}, {1704.95, 16.0974}, {1701.09, 16.0969}, {1697.23, 16.0964}, {1693.38, 16.0959}, {1689.52, 16.0953}, {1685.66, 16.0948}, {1681.8, 16.0943}, {1677.95, 16.0938}, {1674.09, 16.0932}, {1670.23, 16.0927}, {1666.38, 16.0922}, {1662.52, 16.0916}, {1658.66, 16.0911}, {1654.8, 16.0906}, {1650.95, 16.0901}, {1647.09, 16.0895}, {1643.23, 16.089}, {1639.37, 16.0885}, {1635.52, 16.0879}, {1631.66, 16.0874}, {1627.8, 16.0869}, {1623.94, 16.0863}, {1620.09, 16.0858}, {1616.23, 16.0853}, {1612.37, 16.0847}, {1608.51, 16.0842}, {1604.66, 16.0837}, {1600.8, 16.0831}, {1596.94, 16.0826}, {1593.09, 16.0821}, {1589.23, 16.0815}, {1585.37, 16.081}, {1581.51, 16.0804}, {1577.66, 16.0799}, {1573.8, 16.0794}, {1569.94, 16.0788}, {1566.08, 16.0783}, {1562.23, 16.0777}, {1558.37, 16.0772}, {1554.51, 16.0767}, {1550.65, 16.0761}, {1546.8, 16.0756}, {1542.94, 16.075}, {1539.08,

```
16.0745}, {1535.23, 16.0739}, {1531.37, 16.0734}, {1527.51, 16.0728}, {1523.65, 16.0723}, {1519.8, 16.0717}, {1515.94, 16.0712}, {1512.08, 16.0706},
{1508.22, 16.0701}, {1504.37, 16.0695}, {1500.51, 16.069}, {1496.65, 16.0684}, {1492.79, 16.0679}, {1488.94, 16.0673}, {1485.08, 16.0667}, {1481.22, 16.0662},
{1477.37, 16.0656}, {1473.51, 16.065}, {1469.65, 16.0645}, {1465.79, 16.0639}, {1461.94, 16.0634}, {1458.08, 16.0628}, {1454.22, 16.0622}, {1450.36,
16.0617}, {1446.51, 16.0611}, {1442.65, 16.0605}, {1438.79, 16.0599}, {1434.93, 16.0594}, {1431.08, 16.0588}, {1427.22, 16.0582}, {1423.36, 16.0576}, {1419.5,
16.057}, {1415.65, 16.0565}, {1411.79, 16.0559}, {1407.93, 16.0553}, {1404.08, 16.0547}, {1400.22, 16.0541}, {1396.36, 16.0535}, {1392.5, 16.0529}, {1388.65,
16.0524}, {1384.79, 16.0518}, {1380.93, 16.0512}, {1377.07, 16.0506}, {1373.22, 16.05}, {1369.36, 16.0494}, {1365.5, 16.0488}, {1361.64, 16.0482}, {1357.79,
16.0475}, {1353.93, 16.0469}, {1350.07, 16.0463}, {1346.22, 16.0457}, {1342.36, 16.0451}, {1338.5, 16.0445}, {1334.64, 16.0439}, {1330.79, 16.0432}, {1326.93,
16.0426}, {1323.07, 16.042}, {1319.21, 16.0414}, {1315.36, 16.0407}, {1311.5, 16.0401}, {1307.64, 16.0395}, {1303.78, 16.0388}, {1299.93, 16.0382}, {1296.07,
16.0376}, {1292.21, 16.0369}, {1288.35, 16.0363}, {1284.5, 16.0356}, {1280.64, 16.035}, {1276.78, 16.0343}, {1272.93, 16.0337}, {1269.07, 16.033}, {1265.21,
16.0323}, {1261.35, 16.0317}, {1257.5, 16.031}, {1253.64, 16.0303}, {1249.78, 16.0297}, {1245.92, 16.029}, {1242.07, 16.0283}, {1238.21, 16.0276}, {1234.35,
16.0269}, {1230.49, 16.0262}, {1226.64, 16.0255}, {1222.78, 16.0248}, {1218.92, 16.0241}, {1215.07, 16.0234}, {1211.21, 16.0227}, {1207.35, 16.022}, {1203.49,
16.0213}, {1199.64, 16.0206}, {1195.78, 16.0199}, {1191.92, 16.0191}, {1188.06, 16.0184}, {1184.21, 16.0177}, {1180.35, 16.017}, {1176.49, 16.0162},
{1172.63, 16.0155}, {1168.78, 16.0147}, {1164.92, 16.014}, {1161.06, 16.0132}, {1157.21, 16.0124}, {1153.35, 16.0117}, {1149.49, 16.0109}, {1145.63, 16.0101},
{1141.78, 16.0094}, {1137.92, 16.0086}, {1134.06, 16.0078}, {1130.2, 16.007}, {1126.35, 16.0062}, {1122.49, 16.0054}, {1118.63, 16.0046}, {1114.77, 16.0038},
{1110.92, 16.0029}, {1107.06, 16.0021}, {1103.2, 16.0013}, {1099.34, 16.0004}, {1095.49, 15.9996}, {1091.63, 15.9988}, {1087.77, 15.9979}, {1083.92, 15.997},
{1080.06, 15.9962}, {1076.2, 15.9953}, {1072.34, 15.9944}, {1068.49, 15.9936}, {1064.63, 15.9927}, {1060.77, 15.9918}, {1056.91, 15.9909}, {1053.06, 15.99},
{1049.2, 15.989}, {1045.34, 15.9881}, {1041.48, 15.9872}, {1037.63, 15.9862}, {1033.77, 15.9853}, {1029.91, 15.9843}, {1026.06, 15.9834}, {1022.2, 15.9824},
{1018.34, 15.9814}, {1014.48, 15.9805}, {1010.63, 15.9795}, {1006.77, 15.9785}, {1002.91, 15.9775}, {999.053, 15.9764}, {995.196, 15.9754}, {991.339,
15.9744}, {987.481, 15.9733}, {983.624, 15.9723}, {979.767, 15.9712}, {975.909, 15.9702}, {972.052, 15.9691}, {968.195, 15.968}, {964.337, 15.9669}, {960.48,
15.9658}, {956.622, 15.9647}, {952.765, 15.9635}, {948.908, 15.9624}, {945.05, 15.9612}, {941.193, 15.9601}, {937.336, 15.9589}, {933.478, 15.9577}, {929.621,
15.9565}, {925.764, 15.9553}, {921.906, 15.9541}, {918.049, 15.9529}, {914.192, 15.9516}, {910.334, 15.9504}, {906.477, 15.9491}, {902.62, 15.9478},
{898.762, 15.9465}, {894.905, 15.9452}, {891.048, 15.9439}, {887.19, 15.9425}, {883.333, 15.9412}, {879.476, 15.9398}, {875.618, 15.9384}, {871.761, 15.937},
{867.903, 15.9356}, {864.046, 15.9342}, {860.189, 15.9327}, {856.331, 15.9313}, {852.474, 15.9298}, {848.617, 15.9283}, {844.759, 15.9268}, {840.902,
15.9253}, {837.045, 15.9237}, {833.187, 15.9222}, {829.33, 15.9206}, {825.473, 15.919}, {821.615, 15.9173}, {817.758, 15.9157}, {813.901, 15.914}, {810.043,
15.9123}, {806.186, 15.9106}, {802.329, 15.9089}, {798.471, 15.9072}, {794.614, 15.9054}, {790.756, 15.9036}, {786.899, 15.9018}, {783.042, 15.8999},
{779.184, 15.8981}, {775.327, 15.8962}, {771.47, 15.8943}, {767.612, 15.8923}, {763.755, 15.8904}, {759.898, 15.8884}, {756.04, 15.8863}, {752.183, 15.8843},
{748.326, 15.8822}, {744.468, 15.8801}, {740.611, 15.878}, {736.754, 15.8758}, {732.896, 15.8736}, {729.039, 15.8714}, {725.182, 15.8691}, {721.324, 15.8668},
{717.467, 15.8645}, {713.609, 15.8621}, {709.752, 15.8597}, {705.895, 15.8573}, {702.037, 15.8548}, {698.18, 15.8523}, {694.323, 15.8498}, {690.465,
15.8472}, {686.608, 15.8445}, {682.751, 15.8419}, {678.893, 15.8392}, {675.036, 15.8364}, {671.179, 15.8336}, {667.321, 15.8307}, {663.464, 15.8279},
{659.607, 15.8249}, {655.749, 15.8219}, {651.892, 15.8189}, {648.035, 15.8158}, {644.177, 15.8126}, {640.32, 15.8094}, {636.463, 15.8062}, {632.605, 15.8029},
{628.748, 15.7995}, {624.891, 15.7961}, {621.033, 15.7926}, {617.176, 15.789}, {613.318, 15.7854}, {609.461, 15.7817}, {605.604, 15.778}, {601.746, 15.7742},
{597.889, 15.7703}, {594.032, 15.7663}, {590.174, 15.7623}, {586.317, 15.7582}, {582.46, 15.754}, {578.602, 15.7497}, {574.745, 15.7454}, {570.888, 15.7409},
{567.03, 15.7364}, {563.173, 15.7318}, {559.316, 15.7271}, {555.458, 15.7223}, {551.601, 15.7174}, {547.744, 15.7124}, {543.886, 15.7072}, {540.029, 15.702},
{536.171, 15.6967}, {532.314, 15.6913}, {528.457, 15.6857}, {524.599, 15.68}, {520.742, 15.6742}, {516.885, 15.6683}, {513.027, 15.6623}, {509.17, 15.6561},
{505.313, 15.6497}, {501.455, 15.6433}, {497.598, 15.6366}, {493.741, 15.6299}, {489.883, 15.6229}, {486.026, 15.6159}, {482.169, 15.6086}, {478.311,
15.6012}, {474.454, 15.5935}, {470.597, 15.5857}, {466.739, 15.5778}, {462.882, 15.5696}, {459.025, 15.5612}, {455.167, 15.5526}, {451.31, 15.5438}, {447.452,
15.5347}, {443.595, 15.5254}, {439.738, 15.5159}, {435.88, 15.5061}, {432.023, 15.4961}, {428.166, 15.4858}, {424.308, 15.4752}, {420.451, 15.4644},
{416.594, 15.4532}, {412.736, 15.4417}, {408.879, 15.4299}, {405.022, 15.4178}, {401.164, 15.4053}, {397.307, 15.3924}, {393.45, 15.3792}, {389.592, 15.3656},
{385.735, 15.3515}, {381.878, 15.3371}, {378.02, 15.3222}, {374.163, 15.3068}, {370.305, 15.291}, {366.448, 15.2747}, {362.591, 15.2578}, {358.733, 15.2404},
{354.876, 15.2225}, {351.019, 15.2039}, {347.161, 15.1847}, {343.304, 15.1649}, {339.447, 15.1444}, {335.589, 15.1232}, {331.732, 15.1012}, {327.875,
15.0785}, {324.017, 15.055}, {320.16, 15.0306}, {316.303, 15.0053}, {312.445, 14.9791}, {308.588, 14.9518}, {304.731, 14.9236}, {300.873, 14.8942}, {297.016,
14.8637}, {293.159, 14.832}, {289.301, 14.7991}, {285.444, 14.7647}, {281.586, 14.729}, {277.729, 14.6918}, {273.872, 14.653}, {270.014, 14.6125}, {266.157,
14.5702}, {262.3, 14.526}, {258.442, 14.4799}, {254.585, 14.4317}, {250.728, 14.3812}, {246.87, 14.3283}, {243.013, 14.2729}, {239.156, 14.2148}, {235.298,
14.1538}, {231.441, 14.0897}, {227.584, 14.0223}, {223.726, 13.9515}, {219.869, 13.8768}, {216.012, 13.7981}, {212.154, 13.7151}, {208.297, 13.6274},
{204.439, 13.5347}, {200.582, 13.4366}, {196.725, 13.3327}, {192.867, 13.2224}, {189.01, 13.1053}, {185.153, 12.9809}, {181.295, 12.8483}, {177.438, 12.707},
{173.581, 12.5562}, {169.723, 12.3949}, {165.866, 12.2222}, {162.009, 12.037}, {158.151, 11.838}, {154.294, 11.6239}, {150.437, 11.3931}, {146.579, 11.1436},
{142.722, 10.8737}, {138.865, 10.5808}, {135.007, 10.2623}, {131.15, 9.91524}, {127.293, 9.53597}, {123.435, 9.12028}, {119.578, 8.66359}, {115.72, 8.16005},
{111.863, 7.60331}, {108.006, 6.98543}, {104.148, 6.29689}, {100.291, 5.5269}};

ge=Interpolation[geraw];

gaasraw={{7876.71, 11.6491}, {7845.85, 11.6419}, {7814.99, 11.6347}, {7784.13, 11.6275}, {7753.27, 11.6204}, {7722.41, 11.6134}, {7695.41, 11.6073}, {7664.55,
11.6003}, {7633.69, 11.5934}, {7606.69, 11.5874}, {7575.83, 11.5806}, {7548.83, 11.5747}, {7521.83, 11.5688}, {7490.97, 11.5621}, {7463.97, 11.5563},
{7436.97, 11.5505}, {7409.97, 11.5448}, {7382.97, 11.5391}, {7355.96, 11.5334}, {7328.96, 11.5277}, {7301.96, 11.5221}, {7274.96, 11.5166}, {7247.96, 11.511},
{7220.96, 11.5055}, {7197.81, 11.5008}, {7170.81, 11.4954}, {7143.81, 11.49}, {7120.67, 11.4853}, {7093.66, 11.48}, {7070.52, 11.4754}, {7043.52, 11.4701},
{7020.38, 11.4656}, {6993.37, 11.4604}, {6970.23, 11.4559}, {6947.09, 11.4515}, {6923.94, 11.4471}, {6896.94, 11.442}, {6873.8, 11.4376}, {6850.65, 11.4332},
{6827.51, 11.4289}, {6804.36, 11.4246}, {6781.22, 11.4204}, {6758.08, 11.4161}, {6734.93, 11.4119}, {6711.79, 11.4077}, {6692.5, 11.4042}, {6669.36, 11.4},
{6646.21, 11.3959}, {6623.07, 11.3917}, {6603.78, 11.3883}, {6580.64, 11.3842}, {6557.49, 11.3802}, {6538.21, 11.3768}, {6515.06, 11.3728}, {6495.78,
11.3694}, {6472.63, 11.3654}, {6453.34, 11.3621}, {6434.06, 11.3588}, {6410.91, 11.3549}, {6391.63, 11.3516}, {6372.34, 11.3484}, {6353.05, 11.3452},
{6329.91, 11.3413}, {6310.62, 11.3381}, {6291.34, 11.3349}, {6272.05, 11.3317}, {6252.76, 11.3286}, {6233.48, 11.3254}, {6214.19, 11.3223}, {6194.9, 11.3192},
{6175.62, 11.3161}, {6156.33, 11.313}, {6137.04, 11.3099}, {6117.76, 11.3068}, {6098.47, 11.3038}, {6079.18, 11.3007}, {6063.75, 11.2983}, {6044.47,
11.2953}, {6025.18, 11.2923}, {6009.75, 11.2899}, {5990.46, 11.2869}, {5971.18, 11.284}, {5955.75, 11.2816}, {5936.46, 11.2787}, {5917.17, 11.2757}, {5901.74,
11.2734}, {5882.46, 11.2705}, {5867.03, 11.2682}, {5851.6, 11.2659}, {5832.31, 11.263}, {5816.88, 11.2607}, {5797.6, 11.2579}, {5782.17, 11.2556}, {5766.74,
11.2534}, {5747.45, 11.2505}, {5732.02, 11.2483}, {5716.59, 11.2461}, {5701.16, 11.2438}, {5681.88, 11.2411}, {5666.45, 11.2389}, {5651.02, 11.2367},
{5635.59, 11.2345}, {5620.16, 11.2323}, {5604.73, 11.2301}, {5589.3, 11.2279}, {5573.87, 11.2258}, {5558.44, 11.2236}, {5543.01, 11.2215}, {5527.58, 11.2193},
{5512.15, 11.2172}, {5496.72, 11.2151}, {5481.29, 11.213}, {5465.86, 11.2109}, {5450.43, 11.2088}, {5435, 11.2067}, {5423.43, 11.2051}, {5408, 11.203},
```

{5392.57, 11.2009}, {5377.14, 11.1989}, {5365.57, 11.1973}, {5350.14, 11.1953}, {5334.71, 11.1932}, {5319.28, 11.1912}, {5307.71, 11.1897}, {5292.28, 11.1877}, {5280.71, 11.1862}, {5265.28, 11.1841}, {5249.85, 11.1821}, {5238.28, 11.1806}, {5222.85, 11.1786}, {5211.28, 11.1772}, {5195.85, 11.1752}, {5184.28, 11.1737}, {5168.85, 11.1717}, {5157.28, 11.1703}, {5141.85, 11.1683}, {5130.27, 11.1669}, {5118.7, 11.1654}, {5103.27, 11.1635}, {5091.7, 11.162}, {5076.27, 11.1601}, {5064.7, 11.1587}, {5053.13, 11.1572}, {5041.56, 11.1558}, {5026.13, 11.1539}, {5014.55, 11.1525}, {5002.98, 11.1511}, {4987.55, 11.1492}, {4975.98, 11.1478}, {4964.41, 11.1464}, {4952.84, 11.145}, {4941.26, 11.1436}, {4929.69, 11.1422}, {4914.26, 11.1403}, {4902.69, 11.139}, {4891.12, 11.1376}, {4879.55, 11.1362}, {4867.97, 11.1348}, {4856.4, 11.1335}, {4844.83, 11.1321}, {4833.26, 11.1307}, {4821.69, 11.1294}, {4810.11, 11.128}, {4798.54, 11.1267}, {4786.97, 11.1253}, {4775.4, 11.124}, {4763.83, 11.1227}, {4752.25, 11.1213}, {4740.68, 11.12}, {4729.11, 11.1187}, {4717.54, 11.1174}, {4705.97, 11.116}, {4698.25, 11.1152}, {4686.68, 11.1138}, {4675.11, 11.1125}, {4663.54, 11.1112}, {4651.96, 11.1099}, {4640.39, 11.1086}, {4632.68, 11.1078}, {4621.1, 11.1065}, {4609.53, 11.1052}, {4597.96, 11.1039}, {4590.25, 11.1031}, {4578.67, 11.1018}, {4567.1, 11.1005}, {4559.39, 11.0996}, {4547.81, 11.0984}, {4536.24, 11.0971}, {4528.53, 11.0963}, {4516.96, 11.095}, {4505.38, 11.0938}, {4497.67, 11.0929}, {4486.1, 11.0917}, {4474.52, 11.0904}, {4466.81, 11.0896}, {4455.24, 11.0884}, {4447.52, 11.0875}, {4435.95, 11.0863}, {4428.24, 11.0855}, {4416.66, 11.0842}, {4408.95, 11.0834}, {4397.38, 11.0822}, {4389.66, 11.0814}, {4378.09, 11.0802}, {4370.38, 11.0794}, {4358.8, 11.0782}, {4351.09, 11.0773}, {4339.52, 11.0761}, {4331.8, 11.0753}, {4320.23, 11.0741}, {4312.52, 11.0733}, {4304.8, 11.0725}, {4293.23, 11.0714}, {4285.51, 11.0706}, {4273.94, 11.0694}, {4266.23, 11.0686}, {4258.51, 11.0678}, {4246.94, 11.0666}, {4239.23, 11.0658}, {4231.51, 11.065}, {4219.94, 11.0639}, {4212.23, 11.0631}, {4204.51, 11.0623}, {4192.94, 11.0612}, {4185.22, 11.0604}, {4177.51, 11.0596}, {4169.79, 11.0588}, {4158.22, 11.0577}, {4150.51, 11.0569}, {4142.79, 11.0562}, {4135.08, 11.0554}, {4127.36, 11.0546}, {4115.79, 11.0535}, {4108.08, 11.0527}, {4100.36, 11.052}, {4092.65, 11.0512}, {4084.93, 11.0505}, {4073.36, 11.0493}, {4065.65, 11.0486}, {4057.93, 11.0478}, {4050.22, 11.0471}, {4042.5, 11.0463}, {4034.79, 11.0456}, {4027.07, 11.0448}, {4019.36, 11.0441}, {4011.64, 11.0433}, {4000.07, 11.0422}, {3992.36, 11.0415}, {3984.64, 11.0408}, {3976.93, 11.04}, {3969.21, 11.0393}, {3961.5, 11.0386}, {3953.78, 11.0378}, {3946.07, 11.0371}, {3938.35, 11.0364}, {3930.64, 11.0356}, {3922.92, 11.0349}, {3915.21, 11.0342}, {3907.49, 11.0335}, {3899.78, 11.0327}, {3892.07, 11.032}, {3884.35, 11.0313}, {3876.64, 11.0306}, {3868.92, 11.0299}, {3861.21, 11.0292}, {3857.35, 11.0288}, {3849.63, 11.0281}, {3841.92, 11.0274}, {3834.21, 11.0267}, {3826.49, 11.0259}, {3818.78, 11.0252}, {3811.06, 11.0245}, {3803.35, 11.0238}, {3795.63, 11.0231}, {3787.92, 11.0224}, {3784.06, 11.0221}, {3776.34, 11.0214}, {3768.63, 11.0207}, {3760.92, 11.02}, {3753.2, 11.0193}, {3745.49, 11.0186}, {3741.63, 11.0182}, {3733.91, 11.0175}, {3726.2, 11.0168}, {3718.48, 11.0162}, {3710.77, 11.0155}, {3706.91, 11.0151}, {3699.2, 11.0144}, {3691.48, 11.0137}, {3683.77, 11.0131}, {3679.91, 11.0127}, {3672.2, 11.012}, {3664.48, 11.0113}, {3656.77, 11.0107}, {3652.91, 11.0103}, {3645.2, 11.0096}, {3637.48, 11.009}, {3629.77, 11.0083}, {3625.91, 11.0079}, {3618.19, 11.0073}, {3610.48, 11.0066}, {3606.62, 11.0063}, {3598.91, 11.0056}, {3591.19, 11.0049}, {3587.33, 11.0046}, {3579.62, 11.0039}, {3571.91, 11.0032}, {3568.05, 11.0029}, {3560.33, 11.0022}, {3552.62, 11.0016}, {3548.76, 11.0012}, {3541.05, 11.0006}, {3537.19, 11.0003}, {3529.47, 10.9996}, {3521.76, 10.9989}, {3517.9, 10.9986}, {3510.19, 10.9979}, {3506.33, 10.9976}, {3498.62, 10.997}, {3490.9, 10.9963}, {3487.04, 10.996}, {3479.33, 10.9953}, {3475.47, 10.995}, {3467.76, 10.9943}, {3463.9, 10.994}, {3456.18, 10.9934}, {3448.47, 10.9927}, {3444.61, 10.9924}, {3436.9, 10.9917}, {3433.04, 10.9914}, {3425.33, 10.9908}, {3421.47, 10.9904}, {3413.75, 10.9898}, {3409.9, 10.9895}, {3402.18, 10.9888}, {3398.32, 10.9885}, {3390.61, 10.9879}, {3386.75, 10.9876}, {3379.04, 10.9869}, {3375.18, 10.9866}, {3367.47, 10.986}, {3363.61, 10.9856}, {3355.89, 10.985}, {3352.04, 10.9847}, {3348.18, 10.9844}, {3340.46, 10.9837}, {3336.61, 10.9834}, {3328.89, 10.9828}, {3325.04, 10.9825}, {3317.32, 10.9818}, {3313.46, 10.9815}, {3309.61, 10.9812}, {3301.89, 10.9806}, {3298.03, 10.9803}, {3290.32, 10.9796}, {3286.46, 10.9793}, {3278.75, 10.9787}, {3274.89, 10.9784}, {3271.03, 10.9781}, {3263.32, 10.9774}, {3259.46, 10.9771}, {3255.6, 10.9768}, {3247.89, 10.9762}, {3244.03, 10.9759}, {3236.32, 10.9753}, {3232.46, 10.9749}, {3228.6, 10.9746}, {3220.89, 10.974}, {3217.03, 10.9737}, {3213.17, 10.9734}, {3205.46, 10.9728}, {3201.6, 10.9725}, {3197.74, 10.9722}, {3190.03, 10.9716}, {3186.17, 10.9712}, {3182.31, 10.9709}, {3178.46, 10.9706}, {3170.74, 10.97}, {3166.88, 10.9697}, {3163.03, 10.9694}, {3155.31, 10.9688}, {3151.45, 10.9685}, {3147.6, 10.9682}, {3139.88, 10.9676}, {3136.02, 10.9673}, {3132.17, 10.967}, {3128.31, 10.9667}, {3120.6, 10.9661}, {3116.74, 10.9658}, {3112.88, 10.9654}, {3109.02, 10.9651}, {3101.31, 10.9645}, {3097.45, 10.9642}, {3093.59, 10.9639}, {3089.74, 10.9636}, {3082.02, 10.963}, {3078.16, 10.9627}, {3074.31, 10.9624}, {3070.45, 10.9621}, {3066.59, 10.9618}, {3058.88, 10.9612}, {3055.02, 10.9609}, {3051.16, 10.9606}, {3047.31, 10.9603}, {3039.59, 10.9597}, {3035.73, 10.9594}, {3031.88, 10.9591}, {3028.02, 10.9588}, {3024.16, 10.9585}, {3020.3, 10.9582}, {3012.59, 10.9576}, {3008.73, 10.9573}, {3004.88, 10.957}, {3001.02, 10.9568}, {2997.16, 10.9565}, {2993.3, 10.9562}, {2985.59, 10.9556}, {2981.73, 10.9553}, {2977.87, 10.955}, {2974.02, 10.9547}, {2970.16, 10.9544}, {2966.3, 10.9541}, {2958.59, 10.9535}, {2954.73, 10.9532}, {2950.87, 10.9529}, {2947.01, 10.9526}, {2943.16, 10.9523}, {2939.3, 10.952}, {2935.44, 10.9517}, {2931.59, 10.9514}, {2927.73, 10.9511}, {2920.01, 10.9506}, {2916.16, 10.9503}, {2912.3, 10.95}, {2908.44, 10.9497}, {2904.58, 10.9494}, {2900.73, 10.9491}, {2896.87, 10.9488}, {2893.01, 10.9485}, {2889.15, 10.9482}, {2885.3, 10.9479}, {2881.44, 10.9476}, {2873.73, 10.947}, {2869.87, 10.9468}, {2866.01, 10.9465}, {2862.15, 10.9462}, {2858.3, 10.9459}, {2854.44, 10.9456}, {2850.58, 10.9453}, {2846.72, 10.945}, {2842.87, 10.9447}, {2839.01, 10.9444}, {2835.15, 10.9441}, {2831.29, 10.9438}, {2827.44, 10.9436}, {2823.58, 10.9433}, {2819.72, 10.943}, {2815.87, 10.9427}, {2812.01, 10.9424}, {2808.15, 10.9421}, {2804.29, 10.9418}, {2800.44, 10.9415}, {2796.58, 10.9412}, {2792.72, 10.941}, {2788.86, 10.9407}, {2785.01, 10.9404}, {2781.15, 10.9401}, {2777.29, 10.9398}, {2773.43, 10.9395}, {2769.58, 10.9392}, {2765.72, 10.9389}, {2761.86, 10.9387}, {2758, 10.9384}, {2754.15, 10.9381}, {2750.29, 10.9378}, {2746.43, 10.9375}, {2742.58, 10.9372}, {2738.72, 10.9369}, {2734.86, 10.9366}, {2731, 10.9364}, {2727.15, 10.9361}, {2723.29, 10.9358}, {2719.43, 10.9355}, {2715.57, 10.9352}, {2711.72, 10.9349}, {2707.86, 10.9346}, {2704, 10.9344}, {2700.14, 10.9341}, {2696.29, 10.9338}, {2692.43, 10.9335}, {2688.57, 10.9332}, {2684.72, 10.9329}, {2680.86, 10.9326}, {2677, 10.9324}, {2673.14, 10.9321}, {2669.29, 10.9318}, {2665.43, 10.9315}, {2661.57, 10.9312}, {2657.71, 10.9309}, {2653.86, 10.9306}, {2650, 10.9304}, {2646.14, 10.9301}, {2642.28, 10.9298}, {2638.43, 10.9295}, {2634.57, 10.9292}, {2630.71, 10.9289}, {2626.85, 10.9287}, {2623, 10.9284}, {2619.14, 10.9281}, {2615.28, 10.9278}, {2611.43, 10.9275}, {2607.57, 10.9272}, {2603.71, 10.9269}, {2599.85, 10.9267}, {2596, 10.9264}, {2592.14, 10.9261}, {2588.28, 10.9258}, {2584.42, 10.9255}, {2580.57, 10.9252}, {2576.71, 10.925}, {2572.85, 10.9247}, {2568.99, 10.9244}, {2565.14, 10.9241}, {2561.28, 10.9238}, {2557.42, 10.9235}, {2553.57, 10.9233}, {2549.71, 10.923}, {2545.85, 10.9227}, {2541.99, 10.9224}, {2538.14, 10.9221}, {2534.28, 10.9218}, {2530.42, 10.9216}, {2526.56, 10.9213}, {2522.71, 10.921}, {2518.85, 10.9207}, {2514.99, 10.9204}, {2511.13, 10.9201}, {2507.28, 10.9199}, {2503.42, 10.9196}, {2499.56, 10.9193}, {2495.71, 10.919}, {2491.85, 10.9187}, {2487.99, 10.9184}, {2484.13, 10.9181}, {2480.28, 10.9179}, {2476.42, 10.9176}, {2472.56, 10.9173}, {2468.7, 10.917}, {2464.85, 10.9167}, {2460.99, 10.9164}, {2457.13, 10.9162}, {2453.27, 10.9159}, {2449.42, 10.9156}, {2445.56, 10.9153}, {2441.7, 10.915}, {2437.84, 10.9147}, {2433.99, 10.9145}, {2430.13, 10.9142}, {2426.27, 10.9139}, {2422.42, 10.9136}, {2418.56, 10.9133}, {2414.7, 10.913}, {2410.84, 10.9128}, {2406.99, 10.9125}, {2403.13, 10.9122}, {2399.27, 10.9119}, {2395.41, 10.9116}, {2391.56, 10.9113}, {2387.7, 10.911}, {2383.84, 10.9108}, {2379.98, 10.9105}, {2376.13, 10.9102}, {2372.27, 10.9099}, {2368.41, 10.9096}, {2364.56, 10.9093}, {2360.7, 10.909}, {2356.84, 10.9088}, {2352.98, 10.9085}, {2349.13, 10.9082}, {2345.27, 10.9079}, {2341.41, 10.9076}, {2337.55, 10.9073}, {2333.7, 10.907}, {2329.84, 10.9068}, {2325.98, 10.9065}, {2322.12, 10.9062}, {2318.27, 10.9059}, {2314.41, 10.9056}, {2310.55, 10.9053}, {2306.7, 10.905}, {2302.84, 10.9047}, {2298.98, 10.9045}, {2295.12, 10.9042}, {2291.27, 10.9039}, {2287.41, 10.9036}, {2283.55, 10.9033}, {2279.69, 10.903}, {2275.84, 10.9027}, {2271.98, 10.9024}, {2268.12, 10.9022}, {2264.26, 10.9019}, {2260.41, 10.9016}, {2256.55, 10.9013}, {2252.69, 10.901}, {2248.83, 10.9007}, {2244.98, 10.9004}, {2241.12, 10.9001}, {2237.26, 10.8998}, {2233.41, 10.8995}, {2229.55, 10.8993}, {2225.69, 10.899}, {2221.83, 10.8987}, {2217.98, 10.8984}, {2214.12, 10.8981}, {2210.26, 10.8978}, {2206.4, 10.8975}, {2202.55, 10.8972}, {2198.69, 10.8969}, {2194.83, 10.8966}, {2190.97, 10.8963}, {2187.12, 10.896}, {2183.26, 10.8957}, {2179.4, 10.8954}, {2175.55, 10.8952}, {2171.69, 10.8949}, {2167.83, 10.8946}, {2163.97, 10.8943}, {2160.12, 10.894}, {2156.26, 10.8937}, {2152.4, 10.8934}, {2148.54, 10.8931}, {2144.69, 10.8928}, {2140.83, 10.8925}, {2136.97, 10.8922}, {2133.11, 10.8919}, {2129.26, 10.8916}, {2125.4, 10.8913},

{2121.54, 10.891}, {2117.68, 10.8907}, {2113.83, 10.8904}, {2109.97, 10.8901}, {2106.11, 10.8898}, {2102.26, 10.8895}, {2098.4, 10.8892}, {2094.54, 10.8889}, {2090.68, 10.8886}, {2086.83, 10.8883}, {2082.97, 10.888}, {2079.11, 10.8877}, {2075.25, 10.8874}, {2071.4, 10.8871}, {2067.54, 10.8868}, {2063.68, 10.8865}, {2059.82, 10.8862}, {2055.97, 10.8858}, {2052.11, 10.8855}, {2048.25, 10.8852}, {2044.4, 10.8849}, {2040.54, 10.8846}, {2036.68, 10.8843}, {2032.82, 10.884}, {2028.97, 10.8837}, {2025.11, 10.8834}, {2021.25, 10.8831}, {2017.39, 10.8828}, {2013.54, 10.8824}, {2009.68, 10.8821}, {2005.82, 10.8818}, {2001.96, 10.8815}, {1998.11, 10.8812}, {1994.25, 10.8809}, {1990.39, 10.8806}, {1986.54, 10.8803}, {1982.68, 10.8799}, {1978.82, 10.8796}, {1974.96, 10.8793}, {1971.11, 10.879}, {1967.25, 10.8787}, {1963.39, 10.8784}, {1959.53, 10.878}, {1955.68, 10.8777}, {1951.82, 10.8774}, {1947.96, 10.8771}, {1944.1, 10.8767}, {1940.25, 10.8764}, {1936.39, 10.8761}, {1932.53, 10.8758}, {1928.67, 10.8755}, {1924.82, 10.8751}, {1920.96, 10.8748}, {1917.1, 10.8745}, {1913.25, 10.8741}, {1909.39, 10.8738}, {1905.53, 10.8735}, {1901.67, 10.8732}, {1897.82, 10.8728}, {1893.96, 10.8725}, {1890.1, 10.8722}, {1886.24, 10.8718}, {1882.39, 10.8715}, {1878.53, 10.8712}, {1874.67, 10.8708}, {1870.81, 10.8705}, {1866.96, 10.8702}, {1863.1, 10.8698}, {1859.24, 10.8695}, {1855.39, 10.8691}, {1851.53, 10.8688}, {1847.67, 10.8685}, {1843.81, 10.8681}, {1839.96, 10.8678}, {1836.1, 10.8674}, {1832.24, 10.8671}, {1828.38, 10.8667}, {1824.53, 10.8664}, {1820.67, 10.866}, {1816.81, 10.8657}, {1812.95, 10.8653}, {1809.1, 10.865}, {1805.24, 10.8646}, {1801.38, 10.8643}, {1797.53, 10.8639}, {1793.67, 10.8636}, {1789.81, 10.8632}, {1785.95, 10.8629}, {1782.1, 10.8625}, {1778.24, 10.8622}, {1774.38, 10.8618}, {1770.52, 10.8614}, {1766.67, 10.8611}, {1762.81, 10.8607}, {1758.95, 10.8603}, {1755.09, 10.86}, {1751.24, 10.8596}, {1747.38, 10.8592}, {1743.52, 10.8589}, {1739.66, 10.8585}, {1735.81, 10.8581}, {1731.95, 10.8578}, {1728.09, 10.8574}, {1724.24, 10.857}, {1720.38, 10.8566}, {1716.52, 10.8563}, {1712.66, 10.8559}, {1708.81, 10.8555}, {1704.95, 10.8551}, {1701.09, 10.8547}, {1697.23, 10.8543}, {1693.38, 10.854}, {1689.52, 10.8536}, {1685.66, 10.8532}, {1681.8, 10.8528}, {1677.95, 10.8524}, {1674.09, 10.852}, {1670.23, 10.8516}, {1666.38, 10.8512}, {1662.52, 10.8508}, {1658.66, 10.8504}, {1654.8, 10.85}, {1650.95, 10.8496}, {1647.09, 10.8492}, {1643.23, 10.8488}, {1639.37, 10.8484}, {1635.52, 10.848}, {1631.66, 10.8476}, {1627.8, 10.8471}, {1623.94, 10.8467}, {1620.09, 10.8463}, {1616.23, 10.8459}, {1612.37, 10.8455}, {1608.51, 10.8451}, {1604.66, 10.8446}, {1600.8, 10.8442}, {1596.94, 10.8438}, {1593.09, 10.8433}, {1589.23, 10.8429}, {1585.37, 10.8425}, {1581.51, 10.842}, {1577.66, 10.8416}, {1573.8, 10.8412}, {1569.94, 10.8407}, {1566.08, 10.8403}, {1562.23, 10.8398}, {1558.37, 10.8394}, {1554.51, 10.8389}, {1550.65, 10.8385}, {1546.8, 10.838}, {1542.94, 10.8376}, {1539.08, 10.8371}, {1535.23, 10.8366}, {1531.37, 10.8362}, {1527.51, 10.8357}, {1523.65, 10.8352}, {1519.8, 10.8348}, {1515.94, 10.8343}, {1512.08, 10.8338}, {1508.22, 10.8333}, {1504.37, 10.8329}, {1500.51, 10.8324}, {1496.65, 10.8319}, {1492.79, 10.8314}, {1488.94, 10.8309}, {1485.08, 10.8304}, {1481.22, 10.8299}, {1477.37, 10.8294}, {1473.51, 10.8289}, {1469.65, 10.8284}, {1465.79, 10.8279}, {1461.94, 10.8274}, {1458.08, 10.8269}, {1454.22, 10.8264}, {1450.36, 10.8258}, {1446.51, 10.8253}, {1442.65, 10.8248}, {1438.79, 10.8243}, {1434.93, 10.8237}, {1431.08, 10.8232}, {1427.22, 10.8227}, {1423.36, 10.8221}, {1419.5, 10.8216}, {1415.65, 10.821}, {1411.79, 10.8205}, {1407.93, 10.8199}, {1404.08, 10.8194}, {1400.22, 10.8188}, {1396.36, 10.8182}, {1392.5, 10.8177}, {1388.65, 10.8171}, {1384.79, 10.8165}, {1380.93, 10.8159}, {1377.07, 10.8153}, {1373.22, 10.8147}, {1369.36, 10.8142}, {1365.5, 10.8136}, {1361.64, 10.813}, {1357.79, 10.8124}, {1353.93, 10.8117}, {1350.07, 10.8111}, {1346.22, 10.8105}, {1342.36, 10.8099}, {1338.5, 10.8093}, {1334.64, 10.8086}, {1330.79, 10.808}, {1326.93, 10.8074}, {1323.07, 10.8067}, {1319.21, 10.8061}, {1315.36, 10.8054}, {1311.5, 10.8048}, {1307.64, 10.8041}, {1303.78, 10.8034}, {1299.93, 10.8028}, {1296.07, 10.8021}, {1292.21, 10.8014}, {1288.35, 10.8007}, {1284.5, 10.8}, {1280.64, 10.7993}, {1276.78, 10.7986}, {1272.93, 10.7979}, {1269.07, 10.7972}, {1265.21, 10.7965}, {1261.35, 10.7957}, {1257.5, 10.795}, {1253.64, 10.7943}, {1249.78, 10.7935}, {1245.92, 10.7928}, {1242.07, 10.792}, {1238.21, 10.7912}, {1234.35, 10.7905}, {1230.49, 10.7897}, {1226.64, 10.7889}, {1222.78, 10.7881}, {1218.92, 10.7873}, {1215.07, 10.7865}, {1211.21, 10.7857}, {1207.35, 10.7849}, {1203.49, 10.7841}, {1199.64, 10.7832}, {1195.78, 10.7824}, {1191.92, 10.7816}, {1188.06, 10.7807}, {1184.21, 10.7799}, {1180.35, 10.779}, {1176.49, 10.7781}, {1172.63, 10.7772}, {1168.78, 10.7763}, {1164.92, 10.7754}, {1161.06, 10.7745}, {1157.21, 10.7736}, {1153.35, 10.7727}, {1149.49, 10.7717}, {1145.63, 10.7708}, {1141.78, 10.7699}, {1137.92, 10.7689}, {1134.06, 10.7679}, {1130.2, 10.7669}, {1126.35, 10.766}, {1122.49, 10.765}, {1118.63, 10.7639}, {1114.77, 10.7629}, {1110.92, 10.7619}, {1107.06, 10.7609}, {1103.2, 10.7598}, {1099.34, 10.7587}, {1095.49, 10.7577}, {1091.63, 10.7566}, {1087.77, 10.7555}, {1083.92, 10.7544}, {1080.06, 10.7533}, {1076.2, 10.7522}, {1072.34, 10.751}, {1068.49, 10.7499}, {1064.63, 10.7487}, {1060.77, 10.7475}, {1056.91, 10.7463}, {1053.06, 10.7451}, {1049.2, 10.7439}, {1045.34, 10.7427}, {1041.48, 10.7414}, {1037.63, 10.7402}, {1033.77, 10.7389}, {1029.91, 10.7376}, {1026.06, 10.7363}, {1022.2, 10.735}, {1018.34, 10.7337}, {1014.48, 10.7323}, {1010.63, 10.731}, {1006.77, 10.7296}, {1002.91, 10.7282}, {999.053, 10.7268}, {995.196, 10.7254}, {991.339, 10.7239}, {987.481, 10.7225}, {983.624, 10.721}, {979.767, 10.7195}, {975.909, 10.718}, {972.052, 10.7164}, {968.195, 10.7149}, {964.337, 10.7133}, {960.48, 10.7117}, {956.622, 10.7101}, {952.765, 10.7085}, {948.908, 10.7068}, {945.05, 10.7052}, {941.193, 10.7035}, {937.336, 10.7017}, {933.478, 10.7}, {929.621, 10.6982}, {925.764, 10.6965}, {921.906, 10.6946}, {918.049, 10.6928}, {914.192, 10.691}, {910.334, 10.6891}, {906.477, 10.6872}, {902.62, 10.6852}, {898.762, 10.6833}, {894.905, 10.6813}, {891.048, 10.6792}, {887.19, 10.6772}, {883.333, 10.6751}, {879.476, 10.673}, {875.618, 10.6709}, {871.761, 10.6687}, {867.903, 10.6665}, {864.046, 10.6643}, {860.189, 10.662}, {856.331, 10.6597}, {852.474, 10.6574}, {848.617, 10.655}, {844.759, 10.6526}, {840.902, 10.6502}, {837.045, 10.6477}, {833.187, 10.6452}, {829.33, 10.6426}, {825.473, 10.64}, {821.615, 10.6374}, {817.758, 10.6347}, {813.901, 10.632}, {810.043, 10.6292}, {806.186, 10.6264}, {802.329, 10.6235}, {798.471, 10.6206}, {794.614, 10.6177}, {790.756, 10.6147}, {786.899, 10.6116}, {783.042, 10.6085}, {779.184, 10.6054}, {775.327, 10.6022}, {771.47, 10.5989}, {767.612, 10.5956}, {763.755, 10.5922}, {759.898, 10.5887}, {756.04, 10.5852}, {752.183, 10.5817}, {748.326, 10.578}, {744.468, 10.5743}, {740.611, 10.5706}, {736.754, 10.5667}, {732.896, 10.5628}, {729.039, 10.5588}, {725.182, 10.5548}, {721.324, 10.5507}, {717.467, 10.5464}, {713.609, 10.5421}, {709.752, 10.5378}, {705.895, 10.5333}, {702.037, 10.5287}, {698.18, 10.5241}, {694.323, 10.5193}, {690.465, 10.5145}, {686.608, 10.5096}, {682.751, 10.5045}, {678.893, 10.4994}, {675.036, 10.4941}, {671.179, 10.4887}, {667.321, 10.4833}, {663.464, 10.4777}, {659.607, 10.4719}, {655.749, 10.4661}, {651.892, 10.4601}, {648.035, 10.454}, {644.177, 10.4477}, {640.32, 10.4413}, {636.463, 10.4347}, {632.605, 10.428}, {628.748, 10.4212}, {624.891, 10.4141}, {621.033, 10.4069}, {617.176, 10.3996}, {613.318, 10.392}, {609.461, 10.3843}, {605.604, 10.3763}, {601.746, 10.3682}, {597.889, 10.3598}, {594.032, 10.3513}, {590.174, 10.3425}, {586.317, 10.3334}, {582.46, 10.3242}, {578.602, 10.3146}, {574.745, 10.3049}, {570.888, 10.2948}, {567.03, 10.2845}, {563.173, 10.2738}, {559.316, 10.2629}, {555.458, 10.2516}, {551.601, 10.24}, {547.744, 10.2281}, {543.886, 10.2158}, {540.029, 10.2031}, {536.171, 10.19}, {532.314, 10.1765}, {528.457, 10.1626}, {524.599, 10.1483}, {520.742, 10.1334}, {516.885, 10.1181}, {513.027, 10.1022}, {509.17, 10.0858}, {505.313, 10.0689}, {501.455, 10.0513}, {497.598, 10.0331}, {493.741, 10.0142}, {489.883, 9.99466}, {486.026, 9.97436}, {482.169, 9.95329}, {478.311, 9.93138}, {474.454, 9.90862}, {470.597, 9.88493}, {466.739, 9.86027}, {462.882, 9.83458}, {459.025, 9.80779}, {455.167, 9.77984}, {451.31, 9.75065}, {447.452, 9.72014}, {443.595, 9.68822}, {439.738, 9.6548}, {435.88, 9.61977}, {432.023, 9.58302}, {428.166, 9.54442}, {424.308, 9.50383}, {420.451, 9.4611}, {416.594, 9.41607}, {412.736, 9.36854}, {408.879, 9.31831}, {405.022, 9.26515}, {401.164, 9.2088}, {397.307, 9.14898}, {393.45, 9.08537}, {389.592, 9.01758}, {385.735, 8.94524}, {381.878, 8.86786}, {378.02, 8.78488}, {374.163, 8.69575}, {370.305, 8.59971}, {366.448, 8.496}, {362.591, 8.38365}, {358.733, 8.26153}, {354.876, 8.12839}, {351.019, 7.98266}, {347.161, 7.82246}, {343.304, 7.64564}, {339.447, 7.44946}, {335.589, 7.23056}, {331.732, 6.98491}, {327.875, 6.70729}, {324.017, 6.39099}, {320.16, 6.02763}, {316.303, 5.60584}, {312.445, 5.11028}, {308.588, 4.52025}, {304.731, 3.80588}, {300.873, 2.92328}, {297.016, 1.80618}, {293.159, 0.346998}, {289.301, −1.63919}, {285.444, −4.49644}, {281.586, −8.95428}, {277.729, −16.843}, {273.872, −34.3178}, {270.014, −91.5579}, {266.157, 116.2}, {262.3, 57.681}, {258.442, 39.8545}, {254.585, 31.8606}, {250.728, 27.3592}, {246.87, 24.4786}, {243.013, 22.4801}, {239.156, 21.0132}, {235.298, 19.891}, {231.441, 19.0056}, {227.584, 18.2894}, {223.726, 17.6982}, {219.869, 17.2024}, {216.012, 16.7807}, {212.154, 16.4178}, {208.297, 16.1023}, {204.439, 15.8257}, {200.582, 15.5814}, {196.725, 15.364}, {192.867, 15.1695}, {189.01, 14.9946}, {185.153, 14.8365}, {181.295, 14.6929}, {177.438, 14.5622}, {173.581, 14.4426}, {169.723, 14.3329}, {165.866, 14.232}, {162.009, 14.139}, {158.151, 14.053}, {154.294, 13.9734}, {150.437, 13.8994}, {146.579, 13.8307}, {142.722, 13.7666}, {138.865, 13.7069}, {135.007, 13.6512}, {131.15, 13.5991}, {127.293, 13.5503}, {123.435, 13.5046}, {119.578, 13.4618}, {115.72,

13.4217}, {111.863, 13.384}, {108.006, 13.3487}, {104.148, 13.3155}, {100.291, 13.2844}};
gaas=Interpolation[gaasraw];

inpraw={{7876.71, 10.3733}, {7845.85, 10.3625}, {7814.99, 10.3517}, {7784.13, 10.3411}, {7753.27, 10.3304}, {7722.41, 10.3199}, {7695.41, 10.3107}, {7664.55, 10.3003}, {7633.69, 10.2899}, {7606.69, 10.2809}, {7575.83, 10.2706}, {7548.83, 10.2617}, {7521.83, 10.2528}, {7490.97, 10.2428}, {7463.97, 10.234}, {7436.97, 10.2253}, {7409.97, 10.2166}, {7382.97, 10.208}, {7355.96, 10.1994}, {7328.96, 10.1909}, {7301.96, 10.1824}, {7274.96, 10.174}, {7247.96, 10.1656}, {7220.96, 10.1572}, {7197.81, 10.1501}, {7170.81, 10.1418}, {7143.81, 10.1336}, {7120.67, 10.1266}, {7093.66, 10.1185}, {7070.52, 10.1115}, {7043.52, 10.1035}, {7020.38, 10.0966}, {6993.37, 10.0887}, {6970.23, 10.0819}, {6947.09, 10.0751}, {6923.94, 10.0684}, {6896.94, 10.0606}, {6873.8, 10.0539}, {6850.65, 10.0473}, {6827.51, 10.0407}, {6804.36, 10.0341}, {6781.22, 10.0276}, {6758.08, 10.0211}, {6734.93, 10.0146}, {6711.79, 10.0082}, {6692.5, 10.0028}, {6669.36, 9.99642}, {6646.21, 9.99007}, {6623.07, 9.98374}, {6603.78, 9.97849}, {6580.64, 9.97222}, {6557.49, 9.96598}, {6538.21, 9.9608}, {6515.06, 9.95462}, {6495.78, 9.94949}, {6472.63, 9.94335}, {6453.34, 9.93827}, {6434.06, 9.9332}, {6410.91, 9.92715}, {6391.63, 9.92213}, {6372.34, 9.91713}, {6353.05, 9.91215}, {6329.91, 9.9062}, {6310.62, 9.90126}, {6291.34, 9.89634}, {6272.05, 9.89145}, {6252.76, 9.88657}, {6233.48, 9.88171}, {6214.19, 9.87687}, {6194.9, 9.87206}, {6175.62, 9.86726}, {6156.33, 9.86248}, {6137.04, 9.85772}, {6117.76, 9.85298}, {6098.47, 9.84826}, {6079.18, 9.84356}, {6063.75, 9.83981}, {6044.47, 9.83515}, {6025.18, 9.8305}, {6009.75, 9.82679}, {5990.46, 9.82218}, {5971.18, 9.81759}, {5955.75, 9.81393}, {5936.46, 9.80937}, {5917.17, 9.80483}, {5901.74, 9.80121}, {5882.46, 9.7967}, {5867.03, 9.79311}, {5851.6, 9.78953}, {5832.31, 9.78507}, {5816.88, 9.78151}, {5797.6, 9.77709}, {5782.17, 9.77356}, {5766.74, 9.77005}, {5747.45, 9.76567}, {5732.02, 9.76218}, {5716.59, 9.7587}, {5701.16, 9.75524}, {5681.88, 9.75092}, {5666.45, 9.74748}, {5651.02, 9.74405}, {5635.59, 9.74064}, {5620.16, 9.73723}, {5604.73, 9.73384}, {5589.3, 9.73046}, {5573.87, 9.72709}, {5558.44, 9.72373}, {5543.01, 9.72038}, {5527.58, 9.71704}, {5512.15, 9.71372}, {5496.72, 9.7104}, {5481.29, 9.7071}, {5465.86, 9.70381}, {5450.43, 9.70053}, {5435, 9.69726}, {5423.43, 9.69481}, {5408, 9.69156}, {5392.57, 9.68832}, {5377.14, 9.6851}, {5365.57, 9.68268}, {5350.14, 9.67947}, {5334.71, 9.67628}, {5319.28, 9.67309}, {5307.71, 9.67071}, {5292.28, 9.66754}, {5280.71, 9.66517}, {5265.28, 9.66202}, {5249.85, 9.65889}, {5238.28, 9.65654}, {5222.85, 9.65342}, {5211.28, 9.65109}, {5195.85, 9.64799}, {5184.28, 9.64567}, {5168.85, 9.64259}, {5157.28, 9.64029}, {5141.85, 9.63722}, {5130.27, 9.63493}, {5118.7, 9.63265}, {5103.27, 9.62961}, {5091.7, 9.62734}, {5076.27, 9.62433}, {5064.7, 9.62207}, {5053.13, 9.61982}, {5041.56, 9.61758}, {5026.13, 9.61459}, {5014.55, 9.61236}, {5002.98, 9.61014}, {4987.55, 9.60718}, {4975.98, 9.60497}, {4964.41, 9.60276}, {4952.84, 9.60056}, {4941.26, 9.59837}, {4929.69, 9.59618}, {4914.26, 9.59327}, {4902.69, 9.5911}, {4891.12, 9.58893}, {4879.55, 9.58676}, {4867.97, 9.58461}, {4856.4, 9.58245}, {4844.83, 9.58031}, {4833.26, 9.57817}, {4821.69, 9.57603}, {4810.11, 9.5739}, {4798.54, 9.57178}, {4786.97, 9.56966}, {4775.4, 9.56755}, {4763.83, 9.56544}, {4752.25, 9.56334}, {4740.68, 9.56125}, {4729.11, 9.55916}, {4717.54, 9.55707}, {4705.97, 9.555}, {4698.25, 9.55361}, {4686.68, 9.55154}, {4675.11, 9.54948}, {4663.54, 9.54742}, {4651.96, 9.54537}, {4640.39, 9.54332}, {4632.68, 9.54196}, {4621.1, 9.53992}, {4609.53, 9.53789}, {4597.96, 9.53586}, {4590.25, 9.53451}, {4578.67, 9.53249}, {4567.1, 9.53048}, {4559.39, 9.52914}, {4547.81, 9.52714}, {4536.24, 9.52514}, {4528.53, 9.52381}, {4516.96, 9.52182}, {4505.38, 9.51984}, {4497.67, 9.51852}, {4486.1, 9.51654}, {4474.52, 9.51457}, {4466.81, 9.51326}, {4455.24, 9.5113}, {4447.52, 9.50999}, {4435.95, 9.50804}, {4428.24, 9.50674}, {4416.66, 9.5048}, {4408.95, 9.50351}, {4397.38, 9.50157}, {4389.66, 9.50028}, {4378.09, 9.49836}, {4370.38, 9.49708}, {4358.8, 9.49516}, {4351.09, 9.49388}, {4339.52, 9.49198}, {4331.8, 9.49071}, {4320.23, 9.48881}, {4312.52, 9.48754}, {4304.8, 9.48628}, {4293.23, 9.48439}, {4285.51, 9.48314}, {4273.94, 9.48126}, {4266.23, 9.48001}, {4258.51, 9.47876}, {4246.94, 9.47689}, {4239.23, 9.47565}, {4231.51, 9.47441}, {4219.94, 9.47255}, {4212.23, 9.47132}, {4204.51, 9.47008}, {4192.94, 9.46824}, {4185.22, 9.46701}, {4177.51, 9.46579}, {4169.79, 9.46457}, {4158.22, 9.46274}, {4150.51, 9.46152}, {4142.79, 9.4603}, {4135.08, 9.45909}, {4127.36, 9.45788}, {4115.79, 9.45607}, {4108.08, 9.45487}, {4100.36, 9.45366}, {4092.65, 9.45246}, {4084.93, 9.45126}, {4073.36, 9.44947}, {4065.65, 9.44828}, {4057.93, 9.44709}, {4050.22, 9.4459}, {4042.5, 9.44471}, {4034.79, 9.44353}, {4027.07, 9.44235}, {4019.36, 9.44117}, {4011.64, 9.43999}, {4000.07, 9.43823}, {3992.36, 9.43705}, {3984.64, 9.43588}, {3976.93, 9.43471}, {3969.21, 9.43355}, {3961.5, 9.43238}, {3953.78, 9.43122}, {3946.07, 9.43006}, {3938.35, 9.4289}, {3930.64, 9.42775}, {3922.92, 9.42659}, {3915.21, 9.42544}, {3907.49, 9.42429}, {3899.78, 9.42314}, {3892.07, 9.422}, {3884.35, 9.42086}, {3876.64, 9.41971}, {3868.92, 9.41857}, {3861.21, 9.41744}, {3857.35, 9.41687}, {3849.63, 9.41574}, {3841.92, 9.4146}, {3834.21, 9.41347}, {3826.49, 9.41234}, {3818.78, 9.41122}, {3811.06, 9.41009}, {3803.35, 9.40897}, {3795.63, 9.40785}, {3787.92, 9.40673}, {3784.06, 9.40618}, {3776.34, 9.40506}, {3768.63, 9.40395}, {3760.92, 9.40284}, {3753.2, 9.40173}, {3745.49, 9.40062}, {3741.63, 9.40007}, {3733.91, 9.39896}, {3726.2, 9.39786}, {3718.48, 9.39676}, {3710.77, 9.39566}, {3706.91, 9.39511}, {3699.2, 9.39402}, {3691.48, 9.39292}, {3683.77, 9.39183}, {3679.91, 9.39129}, {3672.2, 9.3902}, {3664.48, 9.38911}, {3656.77, 9.38802}, {3652.91, 9.38748}, {3645.2, 9.3864}, {3637.48, 9.38532}, {3629.77, 9.38424}, {3625.91, 9.3837}, {3618.19, 9.38263}, {3610.48, 9.38155}, {3606.62, 9.38102}, {3598.91, 9.37995}, {3591.19, 9.37888}, {3587.33, 9.37834}, {3579.62, 9.37728}, {3571.91, 9.37621}, {3568.05, 9.37568}, {3560.33, 9.37462}, {3552.62, 9.37356}, {3548.76, 9.37303}, {3541.05, 9.37197}, {3537.19, 9.37144}, {3529.47, 9.37039}, {3521.76, 9.36934}, {3517.9, 9.36881}, {3510.19, 9.36776}, {3506.33, 9.36724}, {3498.62, 9.36619}, {3490.9, 9.36514}, {3487.04, 9.36462}, {3479.33, 9.36358}, {3475.47, 9.36306}, {3467.76, 9.36202}, {3463.9, 9.3615}, {3456.18, 9.36046}, {3448.47, 9.35942}, {3444.61, 9.35891}, {3436.9, 9.35787}, {3433.04, 9.35736}, {3425.33, 9.35632}, {3421.47, 9.35581}, {3413.75, 9.35478}, {3409.9, 9.35427}, {3402.18, 9.35324}, {3398.32, 9.35273}, {3390.61, 9.35171}, {3386.75, 9.3512}, {3379.04, 9.35017}, {3375.18, 9.34966}, {3367.47, 9.34865}, {3363.61, 9.34814}, {3355.89, 9.34712}, {3352.04, 9.34661}, {3348.18, 9.34611}, {3340.46, 9.3451}, {3336.61, 9.34459}, {3328.89, 9.34358}, {3325.04, 9.34308}, {3317.32, 9.34207}, {3313.46, 9.34156}, {3309.61, 9.34106}, {3301.89, 9.34006}, {3298.03, 9.33955}, {3290.32, 9.33855}, {3286.46, 9.33805}, {3278.75, 9.33705}, {3274.89, 9.33655}, {3271.03, 9.33605}, {3263.32, 9.33506}, {3259.46, 9.33456}, {3255.6, 9.33406}, {3247.89, 9.33307}, {3244.03, 9.33257}, {3236.32, 9.33158}, {3232.46, 9.33109}, {3228.6, 9.33059}, {3220.89, 9.3296}, {3217.03, 9.32911}, {3213.17, 9.32862}, {3205.46, 9.32763}, {3201.6, 9.32714}, {3197.74, 9.32665}, {3190.03, 9.32566}, {3186.17, 9.32517}, {3182.31, 9.32468}, {3178.46, 9.32419}, {3170.74, 9.32321}, {3166.88, 9.32272}, {3163.03, 9.32224}, {3155.31, 9.32126}, {3151.45, 9.32077}, {3147.6, 9.32029}, {3139.88, 9.31931}, {3136.02, 9.31883}, {3132.17, 9.31834}, {3128.31, 9.31786}, {3120.6, 9.31689}, {3116.74, 9.3164}, {3112.88, 9.31592}, {3109.02, 9.31543}, {3101.31, 9.31447}, {3097.45, 9.31398}, {3093.59, 9.3135}, {3089.74, 9.31302}, {3082.02, 9.31206}, {3078.16, 9.31158}, {3074.31, 9.3111}, {3070.45, 9.31061}, {3066.59, 9.31013}, {3058.88, 9.30918}, {3055.02, 9.3087}, {3051.16, 9.30822}, {3047.31, 9.30774}, {3039.59, 9.30678}, {3035.73, 9.30631}, {3031.88, 9.30583}, {3028.02, 9.30535}, {3024.16, 9.30487}, {3020.3, 9.3044}, {3012.59, 9.30345}, {3008.73, 9.30297}, {3004.88, 9.3025}, {3001.02, 9.30202}, {2997.16, 9.30155}, {2993.3, 9.30107}, {2985.59, 9.30013}, {2981.73, 9.29965}, {2977.87, 9.29918}, {2974.02, 9.29871}, {2970.16, 9.29823}, {2966.3, 9.29776}, {2958.59, 9.29682}, {2954.73, 9.29635}, {2950.87, 9.29588}, {2947.01, 9.2954}, {2943.16, 9.29493}, {2939.3, 9.29446}, {2935.44, 9.29399}, {2931.59, 9.29352}, {2927.73, 9.29306}, {2920.01, 9.29212}, {2916.16, 9.29165}, {2912.3, 9.29118}, {2908.44, 9.29071}, {2904.58, 9.29024}, {2900.73, 9.28978}, {2896.87, 9.28931}, {2893.01, 9.28884}, {2889.15, 9.28837}, {2885.3, 9.28791}, {2881.44, 9.28744}, {2873.73, 9.28651}, {2869.87, 9.28604}, {2866.01, 9.28558}, {2862.15, 9.28511}, {2858.3, 9.28465}, {2854.44, 9.28418}, {2850.58, 9.28372}, {2846.72, 9.28326}, {2842.87, 9.28279}, {2839.01, 9.28233}, {2835.15, 9.28186}, {2831.29, 9.2814}, {2827.44, 9.28094}, {2823.58, 9.28047}, {2819.72, 9.28001}, {2815.87, 9.27955}, {2812.01, 9.27909}, {2808.15, 9.27863}, {2804.29, 9.27816}, {2800.44, 9.2777}, {2796.58, 9.27724}, {2792.72, 9.27678}, {2788.86, 9.27632}, {2785.01, 9.27586}, {2781.15, 9.2754}, {2777.29, 9.27494}, {2773.43, 9.27448}, {2769.58, 9.27402}, {2765.72, 9.27356}, {2761.86, 9.2731}, {2758, 9.27264}, {2754.15, 9.27218}, {2750.29, 9.27172}, {2746.43, 9.27126}, {2742.58, 9.2708}, {2738.72, 9.27034}, {2734.86, 9.26988}, {2731, 9.26942}, {2727.15, 9.26897}, {2723.29, 9.26851}, {2719.43, 9.26805}, {2715.57, 9.26759}, {2711.72, 9.26713}, {2707.86, 9.26668}, {2704, 9.26622}, {2700.14, 9.26576}, {2696.29, 9.26531}, {2692.43, 9.26485}, {2688.57, 9.26439}, {2684.72, 9.26394}, {2680.86, 9.26348}, {2677, 9.26302}, {2673.14,

9.26257}, {2669.29, 9.26211}, {2665.43, 9.26165}, {2661.57, 9.2612}, {2657.71, 9.26074}, {2653.86, 9.26029}, {2650, 9.25983}, {2646.14, 9.25938}, {2642.28, 9.25892}, {2638.43, 9.25847}, {2634.57, 9.25801}, {2630.71, 9.25756}, {2626.85, 9.2571}, {2623, 9.25665}, {2619.14, 9.25619}, {2615.28, 9.25574}, {2611.43, 9.25528}, {2607.57, 9.25483}, {2603.71, 9.25437}, {2599.85, 9.25392}, {2596, 9.25347}, {2592.14, 9.25301}, {2588.28, 9.25256}, {2584.42, 9.2521}, {2580.57, 9.25165}, {2576.71, 9.25119}, {2572.85, 9.25074}, {2568.99, 9.25029}, {2565.14, 9.24983}, {2561.28, 9.24938}, {2557.42, 9.24893}, {2553.57, 9.24847}, {2549.71, 9.24802}, {2545.85, 9.24756}, {2541.99, 9.24711}, {2538.14, 9.24666}, {2534.28, 9.2462}, {2530.42, 9.24575}, {2526.56, 9.2453}, {2522.71, 9.24484}, {2518.85, 9.24439}, {2514.99, 9.24394}, {2511.13, 9.24348}, {2507.28, 9.24303}, {2503.42, 9.24258}, {2499.56, 9.24212}, {2495.71, 9.24167}, {2491.85, 9.24121}, {2487.99, 9.24076}, {2484.13, 9.24031}, {2480.28, 9.23985}, {2476.42, 9.2394}, {2472.56, 9.23895}, {2468.7, 9.23849}, {2464.85, 9.23804}, {2460.99, 9.23759}, {2457.13, 9.23713}, {2453.27, 9.23668}, {2449.42, 9.23622}, {2445.56, 9.23577}, {2441.7, 9.23531}, {2437.84, 9.23486}, {2433.99, 9.23441}, {2430.13, 9.23395}, {2426.27, 9.2335}, {2422.42, 9.23304}, {2418.56, 9.23259}, {2414.7, 9.23213}, {2410.84, 9.23168}, {2406.99, 9.23122}, {2403.13, 9.23077}, {2399.27, 9.23031}, {2395.41, 9.22986}, {2391.56, 9.2294}, {2387.7, 9.22895}, {2383.84, 9.22849}, {2379.98, 9.22803}, {2376.13, 9.22758}, {2372.27, 9.22712}, {2368.41, 9.22666}, {2364.56, 9.22621}, {2360.7, 9.22575}, {2356.84, 9.22529}, {2352.98, 9.22484}, {2349.13, 9.22438}, {2345.27, 9.22392}, {2341.41, 9.22347}, {2337.55, 9.22301}, {2333.7, 9.22255}, {2329.84, 9.22209}, {2325.98, 9.22163}, {2322.12, 9.22117}, {2318.27, 9.22072}, {2314.41, 9.22026}, {2310.55, 9.2198}, {2306.7, 9.21934}, {2302.84, 9.21888}, {2298.98, 9.21842}, {2295.12, 9.21796}, {2291.27, 9.2175}, {2287.41, 9.21704}, {2283.55, 9.21657}, {2279.69, 9.21611}, {2275.84, 9.21565}, {2271.98, 9.21519}, {2268.12, 9.21473}, {2264.26, 9.21426}, {2260.41, 9.2138}, {2256.55, 9.21334}, {2252.69, 9.21287}, {2248.83, 9.21241}, {2244.98, 9.21195}, {2241.12, 9.21148}, {2237.26, 9.21102}, {2233.41, 9.21055}, {2229.55, 9.21009}, {2225.69, 9.20962}, {2221.83, 9.20915}, {2217.98, 9.20869}, {2214.12, 9.20822}, {2210.26, 9.20775}, {2206.4, 9.20729}, {2202.55, 9.20682}, {2198.69, 9.20635}, {2194.83, 9.20588}, {2190.97, 9.20541}, {2187.12, 9.20494}, {2183.26, 9.20447}, {2179.4, 9.204}, {2175.55, 9.20353}, {2171.69, 9.20306}, {2167.83, 9.20258}, {2163.97, 9.20211}, {2160.12, 9.20164}, {2156.26, 9.20116}, {2152.4, 9.20069}, {2148.54, 9.20022}, {2144.69, 9.19974}, {2140.83, 9.19927}, {2136.97, 9.19879}, {2133.11, 9.19831}, {2129.26, 9.19784}, {2125.4, 9.19736}, {2121.54, 9.19688}, {2117.68, 9.1964}, {2113.83, 9.19592}, {2109.97, 9.19544}, {2106.11, 9.19496}, {2102.26, 9.19448}, {2098.4, 9.194}, {2094.54, 9.19351}, {2090.68, 9.19303}, {2086.83, 9.19255}, {2082.97, 9.19206}, {2079.11, 9.19158}, {2075.25, 9.19109}, {2071.4, 9.1906}, {2067.54, 9.19012}, {2063.68, 9.18963}, {2059.82, 9.18914}, {2055.97, 9.18865}, {2052.11, 9.18816}, {2048.25, 9.18767}, {2044.4, 9.18718}, {2040.54, 9.18669}, {2036.68, 9.18619}, {2032.82, 9.1857}, {2028.97, 9.18521}, {2025.11, 9.18471}, {2021.25, 9.18421}, {2017.39, 9.18372}, {2013.54, 9.18322}, {2009.68, 9.18272}, {2005.82, 9.18222}, {2001.96, 9.18172}, {1998.11, 9.18122}, {1994.25, 9.18072}, {1990.39, 9.18021}, {1986.54, 9.17971}, {1982.68, 9.17921}, {1978.82, 9.1787}, {1974.96, 9.17819}, {1971.11, 9.17769}, {1967.25, 9.17718}, {1963.39, 9.17667}, {1959.53, 9.17616}, {1955.68, 9.17564}, {1951.82, 9.17513}, {1947.96, 9.17462}, {1944.1, 9.1741}, {1940.25, 9.17359}, {1936.39, 9.17307}, {1932.53, 9.17255}, {1928.67, 9.17203}, {1924.82, 9.17151}, {1920.96, 9.17099}, {1917.1, 9.17047}, {1913.25, 9.16995}, {1909.39, 9.16942}, {1905.53, 9.1689}, {1901.67, 9.16837}, {1897.82, 9.16784}, {1893.96, 9.16731}, {1890.1, 9.16678}, {1886.24, 9.16625}, {1882.39, 9.16571}, {1878.53, 9.16518}, {1874.67, 9.16464}, {1870.81, 9.16411}, {1866.96, 9.16357}, {1863.1, 9.16303}, {1859.24, 9.16249}, {1855.39, 9.16194}, {1851.53, 9.1614}, {1847.67, 9.16085}, {1843.81, 9.16031}, {1839.96, 9.15976}, {1836.1, 9.15921}, {1832.24, 9.15866}, {1828.38, 9.1581}, {1824.53, 9.15755}, {1820.67, 9.15699}, {1816.81, 9.15644}, {1812.95, 9.15588}, {1809.1, 9.15532}, {1805.24, 9.15475}, {1801.38, 9.15419}, {1797.53, 9.15362}, {1793.67, 9.15306}, {1789.81, 9.15249}, {1785.95, 9.15192}, {1782.1, 9.15135}, {1778.24, 9.15077}, {1774.38, 9.1502}, {1770.52, 9.14962}, {1766.67, 9.14904}, {1762.81, 9.14846}, {1758.95, 9.14787}, {1755.09, 9.14729}, {1751.24, 9.1467}, {1747.38, 9.14611}, {1743.52, 9.14552}, {1739.66, 9.14493}, {1735.81, 9.14433}, {1731.95, 9.14374}, {1728.09, 9.14314}, {1724.24, 9.14254}, {1720.38, 9.14193}, {1716.52, 9.14133}, {1712.66, 9.14072}, {1708.81, 9.14011}, {1704.95, 9.1395}, {1701.09, 9.13888}, {1697.23, 9.13827}, {1693.38, 9.13765}, {1689.52, 9.13703}, {1685.66, 9.1364}, {1681.8, 9.13578}, {1677.95, 9.13515}, {1674.09, 9.13452}, {1670.23, 9.13389}, {1666.38, 9.13325}, {1662.52, 9.13261}, {1658.66, 9.13197}, {1654.8, 9.13133}, {1650.95, 9.13069}, {1647.09, 9.13004}, {1643.23, 9.12939}, {1639.37, 9.12873}, {1635.52, 9.12808}, {1631.66, 9.12742}, {1627.8, 9.12676}, {1623.94, 9.12609}, {1620.09, 9.12542}, {1616.23, 9.12475}, {1612.37, 9.12408}, {1608.51, 9.1234}, {1604.66, 9.12272}, {1600.8, 9.12204}, {1596.94, 9.12136}, {1593.09, 9.12067}, {1589.23, 9.11998}, {1585.37, 9.11928}, {1581.51, 9.11858}, {1577.66, 9.11788}, {1573.8, 9.11718}, {1569.94, 9.11647}, {1566.08, 9.11576}, {1562.23, 9.11504}, {1558.37, 9.11432}, {1554.51, 9.1136}, {1550.65, 9.11288}, {1546.8, 9.11215}, {1542.94, 9.11142}, {1539.08, 9.11068}, {1535.23, 9.10994}, {1531.37, 9.1092}, {1527.51, 9.10845}, {1523.65, 9.1077}, {1519.8, 9.10694}, {1515.94, 9.10618}, {1512.08, 9.10542}, {1508.22, 9.10465}, {1504.37, 9.10388}, {1500.51, 9.1031}, {1496.65, 9.10232}, {1492.79, 9.10154}, {1488.94, 9.10075}, {1485.08, 9.09996}, {1481.22, 9.09916}, {1477.37, 9.09836}, {1473.51, 9.09755}, {1469.65, 9.09674}, {1465.79, 9.09593}, {1461.94, 9.09511}, {1458.08, 9.09428}, {1454.22, 9.09345}, {1450.36, 9.09262}, {1446.51, 9.09178}, {1442.65, 9.09093}, {1438.79, 9.09008}, {1434.93, 9.08923}, {1431.08, 9.08837}, {1427.22, 9.0875}, {1423.36, 9.08663}, {1419.5, 9.08575}, {1415.65, 9.08487}, {1411.79, 9.08398}, {1407.93, 9.08309}, {1404.08, 9.08219}, {1400.22, 9.08129}, {1396.36, 9.08038}, {1392.5, 9.07946}, {1388.65, 9.07854}, {1384.79, 9.07761}, {1380.93, 9.07667}, {1377.07, 9.07573}, {1373.22, 9.07479}, {1369.36, 9.07383}, {1365.5, 9.07287}, {1361.64, 9.07191}, {1357.79, 9.07093}, {1353.93, 9.06995}, {1350.07, 9.06896}, {1346.22, 9.06797}, {1342.36, 9.06697}, {1338.5, 9.06596}, {1334.64, 9.06495}, {1330.79, 9.06392}, {1326.93, 9.06289}, {1323.07, 9.06185}, {1319.21, 9.06081}, {1315.36, 9.05976}, {1311.5, 9.05869}, {1307.64, 9.05763}, {1303.78, 9.05655}, {1299.93, 9.05546}, {1296.07, 9.05437}, {1292.21, 9.05327}, {1288.35, 9.05216}, {1284.5, 9.05104}, {1280.64, 9.04991}, {1276.78, 9.04877}, {1272.93, 9.04763}, {1269.07, 9.04647}, {1265.21, 9.04531}, {1261.35, 9.04413}, {1257.5, 9.04295}, {1253.64, 9.04175}, {1249.78, 9.04055}, {1245.92, 9.03934}, {1242.07, 9.03811}, {1238.21, 9.03688}, {1234.35, 9.03564}, {1230.49, 9.03438}, {1226.64, 9.03312}, {1222.78, 9.03184}, {1218.92, 9.03055}, {1215.07, 9.02926}, {1211.21, 9.02795}, {1207.35, 9.02663}, {1203.49, 9.02529}, {1199.64, 9.02395}, {1195.78, 9.02259}, {1191.92, 9.02122}, {1188.06, 9.01984}, {1184.21, 9.01845}, {1180.35, 9.01704}, {1176.49, 9.01562}, {1172.63, 9.01418}, {1168.78, 9.01274}, {1164.92, 9.01128}, {1161.06, 9.0098}, {1157.21, 9.00832}, {1153.35, 9.00681}, {1149.49, 9.0053}, {1145.63, 9.00376}, {1141.78, 9.00222}, {1137.92, 9.00065}, {1134.06, 8.99908}, {1130.2, 8.99748}, {1126.35, 8.99588}, {1122.49, 8.99425}, {1118.63, 8.99261}, {1114.77, 8.99095}, {1110.92, 8.98927}, {1107.06, 8.98758}, {1103.2, 8.98587}, {1099.34, 8.98414}, {1095.49, 8.9824}, {1091.63, 8.98063}, {1087.77, 8.97885}, {1083.92, 8.97705}, {1080.06, 8.97522}, {1076.2, 8.97338}, {1072.34, 8.97152}, {1068.49, 8.96964}, {1064.63, 8.96773}, {1060.77, 8.96581}, {1056.91, 8.96387}, {1053.06, 8.9619}, {1049.2, 8.95991}, {1045.34, 8.9579}, {1041.48, 8.95586}, {1037.63, 8.9538}, {1033.77, 8.95172}, {1029.91, 8.94961}, {1026.06, 8.94748}, {1022.2, 8.94533}, {1018.34, 8.94314}, {1014.48, 8.94094}, {1010.63, 8.9387}, {1006.77, 8.93644}, {1002.91, 8.93415}, {999.053, 8.93183}, {995.196, 8.92949}, {991.339, 8.92711}, {987.481, 8.92471}, {983.624, 8.92227}, {979.767, 8.91981}, {975.909, 8.91731}, {972.052, 8.91478}, {968.195, 8.91222}, {964.337, 8.90963}, {960.48, 8.907}, {956.622, 8.90434}, {952.765, 8.90164}, {948.908, 8.89891}, {945.05, 8.89614}, {941.193, 8.89333}, {937.336, 8.89049}, {933.478, 8.8876}, {929.621, 8.88468}, {925.764, 8.88172}, {921.906, 8.87871}, {918.049, 8.87566}, {914.192, 8.87258}, {910.334, 8.86944}, {906.477, 8.86626}, {902.62, 8.86304}, {898.762, 8.85977}, {894.905, 8.85645}, {891.048, 8.85308}, {887.19, 8.84967}, {883.333, 8.8462}, {879.476, 8.84268}, {875.618, 8.83911}, {871.761, 8.83548}, {867.903, 8.8318}, {864.046, 8.82806}, {860.189, 8.82427}, {856.331, 8.82041}, {852.474, 8.8165}, {848.617, 8.81252}, {844.759, 8.80848}, {840.902, 8.80438}, {837.045, 8.8002}, {833.187, 8.79596}, {829.33, 8.79165}, {825.473, 8.78728}, {821.615, 8.78282}, {817.758, 8.77829}, {813.901, 8.77369}, {810.043, 8.76901}, {806.186, 8.76425}, {802.329, 8.7594}, {798.471, 8.75447}, {794.614, 8.74946}, {790.756, 8.74435}, {786.899, 8.73916}, {783.042, 8.73387}, {779.184, 8.72849}, {775.327, 8.72301}, {771.47, 8.71742}, {767.612, 8.71174}, {763.755, 8.70595}, {759.898, 8.70005}, {756.04, 8.69403}, {752.183, 8.68791}, {748.326, 8.68166}, {744.468, 8.6753}, {740.611, 8.6688}, {736.754, 8.66219}, {732.896, 8.65543}, {729.039, 8.64855}, {725.182, 8.64152}, {721.324, 8.63435}, {717.467, 8.62703}, {713.609, 8.61956}, {709.752, 8.61193}, {705.895, 8.60414}, {702.037, 8.59618}, {698.18, 8.58805}, {694.323, 8.57975}, {690.465, 8.57126}, {686.608, 8.56258}, {682.751, 8.55371}, {678.893, 8.54463}, {675.036, 8.53535}, {671.179,

```
8.52586}, {667.321, 8.51614}, {663.464, 8.50619}, {659.607, 8.49601}, {655.749, 8.48558}, {651.892, 8.4749}, {648.035, 8.46396}, {644.177, 8.45275}, {640.32,
8.44125}, {636.463, 8.42946}, {632.605, 8.41737}, {628.748, 8.40497}, {624.891, 8.39224}, {621.033, 8.37918}, {617.176, 8.36576}, {613.318, 8.35198},
{609.461, 8.33782}, {605.604, 8.32327}, {601.746, 8.30831}, {597.889, 8.29292}, {594.032, 8.27709}, {590.174, 8.26079}, {586.317, 8.24402}, {582.46, 8.22674},
{578.602, 8.20894}, {574.745, 8.19059}, {570.888, 8.17167}, {567.03, 8.15215}, {563.173, 8.132}, {559.316, 8.1112}, {555.458, 8.08971}, {551.601, 8.06751},
{547.744, 8.04455}, {543.886, 8.02079}, {540.029, 7.99621}, {536.171, 7.97074}, {532.314, 7.94437}, {528.457, 7.91702}, {524.599, 7.88864}, {520.742, 7.8592},
{516.885, 7.82861}, {513.027, 7.79682}, {509.17, 7.76376}, {505.313, 7.72936}, {501.455, 7.69351}, {497.598, 7.65616}, {493.741, 7.6172}, {489.883, 7.57651},
{486.026, 7.534}, {482.169, 7.48955}, {478.311, 7.443}, {474.454, 7.39424}, {470.597, 7.3431}, {466.739, 7.28938}, {462.882, 7.23292}, {459.025, 7.1735},
{455.167, 7.11087}, {451.31, 7.0448}, {447.452, 6.97498}, {443.595, 6.90111}, {439.738, 6.82283}, {435.88, 6.73971}, {432.023, 6.65136}, {428.166, 6.55724},
{424.308, 6.45676}, {420.451, 6.34932}, {416.594, 6.23415}, {412.736, 6.11038}, {408.879, 5.97708}, {405.022, 5.83311}, {401.164, 5.67709}, {397.307,
5.50757}, {393.45, 5.32269}, {389.592, 5.12024}, {385.735, 4.89774}, {381.878, 4.65204}, {378.02, 4.37926}, {374.163, 4.0749}, {370.305, 3.73299}, {366.448,
3.34641}, {362.591, 2.90574}, {358.733, 2.39873}, {354.876, 1.80962}, {351.019, 1.11664}, {347.161, 0.289606}, {343.304, −0.713804}, {339.447, −1.95682},
{335.589, −3.537}, {331.732, −5.61139}, {327.875, −8.45493}, {324.017, −12.5929}, {320.16, −19.1632}, {316.303, −31.2014}, {312.445, −60.3726}, {308.588,
−229.636}, {304.731, 171.942}, {300.873, 71.2249}, {297.016, 47.645}, {293.159, 37.1462}, {289.301, 31.2087}, {285.444, 27.3932}, {281.586, 24.7342},
{277.729, 22.7764}, {273.872, 21.2748}, {270.014, 20.0867}, {266.157, 19.1238}, {262.3, 18.3278}, {258.442, 17.6587}, {254.585, 17.0888}, {250.728, 16.5977},
{246.87, 16.1701}, {243.013, 15.7948}, {239.156, 15.4627}, {235.298, 15.1668}, {231.441, 14.9018}, {227.584, 14.6631}, {223.726, 14.4469}, {219.869, 14.2505},
{216.012, 14.0712}, {212.154, 13.907}, {208.297, 13.7561}, {204.439, 13.617}, {200.582, 13.4886}, {196.725, 13.3696}, {192.867, 13.259}, {189.01, 13.1562},
{185.153, 13.0604}, {181.295, 12.9709}, {177.438, 12.8872}, {173.581, 12.8088}, {169.723, 12.7352}, {165.866, 12.6662}, {162.009, 12.6012}, {158.151,
12.5401}, {154.294, 12.4825}, {150.437, 12.4282}, {146.579, 12.3769}, {142.722, 12.3285}, {138.865, 12.2828}, {135.007, 12.2396}, {131.15, 12.1987}, {127.293,
12.1601}, {123.435, 12.1235}, {119.578, 12.0889}, {115.72, 12.0562}, {111.863, 12.0252}, {108.006, 11.9959}, {104.148, 11.9682}, {100.291, 11.942}};

inp=Interpolation[inpraw];

InAsraw={{7876.71, 12.8467}, {7845.85, 12.8459}, {7814.99, 12.8452}, {7784.13, 12.8445}, {7753.27, 12.8439}, {7722.41, 12.8433}, {7695.41, 12.8429}, {7664.55,
12.8424}, {7633.69, 12.842}, {7606.69, 12.8416}, {7575.83, 12.8413}, {7548.83, 12.841}, {7521.83, 12.8408}, {7490.97, 12.8407}, {7463.97, 12.8405}, {7436.97,
12.8405}, {7409.97, 12.8404}, {7382.97, 12.8404}, {7355.96, 12.8405}, {7328.96, 12.8406}, {7301.96, 12.8407}, {7274.96, 12.8409}, {7247.96, 12.8411},
{7220.96, 12.8414}, {7197.81, 12.8417}, {7170.81, 12.8421}, {7143.81, 12.8425}, {7120.67, 12.8429}, {7093.66, 12.8434}, {7070.52, 12.8439}, {7043.52,
12.8445}, {7020.38, 12.8451}, {6993.37, 12.8459}, {6970.23, 12.8466}, {6947.09, 12.8474}, {6923.94, 12.8482}, {6896.94, 12.8492}, {6873.8, 12.8501}, {6850.65,
12.8511}, {6827.51, 12.8522}, {6804.36, 12.8534}, {6781.22, 12.8546}, {6758.08, 12.8559}, {6734.93, 12.8573}, {6711.79, 12.8588}, {6692.5, 12.8601},
{6669.36, 12.8617}, {6646.21, 12.8635}, {6623.07, 12.8653}, {6603.78, 12.8669}, {6580.64, 12.8689}, {6557.49, 12.871}, {6538.21, 12.8728}, {6515.06, 12.8751},
{6495.78, 12.877}, {6472.63, 12.8793}, {6453.34, 12.8813}, {6434.06, 12.8834}, {6410.91, 12.8858}, {6391.63, 12.8878}, {6372.34, 12.8898}, {6353.05,
12.8918}, {6329.91, 12.8942}, {6310.62, 12.896}, {6291.34, 12.8978}, {6272.05, 12.8996}, {6252.76, 12.9012}, {6233.48, 12.9026}, {6214.19, 12.904}, {6194.9,
12.9052}, {6175.62, 12.9062}, {6156.33, 12.907}, {6137.04, 12.9077}, {6117.76, 12.9081}, {6098.47, 12.9083}, {6079.18, 12.9084}, {6063.75, 12.9082}, {6044.47,
12.9078}, {6025.18, 12.9073}, {6009.75, 12.9066}, {5990.46, 12.9056}, {5971.18, 12.9045}, {5955.75, 12.9034}, {5936.46, 12.9018}, {5917.17, 12.9001},
{5901.74, 12.8987}, {5882.46, 12.8967}, {5867.03, 12.895}, {5851.6, 12.8932}, {5832.31, 12.8909}, {5816.88, 12.889}, {5797.6, 12.8865}, {5782.17, 12.8845},
{5766.74, 12.8825}, {5747.45, 12.8799}, {5732.02, 12.8778}, {5716.59, 12.8757}, {5701.16, 12.8736}, {5681.88, 12.871}, {5666.45, 12.869}, {5651.02, 12.8669},
{5635.59, 12.8649}, {5620.16, 12.863}, {5604.73, 12.861}, {5589.3, 12.8591}, {5573.87, 12.8573}, {5558.44, 12.8555}, {5543.01, 12.8537}, {5527.58, 12.852},
{5512.15, 12.8504}, {5496.72, 12.8488}, {5481.29, 12.8472}, {5465.86, 12.8457}, {5450.43, 12.8443}, {5435, 12.8429}, {5423.43, 12.8419}, {5408, 12.8406},
{5392.57, 12.8394}, {5377.14, 12.8382}, {5365.57, 12.8373}, {5350.14, 12.8362}, {5334.71, 12.8352}, {5319.28, 12.8342}, {5307.71, 12.8335}, {5292.28,
12.8325}, {5280.71, 12.8319}, {5265.28, 12.831}, {5249.85, 12.8302}, {5238.28, 12.8296}, {5222.85, 12.8289}, {5211.28, 12.8283}, {5195.85, 12.8277}, {5184.28,
12.8272}, {5168.85, 12.8266}, {5157.28, 12.8261}, {5141.85, 12.8255}, {5130.27, 12.8251}, {5118.7, 12.8248}, {5103.27, 12.8243}, {5091.7, 12.8239}, {5076.27,
12.8235}, {5064.7, 12.8232}, {5053.13, 12.8229}, {5041.56, 12.8226}, {5026.13, 12.8223}, {5014.55, 12.822}, {5002.98, 12.8218}, {4987.55, 12.8215}, {4975.98,
12.8213}, {4964.41, 12.8211}, {4952.84, 12.821}, {4941.26, 12.8208}, {4929.69, 12.8207}, {4914.26, 12.8205}, {4902.69, 12.8204}, {4891.12, 12.8203},
{4879.55, 12.8202}, {4867.97, 12.8201}, {4856.4, 12.82}, {4844.83, 12.82}, {4833.26, 12.8199}, {4821.69, 12.8199}, {4810.11, 12.8199}, {4798.54, 12.8199},
{4786.97, 12.8199}, {4775.4, 12.8199}, {4763.83, 12.8199}, {4752.25, 12.82}, {4740.68, 12.82}, {4729.11, 12.8201}, {4717.54, 12.8202}, {4705.97, 12.8202},
{4698.25, 12.8203}, {4686.68, 12.8204}, {4675.11, 12.8205}, {4663.54, 12.8206}, {4651.96, 12.8208}, {4640.39, 12.8209}, {4632.68, 12.821}, {4621.1, 12.8212},
{4609.53, 12.8213}, {4597.96, 12.8215}, {4590.25, 12.8217}, {4578.67, 12.8219}, {4567.1, 12.8221}, {4559.39, 12.8222}, {4547.81, 12.8225}, {4536.24, 12.8227},
{4528.53, 12.8229}, {4516.96, 12.8231}, {4505.38, 12.8234}, {4497.67, 12.8236}, {4486.1, 12.8239}, {4474.52, 12.8242}, {4466.81, 12.8244}, {4455.24,
12.8247}, {4447.52, 12.8249}, {4435.95, 12.8253}, {4428.24, 12.8255}, {4416.66, 12.8259}, {4408.95, 12.8261}, {4397.38, 12.8265}, {4389.66, 12.8267},
{4378.09, 12.8271}, {4370.38, 12.8274}, {4358.8, 12.8278}, {4351.09, 12.8281}, {4339.52, 12.8285}, {4331.8, 12.8288}, {4320.23, 12.8293}, {4312.52, 12.8296},
{4304.8, 12.8299}, {4293.23, 12.8304}, {4285.51, 12.8307}, {4273.94, 12.8312}, {4266.23, 12.8316}, {4258.51, 12.8319}, {4246.94, 12.8325}, {4239.23, 12.8328},
{4231.51, 12.8332}, {4219.94, 12.8338}, {4212.23, 12.8341}, {4204.51, 12.8345}, {4192.94, 12.8351}, {4185.22, 12.8355}, {4177.51, 12.8359}, {4169.79,
12.8364}, {4158.22, 12.837}, {4150.51, 12.8374}, {4142.79, 12.8379}, {4135.08, 12.8383}, {4127.36, 12.8388}, {4115.79, 12.8395}, {4108.08, 12.84}, {4100.36,
12.8404}, {4092.65, 12.8409}, {4084.93, 12.8414}, {4073.36, 12.8422}, {4065.65, 12.8427}, {4057.93, 12.8432}, {4050.22, 12.8437}, {4042.5, 12.8442}, {4034.79,
12.8448}, {4027.07, 12.8453}, {4019.36, 12.8459}, {4011.64, 12.8465}, {4000.07, 12.8473}, {3992.36, 12.8479}, {3984.64, 12.8485}, {3976.93, 12.8491},
{3969.21, 12.8497}, {3961.5, 12.8503}, {3953.78, 12.8509}, {3946.07, 12.8516}, {3938.35, 12.8522}, {3930.64, 12.8529}, {3922.92, 12.8536}, {3915.21, 12.8542},
{3907.49, 12.8549}, {3899.78, 12.8556}, {3892.07, 12.8563}, {3884.35, 12.857}, {3876.64, 12.8578}, {3868.92, 12.8585}, {3861.21, 12.8592}, {3857.35,
12.8596}, {3849.63, 12.8604}, {3841.92, 12.8612}, {3834.21, 12.862}, {3826.49, 12.8628}, {3818.78, 12.8636}, {3811.06, 12.8644}, {3803.35, 12.8652}, {3795.63,
12.8661}, {3787.92, 12.867}, {3784.06, 12.8674}, {3776.34, 12.8683}, {3768.63, 12.8692}, {3760.92, 12.8701}, {3753.2, 12.8711}, {3745.49, 12.872}, {3741.63,
12.8725}, {3733.91, 12.8735}, {3726.2, 12.8744}, {3718.48, 12.8755}, {3710.77, 12.8765}, {3706.91, 12.877}, {3699.2, 12.878}, {3691.48, 12.8791}, {3683.77,
12.8802}, {3679.91, 12.8808}, {3672.2, 12.8819}, {3664.48, 12.883}, {3656.77, 12.8842}, {3652.91, 12.8848}, {3645.2, 12.886}, {3637.48, 12.8872}, {3629.77,
12.8884}, {3625.91, 12.8891}, {3618.19, 12.8903}, {3610.48, 12.8916}, {3606.62, 12.8923}, {3598.91, 12.8936}, {3591.19, 12.895}, {3587.33, 12.8957}, {3579.62,
12.8971}, {3571.91, 12.8986}, {3568.05, 12.8993}, {3560.33, 12.9008}, {3552.62, 12.9023}, {3548.76, 12.9031}, {3541.05, 12.9047}, {3537.19, 12.9055},
{3529.47, 12.9072}, {3521.76, 12.9088}, {3517.9, 12.9097}, {3510.19, 12.9114}, {3506.33, 12.9123}, {3498.62, 12.9141}, {3490.9, 12.916}, {3487.04, 12.9169},
{3479.33, 12.9188}, {3475.47, 12.9198}, {3467.76, 12.9218}, {3463.9, 12.9229}, {3456.18, 12.9249}, {3448.47, 12.9271}, {3444.61, 12.9282}, {3436.9, 12.9304},
{3433.04, 12.9316}, {3425.33, 12.934}, {3421.47, 12.9352}, {3413.75, 12.9376}, {3409.9, 12.9389}, {3402.18, 12.9415}, {3398.32, 12.9428}, {3390.61, 12.9455},
{3386.75, 12.9469}, {3379.04, 12.9498}, {3375.18, 12.9512}, {3367.47, 12.9543}, {3363.61, 12.9558}, {3355.89, 12.959}, {3352.04, 12.9606}, {3348.18, 12.9623},
```

{3340.46, 12.9657}, {3336.61, 12.9675}, {3328.89, 12.9711}, {3325.04, 12.973}, {3317.32, 12.9768}, {3313.46, 12.9788}, {3309.61, 12.9808}, {3301.89, 12.985}, {3298.03, 12.9871}, {3290.32, 12.9915}, {3286.46, 12.9937}, {3278.75, 12.9984}, {3274.89, 13.0008}, {3271.03, 13.0032}, {3263.32, 13.0082}, {3259.46, 13.0108}, {3255.6, 13.0134}, {3247.89, 13.0188}, {3244.03, 13.0216}, {3236.32, 13.0273}, {3232.46, 13.0302}, {3228.6, 13.0331}, {3220.89, 13.0391}, {3217.03, 13.0422}, {3213.17, 13.0454}, {3205.46, 13.0518}, {3201.6, 13.055}, {3197.74, 13.0583}, {3190.03, 13.0651}, {3186.17, 13.0685}, {3182.31, 13.0719}, {3178.46, 13.0754}, {3170.74, 13.0825}, {3166.88, 13.0861}, {3163.03, 13.0897}, {3155.31, 13.0969}, {3151.45, 13.1005}, {3147.6, 13.1042}, {3139.88, 13.1115}, {3136.02, 13.1152}, {3132.17, 13.1189}, {3128.31, 13.1225}, {3120.6, 13.1298}, {3116.74, 13.1334}, {3112.88, 13.137}, {3109.02, 13.1405}, {3101.31, 13.1475}, {3097.45, 13.1509}, {3093.59, 13.1543}, {3089.74, 13.1576}, {3082.02, 13.1641}, {3078.16, 13.1672}, {3074.31, 13.1703}, {3070.45, 13.1732}, {3066.59, 13.1761}, {3058.88, 13.1815}, {3055.02, 13.1841}, {3051.16, 13.1866}, {3047.31, 13.1889}, {3039.59, 13.1933}, {3035.73, 13.1953}, {3031.88, 13.1971}, {3028.02, 13.1988}, {3024.16, 13.2004}, {3020.3, 13.2018}, {3012.59, 13.2041}, {3008.73, 13.2051}, {3004.88, 13.2059}, {3001.02, 13.2065}, {2997.16, 13.207}, {2993.3, 13.2072}, {2985.59, 13.2073}, {2981.73, 13.207}, {2977.87, 13.2066}, {2974.02, 13.206}, {2970.16, 13.2052}, {2966.3, 13.2043}, {2958.59, 13.2018}, {2954.73, 13.2003}, {2950.87, 13.1986}, {2947.01, 13.1967}, {2943.16, 13.1947}, {2939.3, 13.1925}, {2935.44, 13.1901}, {2931.59, 13.1875}, {2927.73, 13.1848}, {2920.01, 13.1788}, {2916.16, 13.1756}, {2912.3, 13.1722}, {2908.44, 13.1687}, {2904.58, 13.165}, {2900.73, 13.1611}, {2896.87, 13.1572}, {2893.01, 13.1531}, {2889.15, 13.1488}, {2885.3, 13.1445}, {2881.44, 13.14}, {2873.73, 13.1307}, {2869.87, 13.1259}, {2866.01, 13.121}, {2862.15, 13.1159}, {2858.3, 13.1108}, {2854.44, 13.1057}, {2850.58, 13.1004}, {2846.72, 13.0951}, {2842.87, 13.0897}, {2839.01, 13.0842}, {2835.15, 13.0787}, {2831.29, 13.0731}, {2827.44, 13.0675}, {2823.58, 13.0619}, {2819.72, 13.0562}, {2815.87, 13.0505}, {2812.01, 13.0448}, {2808.15, 13.039}, {2804.29, 13.0332}, {2800.44, 13.0275}, {2796.58, 13.0217}, {2792.72, 13.0159}, {2788.86, 13.0101}, {2785.01, 13.0043}, {2781.15, 12.9986}, {2777.29, 12.9928}, {2773.43, 12.9871}, {2769.58, 12.9814}, {2765.72, 12.9757}, {2761.86, 12.9701}, {2758, 12.9645}, {2754.15, 12.9589}, {2750.29, 12.9533}, {2746.43, 12.9478}, {2742.58, 12.9424}, {2738.72, 12.9369}, {2734.86, 12.9315}, {2731, 12.9262}, {2727.15, 12.9209}, {2723.29, 12.9157}, {2719.43, 12.9105}, {2715.57, 12.9054}, {2711.72, 12.9003}, {2707.86, 12.8953}, {2704, 12.8903}, {2700.14, 12.8854}, {2696.29, 12.8805}, {2692.43, 12.8757}, {2688.57, 12.8709}, {2684.72, 12.8662}, {2680.86, 12.8616}, {2677, 12.857}, {2673.14, 12.8525}, {2669.29, 12.848}, {2665.43, 12.8436}, {2661.57, 12.8392}, {2657.71, 12.8349}, {2653.86, 12.8306}, {2650, 12.8264}, {2646.14, 12.8223}, {2642.28, 12.8182}, {2638.43, 12.8141}, {2634.57, 12.8101}, {2630.71, 12.8062}, {2626.85, 12.8023}, {2623, 12.7984}, {2619.14, 12.7946}, {2615.28, 12.7909}, {2611.43, 12.7872}, {2607.57, 12.7835}, {2603.71, 12.7799}, {2599.85, 12.7763}, {2596, 12.7728}, {2592.14, 12.7693}, {2588.28, 12.7658}, {2584.42, 12.7624}, {2580.57, 12.759}, {2576.71, 12.7557}, {2572.85, 12.7524}, {2568.99, 12.7491}, {2565.14, 12.7459}, {2561.28, 12.7427}, {2557.42, 12.7396}, {2553.57, 12.7364}, {2549.71, 12.7333}, {2545.85, 12.7303}, {2541.99, 12.7273}, {2538.14, 12.7243}, {2534.28, 12.7213}, {2530.42, 12.7184}, {2526.56, 12.7155}, {2522.71, 12.7126}, {2518.85, 12.7097}, {2514.99, 12.7069}, {2511.13, 12.7041}, {2507.28, 12.7013}, {2503.42, 12.6986}, {2499.56, 12.6959}, {2495.71, 12.6932}, {2491.85, 12.6905}, {2487.99, 12.6878}, {2484.13, 12.6852}, {2480.28, 12.6826}, {2476.42, 12.68}, {2472.56, 12.6774}, {2468.7, 12.6749}, {2464.85, 12.6724}, {2460.99, 12.6699}, {2457.13, 12.6674}, {2453.27, 12.6649}, {2449.42, 12.6625}, {2445.56, 12.6601}, {2441.7, 12.6576}, {2437.84, 12.6553}, {2433.99, 12.6529}, {2430.13, 12.6505}, {2426.27, 12.6482}, {2422.42, 12.6459}, {2418.56, 12.6436}, {2414.7, 12.6413}, {2410.84, 12.639}, {2406.99, 12.6367}, {2403.13, 12.6345}, {2399.27, 12.6323}, {2395.41, 12.6301}, {2391.56, 12.6279}, {2387.7, 12.6257}, {2383.84, 12.6235}, {2379.98, 12.6214}, {2376.13, 12.6192}, {2372.27, 12.6171}, {2368.41, 12.615}, {2364.56, 12.6129}, {2360.7, 12.6108}, {2356.84, 12.6087}, {2352.98, 12.6067}, {2349.13, 12.6046}, {2345.27, 12.6026}, {2341.41, 12.6006}, {2337.55, 12.5986}, {2333.7, 12.5966}, {2329.84, 12.5946}, {2325.98, 12.5926}, {2322.12, 12.5907}, {2318.27, 12.5887}, {2314.41, 12.5868}, {2310.55, 12.5849}, {2306.7, 12.5829}, {2302.84, 12.581}, {2298.98, 12.5791}, {2295.12, 12.5773}, {2291.27, 12.5754}, {2287.41, 12.5735}, {2283.55, 12.5717}, {2279.69, 12.5698}, {2275.84, 12.568}, {2271.98, 12.5662}, {2268.12, 12.5644}, {2264.26, 12.5626}, {2260.41, 12.5608}, {2256.55, 12.559}, {2252.69, 12.5572}, {2248.83, 12.5555}, {2244.98, 12.5537}, {2241.12, 12.552}, {2237.26, 12.5502}, {2233.41, 12.5485}, {2229.55, 12.5468}, {2225.69, 12.5451}, {2221.83, 12.5434}, {2217.98, 12.5417}, {2214.12, 12.54}, {2210.26, 12.5383}, {2206.4, 12.5367}, {2202.55, 12.535}, {2198.69, 12.5334}, {2194.83, 12.5317}, {2190.97, 12.5301}, {2187.12, 12.5285}, {2183.26, 12.5269}, {2179.4, 12.5252}, {2175.55, 12.5237}, {2171.69, 12.5221}, {2167.83, 12.5205}, {2163.97, 12.5189}, {2160.12, 12.5173}, {2156.26, 12.5158}, {2152.4, 12.5142}, {2148.54, 12.5127}, {2144.69, 12.5111}, {2140.83, 12.5096}, {2136.97, 12.5081}, {2133.11, 12.5066}, {2129.26, 12.5051}, {2125.4, 12.5036}, {2121.54, 12.5021}, {2117.68, 12.5006}, {2113.83, 12.4991}, {2109.97, 12.4976}, {2106.11, 12.4962}, {2102.26, 12.4947}, {2098.4, 12.4932}, {2094.54, 12.4918}, {2090.68, 12.4904}, {2086.83, 12.4889}, {2082.97, 12.4875}, {2079.11, 12.4861}, {2075.25, 12.4847}, {2071.4, 12.4833}, {2067.54, 12.4819}, {2063.68, 12.4805}, {2059.82, 12.4791}, {2055.97, 12.4777}, {2052.11, 12.4763}, {2048.25, 12.475}, {2044.4, 12.4736}, {2040.54, 12.4722}, {2036.68, 12.4709}, {2032.82, 12.4695}, {2028.97, 12.4682}, {2025.11, 12.4669}, {2021.25, 12.4655}, {2017.39, 12.4642}, {2013.54, 12.4629}, {2009.68, 12.4616}, {2005.82, 12.4603}, {2001.96, 12.459}, {1998.11, 12.4577}, {1994.25, 12.4564}, {1990.39, 12.4551}, {1986.54, 12.4538}, {1982.68, 12.4526}, {1978.82, 12.4513}, {1974.96, 12.45}, {1971.11, 12.4488}, {1967.25, 12.4475}, {1963.39, 12.4463}, {1959.53, 12.4451}, {1955.68, 12.4438}, {1951.82, 12.4426}, {1947.96, 12.4414}, {1944.1, 12.4402}, {1940.25, 12.4389}, {1936.39, 12.4377}, {1932.53, 12.4365}, {1928.67, 12.4353}, {1924.82, 12.4341}, {1920.96, 12.4329}, {1917.1, 12.4318}, {1913.25, 12.4306}, {1909.39, 12.4294}, {1905.53, 12.4282}, {1901.67, 12.4271}, {1897.82, 12.4259}, {1893.96, 12.4248}, {1890.1, 12.4236}, {1886.24, 12.4225}, {1882.39, 12.4213}, {1878.53, 12.4202}, {1874.67, 12.4191}, {1870.81, 12.4179}, {1866.96, 12.4168}, {1863.1, 12.4157}, {1859.24, 12.4146}, {1855.39, 12.4135}, {1851.53, 12.4124}, {1847.67, 12.4113}, {1843.81, 12.4102}, {1839.96, 12.4091}, {1836.1, 12.408}, {1832.24, 12.4069}, {1828.38, 12.4058}, {1824.53, 12.4048}, {1820.67, 12.4037}, {1816.81, 12.4026}, {1812.95, 12.4016}, {1809.1, 12.4005}, {1805.24, 12.3995}, {1801.38, 12.3984}, {1797.53, 12.3974}, {1793.67, 12.3963}, {1789.81, 12.3953}, {1785.95, 12.3943}, {1782.1, 12.3932}, {1778.24, 12.3922}, {1774.38, 12.3912}, {1770.52, 12.3902}, {1766.67, 12.3892}, {1762.81, 12.3881}, {1758.95, 12.3871}, {1755.09, 12.3861}, {1751.24, 12.3851}, {1747.38, 12.3842}, {1743.52, 12.3832}, {1739.66, 12.3822}, {1735.81, 12.3812}, {1731.95, 12.3802}, {1728.09, 12.3793}, {1724.24, 12.3783}, {1720.38, 12.3773}, {1716.52, 12.3764}, {1712.66, 12.3754}, {1708.81, 12.3744}, {1704.95, 12.3735}, {1701.09, 12.3725}, {1697.23, 12.3716}, {1693.38, 12.3707}, {1689.52, 12.3697}, {1685.66, 12.3688}, {1681.8, 12.3679}, {1677.95, 12.3669}, {1674.09, 12.366}, {1670.23, 12.3651}, {1666.38, 12.3642}, {1662.52, 12.3633}, {1658.66, 12.3624}, {1654.8, 12.3615}, {1650.95, 12.3606}, {1647.09, 12.3597}, {1643.23, 12.3588}, {1639.37, 12.3579}, {1635.52, 12.357}, {1631.66, 12.3561}, {1627.8, 12.3552}, {1623.94, 12.3543}, {1620.09, 12.3535}, {1616.23, 12.3526}, {1612.37, 12.3517}, {1608.51, 12.3509}, {1604.66, 12.35}, {1600.8, 12.3491}, {1596.94, 12.3483}, {1593.09, 12.3474}, {1589.23, 12.3466}, {1585.37, 12.3458}, {1581.51, 12.3449}, {1577.66, 12.3441}, {1573.8, 12.3432}, {1569.94, 12.3424}, {1566.08, 12.3416}, {1562.23, 12.3408}, {1558.37, 12.3399}, {1554.51, 12.3391}, {1550.65, 12.3383}, {1546.8, 12.3375}, {1542.94, 12.3367}, {1539.08, 12.3359}, {1535.23, 12.3351}, {1531.37, 12.3343}, {1527.51, 12.3335}, {1523.65, 12.3327}, {1519.8, 12.3319}, {1515.94, 12.3311}, {1512.08, 12.3303}, {1508.22, 12.3295}, {1504.37, 12.3287}, {1500.51, 12.328}, {1496.65, 12.3272}, {1492.79, 12.3264}, {1488.94, 12.3256}, {1485.08, 12.3249}, {1481.22, 12.3241}, {1477.37, 12.3234}, {1473.51, 12.3226}, {1469.65, 12.3218}, {1465.79, 12.3211}, {1461.94, 12.3203}, {1458.08, 12.3196}, {1454.22, 12.3189}, {1450.36, 12.3181}, {1446.51, 12.3174}, {1442.65, 12.3167}, {1438.79, 12.3159}, {1434.93, 12.3152}, {1431.08, 12.3145}, {1427.22, 12.3137}, {1423.36, 12.313}, {1419.5, 12.3123}, {1415.65, 12.3116}, {1411.79, 12.3109}, {1407.93, 12.3102}, {1404.08, 12.3095}, {1400.22, 12.3088}, {1396.36, 12.3081}, {1392.5, 12.3074}, {1388.65, 12.3067}, {1384.79, 12.306}, {1380.93, 12.3053}, {1377.07, 12.3046}, {1373.22, 12.3039}, {1369.36, 12.3032}, {1365.5, 12.3025}, {1361.64, 12.3019}, {1357.79, 12.3012}, {1353.93, 12.3005}, {1350.07, 12.2999}, {1346.22, 12.2992}, {1342.36, 12.2985}, {1338.5, 12.2979}, {1334.64, 12.2972}, {1330.79, 12.2965}, {1326.93, 12.2959}, {1323.07, 12.2952}, {1319.21, 12.2946}, {1315.36, 12.2939}, {1311.5, 12.2933}, {1307.64, 12.2927}, {1303.78, 12.292}, {1299.93, 12.2914}, {1296.07, 12.2907}, {1292.21, 12.2901}, {1288.35, 12.2895}, {1284.5, 12.2889}, {1280.64, 12.2882}, {1276.78, 12.2876}, {1272.93, 12.287}, {1269.07, 12.2864}, {1265.21, 12.2858}, {1261.35, 12.2852}, {1257.5, 12.2845}, {1253.64, 12.2839}, {1249.78, 12.2833},

{1245.92, 12.2827}, {1242.07, 12.2821}, {1238.21, 12.2815}, {1234.35, 12.2809}, {1230.49, 12.2803}, {1226.64, 12.2798}, {1222.78, 12.2792}, {1218.92, 12.2786}, {1215.07, 12.278}, {1211.21, 12.2774}, {1207.35, 12.2768}, {1203.49, 12.2763}, {1199.64, 12.2757}, {1195.78, 12.2751}, {1191.92, 12.2746}, {1188.06, 12.274}, {1184.21, 12.2734}, {1180.35, 12.2729}, {1176.49, 12.2723}, {1172.63, 12.2717}, {1168.78, 12.2712}, {1164.92, 12.2706}, {1161.06, 12.2701}, {1157.21, 12.2695}, {1153.35, 12.269}, {1149.49, 12.2684}, {1145.63, 12.2679}, {1141.78, 12.2674}, {1137.92, 12.2668}, {1134.06, 12.2663}, {1130.2, 12.2658}, {1126.35, 12.2652}, {1122.49, 12.2647}, {1118.63, 12.2642}, {1114.77, 12.2636}, {1110.92, 12.2631}, {1107.06, 12.2626}, {1103.2, 12.2621}, {1099.34, 12.2616}, {1095.49, 12.2611}, {1091.63, 12.2606}, {1087.77, 12.26}, {1083.92, 12.2595}, {1080.06, 12.259}, {1076.2, 12.2585}, {1072.34, 12.258}, {1068.49, 12.2575}, {1064.63, 12.257}, {1060.77, 12.2565}, {1056.91, 12.2561}, {1053.06, 12.2556}, {1049.2, 12.2551}, {1045.34, 12.2546}, {1041.48, 12.2541}, {1037.63, 12.2536}, {1033.77, 12.2531}, {1029.91, 12.2527}, {1026.06, 12.2522}, {1022.2, 12.2517}, {1018.34, 12.2513}, {1014.48, 12.2508}, {1010.63, 12.2503}, {1006.77, 12.2499}, {1002.91, 12.2494}, {999.053, 12.2489}, {995.196, 12.2485}, {991.339, 12.248}, {987.481, 12.2476}, {983.624, 12.2471}, {979.767, 12.2467}, {975.909, 12.2462}, {972.052, 12.2458}, {968.195, 12.2453}, {964.337, 12.2449}, {960.48, 12.2445}, {956.622, 12.244}, {952.765, 12.2436}, {948.908, 12.2431}, {945.05, 12.2427}, {941.193, 12.2423}, {937.336, 12.2419}, {933.478, 12.2414}, {929.621, 12.241}, {925.764, 12.2406}, {921.906, 12.2402}, {918.049, 12.2398}, {914.192, 12.2393}, {910.334, 12.2389}, {906.477, 12.2385}, {902.62, 12.2381}, {898.762, 12.2377}, {894.905, 12.2373}, {891.048, 12.2369}, {887.19, 12.2365}, {883.333, 12.2361}, {879.476, 12.2357}, {875.618, 12.2353}, {871.761, 12.2349}, {867.903, 12.2345}, {864.046, 12.2341}, {860.189, 12.2337}, {856.331, 12.2333}, {852.474, 12.233}, {848.617, 12.2326}, {844.759, 12.2322}, {840.902, 12.2318}, {837.045, 12.2314}, {833.187, 12.2311}, {829.33, 12.2307}, {825.473, 12.2303}, {821.615, 12.23}, {817.758, 12.2296}, {813.901, 12.2292}, {810.043, 12.2289}, {806.186, 12.2285}, {802.329, 12.2281}, {798.471, 12.2278}, {794.614, 12.2274}, {790.756, 12.2271}, {786.899, 12.2267}, {783.042, 12.2264}, {779.184, 12.226}, {775.327, 12.2257}, {771.47, 12.2253}, {767.612, 12.225}, {763.755, 12.2247}, {759.898, 12.2243}, {756.04, 12.224}, {752.183, 12.2237}, {748.326, 12.2233}, {744.468, 12.223}, {740.611, 12.2227}, {736.754, 12.2223}, {732.896, 12.222}, {729.039, 12.2217}, {725.182, 12.2214}, {721.324, 12.221}, {717.467, 12.2207}, {713.609, 12.2204}, {709.752, 12.2201}, {705.895, 12.2198}, {702.037, 12.2195}, {698.18, 12.2192}, {694.323, 12.2189}, {690.465, 12.2186}, {686.608, 12.2183}, {682.751, 12.218}, {678.893, 12.2177}, {675.036, 12.2174}, {671.179, 12.2171}, {667.321, 12.2168}, {663.464, 12.2165}, {659.607, 12.2162}, {655.749, 12.2159}, {651.892, 12.2156}, {648.035, 12.2153}, {644.177, 12.215}, {640.32, 12.2148}, {636.463, 12.2145}, {632.605, 12.2142}, {628.748, 12.2139}, {624.891, 12.2137}, {621.033, 12.2134}, {617.176, 12.2131}, {613.318, 12.2128}, {609.461, 12.2126}, {605.604, 12.2123}, {601.746, 12.2121}, {597.889, 12.2118}, {594.032, 12.2115}, {590.174, 12.2113}, {586.317, 12.211}, {582.46, 12.2108}, {578.602, 12.2105}, {574.745, 12.2103}, {570.888, 12.21}, {567.03, 12.2098}, {563.173, 12.2095}, {559.316, 12.2093}, {555.458, 12.209}, {551.601, 12.2088}, {547.744, 12.2086}, {543.886, 12.2083}, {540.029, 12.2081}, {536.171, 12.2078}, {532.314, 12.2076}, {528.457, 12.2074}, {524.599, 12.2072}, {520.742, 12.2069}, {516.885, 12.2067}, {513.027, 12.2065}, {509.17, 12.2063}, {505.313, 12.206}, {501.455, 12.2058}, {497.598, 12.2056}, {493.741, 12.2054}, {489.883, 12.2052}, {486.026, 12.205}, {482.169, 12.2048}, {478.311, 12.2046}, {474.454, 12.2043}, {470.597, 12.2041}, {466.739, 12.2039}, {462.882, 12.2037}, {459.025, 12.2035}, {455.167, 12.2033}, {451.31, 12.2032}, {447.452, 12.203}, {443.595, 12.2028}, {439.738, 12.2026}, {435.88, 12.2024}, {432.023, 12.2022}, {428.166, 12.202}, {424.308, 12.2018}, {420.451, 12.2017}, {416.594, 12.2015}, {412.736, 12.2013}, {408.879, 12.2011}, {405.022, 12.2009}, {401.164, 12.2008}, {397.307, 12.2006}, {393.45, 12.2004}, {389.592, 12.2003}, {385.735, 12.2001}, {381.878, 12.1999}, {378.02, 12.1998}, {374.163, 12.1996}, {370.305, 12.1994}, {366.448, 12.1993}, {362.591, 12.1991}, {358.733, 12.199}, {354.876, 12.1988}, {351.019, 12.1987}, {347.161, 12.1985}, {343.304, 12.1984}, {339.447, 12.1982}, {335.589, 12.1981}, {331.732, 12.1979}, {327.875, 12.1978}, {324.017, 12.1977}, {320.16, 12.1975}, {316.303, 12.1974}, {312.445, 12.1973}, {308.588, 12.1971}, {304.731, 12.197}, {300.873, 12.1969}, {297.016, 12.1967}, {293.159, 12.1966}, {289.301, 12.1965}, {285.444, 12.1964}, {281.586, 12.1962}, {277.729, 12.1961}, {273.872, 12.196}, {270.014, 12.1959}, {266.157, 12.1958}, {262.3, 12.1957}, {258.442, 12.1955}, {254.585, 12.1954}, {250.728, 12.1953}};

inas=Interpolation[InAsraw];

mgoraw={{7876.71, 2.96066}, {7845.85, 2.96042}, {7814.99, 2.96018}, {7784.13, 2.95994}, {7753.27, 2.95969}, {7722.41, 2.95945}, {7695.41, 2.95923}, {7664.55, 2.95899}, {7633.69, 2.95874}, {7606.69, 2.95852}, {7575.83, 2.95827}, {7548.83, 2.95805}, {7521.83, 2.95782}, {7490.97, 2.95757}, {7463.97, 2.95734}, {7436.97, 2.95711}, {7409.97, 2.95689}, {7382.97, 2.95666}, {7355.96, 2.95643}, {7328.96, 2.95619}, {7301.96, 2.95596}, {7274.96, 2.95573}, {7247.96, 2.95549}, {7220.96, 2.95525}, {7197.81, 2.95505}, {7170.81, 2.95481}, {7143.81, 2.95457}, {7120.67, 2.95436}, {7093.66, 2.95411}, {7070.52, 2.9539}, {7043.52, 2.95365}, {7020.38, 2.95344}, {6993.37, 2.95319}, {6970.23, 2.95297}, {6947.09, 2.95275}, {6923.94, 2.95253}, {6896.94, 2.95228}, {6873.8, 2.95205}, {6850.65, 2.95183}, {6827.51, 2.9516}, {6804.36, 2.95138}, {6781.22, 2.95115}, {6758.08, 2.95092}, {6734.93, 2.95069}, {6711.79, 2.95046}, {6692.5, 2.95026}, {6669.36, 2.95003}, {6646.21, 2.94979}, {6623.07, 2.94955}, {6603.78, 2.94935}, {6580.64, 2.94911}, {6557.49, 2.94886}, {6538.21, 2.94866}, {6515.06, 2.94841}, {6495.78, 2.94821}, {6472.63, 2.94796}, {6453.34, 2.94775}, {6434.06, 2.94754}, {6410.91, 2.94728}, {6391.63, 2.94707}, {6372.34, 2.94685}, {6353.05, 2.94664}, {6329.91, 2.94637}, {6310.62, 2.94616}, {6291.34, 2.94593}, {6272.05, 2.94571}, {6252.76, 2.94549}, {6233.48, 2.94526}, {6214.19, 2.94504}, {6194.9, 2.94481}, {6175.62, 2.94458}, {6156.33, 2.94434}, {6137.04, 2.94411}, {6117.76, 2.94388}, {6098.47, 2.94364}, {6079.18, 2.9434}, {6063.75, 2.94321}, {6044.47, 2.94297}, {6025.18, 2.94273}, {6009.75, 2.94253}, {5990.46, 2.94228}, {5971.18, 2.94204}, {5955.75, 2.94184}, {5936.46, 2.94159}, {5917.17, 2.94133}, {5901.74, 2.94113}, {5882.46, 2.94087}, {5867.03, 2.94067}, {5851.6, 2.94046}, {5832.31, 2.9402}, {5816.88, 2.93999}, {5797.6, 2.93972}, {5782.17, 2.93951}, {5766.74, 2.93929}, {5747.45, 2.93902}, {5732.02, 2.9388}, {5716.59, 2.93858}, {5701.16, 2.93836}, {5681.88, 2.93808}, {5666.45, 2.93786}, {5651.02, 2.93763}, {5635.59, 2.93741}, {5620.16, 2.93718}, {5604.73, 2.93695}, {5589.3, 2.93672}, {5573.87, 2.93648}, {5558.44, 2.93625}, {5543.01, 2.93601}, {5527.58, 2.93578}, {5512.15, 2.93554}, {5496.72, 2.93529}, {5481.29, 2.93505}, {5465.86, 2.93481}, {5450.43, 2.93456}, {5435, 2.93431}, {5423.43, 2.93413}, {5408, 2.93387}, {5392.57, 2.93362}, {5377.14, 2.93337}, {5365.57, 2.93317}, {5350.14, 2.93292}, {5334.71, 2.93266}, {5319.28, 2.9324}, {5307.71, 2.9322}, {5292.28, 2.93193}, {5280.71, 2.93173}, {5265.28, 2.93146}, {5249.85, 2.93119}, {5238.28, 2.93099}, {5222.85, 2.93072}, {5211.28, 2.93051}, {5195.85, 2.93023}, {5184.28, 2.93002}, {5168.85, 2.92974}, {5157.28, 2.92953}, {5141.85, 2.92924}, {5130.27, 2.92903}, {5118.7, 2.92881}, {5103.27, 2.92852}, {5091.7, 2.9283}, {5076.27, 2.928}, {5064.7, 2.92778}, {5053.13, 2.92756}, {5041.56, 2.92733}, {5026.13, 2.92703}, {5014.55, 2.9268}, {5002.98, 2.92657}, {4987.55, 2.92626}, {4975.98, 2.92603}, {4964.41, 2.9258}, {4952.84, 2.92556}, {4941.26, 2.92532}, {4929.69, 2.92508}, {4914.26, 2.92476}, {4902.69, 2.92452}, {4891.12, 2.92428}, {4879.55, 2.92403}, {4867.97, 2.92378}, {4856.4, 2.92353}, {4844.83, 2.92328}, {4833.26, 2.92303}, {4821.69, 2.92278}, {4810.11, 2.92252}, {4798.54, 2.92227}, {4786.97, 2.92201}, {4775.4, 2.92175}, {4763.83, 2.92149}, {4752.25, 2.92122}, {4740.68, 2.92096}, {4729.11, 2.92069}, {4717.54, 2.92042}, {4705.97, 2.92015}, {4698.25, 2.91997}, {4686.68, 2.9197}, {4675.11, 2.91942}, {4663.54, 2.91914}, {4651.96, 2.91887}, {4640.39, 2.91858}, {4632.68, 2.9184}, {4621.1, 2.91811}, {4609.53, 2.91783}, {4597.96, 2.91754}, {4590.25, 2.91734}, {4578.67, 2.91705}, {4567.1, 2.91676}, {4559.39, 2.91656}, {4547.81, 2.91627}, {4536.24, 2.91597}, {4528.53, 2.91577}, {4516.96, 2.91546}, {4505.38, 2.91516}, {4497.67, 2.91496}, {4486.1, 2.91465}, {4474.52, 2.91434}, {4466.81, 2.91413}, {4455.24, 2.91382}, {4447.52, 2.9136}, {4435.95, 2.91329}, {4428.24, 2.91307}, {4416.66, 2.91275}, {4408.95, 2.91254}, {4397.38, 2.91221}, {4389.66, 2.91199}, {4378.09, 2.91166}, {4370.38, 2.91144}, {4358.8, 2.91111}, {4351.09, 2.91088}, {4339.52, 2.91055}, {4331.8, 2.91032}, {4320.23, 2.90998}, {4312.52, 2.90975}, {4304.8, 2.90952}, {4293.23, 2.90917}, {4285.51, 2.90893}, {4273.94, 2.90858}, {4266.23, 2.90835}, {4258.51, 2.90811}, {4246.94, 2.90775}, {4239.23, 2.90751}, {4231.51, 2.90727}, {4219.94, 2.9069}, {4212.23, 2.90665}, {4204.51, 2.90641}, {4192.94, 2.90604}, {4185.22, 2.90579}, {4177.51, 2.90554}, {4169.79, 2.90528}, {4158.22, 2.9049}, {4150.51, 2.90465}, {4142.79, 2.90439}, {4135.08, 2.90413}, {4127.36, 2.90387}, {4115.79, 2.90348}, {4108.08,

2.90322}, {4100.36, 2.90295}, {4092.65, 2.90269}, {4084.93, 2.90242}, {4073.36, 2.90201}, {4065.65, 2.90174}, {4057.93, 2.90147}, {4050.22, 2.9012}, {4042.5, 2.90092}, {4034.79, 2.90064}, {4027.07, 2.90037}, {4019.36, 2.90009}, {4011.64, 2.8998}, {4000.07, 2.89938}, {3992.36, 2.89909}, {3984.64, 2.89881}, {3976.93, 2.89852}, {3969.21, 2.89823}, {3961.5, 2.89794}, {3953.78, 2.89764}, {3946.07, 2.89735}, {3938.35, 2.89705}, {3930.64, 2.89675}, {3922.92, 2.89645}, {3915.21, 2.89615}, {3907.49, 2.89585}, {3899.78, 2.89554}, {3892.07, 2.89523}, {3884.35, 2.89492}, {3876.64, 2.89461}, {3868.92, 2.8943}, {3861.21, 2.89399}, {3857.35, 2.89383}, {3849.63, 2.89351}, {3841.92, 2.89319}, {3834.21, 2.89287}, {3826.49, 2.89255}, {3818.78, 2.89223}, {3811.06, 2.8919}, {3803.35, 2.89157}, {3795.63, 2.89124}, {3787.92, 2.89091}, {3784.06, 2.89074}, {3776.34, 2.89041}, {3768.63, 2.89007}, {3760.92, 2.88973}, {3753.2, 2.88939}, {3745.49, 2.88905}, {3741.63, 2.88887}, {3733.91, 2.88853}, {3726.2, 2.88818}, {3718.48, 2.88783}, {3710.77, 2.88748}, {3706.91, 2.8873}, {3699.2, 2.88694}, {3691.48, 2.88658}, {3683.77, 2.88622}, {3679.91, 2.88604}, {3672.2, 2.88568}, {3664.48, 2.88531}, {3656.77, 2.88495}, {3652.91, 2.88476}, {3645.2, 2.88439}, {3637.48, 2.88402}, {3629.77, 2.88364}, {3625.91, 2.88345}, {3618.19, 2.88307}, {3610.48, 2.88269}, {3606.62, 2.8825}, {3598.91, 2.88211}, {3591.19, 2.88172}, {3587.33, 2.88153}, {3579.62, 2.88114}, {3571.91, 2.88074}, {3568.05, 2.88055}, {3560.33, 2.88015}, {3552.62, 2.87975}, {3548.76, 2.87955}, {3541.05, 2.87914}, {3537.19, 2.87894}, {3529.47, 2.87853}, {3521.76, 2.87812}, {3517.9, 2.87791}, {3510.19, 2.8775}, {3506.33, 2.87729}, {3498.62, 2.87687}, {3490.9, 2.87645}, {3487.04, 2.87624}, {3479.33, 2.87581}, {3475.47, 2.8756}, {3467.76, 2.87517}, {3463.9, 2.87495}, {3456.18, 2.87452}, {3448.47, 2.87408}, {3444.61, 2.87386}, {3436.9, 2.87342}, {3433.04, 2.8732}, {3425.33, 2.87275}, {3421.47, 2.87253}, {3413.75, 2.87208}, {3409.9, 2.87185}, {3402.18, 2.8714}, {3398.32, 2.87117}, {3390.61, 2.87071}, {3386.75, 2.87048}, {3379.04, 2.87001}, {3375.18, 2.86978}, {3367.47, 2.86931}, {3363.61, 2.86907}, {3355.89, 2.8686}, {3352.04, 2.86836}, {3348.18, 2.86812}, {3340.46, 2.86764}, {3336.61, 2.8674}, {3328.89, 2.86692}, {3325.04, 2.86667}, {3317.32, 2.86618}, {3313.46, 2.86594}, {3309.61, 2.86569}, {3301.89, 2.86519}, {3298.03, 2.86494}, {3290.32, 2.86444}, {3286.46, 2.86419}, {3278.75, 2.86368}, {3274.89, 2.86342}, {3271.03, 2.86317}, {3263.32, 2.86265}, {3259.46, 2.86239}, {3255.6, 2.86214}, {3247.89, 2.86161}, {3244.03, 2.86135}, {3236.32, 2.86082}, {3232.46, 2.86056}, {3228.6, 2.86029}, {3220.89, 2.85976}, {3217.03, 2.85949}, {3213.17, 2.85922}, {3205.46, 2.85867}, {3201.6, 2.8584}, {3197.74, 2.85813}, {3190.03, 2.85758}, {3186.17, 2.8573}, {3182.31, 2.85702}, {3178.46, 2.85674}, {3170.74, 2.85618}, {3166.88, 2.8559}, {3163.03, 2.85562}, {3155.31, 2.85505}, {3151.45, 2.85476}, {3147.6, 2.85447}, {3139.88, 2.8539}, {3136.02, 2.85361}, {3132.17, 2.85332}, {3128.31, 2.85302}, {3120.6, 2.85243}, {3116.74, 2.85214}, {3112.88, 2.85184}, {3109.02, 2.85154}, {3101.31, 2.85095}, {3097.45, 2.85064}, {3093.59, 2.85034}, {3089.74, 2.85004}, {3082.02, 2.84943}, {3078.16, 2.84912}, {3074.31, 2.84881}, {3070.45, 2.8485}, {3066.59, 2.84819}, {3058.88, 2.84757}, {3055.02, 2.84725}, {3051.16, 2.84694}, {3047.31, 2.84662}, {3039.59, 2.84599}, {3035.73, 2.84567}, {3031.88, 2.84534}, {3028.02, 2.84502}, {3024.16, 2.8447}, {3020.3, 2.84437}, {3012.59, 2.84372}, {3008.73, 2.84339}, {3004.88, 2.84306}, {3001.02, 2.84273}, {2997.16, 2.8424}, {2993.3, 2.84206}, {2985.59, 2.84139}, {2981.73, 2.84105}, {2977.87, 2.84071}, {2974.02, 2.84037}, {2970.16, 2.84003}, {2966.3, 2.83969}, {2958.59, 2.839}, {2954.73, 2.83865}, {2950.87, 2.8383}, {2947.01, 2.83795}, {2943.16, 2.8376}, {2939.3, 2.83725}, {2935.44, 2.83689}, {2931.59, 2.83654}, {2927.73, 2.83618}, {2920.01, 2.83546}, {2916.16, 2.8351}, {2912.3, 2.83474}, {2908.44, 2.83438}, {2904.58, 2.83401}, {2900.73, 2.83364}, {2896.87, 2.83327}, {2893.01, 2.8329}, {2889.15, 2.83253}, {2885.3, 2.83216}, {2881.44, 2.83178}, {2873.73, 2.83103}, {2869.87, 2.83065}, {2866.01, 2.83027}, {2862.15, 2.82989}, {2858.3, 2.8295}, {2854.44, 2.82912}, {2850.58, 2.82873}, {2846.72, 2.82834}, {2842.87, 2.82795}, {2839.01, 2.82756}, {2835.15, 2.82717}, {2831.29, 2.82677}, {2827.44, 2.82638}, {2823.58, 2.82598}, {2819.72, 2.82558}, {2815.87, 2.82518}, {2812.01, 2.82477}, {2808.15, 2.82437}, {2804.29, 2.82396}, {2800.44, 2.82355}, {2796.58, 2.82314}, {2792.72, 2.82273}, {2788.86, 2.82232}, {2785.01, 2.8219}, {2781.15, 2.82149}, {2777.29, 2.82107}, {2773.43, 2.82065}, {2769.58, 2.82022}, {2765.72, 2.8198}, {2761.86, 2.81937}, {2758, 2.81895}, {2754.15, 2.81852}, {2750.29, 2.81809}, {2746.43, 2.81765}, {2742.58, 2.81722}, {2738.72, 2.81678}, {2734.86, 2.81634}, {2731, 2.8159}, {2727.15, 2.81546}, {2723.29, 2.81501}, {2719.43, 2.81457}, {2715.57, 2.81412}, {2711.72, 2.81367}, {2707.86, 2.81322}, {2704, 2.81276}, {2700.14, 2.81231}, {2696.29, 2.81185}, {2692.43, 2.81139}, {2688.57, 2.81093}, {2684.72, 2.81046}, {2680.86, 2.80999}, {2677, 2.80953}, {2673.14, 2.80906}, {2669.29, 2.80858}, {2665.43, 2.80811}, {2661.57, 2.80763}, {2657.71, 2.80715}, {2653.86, 2.80667}, {2650, 2.80619}, {2646.14, 2.8057}, {2642.28, 2.80522}, {2638.43, 2.80473}, {2634.57, 2.80424}, {2630.71, 2.80374}, {2626.85, 2.80325}, {2623, 2.80275}, {2619.14, 2.80225}, {2615.28, 2.80174}, {2611.43, 2.80124}, {2607.57, 2.80073}, {2603.71, 2.80022}, {2599.85, 2.79971}, {2596, 2.79919}, {2592.14, 2.79868}, {2588.28, 2.79816}, {2584.42, 2.79764}, {2580.57, 2.79711}, {2576.71, 2.79659}, {2572.85, 2.79606}, {2568.99, 2.79553}, {2565.14, 2.79499}, {2561.28, 2.79446}, {2557.42, 2.79392}, {2553.57, 2.79338}, {2549.71, 2.79283}, {2545.85, 2.79229}, {2541.99, 2.79174}, {2538.14, 2.79119}, {2534.28, 2.79064}, {2530.42, 2.79008}, {2526.56, 2.78952}, {2522.71, 2.78896}, {2518.85, 2.78839}, {2514.99, 2.78783}, {2511.13, 2.78726}, {2507.28, 2.78669}, {2503.42, 2.78611}, {2499.56, 2.78553}, {2495.71, 2.78495}, {2491.85, 2.78437}, {2487.99, 2.78378}, {2484.13, 2.78319}, {2480.28, 2.7826}, {2476.42, 2.78201}, {2472.56, 2.78141}, {2468.7, 2.78081}, {2464.85, 2.78021}, {2460.99, 2.7796}, {2457.13, 2.77899}, {2453.27, 2.77838}, {2449.42, 2.77777}, {2445.56, 2.77715}, {2441.7, 2.77653}, {2437.84, 2.7759}, {2433.99, 2.77528}, {2430.13, 2.77465}, {2426.27, 2.77401}, {2422.42, 2.77338}, {2418.56, 2.77274}, {2414.7, 2.7721}, {2410.84, 2.77145}, {2406.99, 2.7708}, {2403.13, 2.77015}, {2399.27, 2.7695}, {2395.41, 2.76884}, {2391.56, 2.76818}, {2387.7, 2.76751}, {2383.84, 2.76684}, {2379.98, 2.76617}, {2376.13, 2.7655}, {2372.27, 2.76482}, {2368.41, 2.76413}, {2364.56, 2.76345}, {2360.7, 2.76276}, {2356.84, 2.76207}, {2352.98, 2.76137}, {2349.13, 2.76067}, {2345.27, 2.75997}, {2341.41, 2.75926}, {2337.55, 2.75855}, {2333.7, 2.75784}, {2329.84, 2.75712}, {2325.98, 2.7564}, {2322.12, 2.75568}, {2318.27, 2.75495}, {2314.41, 2.75422}, {2310.55, 2.75348}, {2306.7, 2.75274}, {2302.84, 2.752}, {2298.98, 2.75125}, {2295.12, 2.7505}, {2291.27, 2.74974}, {2287.41, 2.74898}, {2283.55, 2.74822}, {2279.69, 2.74745}, {2275.84, 2.74668}, {2271.98, 2.74591}, {2268.12, 2.74513}, {2264.26, 2.74434}, {2260.41, 2.74355}, {2256.55, 2.74276}, {2252.69, 2.74197}, {2248.83, 2.74117}, {2244.98, 2.74036}, {2241.12, 2.73955}, {2237.26, 2.73874}, {2233.41, 2.73792}, {2229.55, 2.7371}, {2225.69, 2.73627}, {2221.83, 2.73544}, {2217.98, 2.73461}, {2214.12, 2.73376}, {2210.26, 2.73292}, {2206.4, 2.73207}, {2202.55, 2.73122}, {2198.69, 2.73036}, {2194.83, 2.7295}, {2190.97, 2.72863}, {2187.12, 2.72775}, {2183.26, 2.72688}, {2179.4, 2.72599}, {2175.55, 2.72511}, {2171.69, 2.72422}, {2167.83, 2.72332}, {2163.97, 2.72242}, {2160.12, 2.72151}, {2156.26, 2.7206}, {2152.4, 2.71968}, {2148.54, 2.71876}, {2144.69, 2.71783}, {2140.83, 2.7169}, {2136.97, 2.71596}, {2133.11, 2.71501}, {2129.26, 2.71407}, {2125.4, 2.71311}, {2121.54, 2.71215}, {2117.68, 2.71119}, {2113.83, 2.71022}, {2109.97, 2.70924}, {2106.11, 2.70826}, {2102.26, 2.70727}, {2098.4, 2.70628}, {2094.54, 2.70528}, {2090.68, 2.70427}, {2086.83, 2.70326}, {2082.97, 2.70225}, {2079.11, 2.70123}, {2075.25, 2.7002}, {2071.4, 2.69916}, {2067.54, 2.69812}, {2063.68, 2.69708}, {2059.82, 2.69602}, {2055.97, 2.69497}, {2052.11, 2.6939}, {2048.25, 2.69283}, {2044.4, 2.69175}, {2040.54, 2.69067}, {2036.68, 2.68958}, {2032.82, 2.68848}, {2028.97, 2.68738}, {2025.11, 2.68627}, {2021.25, 2.68515}, {2017.39, 2.68403}, {2013.54, 2.6829}, {2009.68, 2.68176}, {2005.82, 2.68061}, {2001.96, 2.67946}, {1998.11, 2.67831}, {1994.25, 2.67714}, {1990.39, 2.67597}, {1986.54, 2.67479}, {1982.68, 2.6736}, {1978.82, 2.67241}, {1974.96, 2.67121}, {1971.11, 2.67}, {1967.25, 2.66878}, {1963.39, 2.66756}, {1959.53, 2.66633}, {1955.68, 2.66509}, {1951.82, 2.66384}, {1947.96, 2.66259}, {1944.1, 2.66133}, {1940.25, 2.66006}, {1936.39, 2.65878}, {1932.53, 2.65749}, {1928.67, 2.6562}, {1924.82, 2.6549}, {1920.96, 2.65359}, {1917.1, 2.65227}, {1913.25, 2.65094}, {1909.39, 2.6496}, {1905.53, 2.64826}, {1901.67, 2.6469}, {1897.82, 2.64554}, {1893.96, 2.64417}, {1890.1, 2.64279}, {1886.24, 2.6414}, {1882.39, 2.64}, {1878.53, 2.6386}, {1874.67, 2.63718}, {1870.81, 2.63576}, {1866.96, 2.63432}, {1863.1, 2.63288}, {1859.24, 2.63142}, {1855.39, 2.62996}, {1851.53, 2.62849}, {1847.67, 2.62701}, {1843.81, 2.62551}, {1839.96, 2.62401}, {1836.1, 2.6225}, {1832.24, 2.62098}, {1828.38, 2.61944}, {1824.53, 2.6179}, {1820.67, 2.61635}, {1816.81, 2.61478}, {1812.95, 2.61321}, {1809.1, 2.61162}, {1805.24, 2.61002}, {1801.38, 2.60842}, {1797.53, 2.6068}, {1793.67, 2.60517}, {1789.81, 2.60353}, {1785.95, 2.60188}, {1782.1, 2.60021}, {1778.24, 2.59854}, {1774.38, 2.59685}, {1770.52, 2.59515}, {1766.67, 2.59344}, {1762.81, 2.59172}, {1758.95, 2.58999}, {1755.09, 2.58824}, {1751.24, 2.58648}, {1747.38, 2.58471}, {1743.52, 2.58293}, {1739.66, 2.58113}, {1735.81, 2.57932}, {1731.95, 2.5775}, {1728.09, 2.57566}, {1724.24, 2.57381}, {1720.38, 2.57195}, {1716.52, 2.57007}, {1712.66, 2.56819}, {1708.81, 2.56628}, {1704.95, 2.56437}, {1701.09, 2.56244}, {1697.23, 2.56049}, {1693.38, 2.55853}, {1689.52, 2.55656}, {1685.66, 2.55457}, {1681.8, 2.55257}, {1677.95, 2.55055}, {1674.09, 2.54852},

```
{1670.23, 2.54647}, {1666.38, 2.54441}, {1662.52, 2.54233}, {1658.66, 2.54023}, {1654.8, 2.53812}, {1650.95, 2.536}, {1647.09, 2.53386}, {1643.23, 2.5317},
{1639.37, 2.52952}, {1635.52, 2.52733}, {1631.66, 2.52512}, {1627.8, 2.5229}, {1623.94, 2.52066}, {1620.09, 2.5184}, {1616.23, 2.51612}, {1612.37, 2.51382},
{1608.51, 2.51151}, {1604.66, 2.50918}, {1600.8, 2.50683}, {1596.94, 2.50446}, {1593.09, 2.50208}, {1589.23, 2.49967}, {1585.37, 2.49725}, {1581.51, 2.49481},
{1577.66, 2.49234}, {1573.8, 2.48986}, {1569.94, 2.48736}, {1566.08, 2.48483}, {1562.23, 2.48229}, {1558.37, 2.47973}, {1554.51, 2.47714}, {1550.65,
2.47454}, {1546.8, 2.47191}, {1542.94, 2.46926}, {1539.08, 2.46659}, {1535.23, 2.4639}, {1531.37, 2.46119}, {1527.51, 2.45845}, {1523.65, 2.45569}, {1519.8,
2.45291}, {1515.94, 2.4501}, {1512.08, 2.44727}, {1508.22, 2.44442}, {1504.37, 2.44154}, {1500.51, 2.43864}, {1496.65, 2.43571}, {1492.79, 2.43276}, {1488.94,
2.42979}, {1485.08, 2.42679}, {1481.22, 2.42376}, {1477.37, 2.4207}, {1473.51, 2.41762}, {1469.65, 2.41452}, {1465.79, 2.41138}, {1461.94, 2.40822},
{1458.08, 2.40503}, {1454.22, 2.40181}, {1450.36, 2.39857}, {1446.51, 2.3953}, {1442.65, 2.39199}, {1438.79, 2.38866}, {1434.93, 2.3853}, {1431.08, 2.3819},
{1427.22, 2.37848}, {1423.36, 2.37503}, {1419.5, 2.37154}, {1415.65, 2.36802}, {1411.79, 2.36447}, {1407.93, 2.36089}, {1404.08, 2.35728}, {1400.22, 2.35363},
{1396.36, 2.34995}, {1392.5, 2.34623}, {1388.65, 2.34248}, {1384.79, 2.3387}, {1380.93, 2.33488}, {1377.07, 2.33102}, {1373.22, 2.32713}, {1369.36, 2.3232},
{1365.5, 2.31923}, {1361.64, 2.31522}, {1357.79, 2.31118}, {1353.93, 2.3071}, {1350.07, 2.30298}, {1346.22, 2.29881}, {1342.36, 2.29461}, {1338.5, 2.29037},
{1334.64, 2.28608}, {1330.79, 2.28176}, {1326.93, 2.27739}, {1323.07, 2.27298}, {1319.21, 2.26852}, {1315.36, 2.26402}, {1311.5, 2.25947}, {1307.64, 2.25488},
{1303.78, 2.25024}, {1299.93, 2.24556}, {1296.07, 2.24083}, {1292.21, 2.23605}, {1288.35, 2.23122}, {1284.5, 2.22634}, {1280.64, 2.22141}, {1276.78,
2.21643}, {1272.93, 2.2114}, {1269.07, 2.20631}, {1265.21, 2.20117}, {1261.35, 2.19598}, {1257.5, 2.19074}, {1253.64, 2.18543}, {1249.78, 2.18007}, {1245.92,
2.17466}, {1242.07, 2.16918}, {1238.21, 2.16365}, {1234.35, 2.15806}, {1230.49, 2.1524}, {1226.64, 2.14669}, {1222.78, 2.14091}, {1218.92, 2.13507}, {1215.07,
2.12916}, {1211.21, 2.12319}, {1207.35, 2.11715}, {1203.49, 2.11104}, {1199.64, 2.10487}, {1195.78, 2.09862}, {1191.92, 2.09231}, {1188.06, 2.08592},
{1184.21, 2.07946}, {1180.35, 2.07292}, {1176.49, 2.06631}, {1172.63, 2.05962}, {1168.78, 2.05286}, {1164.92, 2.04601}, {1161.06, 2.03909}, {1157.21,
2.03208}, {1153.35, 2.02499}, {1149.49, 2.01782}, {1145.63, 2.01055}, {1141.78, 2.0032}, {1137.92, 1.99577}, {1134.06, 1.98824}, {1130.2, 1.98062}, {1126.35,
1.9729}, {1122.49, 1.96509}, {1118.63, 1.95719}, {1114.77, 1.94918}, {1110.92, 1.94107}, {1107.06, 1.93287}, {1103.2, 1.92456}, {1099.34, 1.91614}, {1095.49,
1.90761}, {1091.63, 1.89897}, {1087.77, 1.89023}, {1083.92, 1.88136}, {1080.06, 1.87239}, {1076.2, 1.86329}, {1072.34, 1.85407}, {1068.49, 1.84473}, {1064.63,
1.83526}, {1060.77, 1.82567}, {1056.91, 1.81595}, {1053.06, 1.80609}, {1049.2, 1.7961}, {1045.34, 1.78597}, {1041.48, 1.7757}, {1037.63, 1.76528}, {1033.77,
1.75472}, {1029.91, 1.74401}, {1026.06, 1.73315}, {1022.2, 1.72213}, {1018.34, 1.71095}, {1014.48, 1.69961}, {1010.63, 1.68809}, {1006.77, 1.67642}, {1002.91,
1.66457}, {999.053, 1.65254}, {995.196, 1.64033}, {991.339, 1.62793}, {987.481, 1.61535}, {983.624, 1.60257}, {979.767, 1.58959}, {975.909, 1.57641},
{972.052, 1.56303}, {968.195, 1.54944}, {964.337, 1.53562}, {960.48, 1.52159}, {956.622, 1.50733}, {952.765, 1.49285}, {948.908, 1.47812}, {945.05, 1.46315},
{941.193, 1.44794}, {937.336, 1.43248}, {933.478, 1.41675}, {929.621, 1.40077}, {925.764, 1.38452}, {921.906, 1.36798}, {918.049, 1.35117}, {914.192,
1.33407}, {910.334, 1.31668}, {906.477, 1.29899}, {902.62, 1.281}, {898.762, 1.26268}, {894.905, 1.24406}, {891.048, 1.22511}, {887.19, 1.20582}, {883.333,
1.18621}, {879.476, 1.16625}, {875.618, 1.14593}, {871.761, 1.12527}, {867.903, 1.10423}, {864.046, 1.08283}, {860.189, 1.06106}, {856.331, 1.0389}, {852.474,
1.01635}, {848.617, 0.993416}, {844.759, 0.970071}, {840.902, 0.946324}, {837.045, 0.922164}, {833.187, 0.897578}, {829.33, 0.872571}, {825.473, 0.847132},
{821.615, 0.821246}, {817.758, 0.79492}, {813.901, 0.768141}, {810.043, 0.740895}, {806.186, 0.713188}, {802.329, 0.685007}, {798.471, 0.656335}, {794.614,
0.62718}, {790.756, 0.597518}, {786.899, 0.567354}, {783.042, 0.536673}, {779.184, 0.505455}, {775.327, 0.473706}, {771.47, 0.441407}, {767.612, 0.408535},
{763.755, 0.375096}, {759.898, 0.341064}, {756.04, 0.306417}, {752.183, 0.271155}, {748.326, 0.235252}, {744.468, 0.198676}, {740.611, 0.161427}, {736.754,
0.123472}, {732.896, 0.0847762}, {729.039, 0.0453319}, {725.182, 0.00510134}, {721.324, −0.035957}, {717.467, −0.0778564}, {713.609, −0.120654}, {709.752,
−0.164365}, {705.895, −0.209043}, {702.037, −0.254744}, {698.18, −0.30149}, {694.323, −0.349344}, {690.465, −0.398373}, {686.608, −0.448609}, {682.751,
−0.500123}, {678.893, −0.552995}, {675.036, −0.607268}, {671.179, −0.663025}, {667.321, −0.72036}, {663.464, −0.779325}, {659.607, −0.84002}, {655.749,
−0.902555}, {651.892, −0.966992}, {648.035, −1.03345}, {644.177, −1.10206}, {640.32, −1.17289}, {636.463, −1.24609}, {632.605, −1.3218}, {628.748, −1.40012},
{624.891, −1.48121}, {621.033, −1.56524}, {617.176, −1.65234}, {613.318, −1.74271}, {609.461, −1.83649}, {605.604, −1.9339}, {601.746, −2.03516}, {597.889,
−2.14044}, {594.032, −2.24999}, {590.174, −2.3641}, {586.317, −2.48297}, {582.46, −2.60691}, {578.602, −2.73625}, {574.745, −2.87126}, {570.888, −3.01232},
{567.03, −3.15985}, {563.173, −3.31418}, {559.316, −3.47579}, {555.458, −3.6452}, {551.601, −3.82286}, {547.744, −4.00938}, {543.886, −4.20543}, {540.029,
−4.4116}, {536.171, −4.62874}, {532.314, −4.85758}, {528.457, −5.09908}, {524.599, −5.35432}, {520.742, −5.62429}, {516.885, −5.91031}, {513.027, −6.21386},
{509.17, −6.53636}, {505.313, −6.87965}, {501.455, −7.24581}, {497.598, −7.63693}, {493.741, −8.05567}, {489.883, −8.50509}, {486.026, −8.98834}, {482.169,
−9.50943}, {478.311, −10.073}, {474.454, −10.6842}, {470.597, −11.3492}, {466.739, −12.0756}, {462.882, −12.8717}, {459.025, −13.7483}, {455.167, −14.7183},
{451.31, −15.7967}, {447.452, −17.0033}, {443.595, −18.3615}, {439.738, −19.902}, {435.88, −21.6645}, {432.023, −23.6991}, {428.166, −26.0748}, {424.308,
−28.8854}, {420.451, −32.2602}, {416.594, −36.3887}, {412.736, −41.5561}, {408.879, −48.2059}, {405.022, −57.0848}, {401.164, −69.5411}, {397.307, −88.2679},
{393.45, −119.599}, {389.592, −182.724}, {385.735, −375.646}, {381.878, 13489.1}, {378.02, 365.071}, {374.163, 187.472}, {370.305, 127.184}, {366.448,
96.846}, {362.591, 78.5793}, {358.733, 66.3738}, {354.876, 57.6468}, {351.019, 51.0962}, {347.161, 45.9978}, {343.304, 41.9193}, {339.447, 38.5823}, {335.589,
35.8011}, {331.732, 33.4492}, {327.875, 31.4341}, {324.017, 29.6882}, {320.16, 28.162}, {316.303, 26.8164}, {312.445, 25.621}, {308.588, 24.5529}, {304.731,
23.5926}, {300.873, 22.7246}, {297.016, 21.9368}, {293.159, 21.2186}, {289.301, 20.561}, {285.444, 19.9573}, {281.586, 19.4008}, {277.729, 18.8867}, {273.872,
18.4103}, {270.014, 17.9676}, {266.157, 17.5555}, {262.3, 17.171}, {258.442, 16.8113}, {254.585, 16.4745}, {250.728, 16.1584}};

mgo=Interpolation[mgoraw];

(* H20, data from Wieliczka, Weng& Querry
(Appl.Opt.28, 1714−1719, 1989) *)

h2oraw={{500, 2.18614}, {504.7, 2.16963}, {510.5, 2.14232}, {515.2, 2.12033}, {521.2, 2.09392}, {526, 2.06978}, {532.1, 2.03678}, {537, 2.01358}, {543.2, 1.98163},
{549.5, 1.94857}, {555.9, 1.91864}, {562.3, 1.8889}, {567.5, 1.86432}, {574.1, 1.83494}, {580.8, 1.80294}, {588.8, 1.76731}, {595.7, 1.73393}, {602.6,
1.70444}, {609.5, 1.67595}, {616.6, 1.64964}, {625.2, 1.61709}, {632.4, 1.58752}, {641.2, 1.55642}, {648.6, 1.53075}, {657.7, 1.50087}, {666.8, 1.47383},
{676.1, 1.44515}, {685.5, 1.41666}, {695, 1.38984}, {704.7, 1.36555}, {714.5, 1.33719}, {724.4, 1.31309}, {734.5, 1.28954}, {746.4, 1.26049}, {756.8,
1.24146}, {769.1, 1.22197}, {781.6, 1.20511}, {794.3, 1.19326}, {807.2, 1.18192}, {820.4, 1.17979}, {833.7, 1.18806}, {847.2, 1.20179}, {863, 1.22012}, {877,
1.24368}, {890, 1.27016}, {894, 1.28034}, {898, 1.29107}, {902, 1.30152}, {906, 1.30702}, {910, 1.31218}, {914, 1.31713}, {918, 1.31971}, {922, 1.32461},
{926, 1.32963}, {930, 1.3394}, {934, 1.34686}, {938, 1.35426}, {942, 1.36162}, {946, 1.36894}, {950, 1.3763}, {954, 1.38361}, {958, 1.3909}, {962, 1.3982},
{966, 1.40314}, {970, 1.41046}, {974, 1.41539}, {978, 1.42269}, {982, 1.42999}, {986, 1.43491}, {990, 1.44223}, {994, 1.44716}, {998, 1.4545}, {1002,
1.45944}, {1006, 1.46435}, {1010, 1.4717}, {1014, 1.47662}, {1018, 1.48155}, {1022, 1.48648}, {1026, 1.49141}, {1030, 1.49635}, {1034, 1.49885}, {1038,
1.50379}, {1042, 1.50874}, {1046, 1.5137}, {1050, 1.51866}, {1054, 1.52116}, {1058, 1.52366}, {1062, 1.52863}, {1066, 1.53361}, {1070, 1.53611}, {1074,
1.54109}, {1078, 1.5436}, {1082, 1.5486}, {1086, 1.55111}, {1090, 1.55612}, {1094, 1.55863}, {1098, 1.56115}, {1102, 1.56617}, {1106, 1.56869}, {1110,
1.5712}, {1114, 1.57372}, {1118, 1.57624}, {1122, 1.57876}, {1126, 1.58129}, {1130, 1.58382}, {1134, 1.58635}, {1138, 1.5914}, {1142, 1.59393}, {1146,
```

1.59647}, {1150, 1.599}, {1154, 1.59901}, {1158, 1.60154}, {1162, 1.60662}, {1166, 1.60916}, {1170, 1.61171}, {1174, 1.61172}, {1178, 1.61426}, {1182, 1.61681}, {1186, 1.61936}, {1190, 1.62192}, {1194, 1.62192}, {1198, 1.62447}, {1202, 1.62702}, {1206, 1.62702}, {1210, 1.62958}, {1214, 1.63214}, {1218, 1.63214}, {1222, 1.6347}, {1226, 1.6347}, {1230, 1.63983}, {1234, 1.63984}, {1238, 1.63984}, {1242, 1.64241}, {1246, 1.64498}, {1250, 1.64755}, {1254, 1.64756}, {1258, 1.65014}, {1262, 1.65015}, {1266, 1.65272}, {1270, 1.65529}, {1274, 1.65529}, {1278, 1.65786}, {1282, 1.65786}, {1286, 1.66044}, {1290, 1.66302}, {1294, 1.66302}, {1298, 1.6656}, {1302, 1.6656}, {1306, 1.66818}, {1310, 1.67077}, {1314, 1.67078}, {1318, 1.67078}, {1322, 1.67337}, {1326, 1.67337}, {1330, 1.67597}, {1334, 1.67856}, {1338, 1.67857}, {1342, 1.67857}, {1346, 1.68117}, {1350, 1.68377}, {1354, 1.68377}, {1358, 1.68377}, {1362, 1.68378}, {1366, 1.68638}, {1370, 1.68639}, {1374, 1.68639}, {1378, 1.68899}, {1382, 1.69159}, {1386, 1.69159}, {1390, 1.69159}, {1394, 1.6942}, {1398, 1.6942}, {1402, 1.6942}, {1406, 1.69681}, {1410, 1.69681}, {1414, 1.69681}, {1418, 1.69942}, {1422, 1.69941}, {1426, 1.70202}, {1430, 1.70463}, {1434, 1.70463}, {1438, 1.70463}, {1442, 1.70463}, {1446, 1.70724}, {1450, 1.70984}, {1454, 1.70721}, {1458, 1.70982}, {1462, 1.71244}, {1466, 1.71243}, {1470, 1.71504}, {1474, 1.71504}, {1478, 1.71765}, {1482, 1.71763}, {1486, 1.72025}, {1490, 1.72023}, {1494, 1.72022}, {1498, 1.72284}, {1502, 1.72545}, {1506, 1.72544}, {1510, 1.73068}, {1514, 1.73066}, {1518, 1.7359}, {1522, 1.73587}, {1526, 1.73845}, {1530, 1.73839}, {1534, 1.74624}, {1538, 1.74618}, {1542, 1.74608}, {1546, 1.75127}, {1550, 1.75118}, {1554, 1.75639}, {1558, 1.76158}, {1562, 1.76677}, {1566, 1.76665}, {1570, 1.77449}, {1574, 1.78235}, {1578, 1.79282}, {1582, 1.80063}, {1586, 1.80303}, {1590, 1.80805}, {1594, 1.81028}, {1598, 1.81236}, {1602, 1.80891}, {1606, 1.80807}, {1610, 1.80429}, {1614, 1.79778}, {1618, 1.77871}, {1622, 1.76923}, {1626, 1.75423}, {1630, 1.73995}, {1634, 1.71545}, {1638, 1.6913}, {1642, 1.66497}, {1646, 1.64202}, {1650, 1.61685}, {1654, 1.59195}, {1658, 1.57222}, {1662, 1.55568}, {1666, 1.54444}, {1670, 1.54087}, {1674, 1.53731}, {1678, 1.53365}, {1682, 1.53357}, {1686, 1.52969}, {1690, 1.52553}, {1694, 1.52132}, {1698, 1.52201}, {1702, 1.52502}, {1706, 1.52788}, {1710, 1.53317}, {1714, 1.5409}, {1718, 1.55358}, {1722, 1.56377}, {1726, 1.56893}, {1730, 1.57407}, {1734, 1.57921}, {1738, 1.58434}, {1742, 1.59199}, {1746, 1.59964}, {1750, 1.60478}, {1754, 1.60746}, {1758, 1.61257}, {1762, 1.61514}, {1766, 1.61771}, {1770, 1.62028}, {1774, 1.62284}, {1778, 1.62286}, {1782, 1.62797}, {1786, 1.63054}, {1790, 1.63822}, {1794, 1.64335}, {1798, 1.64592}, {1802, 1.65107}, {1806, 1.65364}, {1810, 1.65365}, {1814, 1.65623}, {1818, 1.65881}, {1822, 1.66139}, {1826, 1.66397}, {1830, 1.66656}, {1834, 1.66914}, {1838, 1.67173}, {1842, 1.67432}, {1846, 1.67691}, {1850, 1.6795}, {1854, 1.67951}, {1858, 1.6821}, {1862, 1.6847}, {1866, 1.68729}, {1870, 1.6873}, {1874, 1.68989}, {1878, 1.68989}, {1882, 1.69249}, {1886, 1.69249}, {1890, 1.6951}, {1894, 1.6951}, {1898, 1.6977}, {1902, 1.70031}, {1906, 1.70031}, {1910, 1.70292}, {1914, 1.70553}, {1918, 1.70814}, {1922, 1.70814}, {1926, 1.71075}, {1930, 1.71337}, {1934, 1.71337}, {1938, 1.71599}, {1942, 1.71598}, {1946, 1.7186}, {1950, 1.7186}, {1954, 1.7186}, {1958, 1.72122}, {1962, 1.72121}, {1966, 1.72383}, {1970, 1.72383}, {1974, 1.72383}, {1978, 1.72382}, {1982, 1.72645}, {1986, 1.72644}, {1990, 1.72644}, {1994, 1.72643}, {1998, 1.72643}, {2002, 1.72906}, {2006, 1.72905}, {2010, 1.73168}, {2014, 1.73168}, {2018, 1.73167}, {2022, 1.73167}, {2026, 1.7343}, {2030, 1.73429}, {2034, 1.73429}, {2038, 1.73429}, {2042, 1.73692}, {2046, 1.73691}, {2050, 1.73691}, {2054, 1.7369}, {2058, 1.7369}, {2062, 1.7369}, {2066, 1.73689}, {2070, 1.73689}, {2074, 1.73689}, {2078, 1.73952}, {2082, 1.73952}, {2086, 1.73952}, {2090, 1.73952}, {2094, 1.73952}, {2098, 1.73952}, {2102, 1.74216}, {2106, 1.73952}, {2110, 1.73952}, {2114, 1.73952}, {2118, 1.73952}, {2122, 1.73952}, {2126, 1.73952}, {2130, 1.73952}, {2134, 1.73952}, {2138, 1.73953}, {2142, 1.73953}, {2146, 1.73953}, {2150, 1.73953}, {2154, 1.73954}, {2158, 1.73954}, {2162, 1.73954}, {2166, 1.73955}, {2170, 1.73955}, {2174, 1.73956}, {2178, 1.73956}, {2182, 1.73957}, {2186, 1.73957}, {2190, 1.73958}, {2194, 1.73958}, {2198, 1.73959}, {2202, 1.73959}, {2206, 1.73959}, {2210, 1.74224}, {2214, 1.74224}, {2218, 1.74225}, {2222, 1.74225}, {2226, 1.74225}, {2230, 1.74226}, {2234, 1.74226}, {2238, 1.74227}, {2242, 1.74491}, {2246, 1.74491}, {2250, 1.74492}, {2254, 1.74492}, {2258, 1.74493}, {2262, 1.74757}, {2266, 1.74758}, {2270, 1.74758}, {2274, 1.74758}, {2278, 1.74759}, {2282, 1.74759}, {2286, 1.75024}, {2290, 1.75024}, {2294, 1.75024}, {2298, 1.75024}, {2302, 1.75025}, {2306, 1.75025}, {2310, 1.7529}, {2314, 1.7529}, {2318, 1.7529}, {2322, 1.7529}, {2326, 1.75291}, {2330, 1.75291}, {2334, 1.75291}, {2338, 1.75556}, {2342, 1.75556}, {2346, 1.75822}, {2350, 1.75822}, {2354, 1.75822}, {2358, 1.75822}, {2362, 1.76088}, {2366, 1.76088}, {2370, 1.76088}, {2374, 1.76088}, {2378, 1.76354}, {2382, 1.7662}, {2386, 1.7662}, {2390, 1.7662}, {2394, 1.7662}, {2398, 1.76886}, {2402, 1.76886}, {2406, 1.77152}, {2410, 1.77152}, {2414, 1.77152}, {2418, 1.77419}, {2422, 1.77419}, {2426, 1.77685}, {2430, 1.77686}, {2434, 1.77686}, {2438, 1.77686}, {2442, 1.77953}, {2446, 1.77953}, {2450, 1.7822}, {2454, 1.7822}, {2458, 1.7822}, {2462, 1.7822}, {2466, 1.7822}, {2470, 1.78487}, {2474, 1.78487}, {2478, 1.78487}, {2482, 1.78755}, {2486, 1.78755}, {2490, 1.78755}, {2494, 1.78755}, {2498, 1.79022}, {2502, 1.7929}, {2506, 1.7929}, {2510, 1.79558}, {2514, 1.79558}, {2518, 1.79826}, {2522, 1.80095}, {2526, 1.80095}, {2530, 1.80095}, {2534, 1.80363}, {2538, 1.80632}, {2542, 1.80632}, {2546, 1.80632}, {2550, 1.80901}, {2554, 1.80901}, {2558, 1.8117}, {2562, 1.8117}, {2566, 1.81439}, {2570, 1.81709}, {2574, 1.81709}, {2578, 1.81979}, {2582, 1.81979}, {2586, 1.81979}, {2590, 1.82249}, {2594, 1.82249}, {2598, 1.82519}, {2602, 1.82789}, {2606, 1.82789}, {2610, 1.8306}, {2614, 1.8306}, {2618, 1.8333}, {2622, 1.8333}, {2626, 1.8333}, {2630, 1.83601}, {2634, 1.83601}, {2638, 1.83601}, {2642, 1.83601}, {2646, 1.83872}, {2650, 1.84144}, {2654, 1.84144}, {2658, 1.84144}, {2662, 1.84415}, {2666, 1.84687}, {2670, 1.84687}, {2674, 1.84687}, {2678, 1.84959}, {2682, 1.84959}, {2686, 1.85231}, {2690, 1.85231}, {2694, 1.85231}, {2698, 1.85503}, {2702, 1.85503}, {2706, 1.85775}, {2710, 1.85775}, {2714, 1.86048}, {2718, 1.86321}, {2722, 1.86321}, {2726, 1.86594}, {2730, 1.86867}, {2734, 1.86867}, {2738, 1.8714}, {2742, 1.8714}, {2746, 1.87414}, {2750, 1.87688}, {2754, 1.87688}, {2758, 1.87962}, {2762, 1.87962}, {2766, 1.88236}, {2770, 1.8851}, {2774, 1.88785}, {2778, 1.8906}, {2782, 1.89059}, {2786, 1.89334}, {2790, 1.8961}, {2794, 1.89885}, {2798, 1.89885}, {2802, 1.9016}, {2806, 1.90436}, {2810, 1.90712}, {2814, 1.90988}, {2818, 1.91264}, {2822, 1.91264}, {2826, 1.9154}, {2830, 1.91817}, {2834, 1.92094}, {2838, 1.92371}, {2842, 1.92648}, {2846, 1.92648}, {2850, 1.93203}, {2854, 1.93202}, {2858, 1.9348}, {2862, 1.93758}, {2866, 1.94036}, {2870, 1.94314}, {2874, 1.94313}, {2878, 1.94591}, {2882, 1.9487}, {2886, 1.95148}, {2890, 1.95707}, {2894, 1.95706}, {2898, 1.95985}, {2902, 1.96264}, {2906, 1.96543}, {2910, 1.96823}, {2914, 1.97102}, {2918, 1.97382}, {2922, 1.97661}, {2926, 1.98223}, {2930, 1.98503}, {2934, 1.98783}, {2938, 1.99063}, {2942, 1.99626}, {2946, 1.99624}, {2950, 2.00188}, {2954, 2.00469}, {2958, 2.00751}, {2962, 2.01032}, {2966, 2.01596}, {2970, 2.01874}, {2974, 2.02151}, {2978, 2.02714}, {2982, 2.02992}, {2986, 2.0327}, {2990, 2.03832}, {2994, 2.04107}, {2998, 2.04374}, {3002, 2.04933}, {3006, 2.05207}, {3010, 2.05767}, {3014, 2.06042}, {3018, 2.06318}, {3022, 2.06883}, {3026, 2.0716}, {3030, 2.07728}, {3034, 2.08009}, {3038, 2.0829}, {3042, 2.08861}, {3046, 2.0914}, {3050, 2.09707}, {3054, 2.09984}, {3058, 2.10548}, {3062, 2.10819}, {3066, 2.1138}, {3070, 2.11644}, {3074, 2.12199}, {3078, 2.12457}, {3082, 2.13003}, {3086, 2.13257}, {3090, 2.13512}, {3094, 2.13765}, {3098, 2.14309}, {3102, 2.14557}, {3106, 2.14806}, {3110, 2.15058}, {3114, 2.15309}, {3118, 2.15559}, {3122, 2.15806}, {3126, 2.16047}, {3130, 2.1629}, {3134, 2.16825}, {3138, 2.17358}, {3142, 2.17295}, {3146, 2.17225}, {3150, 2.16853}, {3154, 2.16772}, {3158, 2.16684}, {3162, 2.1658}, {3166, 2.16471}, {3170, 2.16062}, {3174, 2.15942}, {3178, 2.15523}, {3182, 2.15396}, {3186, 2.14972}, {3190, 2.14263}, {3194, 2.13834}, {3198, 2.1312}, {3202, 2.1299}, {3206, 2.12575}, {3210, 2.12164}, {3214, 2.11447}, {3218, 2.11035}, {3222, 2.10318}, {3226, 2.09903}, {3230, 2.09205}, {3234, 2.08203}, {3238, 2.07212}, {3242, 2.0623}, {3246, 2.05215}, {3250, 2.03614}, {3254, 2.02603}, {3258, 2.01317}, {3262, 1.99768}, {3266, 1.98797}, {3270, 1.97827}, {3274, 1.97195}, {3278, 1.96253}, {3282, 1.95591}, {3286, 1.94636}, {3290, 1.93682}, {3294, 1.93316}, {3298, 1.92686}, {3302, 1.91733}, {3306, 1.90772}, {3310, 1.89835}, {3314, 1.88575}, {3318, 1.87641}, {3322, 1.86712}, {3326, 1.85774}, {3330, 1.85109}, {3334, 1.83871}, {3338, 1.82318}, {3342, 1.81364}, {3346, 1.79557}, {3350, 1.78322}, {3354, 1.77099}, {3358, 1.75332}, {3362, 1.73884}, {3366, 1.72144}, {3370, 1.7041}, {3374, 1.69526}, {3378, 1.67892}, {3382, 1.66248}, {3386, 1.64931}, {3390, 1.63362}, {3394, 1.61755}, {3398, 1.5989}, {3402, 1.57732}, {3406, 1.5512}, {3410, 1.53404}, {3414, 1.514}, {3418, 1.50214}, {3422, 1.47775}, {3426, 1.4534}, {3430, 1.43428}, {3434, 1.41533}, {3438, 1.39927}, {3442, 1.38358}, {3446, 1.36809}, {3450, 1.35469}, {3454, 1.3419}, {3458, 1.33131}, {3462, 1.31402}, {3466, 1.30187}, {3470, 1.28254}, {3474, 1.27278}, {3478, 1.26805}, {3482, 1.26345}, {3486, 1.24914}, {3490, 1.24689}, {3494, 1.24201}, {3498, 1.23974}, {3502, 1.23276}, {3506, 1.22092}, {3510, 1.21369}, {3514, 1.20649}, {3518, 1.1944}, {3522, 1.1871}, {3526, 1.17528}, {3530, 1.15479}, {3534, 1.14948}, {3538, 1.14431}, {3542,

```
1.13504}, {3546, 1.13904}, {3550, 1.14513}, {3554, 1.14673}, {3558, 1.15909}, {3562, 1.16288}, {3566, 1.16893}, {3570, 1.16835}, {3574, 1.16768}, {3578,
1.1669}, {3582, 1.17257}, {3586, 1.18038}, {3590, 1.19035}, {3594, 1.20242}, {3598, 1.21225}, {3602, 1.22198}, {3606, 1.23163}, {3610, 1.23685}, {3614,
1.23976}, {3618, 1.23369}, {3622, 1.23212}, {3626, 1.23274}, {3630, 1.23119}, {3634, 1.23184}, {3638, 1.23024}, {3642, 1.23315}, {3646, 1.23837}, {3650,
1.24586}, {3654, 1.25781}, {3658, 1.2697}, {3662, 1.27926}, {3666, 1.29106}, {3670, 1.30744}, {3674, 1.31467}, {3678, 1.31953}, {3682, 1.32201}, {3686,
1.32904}, {3690, 1.33838}, {3694, 1.34539}, {3698, 1.35007}, {3702, 1.35941}, {3706, 1.3641}, {3710, 1.37114}, {3714, 1.37819}, {3718, 1.38526}, {3722,
1.38998}, {3726, 1.39707}, {3730, 1.40181}, {3734, 1.40655}, {3740, 1.41369}, {3745, 1.42084}, {3751, 1.428}, {3757, 1.43279}, {3762, 1.4399}, {3768,
1.44479}, {3774, 1.45201}, {3779, 1.45684}, {3785, 1.46167}, {3791, 1.46651}, {3797, 1.47136}, {3802, 1.47622}, {3808, 1.48108}, {3814, 1.48352}, {3820,
1.48839}, {3826, 1.49328}, {3831, 1.49572}, {3837, 1.50062}, {3843, 1.50307}, {3849, 1.50552}, {3855, 1.51044}, {3861, 1.51289}, {3867, 1.51536}, {3873,
1.52028}, {3879, 1.52275}, {3885, 1.52522}, {3891, 1.52769}, {3897, 1.53016}, {3903, 1.53264}, {3909, 1.53512}, {3915, 1.5376}, {3922, 1.54008}, {3928,
1.54256}, {3934, 1.54504}, {3940, 1.54753}, {3946, 1.55002}, {3953, 1.55251}, {3959, 1.555}, {3965, 1.555}, {3971, 1.5575}, {3978, 1.56}, {3984, 1.5625},
{3990, 1.5625}, {3997, 1.565}, {4003, 1.5675}, {4010, 1.57001}, {4016, 1.57001}, {4023, 1.57251}, {4029, 1.57502}, {4036, 1.57502}, {4042, 1.57753}, {4049,
1.58005}, {4055, 1.58005}, {4062, 1.58256}, {4068, 1.58256}, {4075, 1.58508}, {4082, 1.5876}, {4088, 1.5876}, {4095, 1.59012}, {4102, 1.59012}, {4108,
1.59264}, {4115, 1.59517}, {4122, 1.59517}, {4129, 1.59769}, {4136, 1.59769}, {4143, 1.60022}, {4149, 1.60022}, {4156, 1.60276}, {4163, 1.60276}, {4170,
1.60529}, {4177, 1.60529}, {4184, 1.60782}, {4191, 1.60782}, {4198, 1.60782}, {4205, 1.61036}, {4212, 1.6129}, {4219, 1.6129}, {4227, 1.6129}, {4234,
1.61544}, {4241, 1.61544}, {4248, 1.61798}, {4255, 1.61798}, {4263, 1.62053}, {4270, 1.62053}, {4277, 1.62053}, {4284, 1.62308}, {4292, 1.62308}, {4299,
1.62562}, {4307, 1.62562}, {4314, 1.62562}, {4322, 1.62818}, {4329, 1.62818}, {4337, 1.62818}, {4344, 1.63073}, {4352, 1.63073}, {4359, 1.63328}, {4367,
1.63328}, {4374, 1.63328}, {4382, 1.63584}, {4390, 1.63584}, {4398, 1.63584}, {4405, 1.6384}, {4413, 1.6384}, {4421, 1.6384}, {4429, 1.64096}, {4437,
1.64096}, {4444, 1.64096}, {4452, 1.64096}, {4460, 1.64352}, {4468, 1.64352}, {4476, 1.64352}, {4484, 1.64609}, {4492, 1.64609}, {4500, 1.64609}, {4509,
1.64866}, {4517, 1.64866}, {4525, 1.64866}, {4533, 1.65122}, {4541, 1.65122}, {4550, 1.65122}, {4558, 1.65122}, {4566, 1.6538}, {4575, 1.6538}, {4583,
1.6538}, {4591, 1.6538}, {4600, 1.65637}, {4608, 1.65637}, {4617, 1.65637}, {4625, 1.65894}, {4634, 1.65894}, {4643, 1.65894}, {4651, 1.65894}, {4660,
1.65894}, {4669, 1.66152}, {4677, 1.66152}, {4686, 1.66152}, {4695, 1.66152}, {4704, 1.6641}, {4713, 1.6641}, {4721, 1.6641}, {4730, 1.6641}, {4739, 1.66668},
 {4748, 1.66668}, {4757, 1.66668}, {4766, 1.66668}, {4776, 1.66926}, {4785, 1.66926}, {4794, 1.66926}, {4803, 1.66926}, {4812, 1.66926}, {4822, 1.67185},
{4831, 1.67185}, {4840, 1.67185}, {4850, 1.67185}, {4859, 1.67185}, {4869, 1.67444}, {4878, 1.67444}, {4888, 1.67444}, {4897, 1.67444}, {4907, 1.67444},
{4916, 1.67702}, {4926, 1.67702}, {4936, 1.67702}, {4946, 1.67702}, {4955, 1.67962}, {4965, 1.67962}, {4975, 1.67962}, {4985, 1.67961}, {4995, 1.67961},
{5005, 1.67961}, {5015, 1.67961}, {5025, 1.68221}, {5035, 1.68221}, {5045, 1.68221}, {5056, 1.68221}, {5066, 1.68221}, {5076, 1.68221}, {5086, 1.6848}, {5097,
 1.6848}, {5107, 1.6848}, {5118, 1.6848}, {5128, 1.6848}, {5139, 1.6848}, {5149, 1.6848}, {5160, 1.6848}, {5171, 1.6848}, {5181, 1.6848}, {5192, 1.6848},
{5203, 1.6848}, {5214, 1.6848}, {5225, 1.6848}, {5236, 1.6848}, {5247, 1.6848}, {5258, 1.6848}, {5269, 1.6848}, {5280, 1.6848}, {5291, 1.6848}, {5302,
1.6874}, {5313, 1.6874}, {5325, 1.6874}, {5336, 1.6874}, {5348, 1.69}, {5359, 1.69}, {5371, 1.69}, {5382, 1.69}, {5394, 1.6926}, {5405, 1.6926}, {5417,
1.6926}, {5429, 1.6926}, {5441, 1.6926}, {5453, 1.6926}, {5464, 1.6952}, {5476, 1.6952}, {5488, 1.6952}, {5501, 1.6952}, {5513, 1.6952}, {5525, 1.6952},
{5537, 1.69781}, {5549, 1.69781}, {5562, 1.69781}, {5574, 1.69781}, {5587, 1.69781}, {5599, 1.69781}, {5612, 1.69781}, {5624, 1.70042}, {5637, 1.70042},
{5650, 1.70042}, {5663, 1.70042}, {5675, 1.70042}, {5688, 1.70042}, {5701, 1.70042}, {5714, 1.70042}, {5727, 1.70302}, {5741, 1.70302}, {5754, 1.70302},
{5767, 1.70302}, {5780, 1.70302}, {5794, 1.70302}, {5807, 1.70302}, {5821, 1.70564}, {5834, 1.70564}, {5848, 1.70564}, {5862, 1.70564}, {5875, 1.70564},
{5889, 1.70564}, {5903, 1.70564}, {5917, 1.70564}, {5931, 1.70564}, {5945, 1.70825}, {5959, 1.70825}, {5974, 1.70825}, {5988, 1.70825}, {6002, 1.70825},
{6017, 1.70825}, {6031, 1.70825}, {6046, 1.71086}, {6061, 1.71086}, {6075, 1.71086}, {6090, 1.71086}, {6105, 1.71086}, {6120, 1.71086}, {6135, 1.71086},
{6150, 1.71086}, {6165, 1.71086}, {6180, 1.71348}, {6196, 1.71348}, {6211, 1.71348}, {6227, 1.71348}, {6242, 1.71348}, {6258, 1.71348}, {6274, 1.71348},
{6289, 1.71348}, {6305, 1.71348}, {6321, 1.71348}, {6337, 1.7161}, {6353, 1.7161}, {6369, 1.7161}, {6386, 1.7161}, {6402, 1.7161}, {6418, 1.7161}, {6435,
1.7161}, {6452, 1.7161}, {6468, 1.7161}, {6485, 1.71872}, {6502, 1.71872}, {6519, 1.71872}, {6536, 1.71872}, {6553, 1.71872}, {6570, 1.71872}, {6588,
1.71872}, {6605, 1.71872}, {6623, 1.71872}, {6640, 1.71872}, {6658, 1.71872}, {6676, 1.72134}, {6693, 1.72134}, {6711, 1.72134}, {6729, 1.72134}, {6748,
1.72134}, {6766, 1.72134}, {6784, 1.72134}, {6803, 1.72134}, {6821, 1.72134}, {6840, 1.72134}, {6859, 1.72397}, {6878, 1.72397}, {6897, 1.72397}, {6916,
1.72397}, {6935, 1.72397}, {6954, 1.72397}, {6974, 1.72397}, {6993, 1.72397}, {7013, 1.72397}, {7032, 1.72397}, {7052, 1.72397}, {7072, 1.72397}, {7092,
1.72397}, {7112, 1.72397}, {7133, 1.7266}, {7153, 1.7266}, {7174, 1.7266}, {7194, 1.7266}, {7215, 1.7266}, {7236, 1.7266}, {7257, 1.7266}, {7278, 1.7266},
{7299, 1.7266}, {7321, 1.7266}, {7342, 1.7266}, {7364, 1.72922}, {7386, 1.72922}, {7407, 1.72922}, {7429, 1.72922}, {7452, 1.72922}, {7474, 1.72922}, {7496,
1.72922}, {7519, 1.72922}, {7541, 1.72922}, {7564, 1.72922}, {7587, 1.73186}, {7610, 1.73186}, {7634, 1.73186}, {7657, 1.73186}, {7680, 1.73186}, {7704,
1.73186}, {7728, 1.73186}, {7752, 1.73186}, {7776, 1.73186}, {7800, 1.73186}, {7825, 1.73186}, {7849, 1.73186}, {7874, 1.73186}, {7899, 1.73449}, {7924,
1.73449}, {7949, 1.73449}, {7974, 1.73449}, {8000, 1.73449}, {8026, 1.73449}, {8052, 1.73449}, {8078, 1.73449}, {8104, 1.73449}};

h2o=Interpolation[h2oraw];

(* Test  dielectric  function with a single  absorbtion at  2325 to see how absorbtion bands interact with plasmons *)

testabsorbraw={{500, 1.4}, {1000, 1.4}, {1200, 1.4}, {1500, 1.4}, {2000, 1.4}, {2300, 1.4}, {2310, 1.3}, {2320, 1.2}, {2325, 1.02}, {2330, 1.2}, {2340, 1.3}, {2350,
    1.4}, {2500, 1.4}, {3000, 1.4}, {3500, 1.4}, {4000, 1.4}, {4500, 1.4}, {5000, 1.4}, {5500, 1.4}, {6000, 1.4}, {6500, 1.4}, {7000, 1.4}, {7500, 1.4}, {8000,
    1.4}, {8104, 1.4}};
testabsorb=Interpolation[testabsorbraw, InterpolationOrder->1];

CO2e1raw={{3500, 1.00087}, {3490, 1.00087}, {3480, 1.00087}, {3470, 1.00087}, {3460, 1.00087}, {3450, 1.00087}, {3440, 1.00087}, {3430, 1.00087}, {3420, 1.00087},
    {3410, 1.00087}, {3400, 1.00087}, {3390, 1.00087}, {3380, 1.00087}, {3370, 1.00087}, {3360, 1.00087}, {3350, 1.00087}, {3340, 1.00087}, {3330, 1.00087},
    {3320, 1.00087}, {3310, 1.00087}, {3300, 1.00087}, {3290, 1.00087}, {3280, 1.00087}, {3270, 1.00087}, {3260, 1.00087}, {3250, 1.00087}, {3240, 1.00087},
    {3230, 1.00087}, {3220, 1.00087}, {3210, 1.00087}, {3200, 1.00087}, {3190, 1.00087}, {3180, 1.00087}, {3170, 1.00087}, {3160, 1.00087}, {3150, 1.00087},
    {3140, 1.00087}, {3130, 1.00087}, {3120, 1.00087}, {3110, 1.00087}, {3100, 1.00087}, {3090, 1.00087}, {3080, 1.00087}, {3070, 1.00087}, {3060, 1.00087},
    {3050, 1.00087}, {3040, 1.00087}, {3030, 1.00087}, {3020, 1.00087}, {3010, 1.00087}, {3000, 1.00087}, {2990, 1.00087}, {2980, 1.00087}, {2970, 1.00087},
    {2960, 1.00087}, {2950, 1.00087}, {2940, 1.00087}, {2930, 1.00087}, {2920, 1.00087}, {2910, 1.00087}, {2900, 1.00087}, {2890, 1.00087}, {2880, 1.00087},
    {2870, 1.00087}, {2860, 1.00087}, {2850, 1.00087}, {2840, 1.00087}, {2830, 1.00087}, {2820, 1.00087}, {2810, 1.00087}, {2800, 1.00087}, {2790, 1.00087},
    {2780, 1.00087}, {2770, 1.00087}, {2760, 1.00087}, {2750, 1.00087}, {2740, 1.00087}, {2730, 1.00087}, {2720, 1.00087}, {2710, 1.00087}, {2700, 1.00087},
    {2690, 1.00087}, {2680, 1.00087}, {2670, 1.00087}, {2660, 1.00087}, {2650, 1.00087}, {2640, 1.00087}, {2630, 1.00087}, {2620, 1.00087}, {2610, 1.00087},
    {2600, 1.00087}, {2590, 1.00087}, {2580, 1.00087}, {2570, 1.00087}, {2560, 1.00087}, {2550, 1.00087}, {2540, 1.00087}, {2530, 1.00087}, {2520, 1.00087},
```

```
{2510, 1.00087}, {2500, 1.00087}, {2490, 1.00087}, {2480, 1.00087}, {2470, 1.00087}, {2460, 1.00087}, {2450, 1.00087}, {2440, 1.00087}, {2430, 1.00087},
{2420, 1.00087}, {2410, 1.00087}, {2400, 0.9}, {2390, 0.8}, {2380, 0.7}, {2370, 0.4}, {2360, 0.2}, {2350, 1.8}, {2340, 1.6}, {2330, 1.3}, {2320, 1.2}, {2310,
1.1}, {2300, 1.00087}, {2290, 1.00087}, {2280, 1.00087}, {2270, 1.00087}, {2260, 1.00087}, {2250, 1.00087}, {2240, 1.00087}, {2230, 1.00087}, {2220, 1.00087},
{2210, 1.00087}, {2200, 1.00087}, {2190, 1.00087}, {2180, 1.00087}, {2170, 1.00087}, {2160, 1.00087}, {2150, 1.00087}, {2140, 1.00087}, {2130, 1.00087},
{2120, 1.00087}, {2110, 1.00087}, {2100, 1.00087}, {2090, 1.00087}, {2080, 1.00087}, {2070, 1.00087}, {2060, 1.00087}, {2050, 1.00087}, {2040, 1.00087},
{2030, 1.00087}, {2020, 1.00087}, {2010, 1.00087}, {2000, 1.00087}, {1990, 1.00087}, {1980, 1.00087}, {1970, 1.00087}, {1960, 1.00087}, {1950, 1.00087},
{1940, 1.00087}, {1930, 1.00087}, {1920, 1.00087}, {1910, 1.00087}, {1900, 1.00087}, {1890, 1.00087}, {1880, 1.00087}, {1870, 1.00087}, {1860, 1.00087},
{1850, 1.00087}, {1840, 1.00087}, {1830, 1.00087}, {1820, 1.00087}, {1810, 1.00087}, {1800, 1.00087}, {1790, 1.00087}, {1780, 1.00087}, {1770, 1.00087},
{1760, 1.00087}, {1750, 1.00087}, {1740, 1.00087}, {1730, 1.00087}, {1720, 1.00087}, {1710, 1.00087}, {1700, 1.00087}, {1690, 1.00087}, {1680, 1.00087},
{1670, 1.00087}, {1660, 1.00087}, {1650, 1.00087}, {1640, 1.00087}, {1630, 1.00087}, {1620, 1.00087}, {1610, 1.00087}, {1600, 1.00087}, {1590, 1.00087},
{1580, 1.00087}, {1570, 1.00087}, {1560, 1.00087}, {1550, 1.00087}, {1540, 1.00087}, {1530, 1.00087}, {1520, 1.00087}, {1510, 1.00087}, {1500, 1.00087},
{1490, 1.00087}, {1480, 1.00087}, {1470, 1.00087}, {1460, 1.00087}, {1450, 1.00087}, {1440, 1.00087}, {1430, 1.00087}, {1420, 1.00087}, {1410, 1.00087},
{1400, 1.00087}, {1390, 1.00087}, {1380, 1.00087}, {1370, 1.00087}, {1360, 1.00087}, {1350, 1.00087}, {1340, 1.00087}, {1330, 1.00087}, {1320, 1.00087},
{1310, 1.00087}, {1300, 1.00087}, {1290, 1.00087}, {1280, 1.00087}, {1270, 1.00087}, {1260, 1.00087}, {1250, 1.00087}, {1240, 1.00087}, {1230, 1.00087},
{1220, 1.00087}, {1210, 1.00087}, {1200, 1.00087}, {1190, 1.00087}, {1180, 1.00087}, {1170, 1.00087}, {1160, 1.00087}, {1150, 1.00087}, {1140, 1.00087},
{1130, 1.00087}, {1120, 1.00087}, {1110, 1.00087}, {1100, 1.00087}, {1090, 1.00087}, {1080, 1.00087}, {1070, 1.00087}, {1060, 1.00087}, {1050, 1.00087},
{1040, 1.00087}, {1030, 1.00087}, {1020, 1.00087}, {1010, 1.00087}, {1000, 1.00087}};
CO2e1=Interpolation[CO2e1raw, InterpolationOrder->1];

CO2e2raw={{3500, 0}, {3490, 0}, {3480, 0}, {3470, 0}, {3460, 0}, {3450, 0}, {3440, 0}, {3430, 0}, {3420, 0}, {3410, 0}, {3400, 0}, {3390, 0}, {3380, 0}, {3370, 0},
{3360, 0}, {3350, 0}, {3340, 0}, {3330, 0}, {3320, 0}, {3310, 0}, {3300, 0}, {3290, 0}, {3280, 0}, {3270, 0}, {3260, 0}, {3250, 0}, {3240, 0}, {3230, 0},
{3220, 0}, {3210, 0}, {3200, 0}, {3190, 0}, {3180, 0}, {3170, 0}, {3160, 0}, {3150, 0}, {3140, 0}, {3130, 0}, {3120, 0}, {3110, 0}, {3100, 0}, {3090, 0},
{3080, 0}, {3070, 0}, {3060, 0}, {3050, 0}, {3040, 0}, {3030, 0}, {3020, 0}, {3010, 0}, {3000, 0}, {2990, 0}, {2980, 0}, {2970, 0}, {2960, 0}, {2950, 0},
{2940, 0}, {2930, 0}, {2920, 0}, {2910, 0}, {2900, 0}, {2890, 0}, {2880, 0}, {2870, 0}, {2860, 0}, {2850, 0}, {2840, 0}, {2830, 0}, {2820, 0}, {2810, 0},
{2800, 0}, {2790, 0}, {2780, 0}, {2770, 0}, {2760, 0}, {2750, 0}, {2740, 0}, {2730, 0}, {2720, 0}, {2710, 0}, {2700, 0}, {2690, 0}, {2680, 0}, {2670, 0},
{2660, 0}, {2650, 0}, {2640, 0}, {2630, 0}, {2620, 0}, {2610, 0}, {2600, 0}, {2590, 0}, {2580, 0}, {2570, 0}, {2560, 0}, {2550, 0}, {2540, 0}, {2530, 0},
{2520, 0}, {2510, 0}, {2500, 0}, {2490, 0}, {2480, 0}, {2470, 0}, {2460, 0}, {2450, 0}, {2440, 0}, {2430, 0}, {2420, 0}, {2410, 0}, {2400, 0.1}, {2390, 0.2},
{2380, 0.3}, {2370, 0.5}, {2360, 2}, {2350, 2}, {2340, 0.5}, {2330, 0.3}, {2320, 0.2}, {2310, 0.1}, {2300, 0}, {2290, 0}, {2280, 0}, {2270, 0}, {2260, 0},
{2250, 0}, {2240, 0}, {2230, 0}, {2220, 0}, {2210, 0}, {2200, 0}, {2190, 0}, {2180, 0}, {2170, 0}, {2160, 0}, {2150, 0}, {2140, 0}, {2130, 0}, {2120, 0},
{2110, 0}, {2100, 0}, {2090, 0}, {2080, 0}, {2070, 0}, {2060, 0}, {2050, 0}, {2040, 0}, {2030, 0}, {2020, 0}, {2010, 0}, {2000, 0}, {1990, 0}, {1980, 0},
{1970, 0}, {1960, 0}, {1950, 0}, {1940, 0}, {1930, 0}, {1920, 0}, {1910, 0}, {1900, 0}, {1890, 0}, {1880, 0}, {1870, 0}, {1860, 0}, {1850, 0}, {1840, 0},
{1830, 0}, {1820, 0}, {1810, 0}, {1800, 0}, {1790, 0}, {1780, 0}, {1770, 0}, {1760, 0}, {1750, 0}, {1740, 0}, {1730, 0}, {1720, 0}, {1710, 0}, {1700, 0},
{1690, 0}, {1680, 0}, {1670, 0}, {1660, 0}, {1650, 0}, {1640, 0}, {1630, 0}, {1620, 0}, {1610, 0}, {1600, 0}, {1590, 0}, {1580, 0}, {1570, 0}, {1560, 0},
{1550, 0}, {1540, 0}, {1530, 0}, {1520, 0}, {1510, 0}, {1500, 0}, {1490, 0}, {1480, 0}, {1470, 0}, {1460, 0}, {1450, 0}, {1440, 0}, {1430, 0}, {1420, 0},
{1410, 0}, {1400, 0}, {1390, 0}, {1380, 0}, {1370, 0}, {1360, 0}, {1350, 0}, {1340, 0}, {1330, 0}, {1320, 0}, {1310, 0}, {1300, 0}, {1290, 0}, {1280, 0},
{1270, 0}, {1260, 0}, {1250, 0}, {1240, 0}, {1230, 0}, {1220, 0}, {1210, 0}, {1200, 0}, {1190, 0}, {1180, 0}, {1170, 0}, {1160, 0}, {1150, 0}, {1140, 0},
{1130, 0}, {1120, 0}, {1110, 0}, {1100, 0}, {1090, 0}, {1080, 0}, {1070, 0}, {1060, 0}, {1050, 0}, {1040, 0}, {1030, 0}, {1020, 0}, {1010, 0}, {1000, 0}};
CO2e2=Interpolation[CO2e2raw, InterpolationOrder->1];
```

B.2 SPR Kretschmann simulations*

This is the code used to simulate the reflectivity for thin film samples in the Kretschmann configuration in energy and angle space.

```
SetOptions[EvaluationNotebook[],CellContext->Notebook];
(* physical constants *)

c=2.99792458 10^8 ;
e=1.6021773 10^-19;
h=6.6260755 10^-34;
\[HBar]=1.05457 10^-34;
K=1.380658 10^-23;
me=9.109389 10^-31;
\[Epsilon]0=8.85419 10^-12;
q= 1.6021773 10^-19;

(* input parameters *)

ne=2 10^20 1000000 ;       (*free carrier density [cm^-3]*)
\[Mu]=150/10000;                    (*mobility*)
```

```
meeff= 0.21;                          (* relative effective mass: ZnO: 0.36, CdO: 0.21, b-GaO:0.342, GaN: 0.2, ITO: 0.4 *)
einf=5.5;    (* high frequqency dielectric constant: ZnO: 3.2 , CdO: 5.5   InGaAs:9.61    b-GaO:3.57 , GaN: 5.3,ITO: 4 *)

(* calculated variables for Drude equations *)

\[CapitalGamma]= N[q /(\[Mu] meeff me )];(*absorbtion term; damping*)
wp=N[Sqrt[(ne q^2 )/(meeff me \[Epsilon]0)]]; (*plasme frequency*)

(* This section is used to calculate a Lorentzian absorbtion band to simulate an absorption in the environement, Code can be commented if calculations are to be
      performed in an dielectric environment *)

A=0.00957242;
w0=2215;
w1=2235;
\[CapitalGamma]lorentz=20.00;
background=1.00027^2;
\[Epsilon]N2O[wcm_]:=(background+(A w0 \[CapitalGamma]lorentz)/(w0^2-wcm^2-I \[CapitalGamma]lorentz wcm)+(A w1 \[CapitalGamma]lorentz)/(w1^2-
      wcm^2-I \[CapitalGamma]lorentz wcm));
(* Plot the resulting absorbtion band: Re for \[Epsilon]1, Im for \[Epsilon]2 *)

Plot[Re[\[Epsilon]N2O[wcm]],{wcm,2050,2450},ImageSize->{800,800},LabelStyle->Directive[30],AxesLabel->{"[cm^-1]","\[Epsilon]1"},BaseStyle->{FontFamily->"
      Arial"},AspectRatio->1 ,PlotRange->{{2050,2450},{0.99,1.01}},PlotStyle->{Blue,Thickness[0.005]}]

(* The following Module iterates through all calculations necessary for reflectivity simulations in the Kretschman configuration *)

r[wcm_,\[CapitalTheta]_,d_]:=Module[{w, efilm,efilmcomplex,efilmfunction,efreesurface,xa,xb,xc,rs1,rp1,rs2,rp2,b,rp,rs,Refl,\[CapitalTheta]substrate,\[Alpha],\[Beta
      ],\[Gamma],nprism,nsubstrate,\[CapitalTheta]base,esubstrate,rpback,rsback,Rbackrefl,Refltotal},

w=wcm 3 10^10 2 \[Pi] ; (* convert to rad/s *)

(* calculate the actual incident angle at the film/substrate interface using Snell's law, the dielectric properties of the prism and substrate as well as the prism geometry
      *)

\[CapitalTheta]base=45; (* the base angle of the prism *)
nprism=N[Sqrt[caf2[wcm]]]; (* refrective index of prism, called from optical properties database *)
nsubstrate=N[Sqrt[mgo[wcm]]]; (* refrective index of substrate, called from optical properties database  *)
\[Alpha]=\[CapitalTheta]-\[CapitalTheta]base;
\[Beta]= ArcSin[1/nprism Sin[\[Alpha] Degree]] 180/\[Pi];
\[Gamma]=  ArcSin[nprism/nsubstrate Sin[(Abs[\[Beta]+\[CapitalTheta]base]) Degree]] 180/\[Pi];
\[CapitalTheta]substrate=\[Gamma]; (* This sets the angle for the reflectivity calculation to the actual incident angle at the film/substrate interface *)

efreesurface=1.00027^2; (*  permitivity of the surrounding medium*, Air:1.00027^2, \[Epsilon]N2O[wcm] for lorentzian band *)

(* Compute backreflection from Prism/substrate interface *)

rsback=(nprism Cos[(\[Beta]+\[CapitalTheta]base)Degree]-nsubstrate Cos[\[Gamma] Degree])/(nprism Cos[(\[Beta]+\[CapitalTheta]base)Degree]+nsubstrate Cos[\[
      Gamma] Degree]);
rpback=(nsubstrate Cos[(\[Beta]+\[CapitalTheta]base)Degree]-nprism Cos[\[Gamma] Degree])/(nprism Cos[\[Gamma] Degree]+nsubstrate Cos[(\[Beta]+\[
      CapitalTheta]base)Degree]);
Rbackrefl=Abs[rpback]^2/Abs[rsback]^2;

esubstrate=mgo[wcm];
efilmcomplex= einf+wp^2/((w I \[CapitalGamma])-w^2);(* calculate the dielectric function of the plasmonic film using Drude eqautions *)

efilm=Re[efilmcomplex]-I Im[efilmcomplex];

(* compute square roots in fresnel equations*)
xa=Sqrt[(esubstrate-esubstrate Sin[\[CapitalTheta]substrate Degree]^2)];
xb= Sqrt[(efilm-esubstrate Sin[\[CapitalTheta]substrate Degree]^2)];
xc=Sqrt[(efreesurface-esubstrate Sin[\[CapitalTheta]substrate Degree]^2)];
(* reflectance interface 1, s- and p- polarized *)
rs1=(xa-xb)/(xa+xb);
rp1=(efilm xa-esubstrate xb)/(efilm xa+esubstrate xb);
(* reflectance interface 2, s- and p- polarized *)
rs2=(xb-xc)/(xb+xc);
rp2=(efreesurface xb-efilm xc)/(efreesurface xb+efilm xc);
```

```
(* compute Airy formula *)
b=2 \[Pi] d 10^-7wcm xb;
rp=(rp1+rp2 Exp[2 I b])/(1+rp1 rp2  Exp[2 I b]);
rs=(rs1+rs2 Exp[2 I b])/(1+rs1 rs2 Exp[2 I b]);
Refl=(Abs[rp]/Abs[rs])^2;
Refltotal=(Abs[rpback]/Abs[rsback])^2 +Refl;(* Calculate total reflectance as rp/rs including the backreflection *)

Return[Refltotal]; (* Set Return[] value to the desired output, such as Refl for rp/rs, Refltotal for the included backrefelction or Abs[rp]^2 for only p-polarized
    reflectivity *)
]

(* The following commands allow for graphical output of the calculated reflectivities using different representations I found usefull for this work. For further
    information on the individual plotting commands please consult the Mathematica manual *)
(* This creates a contour Plot of the reflectivites in angle/energy space used in this work. The respective ranges can be set freely. The contouring options are also
    customizable. Calculating these plots with a large amount of contour lines can take a long time *)

ContourPlot[r[wcm,\[CapitalTheta],130],{wcm,2150,2300}
,{\[CapitalTheta],45,50},PlotRange->{0.0,1.1},ImageSize->{800,800},Contours->50,ColorFunction->"SunsetColors",PlotPoints->30,LabelStyle->Directive[30],
    FrameLabel->{"[cm^-1]","angle [\[Degree]]"},BaseStyle->{FontFamily->"Arial"}]

(* This creates a 3D Plot of the reflectivites in angle/energy space used in this work. The respective ranges can be set freely. Allows for faster calculation of
    reflectivities *)
Plot3D[r[wcm,\[CapitalTheta],200],
{wcm,1500,4000},{\[CapitalTheta],40,60},PlotRange->{0,1.1},Mesh->None,PlotPoints->40,ColorFunction->"SunsetColors", ImageSize->{800,800},TicksStyle->
    Directive[25]]
(* This creates a 2D representation within Mathematics Manipualte environment. Here R is plotted versus energy, with a slider for the film thickness and incidence
    angle. This is usefull to optimize film thickness to achieve maximum coupling at a certain incident angle *)
Manipulate[Plot[r[wcm,\[CapitalTheta],d],{wcm,1000,7000},PlotRange->{{1000,7000},{0,1.2}},AxesOrigin->{1500,0},AxesLabel->{"[cm^-1]","R"},ImageSize
    ->{800,800}],{d,0,600},{\[CapitalTheta],1,90}]
(* This creates a 2D representation within Mathematics Manipualte environment. Here R is plotted versus angle, with a slider for the film thickness and energy. This is
     usefull to optimize film thickness to achieve maximum coupling at a certain energy *)
Manipulate[Plot[r[wcm,\[CapitalTheta],d],{\[CapitalTheta],1,80},PlotRange->{{45,55},{0,1}},AxesOrigin->{48.6,0},AxesOrigin->{1500,0},AxesLabel->{"Angle[\[
    Degree]]","R"},ImageSize->{800,800}],{wcm,1250,4000},{d,1,800}]

(* Create a movie of several calcualted contour plots. For example, one can create a movie depicting the reflectivity evolution as a function of film thickness; image size
    , intervalls,... are adjustable *)

Parallelize[movie=Table[ContourPlot[r[wcm,\[CapitalTheta],d],{wcm,1750,4000},{\[CapitalTheta],40,60},PlotRange->{0,1},ImageSize->{800,800},ColorFunction->"
    SunsetColors",PlotPoints->30,BaseStyle->{FontSize->25}]
,{d,1,400,4}]];
Export["Movie name.mov", movie]
```

Cell formating for Mathematica:

```
SetOptions[EvaluationNotebook[], CellContext → Notebook];

(*physical constants*)

c = 2.99792458 × 10^8;
e = 1.6021773 × 10^-19;
h = 6.6260755 × 10^-34;
ℏ = 1.05457 × 10^-34;
K = 1.380658 × 10^-23;
me = 9.109389 × 10^-31;
ϵ0 = 8.85419 × 10^-12;
q = 1.6021773 × 10^-19;

(*input parameters*)

ne = 2 × 10^20 × 1 000 000; (*free carrier density [cm^-3]*)
μ = 150 / 10 000; (*mobility*)
meeff = 0.21; (*relative effective mass:ZnO:0.36,
CdO:0.21,b-GaO:0.342,GaN:0.2,ITO:0.4*)
einf = 5.5; (*high frequqency dielectric constant:ZnO:3.2,
CdO:5.5 InGaAs:9.61 b-GaO:3.57,GaN:5.3,ITO:4*)
(*calculated variables for Drude equations*)
Γ = N[q / (μ meeff me)]; (*absorbtion term, damping*)
wp = N[Sqrt[(ne q^2) / (meeff me ϵ0)]]; (*plasme frequency*)

(*This section is used to calculate a Lorentzian absorbtion band
 to simulate an absorption in the environement,Code can be commented
 if calculations are to be performed in an dielectric environment*)

A = 0.00957242;
w0 = 2215;
w1 = 2235;
Γlorentz = 20.00;
background = 1.00027^2;
ϵN2O[wcm_] := (background + (A w0 Γlorentz) / (w0^2 - wcm^2 - I Γlorentz wcm) +
     (A w1 Γlorentz) / (w1^2 - wcm^2 - I Γlorentz wcm));

(*Plot the resulting absorbtion band:Re for ϵ1,Im for \[Epsilon]2*)

Plot[Re[ϵN2O[wcm]], {wcm, 2050, 2450}, ImageSize → {800, 800},
 LabelStyle → Directive[30], AxesLabel → {"[cm^-1]", "ϵ1"},
 BaseStyle → {FontFamily → "Arial"}, AspectRatio → 1,
 PlotRange → {{2050, 2450}, {0.99, 1.01}}, PlotStyle → {Blue, Thickness[0.005]}]



(*The following Module iterates through all calculations necessary
 for reflectivity simulations in the Kretschman configuration*)

r[wcm_, Θ_, d_] :=
 Module[{w, efilm, efilmcomplex, efilmfunction, efreesurface, xa, xb, xc, rs1,
   rp1, rs2, rp2, b, rp, rs, Refl, Θsubstrate, α, β, γ, nprism, nsubstrate,
   Θbase, esubstrate, rpback, rsback, Rbackrefl, Refltotal},
```

```
w = wcm 3 × 10^10 × 2 π; (*convert to rad/s*)

(*calculate the actual incident angle at the
   film/substrate interface using Snell's law,the dielectric
 properties of the prism and substrate as well as the prism geometry*)
θbase = 45; (*the base angle of the prism*)
nprism = N[Sqrt[caf2[wcm]]]; (*refrective index of prism,
called from optical properties database*)nsubstrate = N[Sqrt[mgo[wcm]]];
(*refrective index of substrate,called from optical properties database*)
α = θ - θbase;
β = ArcSin[1 / nprism Sin[α Degree]] 180 / π;
γ = ArcSin[nprism / nsubstrate Sin[(Abs[β + θbase]) Degree]] 180 / π;
θsubstrate = γ; (*This sets the angle for the reflectivity calculation
 to the actual incident angle at the film/substrate interface*)
efreesurface = 1.00027^2; (*permitivity of the surrounding medium*,
Air:1.00027^2,∈N2O[wcm] for lorentzian band*)

(*Compute backreflection from Prism/substrate interface*)
rsback = (nprism Cos[(β + θbase) Degree] - nsubstrate Cos[γ Degree]) /
   (nprism Cos[(β + θbase) Degree] + nsubstrate Cos[γ Degree]);
rpback = (nsubstrate Cos[(β + θbase) Degree] - nprism Cos[γ Degree]) /
   (nprism Cos[γ Degree] + nsubstrate Cos[(β + θbase) Degree]);
Rbackrefl = Abs[rpback]^2 / Abs[rsback]^2;
esubstrate = mgo[wcm];
efilmcomplex = einf + wp^2 / ((w I Γ) - w^2);

(*calculate the dielectric
 function of the plasmonic film using Drude eqautions*)

efilm = Re[efilmcomplex] - I Im[efilmcomplex];
(*compute square roots in fresnel equations*)
xa = Sqrt[(esubstrate - esubstrate Sin[θsubstrate Degree]^2)];
xb = Sqrt[(efilm - esubstrate Sin[θsubstrate Degree]^2)];
xc = Sqrt[(efreesurface - esubstrate Sin[θsubstrate Degree]^2)];
(*reflectance interface 1,s-and p-polarized*)rs1 = (xa - xb) / (xa + xb);
rp1 = (efilm xa - esubstrate xb) / (efilm xa + esubstrate xb);
(*reflectance interface 2,s-and p-polarized*)rs2 = (xb - xc) / (xb + xc);
rp2 = (efreesurface xb - efilm xc) / (efreesurface xb + efilm xc);
(*compute Airy formula*)b = 2 π d 10^-7 wcm xb;
rp = (rp1 + rp2 Exp[2 I b]) / (1 + rp1 rp2 Exp[2 I b]);
rs = (rs1 + rs2 Exp[2 I b]) / (1 + rs1 rs2 Exp[2 I b]);
Refl = (Abs[rp] / Abs[rs])^2;
(*Calculate total reflectance as rp/rs including the backreflection*)
Refltotal = (Abs[rpback] / Abs[rsback])^2 + Refl;
(*Set Return[] value to the desired output,such as Refl for rp/rs,
Refltotal for the included backrefelction or Abs[rp]^2 for only p-
 polarized reflectivity*)
Return[Refltotal]]
```

```
(*The following commands allow for graphical output of the
 calculated reflectivities using different representations I found
 usefull for this work.For further information on the individual
 plotting commands please consult the Mathematica manual*)

(*This creates a contour Plot of the reflectivites in angle/energy
 space used in this work.The respective ranges can be set freely.The
 contouring options are also customizable.Calculating these plots
 with a large amount of contour lines can take a long time*)

ContourPlot[r[wcm, Θ, 130], {wcm, 2150, 2300}, {Θ, 45, 50},
 PlotRange → {0.0, 1.1}, ImageSize → {800, 800}, Contours → 50,
 ColorFunction → "SunsetColors", PlotPoints → 30, LabelStyle → Directive[30],
 FrameLabel → {"[cm^-1]", "angle [°]"}, BaseStyle → {FontFamily → "Arial"}]

(*This creates a 3D Plot of the reflectivites in
 angle/energy space used in this work.The respective ranges can
 be set freely.Allows for faster calculation of reflectivities*)

Plot3D[r[wcm, Θ, 200], {wcm, 1500, 4000}, {Θ, 40, 60}, PlotRange → {0, 1.1},
 Mesh → None, PlotPoints → 40, ColorFunction → "SunsetColors",
 ImageSize → {800, 800}, TicksStyle → Directive[25]]

(*This creates a 2D representation within Mathematics
 Manipualte environment.Here R is plotted versus energy,
with a slider for the film thickness and incidence
 angle.This is usefull to optimize film thickness to
 achieve maximum coupling at a certain incident angle*)

Manipulate[Plot[r[wcm, Θ, d], {wcm, 1000, 7000}, PlotRange → {{1000, 7000}, {0, 1.2}},
  AxesOrigin → {1500, 0}, AxesLabel → {"[cm^-1]", "R
   "}, ImageSize → {800, 800}], {d, 0, 600}, {Θ, 1, 90}]

(*This creates a 2D representation within Mathematics
 Manipualte environment.Here R is plotted versus angle,
with a slider for the film thickness and energy.This is usefull to
 optimize film thickness to achieve maximum coupling at a certain energy*)

Manipulate[Plot[r[wcm, Θ, d], {Θ, 1, 80}, PlotRange → {{45, 55}, {0, 1}},
  AxesOrigin → {48.6, 0}, AxesOrigin → {1500, 0}, AxesLabel → {"Angle[°]", "R"},
  ImageSize → {800, 800}], {wcm, 1250, 4000}, {d, 1, 800}]

(*Create a movie of several calcualted contour plots.For example,
one can create a movie depicting the
 reflectivity evolution as a function of film thickness;
image size,intervalls,... are adjustable*)

Parallelize[movie = Table[ContourPlot[r[wcm, Θ, d], {wcm, 1750, 4000}, {Θ, 40, 60},
      PlotRange → {0, 1}, ImageSize → {800, 800}, ColorFunction → "SunsetColors",
      PlotPoints → 30, BaseStyle → {FontSize → 25}], {d, 1, 400, 4}]];
Export["Movie name.mov", movie]
```

B.3 SPR Kretschmann simulations in wave-vector space*

This is the code used to simulate the reflectivity for thin film samples in the Kretschmann configuration in wave-vector space.

```
SetOptions[EvaluationNotebook[],CellContext−>Notebook]

(*physical constants*)

c=2.99792458 10^8;
e=1.6021773 10^−19;
h=6.6260755 10^−34;
\[HBar]=1.05457 10^−34;
K=1.380658 10^−23;
me=9.109389 10^−31;
\[Epsilon]0=8.85419 10^−12;
q=1.6021773 10^−19;

(*input parameters*)

ne=2 10^20 1000000; (*free carrier density [cm^−3]*)
\[Mu]=150/10000; (*mobility*)
meeff=0.21; (*relative effective mass:ZnO:0.36,CdO:0.21,b−GaO:0.342,GaN:0.2,ITO:0.4*)
einf=5.5; (*high frequqency dielectric constant:ZnO:3.2,CdO:5.5 InGaAs:9.61 b−GaO:3.57,GaN:5.3,ITO:4*)(*calculated variables for Drude equations*)
\[CapitalGamma]=N[q/(\[Mu] meeff me)]; (*absorbtion term, damping*)
wp=N[Sqrt[(ne q^2)/(meeff me \[Epsilon]0)]]; (*plasme frequency*)


r[wcm_,kx_,d_]:=Module[{w, efilm,efilmcomplex,efilmfunction,efreesurface,xa,xb,xc,rs1,rp1,rs2,rp2,b,rp,rs,Refl,\[CapitalTheta]substrate,\[Alpha],\[Beta],\[Gamma],
    nprism,nsubstrate,\[CapitalTheta]base,esubstrate,rpback,rsback,Rbackrefl,Refltotal},
w=wcm 3 10^10 2 \[Pi] ; (* convert to rad/s *)
esubstrate=mgo[wcm];
\[Gamma]=ArcSin[(kx 2.99792458 10^8)/(Sqrt[esubstrate]  w)] 180/\[Pi];
\[CapitalTheta]substrate=\[Gamma];
efreesurface= 1.00027^2; (*permitivity of the surrounding medium*,Air:1.00027^2 *)

efilmcomplex=einf+wp^2/((w I \[CapitalGamma])−w^2);
efilm=Re[efilmcomplex]−I Im[efilmcomplex];
xa=Sqrt[(esubstrate−esubstrate Sin[\[CapitalTheta]substrate Degree]^2)];
xb= Sqrt[(efilm−esubstrate Sin[\[CapitalTheta]substrate Degree]^2)];
xc=Sqrt[(efreesurface−esubstrate Sin[\[CapitalTheta]substrate Degree]^2)];
(* reflectance interface 1, s− and p− polarized *)
rs1=(xa−xb)/(xa+xb);
rp1=(efilm xa−esubstrate xb)/(efilm xa+esubstrate xb);
(* reflectance interface 2, s− and p− polarized *)
rs2=(xb−xc)/(xb+xc);
rp2=(efreesurface xb−efilm xc)/(efreesurface xb+efilm xc);
(* compute Airy formula *)
b=2 \[Pi] d 10^−7wcm xb;
rp=(rp1+rp2 Exp[2 I b])/(1+rp1 rp2  Exp[2 I b]);
rs=(rs1+rs2 Exp[2 I b])/(1+rs1 rs2 Exp[2 I b]);
Refl=(Abs[rp]/Abs[rs])^2;

Return[Refl];
]
(* In the following section, a contour plot of the reflectivities in wave−vector space as well as the plasmon dispersion and light lines in the Kretschmann configuration
    are calculated to compute a composite image  *)

(* Reflectivity *)
x=ContourPlot[r[wcm,kx,300],{kx,1000000,4000000},{wcm,1000,6000},PlotRange−>{0,1.2},ImageSize−>{800,800},Contours−>50,ColorFunction−>"SunsetColors",
    PlotPoints−>100,LabelStyle−>Directive[25],FrameLabel−>{"Subscript[k, x][m^−1]","[cm^−1]"}];
```

```
(* light line, upper limit *)

a=ParametricPlot[{(wcm 3 10^10 2 \[Pi] Sqrt[mgo[wcm]]Sin[ArcSin[1/Sqrt[mgo[wcm]]]])/(2.99792458 10^8),wcm},{wcm,1000,6000},TicksStyle->Directive[25],
    AxesLabel->{"Subscript[k, x]","cm^-1"}, AspectRatio->1,AxesOrigin->{1000000,1000},PlotStyle->{Red,Thickness[0.005]}];
(* light line, lower limit *)
b=ParametricPlot[{(wcm 3 10^10 2 \[Pi] Sqrt[mgo[wcm]]Sin[90 Degree])/(2.99792458 10^8),wcm},{wcm,1000,6000}, AspectRatio->1,AxesOrigin->{1000000,1000},
    PlotStyle->{Red,Thickness[0.005]}];

(* real part of the plasmon dispersion *)
efreesurface=1.00027^2 ;(* dielectric environment for the dispersion calculation  *)
d=ParametricPlot[{Re[(wcm 100 2 \[Pi]) Sqrt[(efreesurface  (einf+wp^2/(((wcm 3 10^10 2 \[Pi]) I \[CapitalGamma])-(wcm 3 10^10 2 \[Pi])^2)))/(efreesurface+(einf+
    wp^2/(((wcm 3 10^10 2 \[Pi]) I \[CapitalGamma])-(wcm 3 10^10 2 \[Pi])^2)))]],wcm},{wcm,1000,6000}, AspectRatio->1,AxesOrigin->{1000000,1000},
    GridLines->{{},{wp/(3 10^10 2 \[Pi])}},PlotStyle->{Blue,Thickness[0.005]} ,LabelStyle->Directive[25],AxesLabel->{"Subscript[k, x][m^-1]","[cm^-1]"},
    ImageSize->{800,800} ];

(* Plot the composite image *)

Show[x,d,a,b,PlotRange->{{0.65 10^6,3.4 10^6},{1000,4000}},AxesOrigin->{650000,1000},BaseStyle->{FontFamily->"Arial"}]
```

Cell formating for Mathematica:

```
SetOptions[EvaluationNotebook[], CellContext → Notebook]

(*physical constants*)

c = 2.99792458 × 10^8;
e = 1.6021773 × 10^-19;
h = 6.6260755 × 10^-34;
ℏ = 1.05457 × 10^-34;
K = 1.380658 × 10^-23;
me = 9.109389 × 10^-31;
ϵ0 = 8.85419 × 10^-12;
q = 1.6021773 × 10^-19;

(*input parameters*)

ne = 2 × 10^20 × 1 000 000; (*free carrier density [cm^-3]*)
μ = 150 / 10 000; (*mobility*)
meeff = 0.21; (*relative effective mass:ZnO:0.36,
CdO:0.21,b-GaO:0.342,GaN:0.2,ITO:0.4*)
einf = 5.5; (*high frequqency dielectric constant:ZnO:3.2,
CdO:5.5 InGaAs:9.61 b-GaO:3.57,GaN:5.3,ITO:4*)
(*calculated variables for Drude equations*)
Γ = N[q / (μ meeff me)]; (*absorbtion term, damping*)
wp = N[Sqrt[(ne q^2) / (meeff me ϵ0)]]; (*plasme frequency*)
```

```
r[wcm_, kx_, d_] :=
 Module[{w, efilm, efilmcomplex, efilmfunction, efreesurface, xa, xb, xc, rs1,
   rp1, rs2, rp2, b, rp, rs, Refl, θsubstrate, α, β, γ, nprism, nsubstrate,
   θbase, esubstrate, rpback, rsback, Rbackrefl, Refltotal},
  w = wcm 3 × 10^10 2 π ; (* convert to rad/s *)
  esubstrate = mgo[wcm];
  γ = ArcSin[(kx 2.99792458 × 10^8) / (√esubstrate w)] 180/π;
  θsubstrate = γ;
  efreesurface = 1.00027^2;
  (*permitivity of the surrounding medium*,Air:1.00027^2 *)

  efilmcomplex = einf + wp^2/((w i Γ) - w^2);
  efilm = Re[efilmcomplex] - i Im[efilmcomplex];
  xa = √((esubstrate - esubstrate Sin[θsubstrate Degree]^2)) ;
  xb = √((efilm - esubstrate Sin[θsubstrate Degree]^2)) ;
  xc = √((efreesurface - esubstrate Sin[θsubstrate Degree]^2)) ;
  (* reflectance interface 1, s- and p- polarized *)
  rs1 = (xa - xb)/(xa + xb);
  rp1 = (efilm xa - esubstrate xb)/(efilm xa + esubstrate xb);
  (* reflectance interface 2, s- and p- polarized *)
  rs2 = (xb - xc)/(xb + xc);
  rp2 = (efreesurface xb - efilm xc)/(efreesurface xb + efilm xc);
  (* compute Airy formula *)
  b = 2 π d 10^-7 wcm xb;
  rp = (rp1 + rp2 Exp[2 i b])/(1 + rp1 rp2 Exp[2 i b]);
  rs = (rs1 + rs2 Exp[2 i b])/(1 + rs1 rs2 Exp[2 i b]);
  Refl = (Abs[rp]/Abs[rs])^2;

  Return[Refl];
 ]
```

```
(* In the following section, a contour plot of the reflectivities in wave-
 vector space as well as the plasmon dispersion and light lines in the
  Kretschmann configuration are calculated to compute a composite image  *)

(* Reflectivity *)
x = ContourPlot[r[wcm, kx, 300], {kx, 1 000 000, 4 000 000},
    {wcm, 1000, 6000}, PlotRange → {0, 1.2}, ImageSize → {800, 800},
    Contours → 50, ColorFunction → "SunsetColors", PlotPoints → 100,
    LabelStyle → Directive[25], FrameLabel → {"k_x[m^-1]", "[cm^-1]"}];


(* light line, upper limit *)

a = ParametricPlot[
    {(wcm 3 × 10^10 2 π √(mgo[wcm]) Sin[ArcSin[1 / √(mgo[wcm])]]) / (2.99792458 × 10^8),
     wcm}, {wcm, 1000, 6000}, TicksStyle → Directive[25],
    AxesLabel → {"k_x", "cm^-1"}, AspectRatio → 1, AxesOrigin → {1 000 000, 1000},
    PlotStyle → {Red, Thickness[0.005]}];
(* light line, lower limit *)
b = ParametricPlot[{ (wcm 3 × 10^10 2 π √(mgo[wcm]) Sin[90 Degree]) / (2.99792458 × 10^8), wcm},
    {wcm, 1000, 6000}, AspectRatio → 1, AxesOrigin → {1 000 000, 1000},
    PlotStyle → {Red, Thickness[0.005]}];

(* real part of the plasmon dispersion *)
efreesurface = 1.00027^2 ;
(* dielectric environment for the dispersion calculation  *)
d = ParametricPlot[{Re[(wcm 100 × 2 π)
      √(((efreesurface (einf + wp^2 / ((wcm 3 × 10^10 2 π) i Γ) - (wcm 3 × 10^10 2 π)^2)) /
         (efreesurface + (einf + wp^2 / ((wcm 3 × 10^10 2 π) i Γ) - (wcm 3 × 10^10 2 π)^2))))], wcm},
    {wcm, 1000, 6000}, AspectRatio → 1, AxesOrigin → {1 000 000, 1000},
    GridLines → {{}, {wp / (3 × 10^10 2 π)}},
    PlotStyle → {Blue, Thickness[0.005]} , LabelStyle → Directive[25],
    AxesLabel → {"k_x[m^-1]", "[cm^-1]"}, ImageSize → {800, 800} ];


(* Plot the composite image *)

Show[x, d, a, b, PlotRange → {{0.65 × 10^6, 3.4 × 10^6}, {1000, 4000}},
 AxesOrigin → {650 000, 1000}, BaseStyle → {FontFamily → "Arial"}]
```

B.4 Grating coupling simulation*

This code is used to simulate the coupling to the SPP dispersion using a grating. The SPP, grating vector and materials can be freely defined.

```
SetOptions[EvaluationNotebook[],CellContext->Notebook]

(*physical constants*)

c=2.99792458 10^8;
e=1.6021773 10^-19;
h=6.6260755 10^-34;
\[HBar]=1.05457 10^-34;
K=1.380658 10^-23;
me=9.109389 10^-31;
\[Epsilon]0=8.85419 10^-12;
q=1.6021773 10^-19;

(*input parameters*)

ne=2 10^20 1000000; (*free carrier density [cm^-3]*)
\[Mu]=150/10000; (*mobility*)
meeff=0.21; (*relative effective mass:ZnO:0.36,CdO:0.21,b-GaO:0.342,GaN:0.2,ITO:0.4*)
einf=5.5; (*high frequqency dielectric constant:ZnO:3.2,CdO:5.5 InGaAs:9.61 b-GaO:3.57,GaN:5.3,ITO:4*)(*calculated variables for Drude equations*)
\[CapitalGamma]=N[q/(\[Mu] meeff me)]; (*absorbtion term, damping*)
wp=N[Sqrt[(ne q^2)/(meeff me \[Epsilon]0)]]; (*plasme frequency*)

(* This defines the grating vector *)
pitch=10 10^-6;              (* grating pitch in [m] *)
M=N[2 Pi/(pitch)]; (* Grating Vector *)

(* This Manipulate builds a simulation that lets the user visualize the different possiblities to couple to SPP with gratings. The incidence angle is variable, so is the
      selection of the grating vector (M=\[PlusMinus]0,1,2 ..). *)
Manipulate[
ParametricPlot[{

{((w/c)Sin[-angle Degree])uu,w},
{((w/c)Sin[angle Degree]) uu,w},
{((w/c)Sin[-angle Degree]+(M 0.5)) hh,w},
{((w/c)Sin[angle Degree]+(M 0.5)) hh,w},
{((w/c)Sin[-angle Degree]-(M 0.5)) jj,w},
{((w/c)Sin[angle Degree]-(M 0.5)) jj,w},
{((w/c)Sin[-angle Degree]+M 1) x,w},
{((w/c)Sin[-angle Degree]+M 2)y,w},
{((w/c)Sin[-angle Degree]-M 1)z,w},
{((w/c)Sin[-angle Degree]-M 2) u,w},
{((w/c)Sin[angle Degree]-M 1) z,w},
{((w/c)Sin[angle Degree]-M 2)u,w},
{((w/c)Sin[angle Degree]+M 1) x,w},
{((w/c)Sin[angle Degree]+M 2) y,w},
{((w/c)Sin[-angle Degree]+M 3) r,w},
{((w/c)Sin[angle Degree]+M 3) r,w},
{((w/c)Sin[-angle Degree]-M 3) rr,w},
{((w/c)Sin[angle Degree]-M 3) rr,w},
{(Re[w/c Sqrt[(efreesurface  (einf+wp^2/((w I \[CapitalGamma])-w^2)))/(efreesurface+(einf+wp^2/((w I \[CapitalGamma])-w^2)))]]) xx,w},
{(Re[w/c Sqrt[( mgo[(w/(2 Pi 3 10^10))](einf+wp^2/((w I \[CapitalGamma])-w^2)))/(mgo[(w/(2 Pi 3 10^10))]+(einf+wp^2/((w I \[CapitalGamma])-w^2)))]]) yy,w
      },          (* Plot dispersion curves for the SPP for thin/freesurface and film/substrate *)
{(-Re[w/c Sqrt[(efreesurface  (einf+wp^2/((w I \[CapitalGamma])-w^2)))/(efreesurface+(einf+wp^2/((w I \[CapitalGamma])-w^2)))]]) xx,w},
{(-Re[w/c Sqrt[( mgo[(w/(2 Pi 3 10^10))](einf+wp^2/((w I \[CapitalGamma])-w^2)))/(mgo[(w/(2 Pi 3 10^10))]+(einf+wp^2/((w I \[CapitalGamma])-w^2)))]]) yy,
      w}
},
{w,1 10^14,10^15}, AspectRatio->800/1200,ImageSize->{1100,800},PlotRange->{{-3 10^6,3 10^6},{0.9 10^14,4 10^14}},Frame->True,LabelStyle->Directive[25],
      FrameLabel->{"[Subscript[k, x]]","\[Omega]"},PlotStyle->{Black,Black,Black,Black,Black,Black,Black,Black,Black,Black,Black,Black,Black,Black,Black,Black,
```

```
    Black,Black,Blue,Red,Blue,Red}],

Row[{Control[{{angle,90,"Incident Angle [\[Degree]]"},1,90}],Control[{{xx,0,"Subscript[k, spp] Air/Metal"},{0,1}}],Control[{{yy,0,"Subscript[k, spp] Substrate/Metal
    "},{0,1}}],Control[{{uu,0,"light lines free space"},{0,1}}],Control[{{x,0,"+Subscript[k, g]"},{0,1}}],Control[{{hh,0,"+1/2Subscript[k, g]"},{0,1}}],Control[{{jj,0,"−1/2
    Subscript[k, g]"},{0,1}}],Control[{{y,0,"+2Subscript[k, g]"},{0,1}}],Control[{{z,0,"−Subscript[k, g]"},{0,1}}],Control[{{u,0,"−2Subscript[k, g]"},{0,1}}],Control[{{r,0,"+3
    Subscript[k, g]"},{0,1}}],Control[{{rr,0,"−3Subscript[k, g]"},{0,1}}]},Spacer[15]]]
```

Cell formating for Mathematica:

```
SetOptions[EvaluationNotebook[], CellContext → Notebook]

(*physical constants*)

c = 2.99792458 × 10^8;
e = 1.6021773 × 10^-19;
h = 6.6260755 × 10^-34;
ℏ = 1.05457 × 10^-34;
K = 1.380658 × 10^-23;
me = 9.109389 × 10^-31;
ϵ0 = 8.85419 × 10^-12;
q = 1.6021773 × 10^-19;

(*input parameters*)

ne = 2 × 10^20 × 1 000 000; (*free carrier density [cm^-3]*)
μ = 150 / 10 000; (*mobility*)
meeff = 0.21; (*relative effective mass:ZnO:0.36,
CdO:0.21,b-GaO:0.342,GaN:0.2,ITO:0.4*)
einf = 5.5; (*high frequqency dielectric constant:ZnO:3.2,
CdO:5.5 InGaAs:9.61 b-GaO:3.57,GaN:5.3,ITO:4*)
(*calculated variables for Drude equations*)
Γ = N[q / (μ meeff me)]; (*absorbtion term, damping*)
wp = N[Sqrt[(ne q^2) / (meeff me ϵ0)]]; (*plasme frequency*)

(* This defines the grating vector *)
pitch = 10 × 10^-6;        (* grating pitch in [m] *)
M = N[2 Pi / (pitch)]; (* Grating Vector *)

 (* This Manipulate builds a simulation that lets
 the user visualize the different possiblities to couple
 to SPP with gratings. The incidence angle is variable,
so is the selection of the grating vector (M=±0,1,2 ..). *)
```

Out[66]= 1.74099×10^{15}

```
In[68]:= Manipulate[
 ParametricPlot[{

   {((w / c) Sin[-angle Degree]) uu, w},
   {((w / c) Sin[angle Degree]) uu, w},
   {((w / c) Sin[-angle Degree] + (M 0.5)) hh, w},
   {((w / c) Sin[angle Degree] + (M 0.5)) hh, w},
   {((w / c) Sin[-angle Degree] - (M 0.5)) jj, w},
   {((w / c) Sin[angle Degree] - (M 0.5)) jj, w},
   {((w / c) Sin[-angle Degree] + M 1) x, w},
   {((w / c) Sin[-angle Degree] + M 2) y, w},
   {((w / c) Sin[-angle Degree] - M 1) z, w},
   {((w / c) Sin[-angle Degree] - M 2) u, w},
   {((w / c) Sin[angle Degree] - M 1) z, w},
   {((w / c) Sin[angle Degree] - M 2) u, w},
```

```
  {((w / c) Sin[angle Degree] + M 1) x, w},
  {((w / c) Sin[angle Degree] + M 2) y, w},
  {((w / c) Sin[-angle Degree] + M 3) r, w},
  {((w / c) Sin[angle Degree] + M 3) r, w},
  {((w / c) Sin[-angle Degree] - M 3) rr, w},
  {((w / c) Sin[angle Degree] - M 3) rr, w},

  {(Re[w / c Sqrt[efreesurface (einf + wp^2/((w i Γ) - w^2)) / (efreesurface + (einf + wp^2/((w i Γ) - w^2)))]) xx, w},

  {(Re[w / c Sqrt[mgo[(w / (2 Pi 3 × 10^10))] (einf + wp^2/((w i Γ) - w^2)) / (mgo[(w / (2 Pi 3 × 10^10))] + (einf + wp^2/((w i Γ) - w^2)))]) yy, w},      (* Plot
   dispersion curves for the SPP for thin/freesurface and film/substrate *)
  {(-Re[w / c Sqrt[efreesurface (einf + wp^2/((w i Γ) - w^2)) / (efreesurface + (einf + wp^2/((w i Γ) - w^2)))]) xx, w},

  {(-Re[w / c Sqrt[mgo[(w / (2 Pi 3 × 10^10))] (einf + wp^2/((w i Γ) - w^2)) / (mgo[(w / (2 Pi 3 × 10^10))] + (einf + wp^2/((w i Γ) - w^2)))]) yy, w}
 },
 {w, 1 × 10^14, 10^15}, AspectRatio → 800 / 1200, ImageSize → {1100, 800},
 PlotRange → {{-3 10^6, 3 × 10^6}, {0.9 × 10^14, 4 × 10^14}},
 Frame → True, LabelStyle → Directive[25], FrameLabel → {"[k_x]", "ω"},
 PlotStyle → {Black, Black, Black, Black, Black, Black, Black, Black, Black, Black,
   Black, Black, Black, Black, Black, Black, Black, Blue, Red, Blue, Red}],

Row[{Control[{{angle, 90, "Incident Angle [°]"}, 1, 90}],
  Control[{{xx, 0, "k_spp Air/Metal"}, {0, 1}}],
  Control[{{yy, 0, "k_spp Substrate/Metal"}, {0, 1}}], Control[
   {{uu, 0, "light lines free space"}, {0, 1}}], Control[{{x, 0, "+k_g"}, {0, 1}}],
  Control[{{hh, 0, "+1/2 k_g"}, {0, 1}}], Control[{{jj, 0, "-1/2 k_g"}, {0, 1}}],
  Control[{{y, 0, "+2k_g"}, {0, 1}}], Control[{{z, 0, "-k_g"}, {0, 1}}],
  Control[{{u, 0, "-2k_g"}, {0, 1}}], Control[{{r, 0, "+3k_g"}, {0, 1}}],
  Control[{{rr, 0, "-3k_g"}, {0, 1}}]}, Spacer[15]]
```

B.5 Simulation of the N_2O ν_3 mode

This code allows to compute a pressure dependent N_2O dielctric function around the 2220 cm^{-1} absorption band. This dielectric function can then be fed into the SPR calculations by replacing the constant dielectric environment with the calculated, frequency dependent function within the reflectivity module.

```
A = 0.00957242;
wb = 2224;
w0 = 2210;
(* added assymetry parameter according to: A.L. Stancik, E.B. Brauns \
/Vibrational Spectroscopy 47 (2008) 66−69*)
w1 = 2237;
\[CapitalGamma]lorentz = 30.00;
background = 1.00087^2;
asymmetryw0 = 0.20;
asymmetryw1 = −0.05;
\[CapitalGamma]lorentzassymw0[wcm_] := \[CapitalGamma]lorentz/(
1 + (E^(asymmetryw0 (wcm − w0 ))));

\[CapitalGamma]lorentzassymw1[wcm_] :=  \[CapitalGamma]lorentz/(
1 + (E^(asymmetryw1 (wcm − w1 ))));
\[Epsilon]N2O[
wcm_] := (background + (
0.8 A w0 \[CapitalGamma]lorentzassymw0[wcm])/(
w0^2 − wcm^2 − I \[CapitalGamma]lorentzassymw0[wcm] wcm) + (
1.4 A w1 \[CapitalGamma]lorentzassymw1[wcm])/(
w1^2 − wcm^2 − I \[CapitalGamma]lorentzassymw1[wcm] wcm))

Plot[Re[\[Epsilon]N2O[wcm]], {wcm, 2100, 2350},
ImageSize −> {800, 800}, LabelStyle −> Directive[30],
AxesLabel −> {"[\!\(\*SuperscriptBox[\(cm\), \(−1\)]\)]",
"\[Epsilon]1"}, BaseStyle −> {FontFamily −> "Arial"},
AspectRatio −> 1 , PlotRange −> All,
PlotStyle −> {Blue, Thickness[0.005]}]
```

Cell formatting for Mathematica:

```
A = 0.00957242;
wb = 2224;
w0 = 2210;
(* added assymetry parameter according to: A.L. Stancik,
E.B. Brauns /Vibrational Spectroscopy 47 (2008) 66-69*)
w1 = 2237;
Γlorentz = 30.00;
background = 1.00087^2;
asymmetryw0 = 0.20;
asymmetryw1 = -0.05;
Γlorentzassymw0[wcm_] := Γlorentz / (1 + (e^(asymmetryw0 (wcm-w0))));

Γlorentzassymw1[wcm_] := Γlorentz / (1 + (e^(asymmetryw1 (wcm-w1))));

ϵN2O[wcm_] := (background + 0.8 A w0 Γlorentzassymw0[wcm] / (w0^2 - wcm^2 - i Γlorentzassymw0[wcm] wcm) +
    1.4 A w1 Γlorentzassymw1[wcm] / (w1^2 - wcm^2 - i Γlorentzassymw1[wcm] wcm))

Plot[Re[ϵN2O[wcm]], {wcm, 2100, 2350}, ImageSize → {800, 800},
 LabelStyle → Directive[30], AxesLabel → {"[cm^-1]", "ϵ1"},
 BaseStyle → {FontFamily → "Arial"}, AspectRatio → 1 ,
 PlotRange → All, PlotStyle → {Blue, Thickness[0.005]}]
```